

**PROCEEDINGS OF THE
WORKSHOP ON RADIATION DAMAGE TO WIRE CHAMBERS**

Lawrence Berkeley Laboratory, Berkeley California

January 16-17, 1986

John Kadyk
Workshop Organizer

April 1986

Lawrence Berkeley Laboratory
University of California
Berkeley, California 94720

This work was supported by the U.S. Department of Energy under contract DE-AC03-76SF00098.

MASTER

DISTRIBUTION OF THIS DOCUMENT IS UNLIMITED



LEGAL NOTICE

This book was prepared as an account of work sponsored by an agency of the United States Government. Neither the United States Government nor any agency thereof, nor any of their employees, makes any warranty, express or implied, or assumes any legal liability or responsibility for the accuracy, completeness, or usefulness of any information, apparatus, product, or process disclosed, or represents that its use would not infringe privately owned rights. Reference herein to any specific commercial product, process, or service by trade name, trademark, manufacturer, or otherwise, does not necessarily constitute or imply its endorsement, recommendation, or favoring by the United States Government or any agency thereof. The views and opinions of authors expressed herein do not necessarily state or reflect those of the United States Government or any agency thereof.

Printed in the United States of America
Available from
National Technical Information Service
U.S. Department of Commerce
5285 Port Royal Road
Springfield, VA 22161
Price Code: A15

Lawrence Berkeley Laboratory is an equal opportunity employer.

DISCLAIMER

This report was prepared as an account of work sponsored by an agency of the United States Government. Neither the United States Government nor any agency thereof, nor any of their employees, makes any warranty, express or implied, or assumes any legal liability or responsibility for the accuracy, completeness, or usefulness of any information, apparatus, product, or process disclosed, or represents that its use would not infringe privately owned rights. Reference herein to any specific commercial product, process, or service by trade name, trademark, manufacturer, or otherwise does not necessarily constitute or imply its endorsement, recommendation, or favoring by the United States Government or any agency thereof. The views and opinions of authors expressed herein do not necessarily state or reflect those of the United States Government or any agency thereof.

LBL--21170

DE86 014077

This report was done with support from the Department of Energy. Any conclusions or opinions expressed in this report represent solely those of the author(s) and not necessarily those of The Regents of the University of California, the Lawrence Berkeley Laboratory or the Department of Energy.

Reference to a company or product name does not imply approval or recommendation of the product by the University of California or the U.S. Department of Energy to the exclusion of others that may be suitable.

PREFACE

This workshop is perhaps the first directed toward the understanding and ultimate solution of a particular set of instrumental problems: the deterioration of wire chamber performance due to radiation-induced coating of the wires. Wire chambers have developed into enormously sophisticated and versatile instruments over recent years, especially for use in high energy physics experiments, and are devices whose fabrication frequently involves large investments of time and money. It is therefore appropriate to bring together colleagues who have used wire chambers to try to gain some insight from their collective experiences regarding the problem of wire "aging", and perhaps learn how to prevent or cure it.

About 90 people attended the two-day workshop, and twenty-six papers were presented, twenty-four of which are contained in these Proceedings in the order presented. There are quite a few similarities in the experiences related, leading to certain helpful guidelines and procedural advice, which are nicely summarized by the last speaker, Jaroslav Va'vra. Clarification of some of the fundamental processes of plasma chemistry at work was provided by two members of the faculty of the Department of Chemical Engineering, University of California at Berkeley: Dennis Hess and Michael Williams. They discussed some of the fundamental reactions that might typically occur via plasma chemistry and applied this to an actual example of a defunct chamber where the composition of the wire deposits was analyzed. Little quantitative data exists regarding aging in wire chambers under carefully monitored or controlled conditions. The conditions of atmospheric pressure and d.c. avalanche could lead to substantially different results from those observed in the conventional plasma chemistry studies at low pressure (~ 1 Torr) and using r.f. discharges. Nevertheless, there are indications that the information obtained in plasma chemistry studies may have considerable relevance to the present aging problems.

Some general negative experiences described were the deposits of silicon found on sense wires, plasticisers found on field and sense wires, and excessive currents which were probably caused by cathode wire coatings. Rapid deposit rates were found when halogens (esp. chlorine) were suspected of being in the system. On the positive side, small amounts of alcohol (esp. ethanol) and/or water vapor seem to have very beneficial effects (with gold-plated wire), and some gases containing CO_2 can actually remove "whiskers". Generally speaking, there seems to be considerable evidence that quite small concentrations of certain contaminants can greatly accelerate the deposit rates. Although this information has more the nature of "lore" than science, it nevertheless has a utilitarian value at the present stage, and hopefully will lead to a deeper understanding and better control of the aging processes.

In Appendix A, a selected set of questions and answers (usually paraphrased by me) have been reproduced from the four scheduled discussion periods, and the beginning and final speakers preceding each discussion, to whom questions are generally directed, are indicated. These were taken from audio and video tapes, and I accept the blame for any mistakes in interpretation, or judgment in selection of questions, which was necessary due to space limitations. In some cases the question and/or answer was inaudible on both tapes, and had to be omitted. Appendix B contains descriptions of individual results on aging from laboratory tests or experiments, one result per page (usually). It is

hoped that this may provide a convenient summary of results. The last two appendices contain: C. a partial bibliography of publications and D. a list of attendees to this workshop, with affiliation, address and phone numbers.

The success of the workshop is largely due to the interest of all attendees. However, the organizing committee, consisting of Muzaffer Atac, David Binnie, and Jaroslav Va'vra, was indispensable during the organizing process. The sessions were conducted in a most efficient manner by the chairmen: David Binnie, Hans Juergen Hilke, Muzaffer Atac, and Albrecht Wagner. This was a considerable challenge, considering the nature of the subject and the very limited time for the program. Valerie Heatlie of the Physics Division has been the primary person responsible for the enormous amount of detailed work, before, during, and especially after the workshop in helping with the preparation of this Proceedings. Thanks also to Karen Larsen and Marian Golden for their help at early stages of preparation. Professional conference organizational help from Peggy Little and Lee Merrill of the Technical Information Department are gratefully acknowledged. Ralph Dennis prepared the design for the flyer as well as the present cover design. Loretta Lizama has very ably put together all the contributed papers, plus the other parts of this Proceedings, to make this a timely publication.

Finally, I must thank George Trilling, Head of the Physics Division, for his encouragement and strong support for this workshop, and for the help from his office staff.

John Kadyk
Workshop Organizer

TABLE OF CONTENTS

Preface	iii
When Everything Was Clear F. Sauli	1
Plasma Chemistry in Wire Coating D.W. Hess	15
Analysis of TPC Inner Drift Chamber Wire Coatings M.C. Williams	25
New Technics to Analyse Wire Coatings H. Boerner and R.D. Heuer (Presented by R.D. Heuer)	47
Wire Chamber Aging M. Atac	55
Our Ageing Experience with the UA1 Central Detector S. Beingssner, T. Meyer, V. Vuillemin, and M. Yvert (Presented by M. Yvert)	67
Experience with the UA1 Micro Vertex Detector in the SPS Collider UA1 Coliaboration (Presented by D. Smith)	91
Wire Chamber Degradation at the Argonne ZGS W. Haberichter and H. Spinka (Presented by H. Spinka)	99
The OMEGA and SFMD Experience in Intense Beams OMEGA and SFMD Collaborations (Presented by O. Ullaland)	107
Ageing Effects in Gaseous Detectors and Search for Remedies A. Dwurazny, Z. Hajduk, and M. Turala (Presented by M. Turala)	113
Investigation of Breakdown Conditions of Drift Chambers H.F.-W. Sadrozinski	121
Lifetime Tests for MAC Vertex Chamber H. Nelson	131
Results from Some Anode Wire Aging Tests I. Juricic and J.A. Kadyk (Presented by J.A. Kadyk)	141
Summary of Aging Studies in Wire Chambers by AFS, DELPHI and EMC Groups H.J. Hilke	153

A Laboratory Study of Radiation Damage to Drift Chambers R. Kotthaus	161
Long Term Behaviour of the Jet Chamber at JADE K. Ambrus, J. Heintze, P. Lennert, H. Rieseberg, and A. Wagner (Presented by A. Wagner)	195
Performance of the JADE Vertex Detector H. Kado	207
Experience with the TASSO Chambers D.M. Binnie	213
Radiation Damage Control in the BNL Hypernuclear Spectrometer Drift Chamber System P.H. Pile	219
Whisker Growth in Test Cells B. Foster	227
Aging Effects in a Large Drift Chamber in the Fermilab Tagged Photon Spectrometer P. Estabrooks	231
Results on Ageing and Stability with Pure DME and Isobutane/Methylal Mixture in Thin High-Rate Multiwire Chambers S. Majewski	239
Proportional Tube Lifetimes (Magic Gas, A-CO ₂ , DME) G. Godfrey	257
Review of Wire Chamber Aging J. Va'vra	263
Appendix A Discussion Sessions	295
Appendix B Result Summaries	307
Appendix C Bibliography	335
Appendix D List of Workshop Attendees	337

WHEN EVERYTHING WAS CLEAR

F. Sauli, CERN, Geneva, Switzerland

ABSTRACT

This paper, which is the introduction to the workshop, describes the early observations of degeneracy in multiwire chambers operated with hydrocarbon quenchers after continued exposure to ionizing radiation. A phenomenological explanation of the observations, involving the formation of carbon polymer coatings on anodes and cathodes and the subsequent induced secondary electron emission, was suggested at the time, as well as a way to prevent ageing by addition of a low-ionization-potential, non-polymerizing vapour to the gas mixture. The subsequent observation of ageing in non-polymerizing mixtures and the discovery of silicon and sulfur compounds on the wires have somewhat invalidated this simple picture.

1. INTRODUCTION

Ageing problems were found in multiwire proportional chambers (MWPCs) soon after their development by Charpak and collaborators. It was observed that an initially well-working chamber (having negligible dark current and good detection efficiency), when exposed to radiation for even limited amounts of time, would gradually develop a slowly increasing current often reaching several tens of microamperes and remaining at that value even after removal of the source. Upon switching the high voltage off and on again, this steady current vanished, to reappear slowly again in the absence of radiation; exposure to an ionizing source would almost instantly re-establish the current at its previous value. The damage was obviously local and permanent; thin layers of translucent, whitish, or darkened material were uncovered in the exposed regions. A similar phenomenology observed in new chambers was readily associated with the presence of greasy layers on the electrodes due to improper cleaning. Hard rubbing of the suspicious regions with various solvents removed indeed in most cases the current build up. Since, at the time, gas mixtures rich in heavy hydrocarbon quenchers were used in order to allow large gains, the conjecture that one was observing a polymerization process caused by the ions produced in the gas under avalanche conditions was very natural. These polymers, appearing in the liquid or solid phase, would deposit on all electrodes, inducing various kinds of secondary phenomena. Such processes were indeed well known to take place in sealed, proportional and Geiger counters.

Together with an explanation of the observed ageing came the idea of preventing, or at least slowing down, the process with the addition of a non-polymerizing quencher having the lowest ionization potential in the mixture; the very efficient charge transfer process known to occur between ions and molecules would then quickly transform the hydrocarbons' dangerous ions into harmless non-polymerizing ions of the additive. Indeed, addition of isopropyl alcohol (C_3H_7OH) or methylal $[(OCH_3)_2CH_2]$ to an argon + isobutane + freon mixture (the magic gas) prolonged the lifetime of a test chamber by three orders of magnitude [1]. It was also observed that MWPCs realized with continuous cathodes started showing ageing effects at integral radiation fluxes one or two orders of magnitude higher than chambers having wire cathodes; this indicated again that the deterioration was mainly caused by the deposits on cathodes, obviously reaching a perturbing thickness faster for reduced surfaces.

Subsequent observations by many authors, documented throughout these proceedings, have somewhat invalidated this simple picture. On one hand, ageing has been reported also for gas mixtures that did not contain a polymerizing quencher (as, for example, CO_2); on the other hand, chemical analysis of the deposits found on damaged wires has shown the presence, sometime as dominant species, of silicon and sulfur compounds that could not have been present in the gas mixture itself. While deposits of various kind are always reported to be present on anode wires in damaged chambers, many experimenters could not detect any layer on cathodes, thus voiding the explanation, given below, of the continuous current build up as being due to secondary-cathode field emission. It also appears that the process of polymer formation depends more on the presence in the gas of free radicals produced in the dissociation of molecules than on the presence of ions; the observation of an increased lifetime, when adding to the hydrocarbon mixture a vapour with low ionization potential, may not be explained then by a charge-transfer process.

In what follows I will recall the early observations of ageing and the phenomenological explanation that was given at the time.

2. DETERIORATION OF PROPORTIONAL AND GEIGER TUBES

A deterioration with time of single-wire proportional and Geiger tubes has been reported since the early works on the matter (see for example the sections devoted to this subject in the books of Korff and Kallmann [2] and Wilkinson [3]). The detected total charge at which ageing effects appear varies considerably with the application; in proportional counters used for X-ray detection a degradation in energy resolution appears rather soon, while in low-pressure Geiger counters, used only as digital devices, higher rates could be withstood. Since most of the early detectors were sealed, it was often difficult to distinguish ageing effects due to a change in the gas composition (following molecular dissociations in the avalanches) from those due to permanent coatings on electrodes. References [4] to [9] provide a representative selection of works on the subject.

Figure 1 (from Ref. [6]) shows the typical counting rate characteristics of a Geiger-Muller tube filled with pure methane at low pressure, after various exposure times; curve 4 was measured after 10^8 counts. Estimating the charge gain of the tube to be around 10^{10} (typical for a Geiger counter, and independent from the initial ionization), this gives a total charge flow corresponding to about 0.1 C.

The deterioration of a proportional counter, which appears as a gradual worsening of energy resolution under prolonged irradiation, is illustrated in Fig. 2 [8]. The counter was operated in argon + methane (90% + 10%) and exposed to an ^{55}Fe X-ray source collimated over about 1 cm of length of the wire. After about 10^8 counts (at a proportional gain of 5×10^4 , this corresponds to 10^{-4} C) a clear two-peak structure appears. The authors analysed by X-ray fluorescence the irradiated section of the wire, finding a strong carbon signal, thus confirming the presence of a polymer coating. Similar observations are reported in the quoted references, although the total flux at which deterioration appears varies considerably. It was also found that the use in Geiger counters of quenchers other than hydrocarbons, as for example alcohol, methylal, ethyl acetate, could increase their lifetime by one or two orders of magnitude. Because of their low vapour pressure and X-ray cross-section, of course, these gases were seldom used in proportional counters.

3. OBSERVATION OF THE AGEING PROCESS IN MWPCs

The general operating characteristics of a MWPC are well described by the singles counting rate as a function of voltage, for a fixed source of radiation. Compared to a measurement in coincidence, the singles rate provides information not only on the (relative) efficiency, but also on the background or source-induced noise. An example is shown in Fig. 3 [1]. The full lines provide the count rate recorded in a MWPC detecting a collimated ^{55}Fe X-ray source, as a function of voltage and for a fixed discrimination threshold, at several fluxes of radiation; the chamber used for the measurement had 2 mm anode-wire spacing, wire planes in both cathodes, and was operated with the 'magic' gas filling [argon (75%) + isobutane (24.5%) + freon (0.5%)] allowing very large and saturated gains to be obtained.

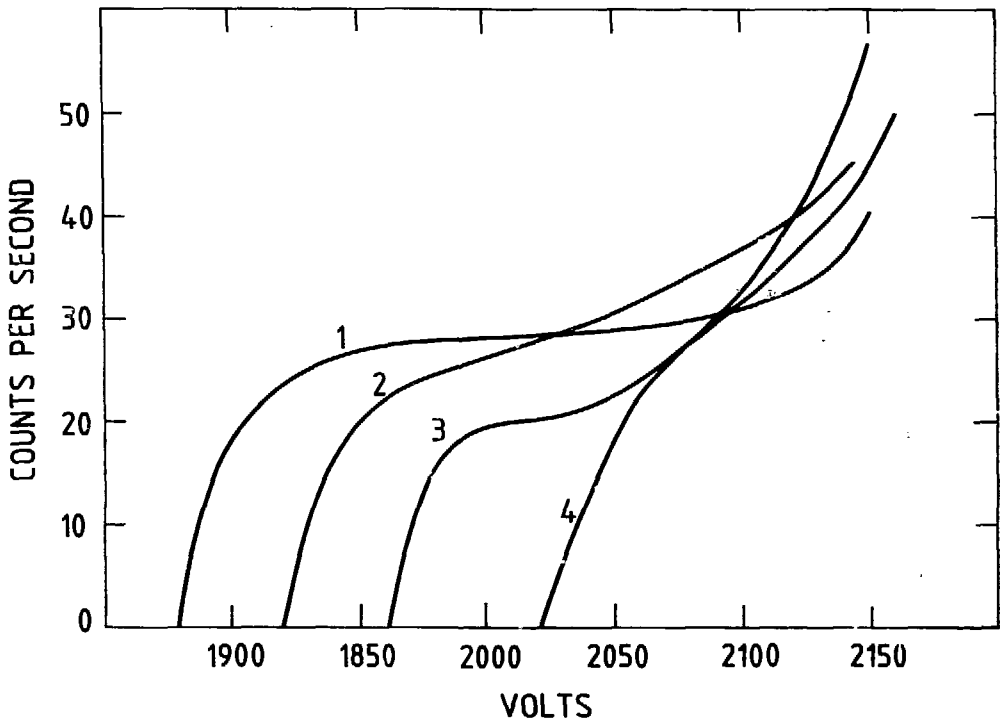


Fig. 1 Operating characteristics of a methane-filled Geiger-Muller tube of various ages. Curve 1 was measured after 10^7 counts, curve 4 after 10^8 counts [6].

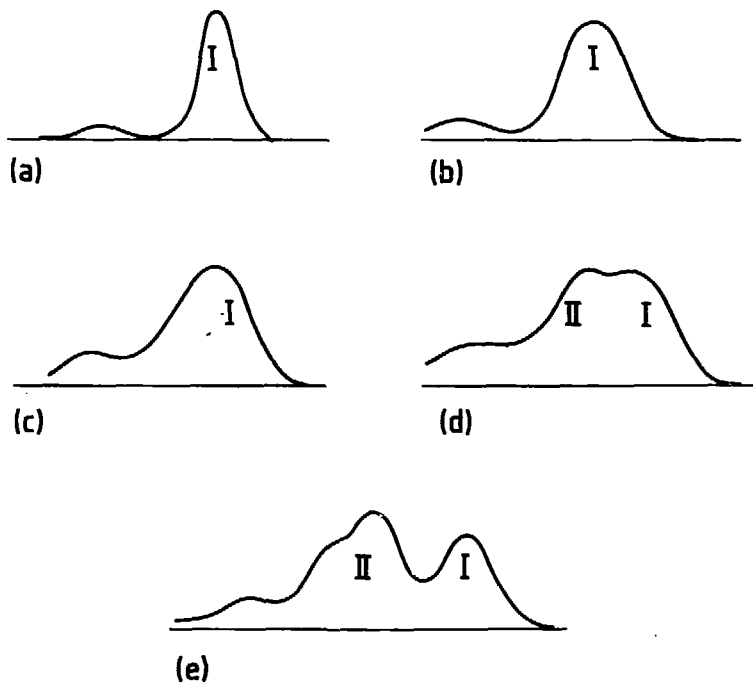


Fig. 2 Five successive pulse-height distributions as they develop during irradiation with a 5.9 keV X-ray source of a proportional counter filled with 10% methane in argon [8].

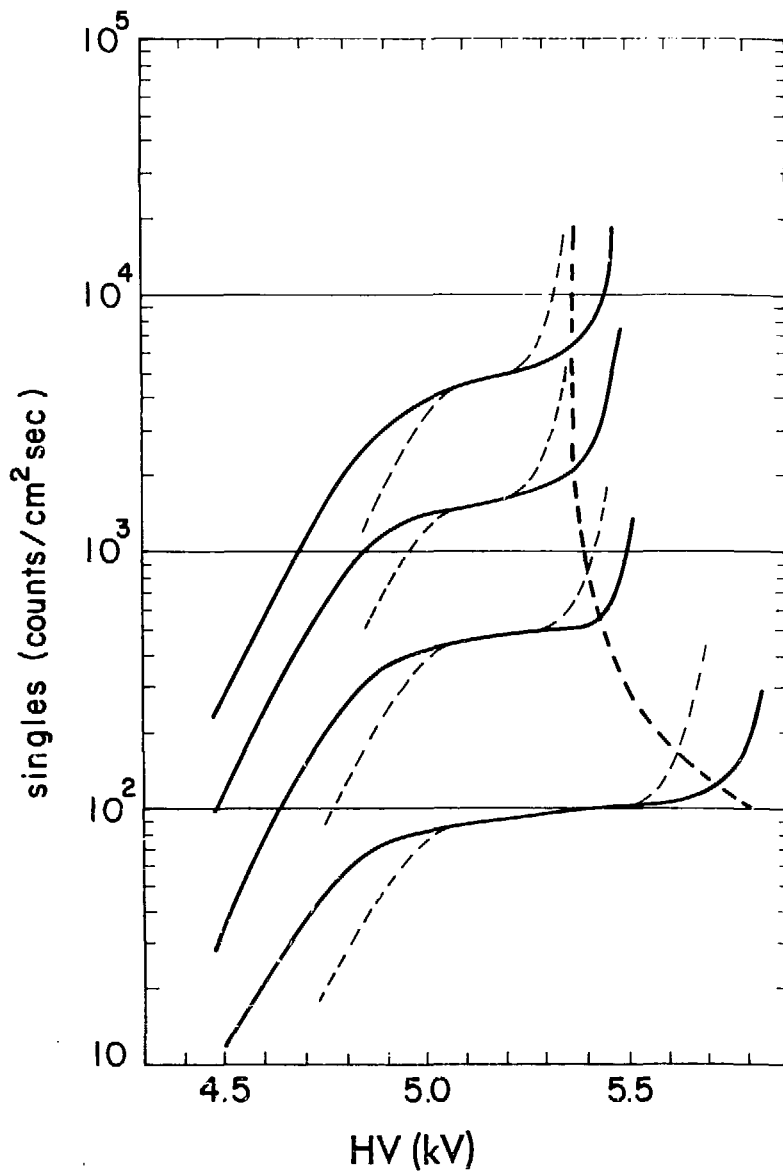


Fig. 3 Singles rate measured with 5.9 keV X-rays at various fluxes in a MWPC operated with magic gas. Full lines: early in the life of the chamber. Broken lines: after an irradiation corresponding to $10^{-4} \text{ C} \cdot \text{cm}^{-1}$ [1].

Note that all plateaux set in at roughly the same value of high voltage, independently of the source intensity; the point at which the noise increases abruptly is instead rate-dependent.

When the chamber is left operating for an extended period under irradiation, a considerable shift in the counting-rate characteristics is observed—see the broken lines in Fig. 3. This measurement was realized after a total exposure to 10^7 5.9 keV photons per square centimetre; since the chamber was operated at a gain delivering about 50 picocoulombs per pulse, the overall detected charge is therefore $5 \times 10^{-4} \text{ C} \cdot \text{cm}^{-2}$, or $10^{-4} \text{ C} \cdot \text{cm}^{-1}$ of anode wire^{*)}. Comparing the two sets of curves, one can see that, as a result of irradiation, there is a constant shift upwards of the efficiency plateau (showing a decrease of gain at a given voltage) and a rate-dependent shift of the breakdown knee towards lower voltages. The change is permanent, and the trend continues if the chamber is further irradiated. It is clear that, unless one measures pulse heights, the chamber can still be efficiently used for detection at low rates; at high fluxes, however, very quickly one will notice a loss of efficiency and a large increase in the noise rate.

It should be mentioned that the large steady current observed to settle in a damaged chamber often does not result in an increased noise rate. This suggests that the current results from a large number of small, single-electron avalanches, usually producing a signal well below the electronics discrimination threshold; they start being detected only at high rates when avalanches overlap in time.

The ageing process has been observed to occur in all gases using hydrocarbon quenchers (and, as a matter of fact, in other gases too, see later); the rate of damage appears, however, to be smaller for the lighter molecules ([10]–[16]). As an example, Fig. 4 [10] compares the single and noise rates measured in a standard MWPC operated in argon (60%) + ethane (40%) at various discrimination thresholds before and after a total detected charge of $1 \text{ C} \cdot \text{cm}^{-2}$ ($0.2 \text{ C} \cdot \text{cm}^{-1}$). Although some sign of deterioration appears, the chamber can still be considered operational after a rate three orders of magnitude larger than for the previously quoted measurement in magic gas. Similar ‘safe’ exposures have been reported in argon + methane (see, for example, the summary paper of J. Va’vra in these proceedings).

4. POLYMERIZATION PROCESSES AND SECONDARY EMISSION

Oily deposits of various kinds were found decades ago by visual inspection of the electrodes in radiation-damaged gaseous counters, and because of the common use of hydrocarbon quenchers in the gas mixture it was natural to think of polymer formation either directly in the avalanche process or mediated by the appearance of free radicals in the discharges. Abundant data exist on the dissociation and polymerization processes of hydrocarbons under discharge conditions or nuclear bombardment; Refs. [17] to [20] are a representative sample of works on the subject. I have reproduced in Fig. 5 [19] an example of what reveals the chemical analysis of a methane sample under bombardment from alpha particles (although similar processes are expected to occur under avalanche conditions, their relative importance may be entirely different). Methane dissociates into lighter molecules, some of the concentrations going through a maximum with time of exposure. The analysis only shows gaseous products, but large amounts of oily deposits are reported to be present on the walls of the cell. A detailed mass spectrographic analysis of dissociation and polymerization products in methane under glow discharge appears, for example, in Ref. [18]; these experimental conditions are maybe energetically closer to the normal operation of a counter at high gains. The author unambiguously identifies the solid products as being a polymer of composition $(\text{CH}_2)_n$; the other species appearing in the discharge are hydrogen, ethane, ethylene, and acetylene.

The various dissociation products can interact and modify the original populations; in the quoted work [18] the presence of hydrogen, for example, increased ethylene and acetylene production at the expense of ethane. This is shown in Fig. 6, where the concentration of various products is measured as a

*) Various notations have been introduced to describe the level of exposure of a MWPC to radiation, and are used throughout these proceedings: the integral counting rate per unit surface, and the total charge per unit surface or unit length of the wire. The last unit is perhaps the best for comparing different chamber geometries. Note, however, that there is evidence that ageing depends strongly on the gain of the detector.

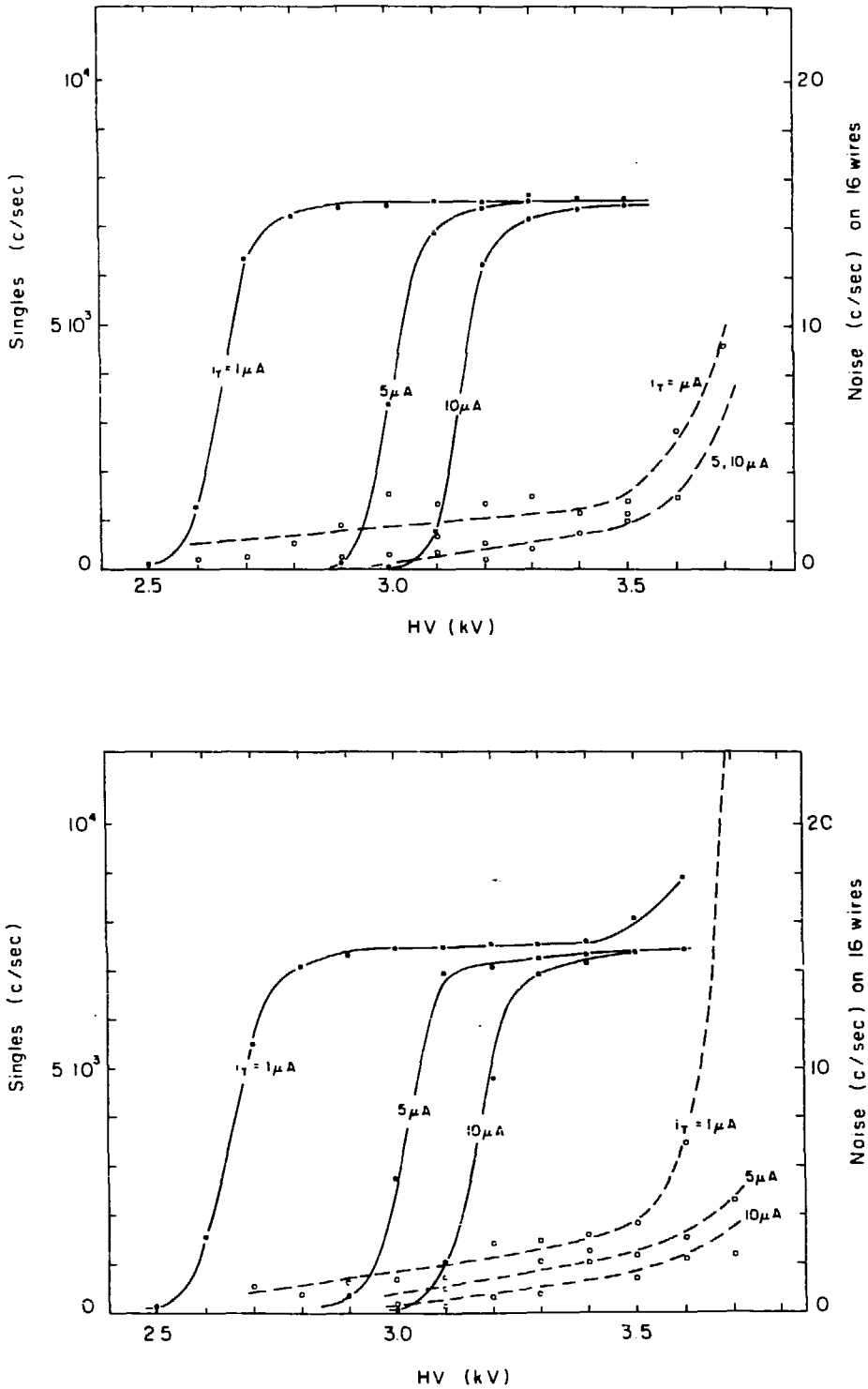


Fig. 4 Singles plateaux and noise rates measured in a MWPC operated in argon (60%) + ethane (40%) before (top) and after (bottom) an irradiation level corresponding to $0.2 \text{ C} \cdot \text{cm}^{-1}$ [10].

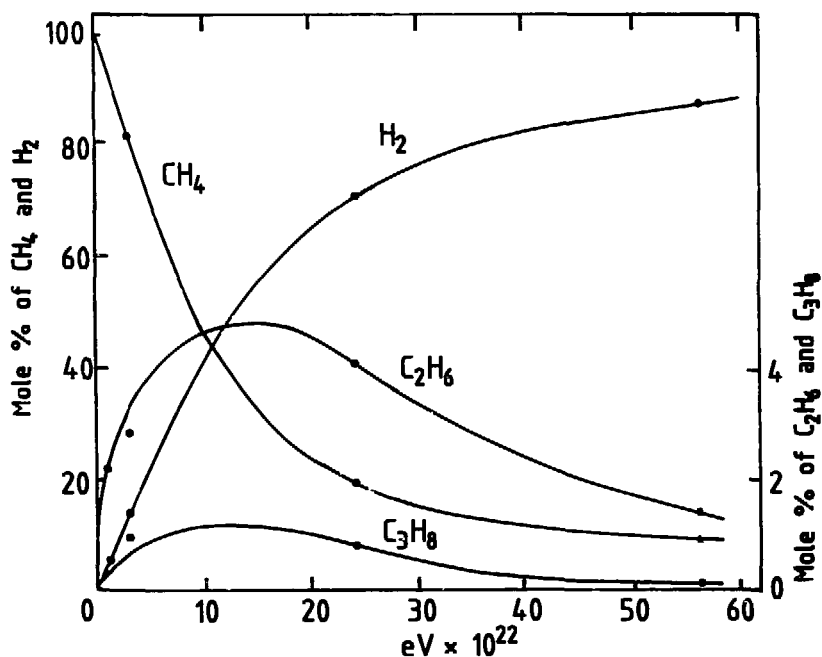


Fig. 5 Dissociation of methane under alpha-particle bombardment. The abscissa gives the integral energy dissipated in the gas cell by the ionizing radiation [19].

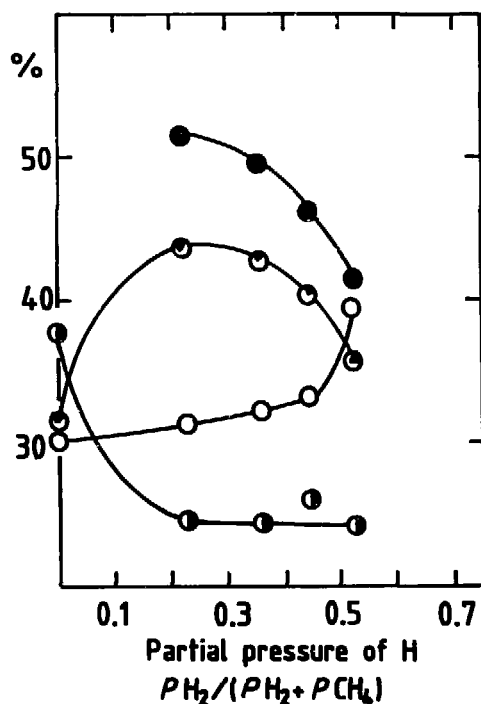


Fig. 6 Influence of hydrogen addition on the decomposition products of methane in a glow discharge. The points refer to polymers (filled circles), ethane (half-filled), ethylene (quarter-filled), and acetylene (empty circles) [18].

Figure 8. Early gastrula where the fracture has fallen to the outside of the archenteron. The animal pole is not visible. The blastocoel (BC), archenteron (A) and two groups of PM cells (PM) are designated. Confirmation of the fracture plane location and PM presence was made with the aid of the frozen dried image.

to be used with a noble gas. A reasonable attempt to preserve the operating characteristics of a well-quenched, hydrocarbon rich gas is to add to the mixture a non-polymerizing agent with the lowest ionization potential. Because of the charge-transfer mechanism, known to be very efficient from previous work, one expects that shortly after an avalanche has occurred only ions of the species with the lowest ionization potential would survive. Such is the case, as will be shown in what follows, and indeed the lifetimes of MWPCs filled with the above-mentioned additives have been extended by several orders of magnitude [1, 22] (see also the contribution by M. Atac to this workshop).

As can be seen in Fig. 7 [1], the singles counting rate plateaux are much better in a gas mixture such as the magic gas after addition of methylal (compare with Fig. 3 measured in the same conditions without the additive). The improvement may be due to the absence of polymerization processes from the very beginning of operation, or to the improved photon-quenching properties of the mixture that suppress more efficiently secondary cathode effects [22].

After long-term irradiation, a MWPC containing the non-polymerizing additives maintains its operational characteristics almost unchanged. Figure 8 shows efficiency, noise rate, and single counting rate measured in a MWPC (indeed the same used for the measurement of Fig. 3 where strong degradation was observed) before and after a total irradiation corresponding to 3.3×10^{10} minimum ionizing particles per square centimetre ($0.3 \text{ C} \cdot \text{cm}^{-1}$); the gas filling was argon + isobutane + freon as before with 4% of methylal added. About the same behaviour is observed adding isopropyl or ethyl alcohols. One should, however, bear in mind that the accidental absence of the additive (commonly used in the liquid phase within a gas bubbler), even for short times and moderate radiation fluxes, can result in irreversible damage to the chamber.

The efficiency of the charge-transfer mechanism can be verified by measuring the mobility of the positive ions in a mixture. A simple linear dependence exists of the inverse mobility of a given ion on the density of the gas mixture in which the ion is drifting under the effect of an electric field (Blanc's law); the slope of the correlation depends on the nature of the ion and on the component gases. The mobility of the dominant ionic species can be measured in a MWPC, looking at the length of the signal induced by ions in their trip from anode to cathode with a high-impedance charge amplifier. Alternatively, a special chamber having thin cathode wires can be built; the increase in drift velocity close to the wires produces a very clear signal at the arrival of the ions. An example is shown in Fig. 9, where experimental values of inverse mobility are plotted, in various gas mixtures as a function of their density [23]. Line F is a fit through the points measured in argon + isobutane mixtures; the relative isobutane concentration is indicated close to each point. It is reasonable to assume that one is measuring the motion of isobutane ions (although, of course, mass identification was not done). The points on line A correspond to measurements in argon + methylal mixtures, while lines B to E correspond to argon + isobutane + methylal mixtures; the relative percentage of methylal is indicated close to each point, and the percentage of isobutane increases from B to E. The interpretation of the data is again straightforward: in all mixtures containing methylal, one is measuring the drift of methylal ions, as far as the percentage of this vapour exceeds 2-3%; below that concentration, the measured mobilities tend to be those of isobutane. This sets a limit to the minimum amount of methylal that should be used for efficient charge transfer. Although similar measurements have not been done for other mixtures, it is reasonable to assume that the majority of ions in a mixture are always those having the lowest ionization potential, provided the concentration of the additive is above a few percent.

I should mention here that an alternative explanation for the observation is that ions with the lowest potential are preferentially and directly produced in the avalanches, at the expense of the other species.

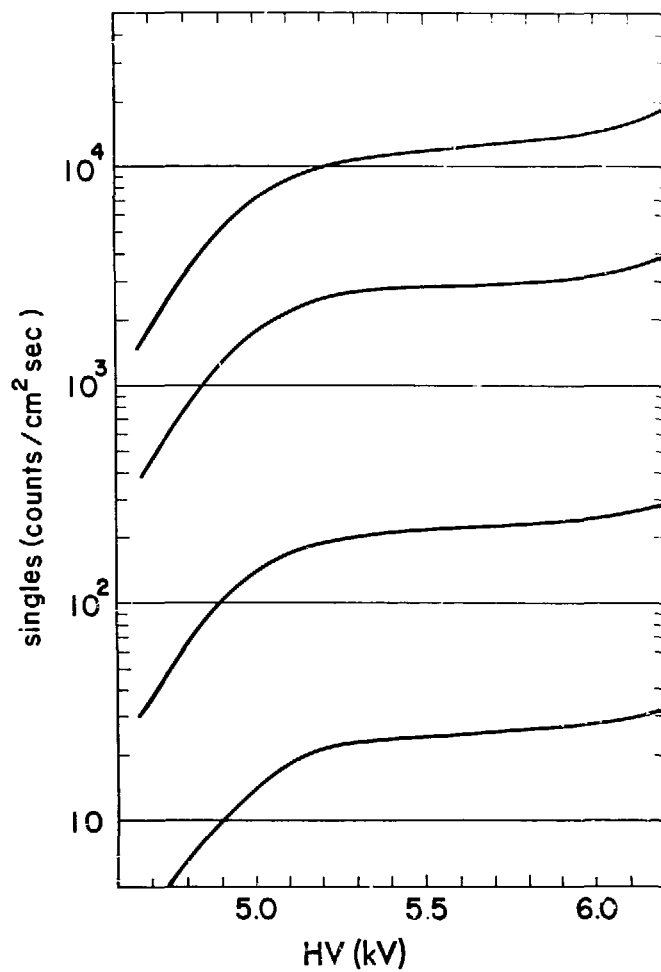


Fig. 7 Singles rate measured in a MWPC for ⁵⁵Fe X-rays at various source intensities; magic gas with the addition of 4% methylal [1].

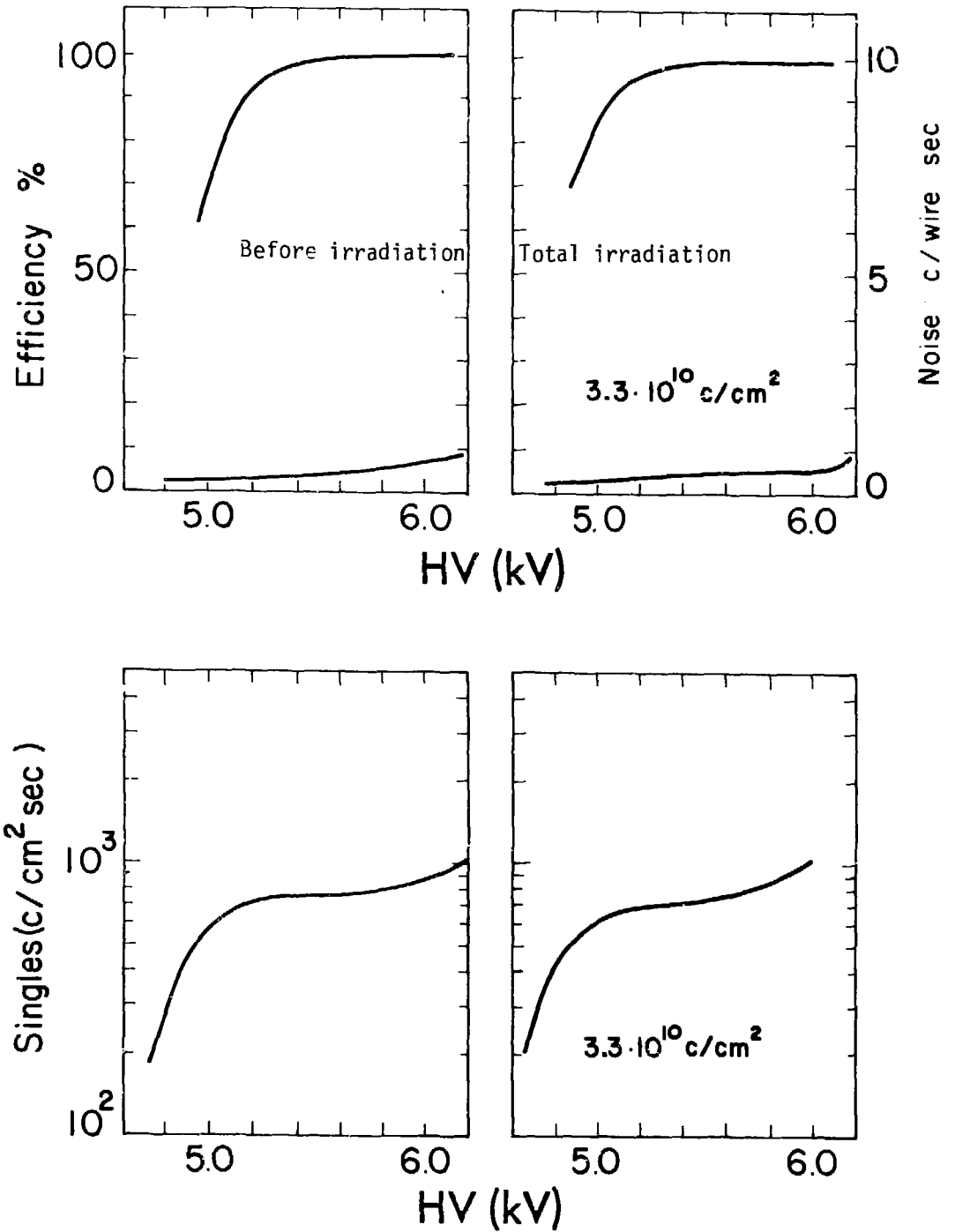


Fig. 8 Efficiency plateau for minimum ionizing particles, and noise and singles rates on 5.9 keV measured in a MWPC operated in magic gas with methylal, before (left) and after (right) prolonged exposure to radiation (3.3×10^{10} particles per square centimetre or $0.3 \text{ C} \cdot \text{cm}^{-1}$) [1].

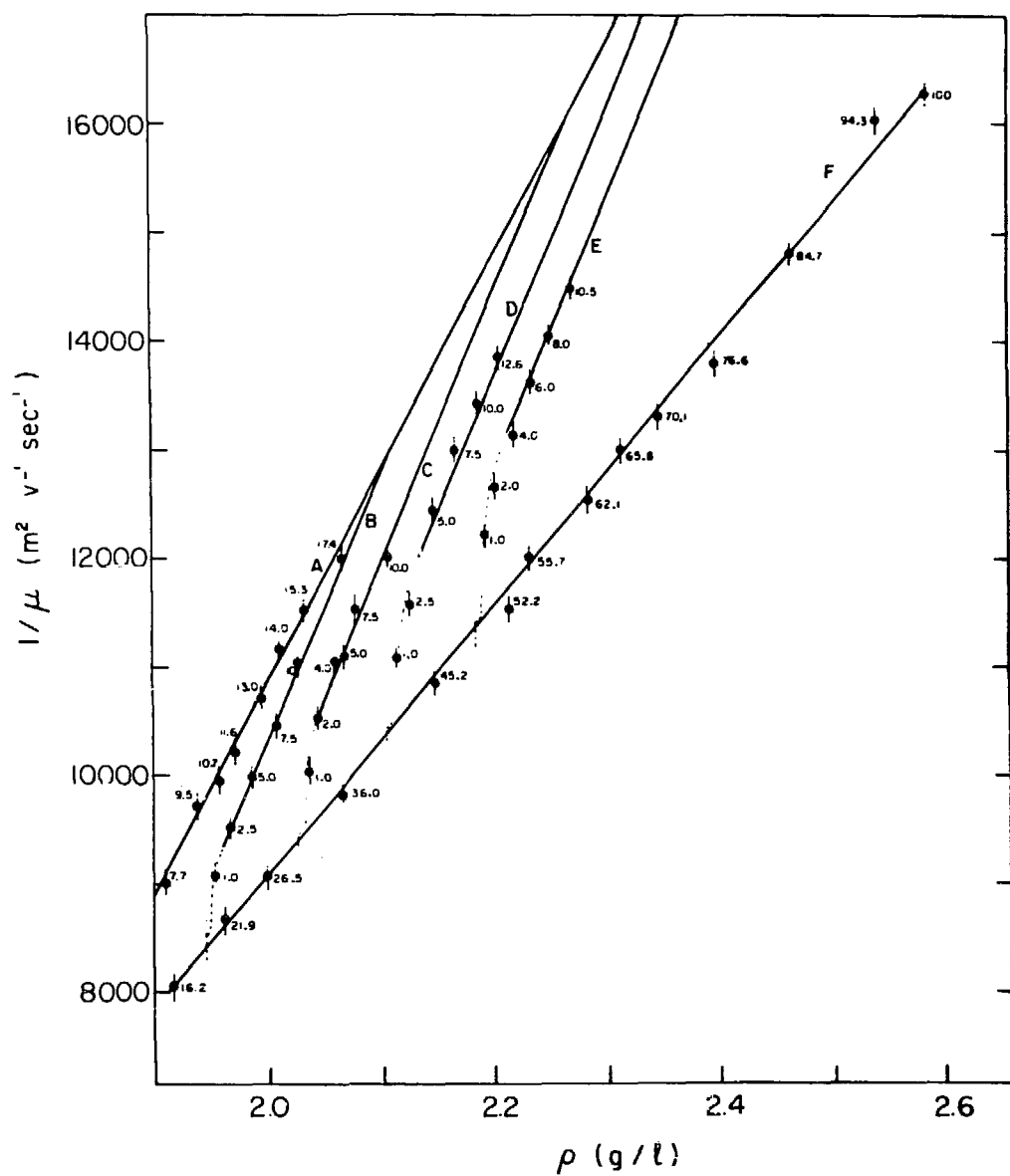


Fig. 9 Experimental values of the inverse mobility of ions as a function of density in various mixtures. A: argon + methylal; B to E: argon + isobutane + methylal; F: argon + isobutane [23].

REFERENCES

- [1] G. Charpak, H.G. Fisher, C.R. Gruhn, A. Minten, F. Sauli, G. Plch and G. Flugge, Nucl. Instrum. Methods **99**, 279 (1972).
- [2] S.A. Korff and H. Kallmann, Electron and nuclear counters (Van Nostrand, New York, 1946, 1955).
- [3] D.H. Wilkinson, Ionization chambers and counters (Cambridge Univ. Press, 1950).
- [4] W.D.B. Spatz, Phys. Rev. **64**, 236 (1943).
- [5] S.S. Friedland, Phys. Rev. **74**, 898 (1948).
- [6] E.C. Farmer and S.C. Brown, Phys. Rev. **74**, 902 (1948).
- [7] S.S. Friedland and H.S. Katzenstein, Rev. Sci. Instrum. **24**, 109 (1952).
- [8] A. den Boggende, A. Brinkman and W. de Graaff, J. Sci. Instrum. **2**, 701 (1969).
- [9] N. Spielberg and D. Tsarnas, Rev. Sci. Instrum. **46**, 1086 (1975).
- [10] D. Friedrich and F. Sauli, CERN, EP Int. Rep. 77-10 (1977).
- [11] H. Sipila and M.L. Jarvinen, Nucl. Instrum. Methods **217**, 282 (1983).
- [12] A.R. Faruqui, IEEE Trans. Nucl. Sci. NS-27, 644 (1980).
- [13] D.J. Grady and J.C. Robertson, Nucl. Instrum. Methods **179**, 317 (1981).
- [14] M. Turala and J.C. Vermeulen, Nucl. Instrum. Methods **205**, 141 (1983).
- [15] A. Smith and M.J.L. Turner, Nucl. Instrum. Methods **192**, 475 (1982).
- [16] J. Adam, C. Baird, D. Cockerill, P.K. Fransen, H.J. Hilke, H. Hofmann, T. Ludlam, E. Rosso, D. Soria and D. Vaughan, Nucl. Instrum. Methods **217**, 291 (1983).
- [17] E.G. Linder, Phys. Rev. **36**, 1375 (1930).
- [18] L.M. Yeddanapalli, J. Chem. Phys. **10**, 249 (1942).
- [19] R.E. Honig and W. Sheppard, J. Phys. Chem. **50**, 119 (1946).
- [20] C.E. Melton, J. Chem. Phys. **33**, 647 (1960).
- [21] L. Malter, Phys. Rev. **50**, 48 (1936).
- [22] M. Atac, IEEE Trans. Nucl. Sci. NS-31, 99 (1984).
- [23] G. Schultz, G. Charpak and F. Sauli, Rev. Phys. Appl. **12**, 67 (1977).

PLASMA CHEMISTRY IN WIRE COATING

DENNIS W. HESS, DEPARTMENT OF CHEMICAL ENGINEERING

UNIVERSITY OF CALIFORNIA, BERKELEY, CALIFORNIA 94720

ABSTRACT

Properties of rf glow discharges (plasmas) used for the deposition of polymer films from organic monomers are reviewed. The dynamic equilibrium between film deposition and film removal (ablation and/or etching) is also discussed. Changes in the plasma chemistry that result from additives or impurities in the hydrocarbon-based plasmas are described and related to the extent of polymerization. Relationships between discharge chemistry in these low pressure plasmas and the atmospheric pressure plasmas that might be used in wire chambers are presented. Possible approaches for further investigations of wire chamber deterioration due to polymer residue formation are suggested.

INTRODUCTION

A degradation in the operation of drift and proportional chambers using hydrocarbon gases or vapors has been observed by numerous investigators¹⁻³. The cause of such deterioration appears to be the formation of polymer or organic film materials on the anode and/or cathode wire. This phenomenon can be viewed within the framework of plasma or discharge chemistry that occurs between hydrocarbon fragments and between hydrocarbons and other reactive species (oxygen, hydrogen, halogens, etc.) in the gas atmosphere and on chamber or wire surfaces. This paper will discuss the chemistry involved in plasma-enhanced polymerization processes used to intentionally deposit polymer thin films^{4,5}. The effects of additives, impurities, and surfaces will be considered to indicate the qualitative changes in plasma chemistry that can result from such modifications. Likely relationships between the chemistry occurring in these low pressure plasmas and that taking place at higher (atmospheric) pressure will be briefly discussed. Finally, conclusions and recommendations for further investigation will be presented.

PLASMA POLYMERIZATION CHEMISTRY

The rf glow discharges (plasmas) used for plasma polymerization are partially ionized gases composed of ions, electrons, and a host of neutral species in both ground and in excited states. Typical conditions that exist in these glow discharges are indicated in Table I⁶. Because of the large difference in energy between electrons, which are highly mobile and can thus respond to the alternating electric field, and positive (or negative) ions, such discharges are termed nonequilibrium plasmas. The primary chemical species responsible for the formation of film materials (polymers) are the neutrals. This conclusion arises because of the high concentration of neutral species, not necessarily because they are more reactive than ions.

Due to the difference in mobility between ions and electrons, all surfaces in contact with the plasma assume a negative potential with respect to the plasma^{7,8}. As a result, positive ions are accelerated into surfaces, and typically attain energies before impact of a few eV up to nearly 1000 eV⁹. It

Table I. rf Glow Discharges Used for Plasma Polymerization

Frequency	= 50 ⁺ kHz-40MHz
Pressure	= 0.1-5 Torr
Electron and Positive Ion Density	= 10 ⁸ -10 ¹¹ cm ⁻³
Neutral Species Density	≅ 10 ¹⁵ cm ⁻³
Electron Energy	= 1-10 eV
Ion Energy	≅ 0.04 eV

Table II. Bond Dissociation and Ionization Energies¹²

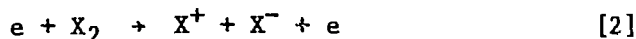
<u>Bond Dissociation Energy (eV)</u>		<u>Ionization Potential (eV)</u>	
N-N	9.8	N ₂	15.5
C-C	6.5	H ₂	15.6
CH ₃ O-H	4.3	CH ₄	14.5
		Ar	15.7
C-H	3.5	CH ₂ (OCH ₃)	9.7

should be noted that this process is distinctly different from the ones that occur in wire chambers. In the latter situation, negative electrons or ions (rather than positive ions) have high energy; these particles bombard the anode. Little (near thermal) energy is imparted to the cathode by bombarding positive ions. However, the phenomena that take place at the surface due to particle bombardment are similar in both types of discharges.

When a surface undergoing chemical reactions leading to film growth is bombarded by radiation, a number of processes, which depend upon radiation flux and energy, can occur^{10,11}. Momentum transfer to the surface from impinging particles can result in local heating and defect generation, thereby enhancing surface diffusion even at low (< 10 eV) particle energies. Physisorbed or chemisorbed species on surfaces can be desorbed by several eV particle bombardment. Particles with energy above a few eV can break surface chemical bonds and thus create adsorption or reaction sites that enhance film growth rates. When particle energies exceed ~ 30 eV, sputtering or ablation of surface material can take place. Finally, at energies above a few hundred eV, direct implantation of particles into the surface can occur.

In the gas phase, collisions of neutral molecules with high energy electrons and heavy particles (ions or neutrals) or photon absorption result in the generation of reactive chemical species. "Generic" reactions for these processes are indicated in Eqs. [1] + [6], where X_2 represents any molecular chemical species, and B represents an ion, molecule, or atom.

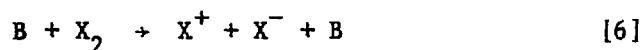
Electron impact collisions



Photon exposure



Heavy particle collisions



Of course, similar bond breaking and ionization processes can occur with molecules or atoms attached to the surface of a solid. Obviously, the chemistry occurring in plasmas is extremely complex, and thus virtually impossible to define completely.

Bond dissociation and ionization energies for bonds and molecules typically encountered in wire chambers are shown in Table II¹². Clearly, ionization potentials for molecules such as nitrogen (N_2), hydrogen (H_2), methane (CH_4), and argon (Ar) are significantly higher than most bond strengths. Furthermore, since average electron energies in glow discharges are less than 10 eV, the neutral species concentration is considerably higher

than the ion concentration. A notable exception to the high ionization potentials of many molecules is that of species such as methylal ($\text{CH}_2(\text{OCH}_3)_2$) or alcohols. Indeed, the ability of such molecules to ionize easily may inhibit chamber breakdown by charge exchange³. In addition, however, alcohols and ethers contain oxygen, which can reduce polymer formation in glow discharges (see following sections).

Polymerization processes can be divided into three basic types of reactions¹³. First, a reactive species (M^*) must be generated to initiate polymerization. If we call the initiator for such a process I, and recognize that in a discharge, the initiator could be a high energy electron, photon, etc., then we can express the bond breakage or ionization of a monomer (chemical species) as

Initiation



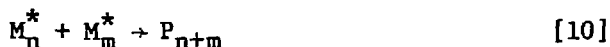
The chemical species M^* can react with other species to increase the molecular weight, and thus lower the volatility of the resulting product. This step (or steps) is termed propagation

Propagation



The reactive fragment(s) will continue to grow in size, ultimately forming a residue or polymer. If two reactive species come together, they can terminate the chain growth process, resulting in a higher molecular weight product or a polymer film if the mass is sufficiently high.

Termination



Of course, M^* can be a neutral (free radical) or ionic species. In glow discharges, M^* is usually a neutral fragment due to the relative concentrations involved.

A specific example of this reaction sequence is shown in Fig. 1 for a methane plasma. Only a few of the possible reactions are presented to illustrate the key considerations. Electron impact collisions create reactive free radicals (ions are also created, but I will not consider them in this discussion). Propagation reactions such as [12] and [13] then occur. It is important to recognize that species such as $\text{CH}_2\cdot$ and hence reactive fragments such as those indicated by reaction [13] are precursors to polymerization. Indeed, ethylene ($\text{CH}_2=\text{CH}_2$) is an easily polymerizable monomer. Thus, when highly reactive fragments such as methylene ($\text{CH}_2\cdot$) impinge on a surface, a polymer is easily formed (reaction [14]). However, termination reactions can occur ([15]-[17]), wherein stable volatile species are formed or reformed. These reactions minimize polymerization by reacting with and eliminating the most reactive polymerizable species ($\text{CH}_2\cdot$) in the discharge or on a surface.

Fig. 1. Example of Hydrocarbon Fragmentation and Reaction in a Methane Glow Discharge.

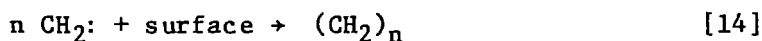
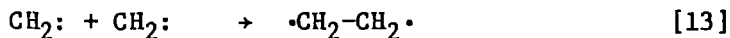
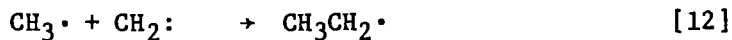
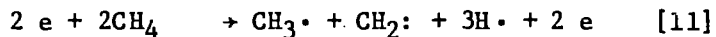
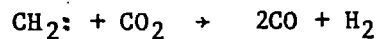
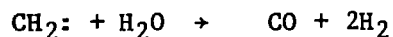
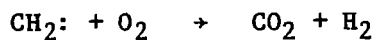
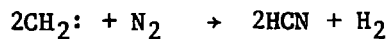
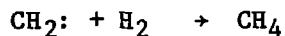


Figure 2. Effect of Additives or Impurities on Polymerization Precursors



Effect of Plasma Parameters and Gas Phase Composition on Polymerization

As mentioned previously, plasma chemistry is quite complex. In addition, surface reactions are equally complicated. Further, a synergism exists between gas phase and surface chemistry; polymerization and ablation or etching of surface films occur simultaneously¹⁴. The process that dominates the overall reaction scheme is determined by the gas phase chemical composition and the particle bombardment energy. The gas phase chemistry can also be altered by the addition of gases that react with polymer precursors to shift the equilibrium from film deposition or polymerization to etching or volatile product formation.

Unintentional contaminants as well as intentionally added vapors or gases can significantly modify the chemistry occurring in plasmas. For instance, residues from chamber cleaning, outgassing from elastomers or other plastics used in the construction of the chamber or in gas introduction lines can be incorporated into the gas phase, thereby affecting chemical reactions. These impurities are ultimately incorporated into the polymer residues. Similarly, chamber leaks or impurities in the gases and vapors used in wire chambers can introduce unwanted and/or unexpected contaminants that affect chamber operation through gas phase and surface chemistry.

Likely reaction "types" that result from the introduction of species such as hydrogen (H_2), nitrogen (N_2), oxygen (O_2), water vapor (H_2O), carbon dioxide (CO_2), and carbon tetrafluoride (CF_4) into a methane or other hydrocarbon plasma are shown in Fig. 2. In these examples, the most reactive fragment in a methane plasma is assumed to be methylene (CH_2). Naturally, any additive that generates oxygen, hydrogen, or halogen (F, Cl, Br) atoms or fragments can undergo analogous reactions. The important concept here is that polymerization can be reduced by addition of a chemical species that reacts with polymer precursors to form stable volatile products. Clearly, Fig. 2 only suggests certain reactions; the exact reactions are nearly impossible to predict. Every conceivable reaction probably occurs. Further, other hydrocarbons will result in somewhat different reactions, although the general concept is still valid.

RELATIONSHIP OF PLASMA CHEMISTRY IN rf GLOW DISCHARGES TO ATMOSPHERIC PRESSURE PLASMAS

Thus far, the plasma chemistry discussed has been characteristic of low pressure (< 5 Torr) rf discharges. It is important to consider the applicability of these concepts to discharges operating at lower frequency and considerably higher pressure (~ 1 atm). There is no reason to expect significant differences in the overall reaction schemes presented earlier, although the chemical kinetics and particle energies involved will surely change. Indeed, a recent study of nitrogen discharges at 60 Hz, 1 mA current, and atmospheric pressure confirm such conclusions¹⁵. In this study, 560 ppm of methane and varying amounts of oxygen were introduced into a nitrogen discharge, and the concentrations of primary product molecules were detected using mass spectrometry and gas chromatography. The results shown in Fig. 3 indicate that methane (CH_4) is only partly dissociated in the N_2 discharge, and the amount of dissociation is not significantly affected by oxygen addition. Further, when the oxygen concentration exceeds the methane concentration, the excess oxygen simply appears in the discharge effluent. With

Figure 3. Effect of Oxygen Additions on Effluent Yield
for AC Discharges in N_2/CH_4^{15}

Conditions: 60 Hz at 1 atm

$I \cong 1$ mA

Total flow rate = $350 \text{ cm}^3/\text{min}$.

$(CH_4)_{in} = 560 \text{ pm}$

Effluent Species	Input O_2 Concentration (ppm)		
	35	500	1100
O_2	25	75	800
CH_4	345	360	360
C_2H_6	0.7	< 0.2	< 0.2
H_2	370	110	90
HCN	100	10	7.3
NCCN	1.2	< 0.2	< 0.2
CH_3CN	0.6	< 0.4	< 0.4
CO	4.8	45	60
CO_2	4.0	135	125

little oxygen present, the ethane (C_2H_6) concentration is 0.7 ppm, but it falls below the detectability limit when more oxygen is added. Apparently, $CH_3\cdot$ radicals are oxidized to CO or CO_2 (and H_2O), thereby reducing C_2H_6 and increasing CO and CO_2 . The authors¹⁵ indicate that water vapor was also present in the effluent, but no quantitative data were presented. Similar effects occur with cyanide (CN) groups formed by the reaction of nitrogen atoms with carbon species. With small oxygen concentrations, cyanide compounds appear in the effluent, but oxygen reacts with these at higher concentrations to yield CO, CO_2 , and H_2O . Therefore, with added oxygen, the carbon-containing fragments in a N_2/CH_4 plasma are oxidized to stable, volatile products.

SUMMARY AND CONCLUSIONS

The chemistry that occurs in plasmas is extraordinarily complex. In general, gas phase impact collisions generate reactive chemical species while surface reactions result in film formation and in the synthesis of additional chemical species that are desorbed into the gas phase.

In discharge atmospheres containing carbonaceous species, ablation, etching, and polymerization occur simultaneously. Polymerization can be reduced by addition of gases or vapors that react with polymerization precursors to form volatile, stable compounds. For instance, O_2 , H_2 , and F_2 can result in the formation of CO_2 , CH_4 , and CF_4 . Unfortunately, highly electronegative vapors can have deleterious effects on wire chamber operation.

The general types of chemical reactions that occur between hydrocarbon fragments and hydrogen, nitrogen, oxygen or halogens is qualitatively understood. However, the specific reactions taking place in different reactors under different conditions, and the particular impurities present in each are ill-understood and ill-defined. Therefore, further improvements in the control of processes occurring in wire chambers, and in the development of vapors suitable for such applications demand careful experimental studies. In particular, systematic investigations of polymerization and chamber deterioration as function of impurities (H_2O , N_2 , O_2 , etc.), additives (CO_2 , alcohols, freons, etc.), and plasma conditions (power, pressure, etc.) are sorely needed. Also, polymer composition analysis can provide useful information and insight.

If the removal of polymer residues can "regenerate" chamber wires, the use of oxygen containing discharges (e.g., H_2O , O_2 , etc.) when the chamber is not in use might accomplish this task. Care should be exercised, however, if oxidation of materials in the chamber (including the wire) is detrimental. Finally, if the residues to be removed contain species that do not form volatile products with oxygen (e.g., silicon), such a "regenerative" procedure will not be successful.

REFERENCES

1. G. Charpak, H. G. Fisher, C. R. Gruhn, A. Minten, F. Sauli, G. Plch, and G. Flugge, Nuc. Instr. and Meth. 99, 279 (1972).
2. M. Turala and J. C. Vermeulen, Nuc. Instr. and Meth. 205, 141 (1983).
3. K. Kwong, J. C. Layter, C. S. Lindsey, S. O. Melnikoff, B. C. Shen, G. J. Vandalen, and M. C. Williams, Nuc. Instr. and Meth. Phys. Res., A238, 265 (1985).
4. Plasma Polymerization, ed. by M. Shen and A. T. Bell, ACS Symp. Series, No. 108, Amer. Chem. Soc., Washington, D.C., 1979.
5. H. Yasuda, Plasma Polymerization, Academic Press Inc., New York, 1985.
6. J. A. Mucha and D. W. Hess, in Introduction to Microlithography, ed. by L. F. Thompson, C. G. Willson, and M. J. Bowden, ACS Symp. Series, No. 219, Amer. Chem. Soc., Washington, D.C. 1983, p. 215.
7. H. S. Butler and G. S. Kino, Phys. Fluids, 6, 1346 (1963).
8. J. L. Vossen, J. Electrochem Soc., 126, 319 (1979).
9. R. H. Bruce, J. Appl. Phys., 52, 7064 (1981).
10. T. Takagi, J. Vac. Sci. Technol. A2, 382 (1984).
11. D. W. Hess, in Ann. Rev. Mat. Sci., Vol. 16, to be published, 1986.
12. CRC Handbook of Chemistry and Physics, 44th Edition, 1963.
13. Ref. 5, p. 50.
14. Ref. 5, p. 180
15. M. E. Fraser, D. A. Fee, and R. S. Sheinson, Plasma Chem. Plasma Proc., 5, 163 (1985).

ANALYSIS OF TPC INNER DRIFT CHAMBER WIRE COATINGS

MICHAEL C. WILLIAMS, DEPARTMENT OF CHEMICAL ENGINEERING

UNIVERSITY OF CALIFORNIA, BERKELEY, CALIFORNIA 94720

ABSTRACT

In the context of analyzing the chemical composition of deposits on wires in a drift chamber at SLAC that failed with an argon/methane gas, the techniques of mass spectroscopy (MS) and Auger electron spectroscopy (AES) are demonstrated. Chemical mechanisms are proposed for conversion of methane gas to polyethylene-like insulating coatings on the wires. Discussion of mass spectra for model compounds is turned toward evaluation of spectra from both field wires and sense wires. Contamination from phthalate plasticizers is found on both sets of wires, while silicone polymer is detected only on sense wires. AES data on field wires show mostly (90%+) carbon; profiles of carbon/gold/copper implicate nonuniformities in the gold coating and/or the underlying copper-beryllium alloy. Successful chamber operation was subsequently achieved by reducing the wire potentials, though polymeric deposition continued at a slower rate.

INTRODUCTION

The impetus for the chemical analysis to be discussed here was the failure of the inner drift chamber (IDC) used as a trigger element to initiate readout of events in the time projection chamber (TPC) detector at the PEP electron-positron storage ring at SLAC. Details of the IDC construction, operation, and evaluation are given elsewhere¹, along with results of the wire coating investigation. To summarize: the IDC operated in a mixture of 80% argon and 20% methane at 8.5 atm; sense wires were gold-plated tungsten of 25 μm diameter; field wires were gold-plated beryllium/copper of 100 μm diameter; and the potentials were approximately +4400 V and -1600 V on the sense and field wires, respectively. Failure was characterized by dark currents in the IDC exceeding 1 μA and recurring discharges. Subsequent visual examination of the chamber revealed the presence of long black filaments ("whiskers") normal to the surfaces of both types of wires in certain regions of the chamber and -- as found subsequently -- the deposition of polymeric coatings on both types of wires. Scanning electron microscopy (SEM) showed¹ that all wire surfaces were coated, not just the whisker regions or other areas of discoloration.

Chemical characterization of these wire deposits will be discussed here in a general fashion, in connection with the use of mass spectroscopy (MS) and Auger electron spectroscopy (AES). These two techniques provide, respectively, information on molecular structure and atomic composition, a highly useful combination. While details of the IDC/TPC operation at SLAC are not germane to our treatment, it is true that use of the simplest possible organic gas (methane, CH_4) facilitates the discussion and also builds a bridge to MS technology.

CHEMICAL MODEL

The creation of chemically active molecular species in gas plasmas is well known^{2,3}, with most of the previous work focused on hydrocarbon gases. These active species -- free radicals and ions -- participate in reactions involving also neutral and non-radical species, producing chain-like molecular assemblies of the original (and modified) species. Such reactions begin in the gas phase but continue in the viscous liquid phase which appears on solid surfaces, as is inevitable when the growing gaseous chains become long enough for condensation to occur. Liquid- and solid-phase reactions are accelerated and made more variegated by the high density of active species in these condensed phases, so that complex structures are possible and heavy deposits with considerable mechanical strength can form.

Starting from CH_4 as a monomer, however, one should expect the deposits to be intrinsically like polyethylene: $\text{H}(\text{CH}_2)_n\text{H}$ where n is large (with $n=1$ giving methane again). A schematic representation of this polymer is given in Fig. 1. Variations in the fundamentally linear alkane (H-saturated) structure will occur frequently, however. Nonlinear topology is seen in the form of branching, wherein a chain C is bonded to three other C's and (rarely) to four others; this is illustrated at three places in Fig. 1. Sometimes ring molecules can also be formed, as will be discussed further below.

Deviations from alkane nature also appear when carbon-carbon single covalent (sigma) bonds are replaced by double (pi) bonds, to appear as $-\text{HC}=\text{CH}-$ units in the middle of the chain. These unsaturated bonds can be triggered by free radicals to open up and react, thus causing branching and further polymerization to occur. A special case of branching is crosslinking, wherein the branches interconnect the linear chains to the extent that a huge (macroscopic) network is formed. Crosslinked deposits will adhere to a wire tenaciously, not being soluble at all, and can only be removed by chemical attack⁴ or mechanical means.

Figure 1 (bottom) also shows that the crosslinked network does not prevent uncrosslinked species from retaining their identity and mobility. These are essentially liquids (oils and greases), even when rather high molecular weights prevail, since crystallization is suppressed due to heterogeneity of the molecular structure. [This explains why the wire deposits are often invisible to the eye; the liquid film and the (amorphous) crosslinked film are clear and transparent under most circumstances.] Solid-like character occurs when the amorphous film crosslinking becomes very dense, thus forming a glass, or when some crystallinity occurs. Linear polyethylene forms crystals more easily, and to a greater extent, than any other polymer. However, such crystals consist of "folded chains" packed in parallel arrays (e.g., a straight 30-nm-length of the molecule is followed by a 180° bend; the chain then returns parallel to itself, then bends back, etc.), and the extensive branching of chains in the wire deposits reduces the long-range regularity needed to form such crystals⁵. For example, highly branched commercial polyethylene may be only 40% crystalline (with $T_m \approx 105^\circ\text{C}$), while linear polyethylene can be over 70% crystalline (with $T_m \approx 138^\circ\text{C}$).

However, as long as the molecules on the wire are not crosslinked, they can be vaporized at some elevated temperature. These are the species analyzed

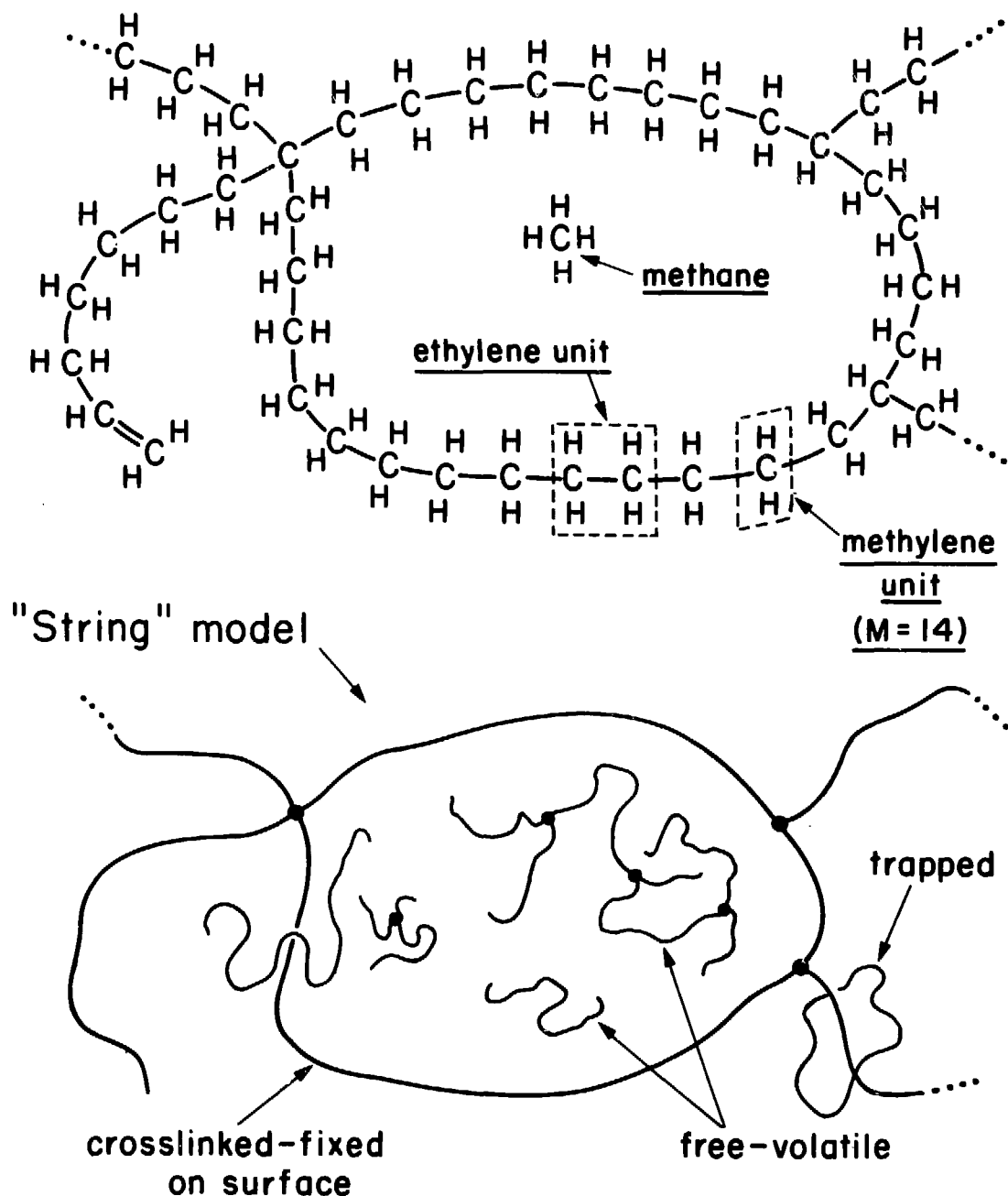
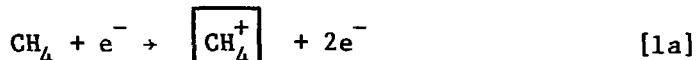


FIG. 1: Mixture of polyethylene-like species deposited on a solid surface. The crosslinked (solid) phase and the unlinked species both show branching at random locations. Above: Hydrocarbon nature and bonding of the crosslinked phase is detailed; note the chain unit of $-\text{CH}_2-$ corresponding to $M = 14$. Below: Topological representation of various types of polymer molecules in the mixture.

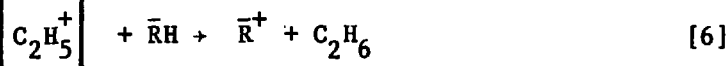
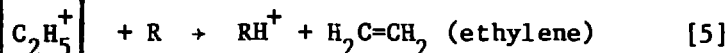
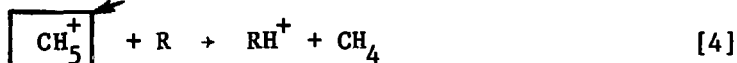
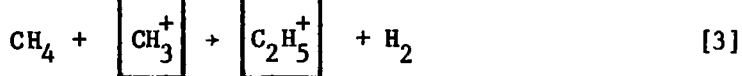
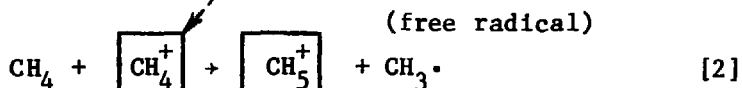
in gas phase by MS, and they are representative of everything deposited on the wire.

It remains to suggest a plausible chemical mechanism for forming polyethylene from methane. This actually proves to be quite well known, since the key initial reactions were studied extensively by MS researchers⁶ who used methane deliberately to implant its hydrogen atoms in other species to assist discrimination and identification of the latter. Thus, at relatively low energies (70 eV) and low pressure (1 torr), the following sequence occurs:

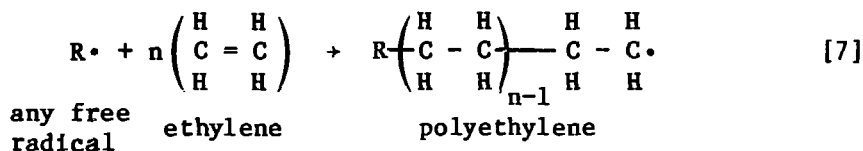
Electron impact



Chemical ionization



Polymerization



The symbol R represents any neutral and non-radical component, either shown explicitly as a product in Eqs. 4-6 (CH_4 , C_2H_4 , C_2H_6) or occurring further along in similar sequences. Note that $\text{R}\cdot$ in Eq. 7 could be $\text{CH}_3\cdot$ from Eq. 2, but need not be. Also, $\bar{\text{R}}$ in Eq. 6 is simply a molecular fragment, such that the whole molecule is R ($= \bar{\text{R}}\text{H}$). In high-pressure high-energy systems such as those of concern here, the sequence in Eqs. 1-7 would be just one of many sequences leading to polymer formation; a variety of polymer structures would also be expected.

MASS SPECTROMETRY

Operation

While the MS is an analytical device, it is of special interest here because its gas-phase reactions mimic and thus demonstrate the reactions occurring in the IDC and other chambers where plasma chemistry occurs. In typical operation⁶, the unknown compound is heated continuously at near-vacuum (10^{-6} torr) conditions to produce a vapor mixture whose composition changes with time because the temperature (T) is steadily increasing. Thus, as T(t) increases, the vapor changes from a low-M high-volatility mixture to higher-M mixtures (i.e., the oils and greases will then have sufficient vapor pressure to be analyzed in the gas phase). This evolution was stopped, in the present case, at about 180°C to avoid thermal degradation of the samples.

Vapors are passed through an electron beam at about 70 eV, which leads to molecular excitation and loss of an electron, creating a molecular ("parent") ion -- e.g., for methane, CH_4^+ . The parent ion, however, is rarely stable. Usually it fragments into a variety of smaller species -- positive ions and neutral species, some of which could be free radicals as well. Application of an electromagnetic field then causes discrimination and identification of the ionic species, as they are accelerated and displayed in proportion to their e/m ratio. Interpretation of the abundance spectrum is simplified by the preponderance of singly-ionized species, so $m/e = M$. The pattern of fragment abundance vs. M is essentially a fingerprint for identifying the parent molecule.

Alkane (Mini-Polyethylene) Patterns

Since alkanes are of major interest here, it is appropriate to begin a discussion of MS pattern recognition with a low-M representative which is liquid at room temperature: hexane, C_6H_{14} . Figure 2 shows the MS line spectrum for hexane; note that the parent ion $\text{C}_6\text{H}_{14}^+$ is significant but far less prominent than other species, and this is generally true for linear hydrocarbons. One notable feature of the spectrum is its periodicity; the clusters of species occur at intervals of $\Delta M = 14$, representing chains with differing numbers of CH_2 groups. To assist the eye, lines are drawn in Fig. 2 to connect peaks representing the two major types of ions: the alkane ions, $\text{C}_n\text{H}_{2n+2}^+$ with $M = 14n+2$, and the alkene ions (one double bond), $\text{C}_n\text{H}_{2n}^+$ with $M = 14n$. Such lines assist one in recognizing the hexane fingerprint. It is clear that the alkane ions are in greater abundance than the alkenes throughout the spectrum. Subsequently, such patterns will be used in analyzing the vapors evolved from the IDC wire coatings.

The parent chain length has some effect on the MS, which shows systematic changes as hexane grows toward polyethylene. An intermediate case is dodecane, $\text{C}_{12}\text{H}_{26}$, shown in Fig. 3. The same periodicity, with $\Delta M = 14$, prevails here, and again the alkane ion abundance exceeds that of the alkenes at every carbon number. Now, however, the parent ion can barely be detected, and the alkane distribution peaks at C_3 rather than at C_4 as with hexane. A broader distribution is evident for both alkanes and alkenes, though the abundance of species with C_7 and higher is notably small.

M = 86
Hexane
 C_6H_{14}

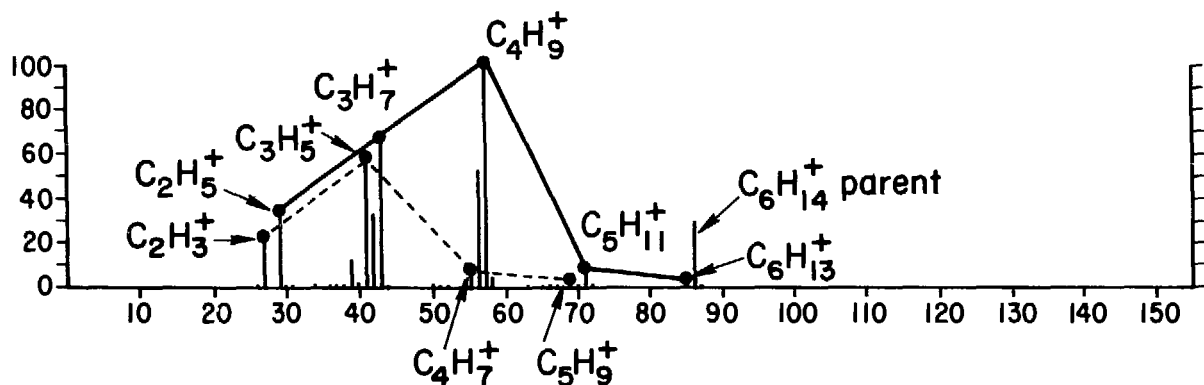
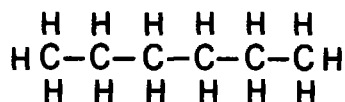


FIG. 2: Mass spectrum⁷ for hexane. Chemical structure at upper right. Solid line (—) connects peaks for ion species without double bonds, $C_nH_{2n+1}^+$ (alkane ions), and dashed line (---) connects peaks for species with one double bond, $C_nH_{2n-1}^+$ (alkenes).

M = 170
Dodecane
 $C_{12}H_{26}$

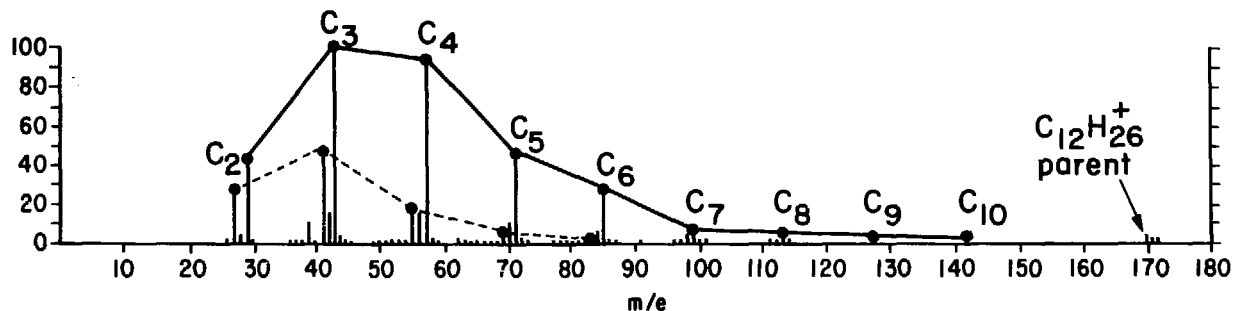
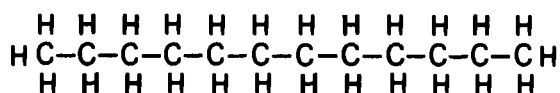


FIG. 3: Mass spectrum⁷ for dodecane. Treatment same as in Fig. 2.

A less cluttered view of the alkane MS patterns is given in Fig. 4, for parent molecules C_6 , C_7 , C_8 , C_{12} . Periodicity is clearly identical in all, though abundance patterns for the ion fragments show characteristic differences. Parent ions (P) become less prominent as their M grow, while C_3 and sometimes also C_4 species are generally the most abundant.

Other Hydrocarbon Patterns

An important question is whether the patterns in Figs. 2-4 are unique to linear alkanes. The answer is yes, with the degree of uniqueness illustrated by a comparison with the class of unsaturated ring compounds (aromatics) in Fig. 5. The comparison between the C_6 alkane and aromatic (hexane vs. benzene) shows that the aromatic MS produces a vastly stronger P line and no periodicity in fragment pattern. A comparison of the C_7 compounds yields similar results, except for the abundant fragment at $M-1 = 91$ caused by stripping a single hydrogen atom from the methyl group on the ring. Clearly the aromatic ring is far more stable than the linear chains, and aromatic patterns are easily distinguishable from alkane patterns.

One might anticipate that linear chains of moderately differing character would not be so easily distinguished. However, Fig. 6 displays the MS spectra from three C_7 compounds to demonstrate that even minor differences in linear species can produce recognizable pattern variations. The alkane (heptane) and alkene (heptene) patterns both show $\Delta M = 14$ periodicity and an abundance peak at C_3 ; however, the connecting lines show clearly that the relative abundances of alkane and alkene ion fragments are opposite in the two cases, a unique distinction. Then, for the branched compound, a totally dissimilar pattern appears. Species that might be clustered at C_2 and C_5 , so prominent for heptane and heptene, are virtually absent; a major peak at C_6 ($M = 83$) has no analogue in the other two compounds (the branching serves to stabilize it). The peak at $M = 55$ arises from an alkene fragment at C_4 , but it is a different one than arises with 3-heptene and its abundance is much greater. Overall, the visual impression created by the spectrum of the branched C_7 compound differs greatly from those of the two linear C_7 compounds.

Field Wire Results

Field wires placed in the MS produced spectra that changed with time, as first the low-M components of the deposit were volatilized at lower temperature and then higher-M components were vaporized as $T(t)$ increased. Results presented here correspond to about 130°C .

Figure 7a shows the results to $M = 500$, with a 20-fold magnification of scale above $M = 170$ for clarity. While the pattern is more complex than for the single molecules shown in Figs. 2-6, the major and rather dramatic impression is the $\Delta M = 14$ periodicity of the peak clusters. Clearly, linear hydrocarbons must dominate this mixture, validating the qualitative picture of Fig. 1. While the crosslinked part of the pseudo-polyethylene network on the wires cannot evaporate to register in this test, some rather high-M unlinked molecules of the same chain character are present; for example, the component at $M = 449$ corresponds to an alkane ion chain at C_{32} .

Of course, the chains represented in Fig. 7a are not all alkanes. Many are unsaturated, with one or more double bonds. The relative abundance of

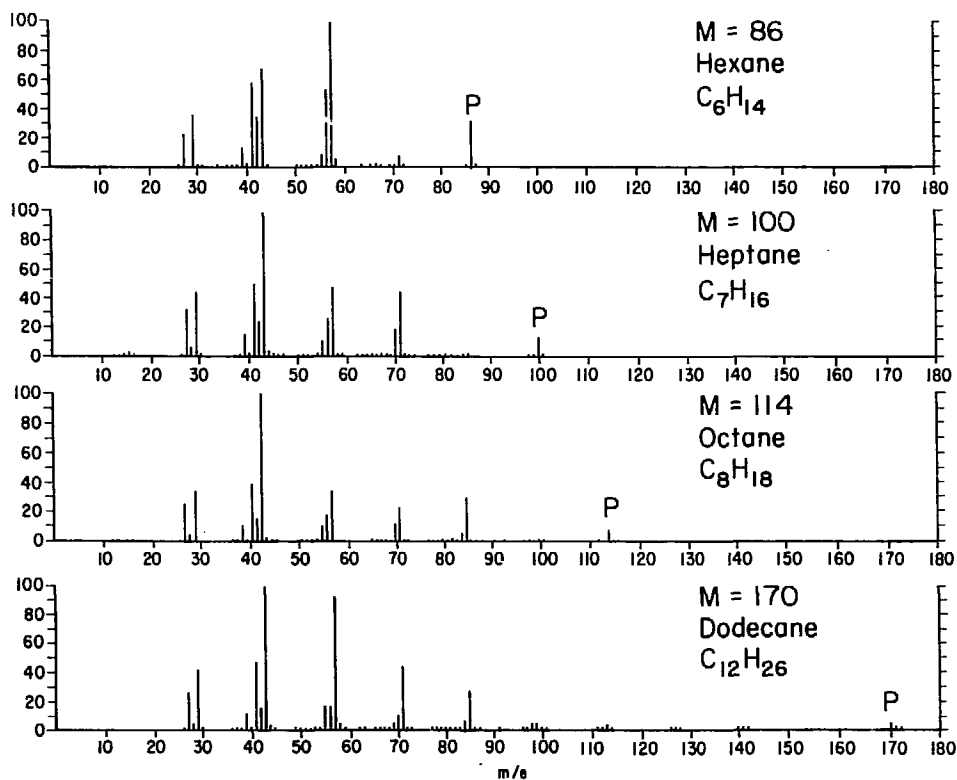


FIG. 4: Mass spectra⁷ for four alkanes. Parent ions designated by P.

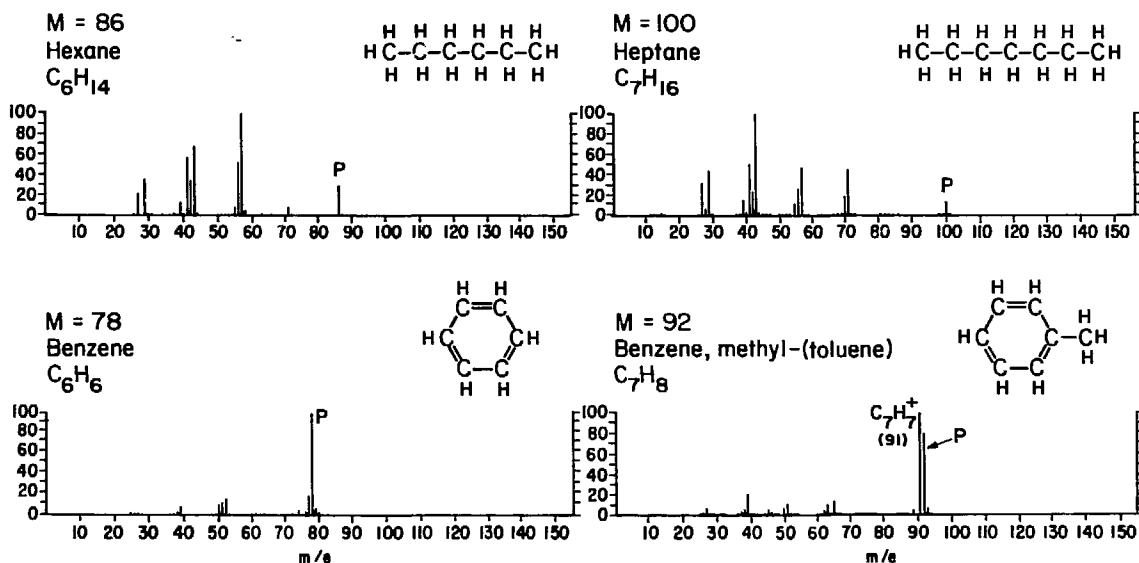


FIG. 5: Mass spectra⁷ for two C_6 compounds (left) and two C_7 compounds (right). The top two are linear alkanes, the bottom two aromatics.

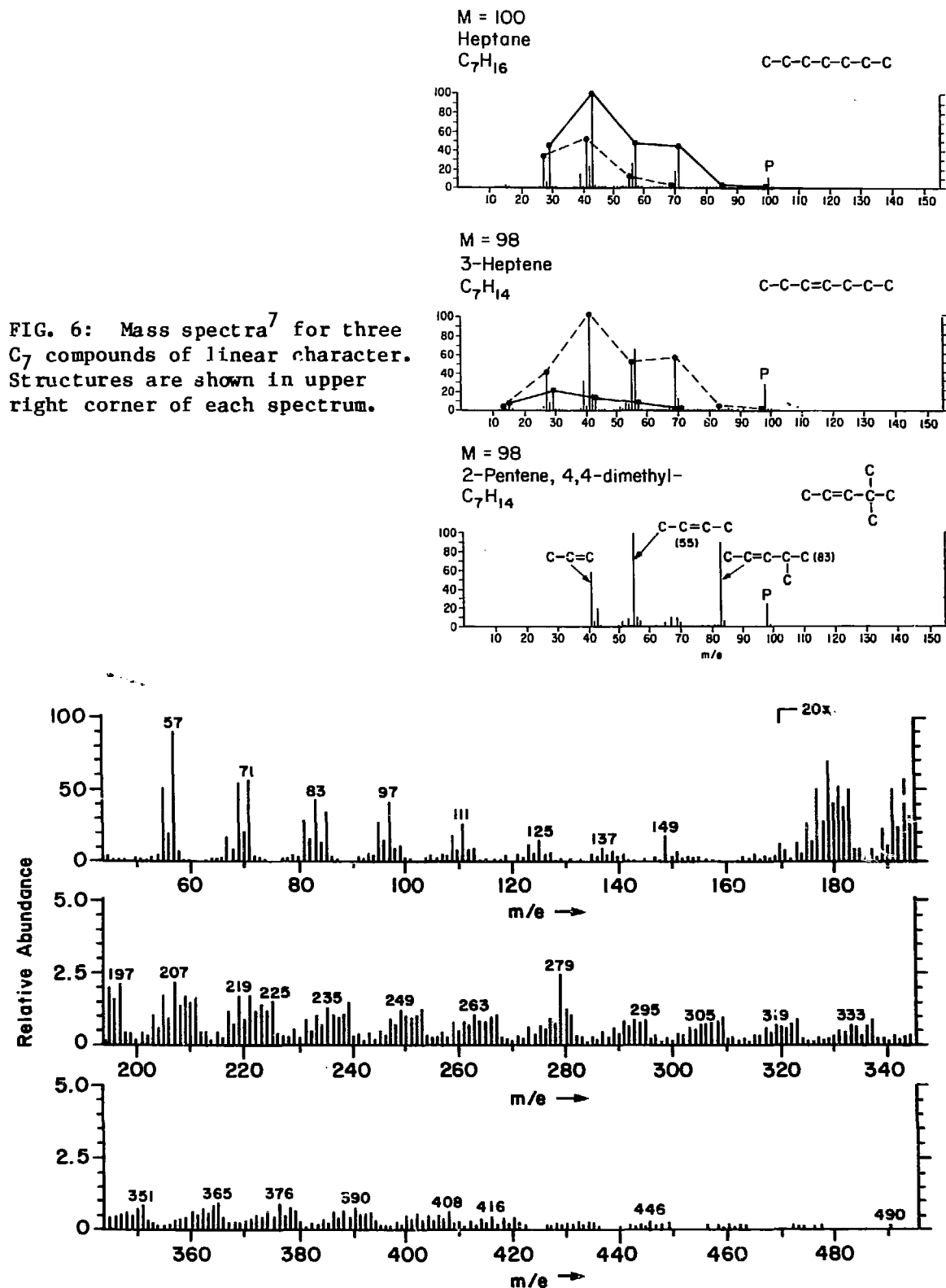


FIG. 7a: Mass spectrum of field wires at about 130°C. Note vertical scale magnification just before M = 170.

Gaussian.

In general a static isolated deuteron produces a powder pattern with singularities appearing at²³ $\nu_1 = \nu_0 \pm (3e^2qQ/8h)(1-\eta)$ and steps or edges appearing at $\nu_3 = \nu_0 \pm (3e^2qQ/4h)$ where ν_0 is the resonance frequency of the deuteron in the absence of the quadrupolar interaction. Shoulders can appear at $\nu_2 = \nu_0 \pm (3e^2qQ/h)(1+\eta)$. In most of the situations we shall encounter below $\eta \leq 0.05$ and the features at ν_1 and ν_2 are unresolved. In the case of larger η the ν_2 shoulders are often broadened out by the dipolar interaction.²⁴

Figure 5.1 shows the well known spectrum predicted for the case of $\eta=0$. The splitting between the "horns" is given by $\Delta\nu_1 = 3e^2qQ/4h$ and the edges of the powder pattern are separated by $\Delta\nu_3 = 3e^2qQ/2h$, thus for a theoretical powder pattern $\Delta\nu_2 = 2\Delta\nu_1$. Symmetric lineshapes similar to that of Figure 5.1 are expected for the majority of "static" sites since they will usually have $\eta \leq 0.05$.¹ Very often, as e^2qQ/h increases, the signal-to-noise will be such, however, that only the horns of a given site will be visible. Rotating methyl groups (for which e^2qQ/h are typically $\sim 40\text{kHz}$) will be a notable exception.

C). Experimental Details.

The quadrupolar echo spectra were obtained using the quadrupolar echo sequence with τ typically equal to $20 \mu\text{sec}$. The quadrupolar echo spectra were obtained with ninety times of $3.0 \mu\text{sec}$ obtained using a Drake L7 tuned amplifier driven by an ENI 5100L ($\sim 1 \text{ kW}$ final output). Spectra utilizing the composite sequence, given in equation (1) below, were obtained with ninety times of $6.4 \mu\text{sec}$ using the ENI alone. Pulse shapes and pulse droop encountered with the L7 produced poor

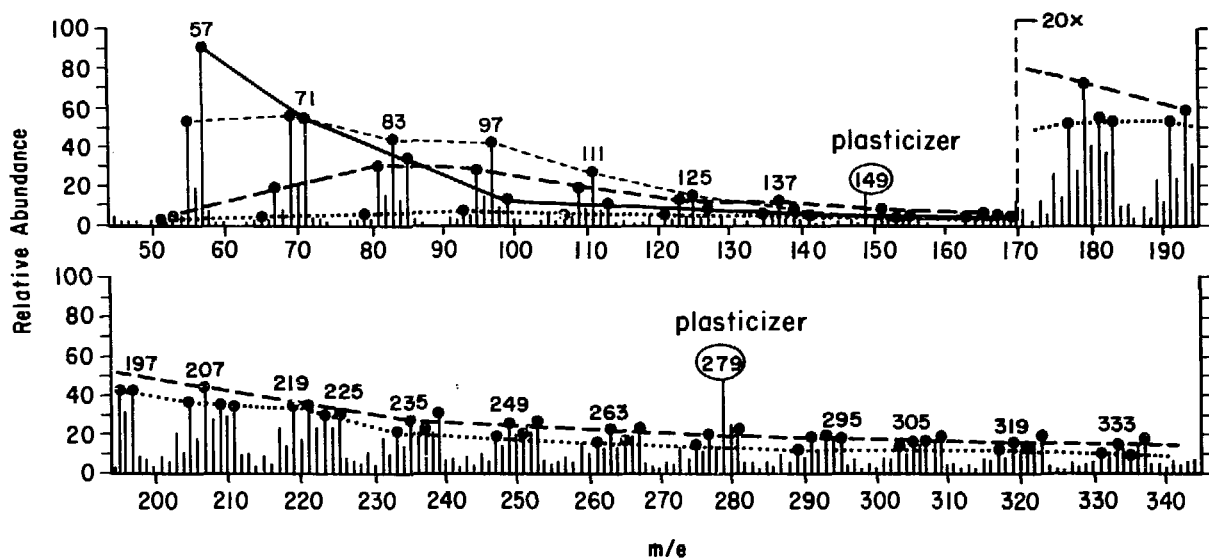
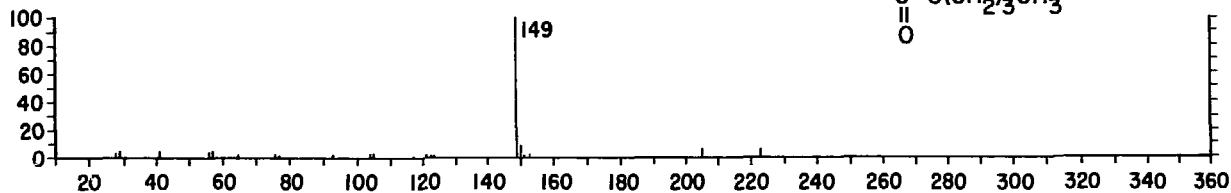
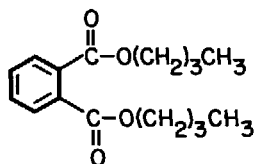


FIG. 7b: Mass spectrum of field wires. Lines connecting peaks for four linear chemical series are: ————— no double bonds; - - - - one double bond; — · — · — two double bonds; ····· three double bonds.

M = 278
Dibutyl phthalate
 $C_{16}H_{22}O_4$



M = 390
Diethyl phthalate
 $C_{24}H_{38}O_4$

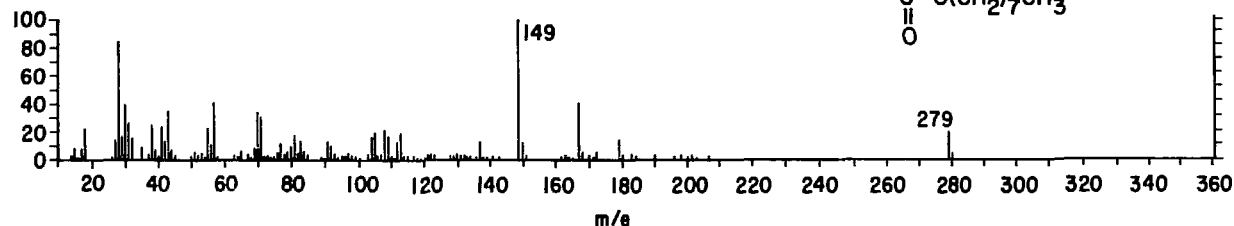
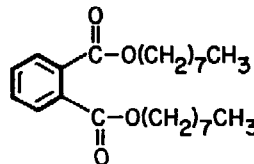


FIG. 8: Mass spectra⁹ for two common phthalate plasticizers. Structures appear in upper right of each spectrum.

Speculation that the phthalate contamination originated from the plastic insulation on cables in the IDC/TPC -- perhaps by normal outgassing and perhaps by reaction with the plasma -- led to MS testing of that insulation. Extremely strong peaks at 149 and 279 were registered.

It should be noted that the phthalates on the field wires were not destroyed by the intensity of chemical reactions in the IDC plasma, nor by any chemistry on the wire surfaces. Since the phthalates contain aromatic rings, a stripping of the chain appendages would have led to spectra similar to those shown for the aromatics in Fig. 5. No such evidence appears in Fig. 7. There is also no evidence of silicone polymers in Fig. 7, as will be discussed below in connection with sense wires.

Sense Wire Results

The MS spectrum for the sense wires, at about 130°C is given in Fig. 9. The untouched pattern in Fig. 9a is immediately seen to be considerably more cluttered than the corresponding field wire pattern (Fig. 7a). While there is still periodicity in this, at roughly $\Delta M = 14$ intervals, it is clear that a great variety of chemical species must be present.

Figure 9b provides the connecting lines for the nominal ion species having 0, 1, 2, 3 double bonds in linear chains. The pattern is quite different than for the field wire in Fig. 7b. There is also more extensive evidence of contamination. In addition to the same phthalate peaks ($M = 149, 279$) seen with the field wires, there are new peaks at $M = 207$ and 281 that are always found when polydimethylsiloxane (the most common silicone polymer, $-\text{Si}(\text{CH}_3)_2-\text{O}-$)_n is present. Note that the spacing of these two peaks, $\Delta M = 74$, corresponds to the mass of one repeat unit of this polymer chain. A GC/MS analysis also confirmed that silicone species were present. This is consistent with several reports¹⁰ that the element silicon was found on sense wires but not on field wires.

The origin of silicone polymer in wire chambers could be one or more of several sources: RTV ("room temperature vulcanizate") adhesive, silicone grease on stopcocks and other fittings, silicone oils whose vapors can reach the chamber through some channel, silicone rubber in O-rings and other seals, etc. However, this is not the only possible source of the element Si. Ordinary glass could be attacked in some plasmas, and silica (SiO_2) is used as a filler to strengthen weak polymers -- most notably silicone. Glass fibers are also present in many structural composites, such as G10 (fiberglass in epoxy matrix) which is sometimes used in chamber construction.

It is worth noting that MS devices themselves produce a background signal for the same reasons as these wire chambers. Silicone and phthalate species were found to be present in the background of the device used in the present study. However, the background has automatically been subtracted from the MS spectra for samples being analyzed, so this could not be the origin of the net signals shown here for silicone, phthalates, and other species. Indeed, the success of this procedure is demonstrated by the absence of silicone signals (peaks at $M = 207$ and 281 inconsistent with linear hydrocarbon spectra) in the field wire analysis, Fig. 7.

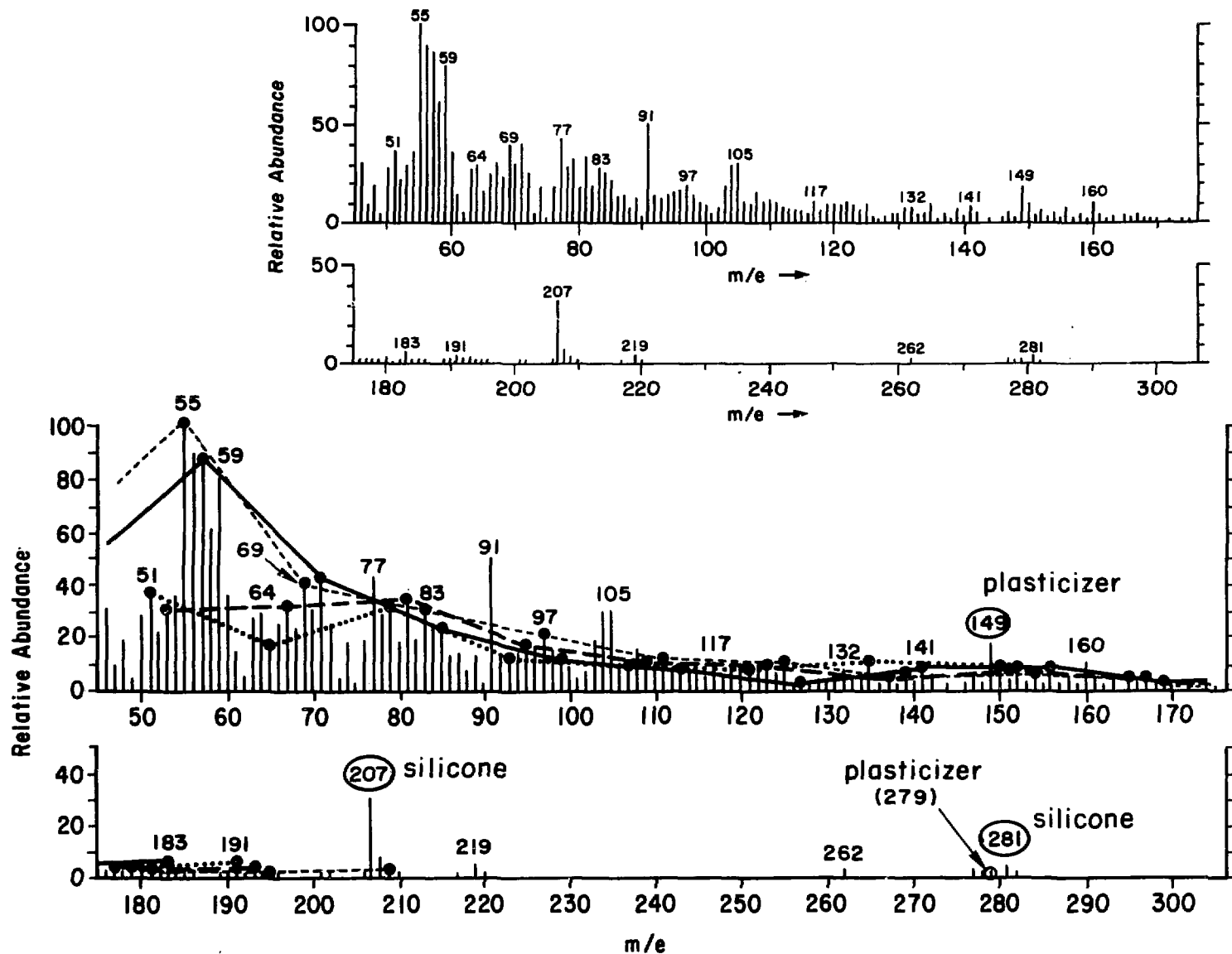


FIG. 9: Mass spectrum of sense wires. (a) Above, as produced. (b) Below, with lines connecting peaks for four linear chemical series — see caption of Fig. 7b for identification.

There are still other peaks in Fig. 9 that need to be explained. In particular, the peaks at $M = 77$, 91 , and 105 (with $\Delta M = 14$) have no counterparts in Fig. 7. Identifying them is easier than explaining their presence. Collectively, they represent aromatic ion species — e.g., note $M = 91$ in the toluene fragment of Fig. 5: $\phi\text{-CH}_2^+$. For $M = 105$ the side chain is simply one methylene unit larger, $\phi\text{-CH}_2\text{CH}_2^+$, while for $M = 77$ one expects ϕ^+ .

However, the presence of these aromatic ions does not uniquely reveal their origin. The simplest explanation would be to point to the phthalates, which contain the aromatic ring. Figure 8 shows that dioctyl phthalate in the MS produces fragments at $M = 77$, 91 , and 105 in significant amount, but still vastly less than the $M = 149$ fragment (which does not agree with the relative abundances seen in Fig. 9, even assuming plausible superposition of these peaks on those of linear species at the same M).

An alternative explanation, also involving the phthalates, would suggest complex gas-phase chemistry in the original plasma which entirely stripped all chains from the aromatic ring and then built new molecules by adding hydrocarbon chains to it. While this might seem to be rather severe, it is indeed believed to be the origin of the fragment ions in the MS at those M for dioctyl phthalate (Fig. 8). But if this had occurred in the original plasma, these species ($M = 77$, 91 , 105) would ultimately have been drawn to the cathode and would have appeared in the field wire MS — but they do not appear in Fig. 7, despite the clear evidence of phthalate itself there.

A third explanation involving plasma chemistry (but not phthalates) would argue that aromatic species can be formed from linear species at sufficiently high energies. For example, in gas-phase reactions at high temperature one can expect such chemistry ("dehydrocyclization"), and the high energies in wire chambers might be sufficient to accomplish this even at moderate temperatures. However, this explanation is also inconsistent with the absence of aromatics on the field wire.

Presumably the answer lies with the sense wire itself, where condensed-phase chemistry is occurring in the presence of extremely strong electric fields. It may involve the phthalates, but this seems doubtful in view of the fact that quite a bit of the regular phthalates remain intact (e.g., the $M = 149$ ion detected by MS) under such conditions. Perhaps attention should be drawn to the metal itself. If the tungsten was exposed because of a porous or otherwise imperfect gold coating (see comments about gold coatings, below), certain catalytic reactions might occur. In petroleum refining, the "reforming" process converts linear hydrocarbons to aromatics by means of a solid metal catalyst (in that case, usually platinum). It may be possible for tungsten to exert a similar effect under these unusual conditions, especially if the high local fields cause field ionization at the surface.

AUGER ELECTRON SPECTROMETRY

Operation

The AES technique provides information about surface composition (sensitive to a depth of about 2–3 nm) at the elemental level, and thus is not useful in general for identification of molecular species. However, knowledge of the atomic composition of materials is useful for other purposes,

and sometimes it can also serve as the discriminator between several chemical species that seem equally plausible [e.g., the MS method might attribute a strong peak at $M = 91$ to either the toluene ion or a silicone fragment such as $\text{HO-Si}(\text{CH}_3)_2\text{O-}$].

Both qualitative and quantitative analyses are possible. AES spectra, covering an energy range roughly 0-2500 eV for all elements of interest, are readily available¹¹; their major peaks can be used to identify the elements in a mixture. (While hydrogen cannot be registered by AES, this is not a major drawback in the present application.) Quantitative results are obtained by assessing the peak-to-peak height of one or more key peaks for each element in a mixture, and comparing this with the standard spectra peak heights at the same energy.

The AES device employed in this study had a beam size too large (about 50 μm) to be used with the sense wires. Therefore, results can be presented only for the field wires. However, another feature of the device was very helpful: argon ion beam sputter-etching, by which the surface material is removed slowly and the usual AES analysis performed continuously. In this fashion, information on elemental composition is obtained at all depths of the film being studied. The only complication is that the specific depth being examined at a given instant is not known precisely, as the etch rate varies with film composition. Results are generally presented as composition vs. time of etching; considerably more work would be needed to convert such data to a true depth profile. Base pressures (inside the device) were in the range $0.5\text{--}1 \times 10^{-9}$ torr, an indication of excellent cleanliness.

Field Wire Results

Because AES is so sensitive, any contamination from handling procedures will produce signals from the surface that are spurious. For this reason, the etching technique is recommended for getting reliable results. The present study encountered this problem after transmitting field wires in test tubes that subsequently were discovered to be designed for biological samples. Such test tubes are coated with a thin film of silicone (very soft) for purposes of biocompatibility, which led to the field wires giving a positive AES test for Si at the outer surface -- which has apparently never been reported for field wires. Compositions of 1-22% Si were registered for various wires. However, ion etching showed that the Si was present only in the outer 30-50 nm of the film. Changing to bare glass test tubes eliminated this Si contamination in later work.

One of the major results was that all regions of the wires were coated with carbon, even those regions that were not darkened or bearing other visible deposits. The atomic abundance of film carbon was 90-98% (H-free basis) throughout the film thickness, at all linear positions along the wire, and in the darkened areas as well as the clear areas. Darkening was probably a consequence of polymer decomposition ("charring"), which would evolve hydrogen, but since H could not be detected by AES there was no way to confirm this possible difference between dark and clear regions.

A representative AES spectrum of a field wire is given in Fig. 10. This wire had both darkened and clear regions on it, and Fig. 10 analyzes the outer surface of a clear region. Film composition, from peak heights, is

approximately 0.5% Cl, 1-2% N, 2-3% O, 2-3% Cu, and 92-95% C. The carbon is expected to be dominant in a hydrocarbon polymer film (100% for pure hydrocarbon, on an H-free basis), but the other elements require alternative explanations.

Oxygen should appear because the phthalates contain it, and this signal persisted throughout the film thickness. Nitrogen could be present in other contaminants (not identified by MS, but not uncommon in commercial plastics -- e.g., N is part of the amide bond in all nylons, and certain amines are used as plastics additives). However, it also seems possible that some of the N and O found in AES spectra came from air, since samples were exposed to air continuously for weeks before tests were made. The Cl in Fig. 10 is a somewhat tentative identification, but could arise from plasma reaction with PVC cable insulation in the IDC/TPC.

The Cu signal is the most surprising aspect of Fig. 10. It was seen at film exteriors only on clear regions of the wire where polymer coatings were thin; thicker coatings (e.g., black spots) produced no Cu signal at the surface. This may indicate that the apparent presence of Cu in Fig. 10 is an artifact, manifesting the relatively long mean free path of Auger electrons from Cu (originating in the Cu/Be wire) which might reach the surface of very thin films. Perhaps significantly, no gold is registered in Fig. 10, and it is known that Auger electrons from Au have a short mean free path.

However, it is surprising that Cu signals should not be screened by the Au coating, suggesting that the Au did not indeed cover the Cu/Be wire completely. The absence of a Be signal (at $E = 104$ eV) from Fig. 10 does not eliminate this possibility, as Be electrons would not penetrate the polymer film. What is really needed for interpretation here is information about the surface texture/coating of the wire as it was installed in the IDC. Unfortunately, the original wire batch was not available for testing by SEM or chemical methods, both of which should be performed in future work.

If the gold was porous or broken in places -- thus revealing the underlying Cu/Be alloy -- or if the copper diffused far out into the gold -- then the wire surface exposed to the plasma would have some Cu content. Either of these two phenomena could explain the Cu signal in Fig. 10. If the former prevailed, then some regions would have Cu "spots" where electrical conduction would be higher and thus favored over Au-coated locations. A consequence of this would be preferential channeling of current through these spots, more chemical reaction, and possibly thicker deposits nearby. Certainly such localization of current would create excess heating, perhaps the cause of darkening or charring of the polymer film. Eventually the degradation of the film would proceed far enough to convert the insulating hydrocarbon deposit to conductive carbon, causing abrupt current avalanche at that point and a possible origin of whisker growth.

The argon ion beam etch was used to track compositions through the polymer film and beyond, into the wire. Film thickness was scaled by near-disappearance of C from the signal. In this way, it was determined (see further discussion below) that the clear films were relatively thin -- in the range 0.1-1 μm -- and the dark films thicker, with the blackest spots over 10 μm thick. These thicknesses were consistent with those scaled roughly from SEM micrographs¹.

FIG. 10: Auger spectrum of field wire, exterior surface. Spot is focused on a clear region of the wire. Ordinate is dN/dE , where $N(E)$ is the number of electrons of energy E (abscissa).

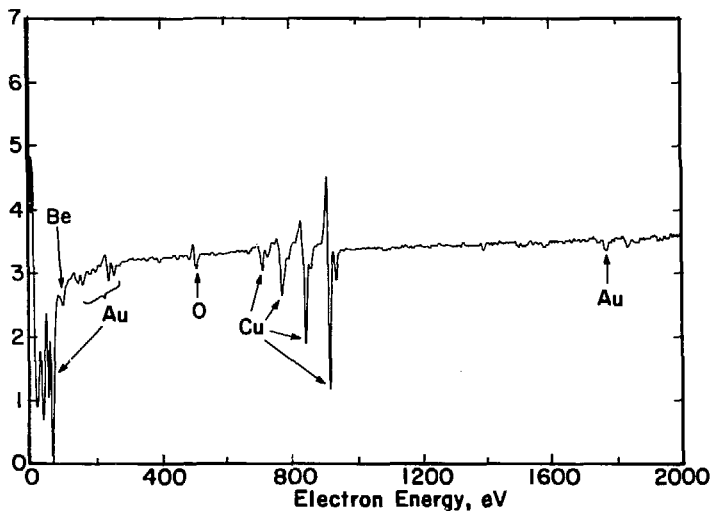
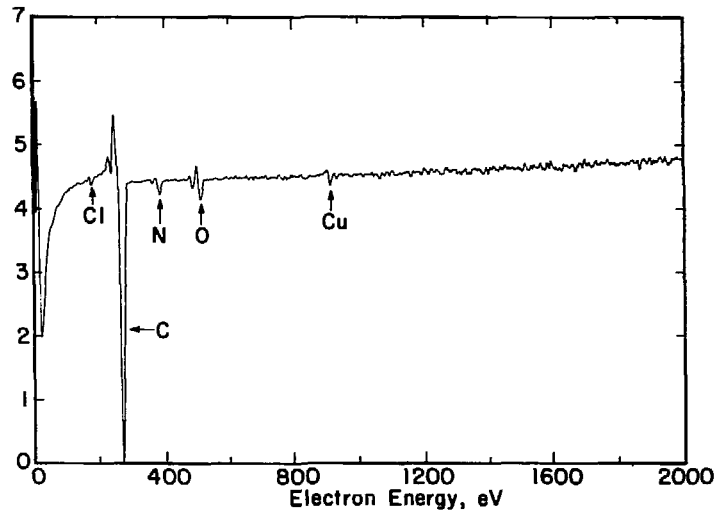
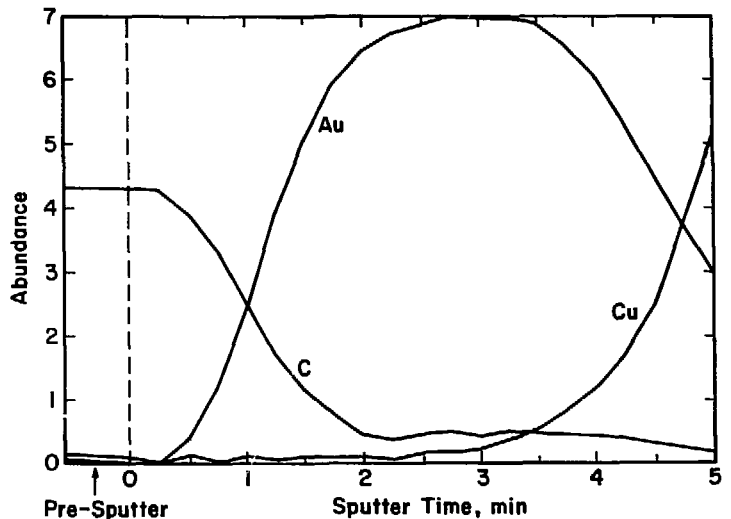


FIG. 11: Auger spectrum of field wire with polymer deposit removed by argon ion sputtering, exposing metal surface.

FIG. 12: Auger signals for carbon, gold, and copper during sputtering.



The signal from a wire surface devoid of its carbon deposits is shown in Fig. 11. In this case, the etching has not penetrated the Cu/Be core and -- at this depth -- one would expect to find only Au. However, the ubiquitous oxygen signal remains, though weaker than with the polymer film; the AES operator suspected it arose from the device itself. It is known that AES ion pumps are least effective in removing H_2O and CO from the chamber; consequently these molecules get "cracked" and atomic oxygen signals tend to grow even on freshly sputtered surfaces. More importantly, the Cu signal is extremely strong. Three explanations can be advanced: (a) the Cu Auger electrons manage to penetrate a substantial thickness of Au; (b) there is indeed an expanse of Cu/Be surface uncoated by gold; (c) Cu has diffused into and across the Au coating.

An example of composition "profiles" (actually, composition vs. etching time) is given in Fig. 12 for C, Au, and Cu; it was from the end of this etch that Fig. 11 was taken. The conversion of etching time to depth is known precisely only for a standard Ta_2O_5 : $0.1 \mu\text{m}/\text{min}$. However, all elements involved here are etched faster -- for Au, from 1.5-3 times faster; for Cu, slightly faster than Au; and for C, perhaps 5 times faster than Au. Thus, at any instant, the speed of etching is varying also with the local composition.

Despite this complication, some semiquantitative information emerges from Fig. 12, which was taken from a clear region of a wire bearing also extensive regions of discoloration. The C signal is constant for about 15 s, and if we assume a C etch rate of $1 \mu\text{m}/\text{min}$ this corresponds to a depth of about $0.25 \mu\text{m}$. From there until 2 min there are overlapping signals of C and Au, representing either a broad interphase (perhaps caused by penetration of high-momentum hydrocarbon ions into the soft gold) or regions of bare gold being uncovered next to regions of polymer that were initially thicker. Using an average etch rate of $0.25 \mu\text{m}/\text{min}$ through this dual-signal region (which presumes the interphase hypothesis) gives a C/Au interphase thickness of about $0.2 \mu\text{m}$. However, for the variable-thickness model of the C film, the fall-off of the C signal corresponds to another polymer increment of $0.75 \mu\text{m}$, for a maximum (local) polymer film depth of about $1 \mu\text{m}$.

This would correspond to the thinnest films (i.e., clear ones) encountered in the present work. When etching was focused on a black spot¹ the signal was 98.5% C, 1% O, and 0.5% N, and there was no change in the C signal for about 10 minutes (hence, a gross deposit with thickness exceeding $10 \mu\text{m}$).

Figure 12 also displays overlapping of Au and Cu signals, and again one cannot be sure whether this represents an interphase (commencing at about 3 min etch time) or an uneven gold coating that is removed at different times in different local regions. The extended Cu signal reaches uniformly through all the Au from 0 to 2.5 min, suggesting that true interdiffusion had occurred since wire manufacture. However, patchiness of the gold coating would be consistent with the upswing of the Cu signal (and downturn of the Au signal) after the 3-minute sputter, perhaps indicating that Au and Cu surfaces are simultaneously exposed and their area ratio changing with time. This is further supported by the appearance of what may be a Be signal in Fig. 11.

Thickness of the Au coating can be gauged from the overall width of the Au signal, estimated as 6 minutes of etch time and thus (using a rate of $0.2 \mu\text{m}/\text{min}$) giving about $1.2 \mu\text{m}$ depth. This seems very reasonable for a

wire-coating process to achieve. Yet, if the Au gradients are interpreted as superpositions of signals from adjoining local regions, then either the Au coating thickness is surprisingly variable or the coating is patchy and broken as proposed above.

A PARTIAL FIX

After the failure, the IDC was completely restrung; the field wire size was increased to 150 μm diameter but the sense wire diameter was unchanged. Since it was not feasible to segregate the IDC gas volume from that of the TPC, changes in gas composition or introduction of certain additives (such as "magic gas") could not be carried out. Electronegative species such as oxygen-containing gases would degrade TPC performance even at levels as dilute as 1 ppm. Instead, the sense wire voltage was reduced to about +3600 V and field wire voltage to -1200 V, and the electronic gain increased to compensate.

While spatial resolution was indeed degraded by these changes, the principal goal of prolonging the lifetime of the IDC as a trigger element was achieved. As of this conference date, the IDC has been in continuous and stable operation for about 24 mo. Whether this is due to any fundamental change in the plasma and/or surface chemistry is not clear. It is possible that some of the gas-phase polymerizable species created previously in the higher-energy electric field are not now being produced; a similar conjecture would apply to complex liquid-phase chemistry on the sense wires.

However, there is an obvious correlation with the total number of charges taken by the wires to date. While the earlier failure occurred with an integrated dosage of about 2×10^{17} charges/cm of sense wire, comparable to other reports of failure in similar chambers¹⁰, the integrated dosage under the new conditions is still less than 10^{16} charges/cm. This permits conjecture that failure conditions may only have been deferred, not eliminated; however, as a practical matter, IDC failure is no longer a limiting factor in TPC operation.

Examination of wires removed from the modified IDC after 8 months of operation¹ confirmed that polymeric deposits were still being formed. SEM micrographs of the field wires showed a distribution of small black spots, though no coatings were visible (Fig. 13a). Micrographs of the sense wires (Fig. 13b) revealed no heavy deposits of the sort found previously¹ on visibly dirty regions, but were somewhat similar to the earlier clear regions (Figs. 2c and 2b of Ref. 1, respectively). Figure 13b gives a representative picture of the small blobs and specks, presumably polymeric, scattered around the surface. There appears to be a porous and broken coating beneath these specks, but one cannot discern whether this a fluffy polymer or an imperfect gold layer.

The MS analysis demonstrated that field wires were vastly cleaner than before. Vaporizable linear hydrocarbons had few high-M species, and the low-M species were generally less abundant than the ubiquitous phthalate peak at $M = 149$ (hydrocarbons at $M = 44$ and 57 had somewhat higher peaks). The sense wires exhibited even more dramatic changes, with an MS spectrum very sparse in the low-M range and virtually vacant in the high-M range — except for phthalate signals. Strangely, there was no trace of silicone ($M = 207, 281$) and almost nothing for the aromatics at $M = 77, 91, \text{ and } 105$. The juxtaposition of these two factors may be the only evidence that fundamental

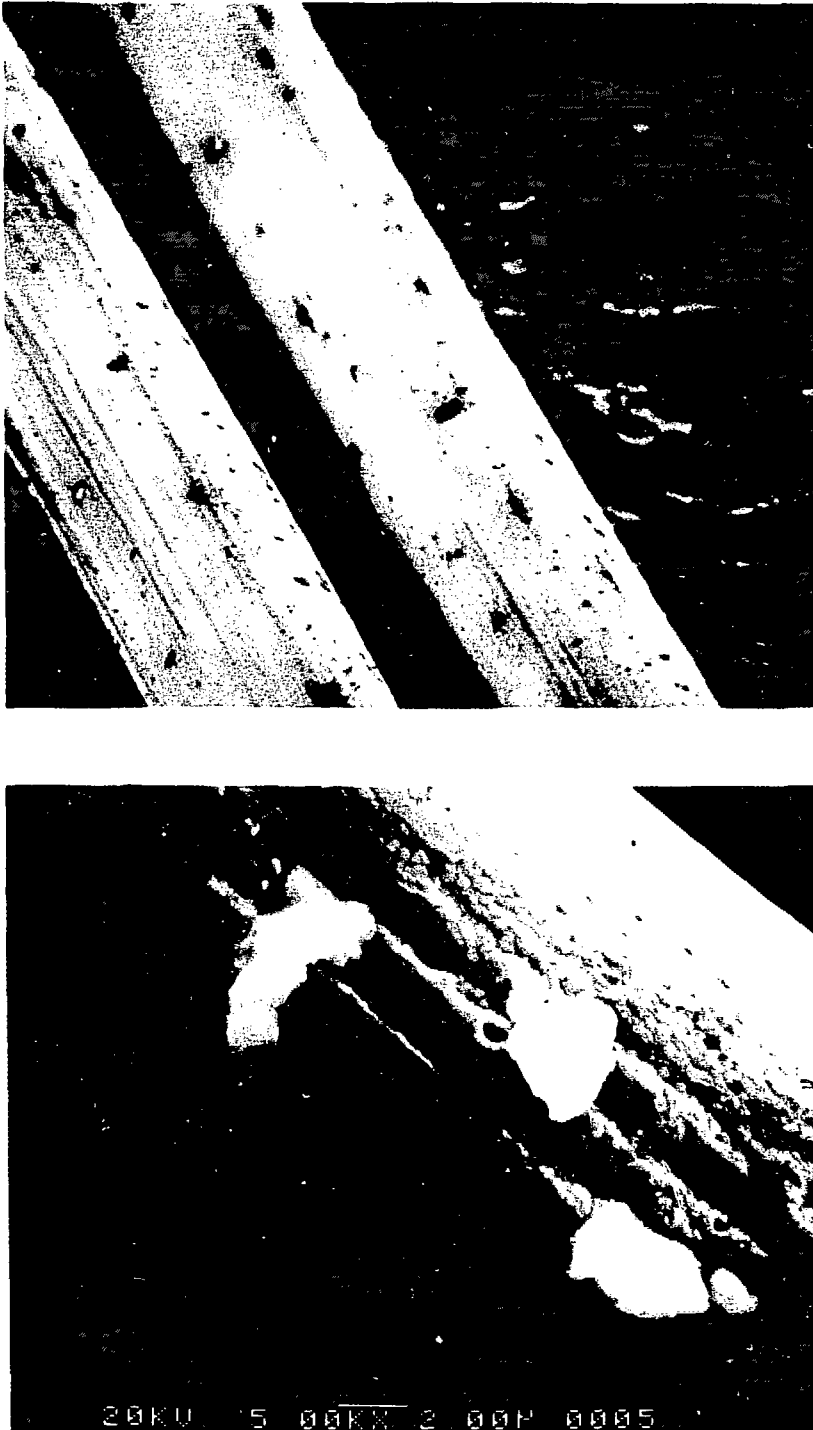


FIG. 13: Scanning electron micrographs of wires after change of operating conditions and 8 months of operation. (a) Above, field wires (150 μm diameter) with black spots later determined by AES to be carbon with considerable thickness. (b) Below, sense wire with polymeric debris of size 2-4 μm and broken coating of undetermined composition.

differences in chemical processes resulted from the changed IDC operating conditions. It may also imply that Si was previously implicated in a catalytic production of the aromatic species. Note that those species vanished even though phthalates were strongly present, reinforcing our previous speculation that the latter were not necessarily the origin of the former

AES analysis of the field wires was also performed. Again a carboniferous film was found in the clear regions, but it was very thin (about 0.02 μm). On the outer surface N, O, and Cl were noted as before, but traces of S, P, Sn, and Na were also detected. The Cu signal was very strong, as expected for a thin film. Etching for 5 s removed the Na, Cl, and P signals, and any remaining S was obscured by the large Au signal. Remarkably, however the Cu signal was also substantially reduced, and another 5 s of etching caused it almost to vanish. This behavior is not at all understood (except to appeal to instrument malfunction), since it implies a separate and unidentified source of Cu in the IDC beyond that of the field wire core. Further, this would alter the previous interpretation of data in Figs. 10-12. Clearly some mysteries still remain, and much more work is needed to unravel them.

REFERENCES

1. K. Kwong, J.G. Layter, C.S. Lindsey, S.O. Melnikoff, B.C. Shen, G.J. VanDalen, and M.C. Williams, Nucl. Inst. Meth. Phys. Res., A238, 265 (1985).
2. M. Shen, ed., Plasma Chemistry of Polymers, Dekker, New York, 1976.
3. H. Yasuda, Plasma Polymerization, Academic Press, New York, 1985.
4. D.W. Hess, "Plasma Chemistry in Wire Coating," Proc. Workshop on Radiation Damage to Wire Chambers, ed. J. Kadyk, 1986 (this volume).
5. L. Mandelkern, Crystallization of Polymers, McGraw-Hill, New York, 1964.
6. M.M. Bursey, "Mass Spectrometry," in Encyclopedia of Science and Technology, Vol. 8, McGraw-Hill, New York, 1977.
7. S.R. Heller and G.W.A. Milne (eds.), EPA/NIH Mass Spectral Data Base, Suppl. 1, U.S. Dept. Commerce, U.S. Government Printing Office, Washington, D.C. 1980.
8. F. Rodriguez, Principles of Polymer Systems, 2nd ed., McGraw-Hill, New York, 1982.
9. E. Steghagen, S. Abrahamsson, F.W. McLafferty (eds.), Registry of Mass Spectral Data, Vol. 3, Wiley-Interscience, New York, 1974.
10. M. Turala and J.C. Vermeulen, Nucl. Instr. Meth., 205, 141 (1983). Other reports of finding silicon are contained in the present volume.
11. L. Davis, N. MacDonald, et al. (eds.), Handbook of Auger Electron Spectroscopy, 2nd edn., Physical Electronics Industries, Eden Prairie Minn., 1976.

ACKNOWLEDGMENTS

Many thanks are due to Dr. John G. Layter, Physics Department, University of California, Riverside, who initially brought the IDC wire problem to my attention and co-authored Ref. 1. Analytical assistance was provided by Dr. K.A. Gaugler (AES and SEM) of the Molecular and Materials Research Division, Lawrence Berkeley Laboratory, and by Dr. A. Falick and others in the MS Laboratory, College of Chemistry, University of California, Berkeley.

NEW TECHNIQUES TO ANALYSE WIRE COATINGS

H. Boerner and R.D. Heuer, CERN, Geneva

ABSTRACT : Two methods for the analysis of coatings on wires used in wire chambers which suffered from radiation damage are described : secondary ion mass spectroscopy and laser microprobe mass analysis. Both methods allow molecules and not only elements to be detected and both are sensitive to hydrogen and its compounds. The methods are compared to Auger electron spectroscopy.

Radiation damage to wire chambers usually results in deposits on the wires which in turn can lead to electrical breakdown of the chambers. The analysis of these contamination films is important for the understanding of the processes which lead to the coating. Up to now electron microscopy and Auger Electron Spectroscopy (AES)¹ have widely been used to analyse wire coatings. With these methods hydrogen cannot be detected. Information on chemical compounds is only possible in certain cases with AES from the analysis of the exact positions and shapes of the Auger lines. We have therefore searched for methods which are sensitive to hydrogen and which also allow to analyse the chemical composition of the deposits.

Secondary Ion Mass Spectroscopy (SIMS)² and Laser Microprobe Mass Analysis (LAMMA)^{*) 3} are well known techniques in solid state physics for the analysis of surfaces.

The SIMS method is based on the fact that surfaces bombarded with ions (in this case : noble gas ions) emit positive and negative secondary ions which are characteristic for the chemical composition of the emitting surface. With the energy of the probing ion in the KeV range the secondary ions have a low kinetic energy of several eV, so they can only originate from the outermost atomic layers. The high sensitivity of the method⁴ is obtained by the use of an ion-detecting system (usually a quadrupole mass analyzer) which counts individual secondary ions, yet also at the expense of a relatively large beam spot size of the order of 0.1 cm².

The LAMMA method uses a pulsed UV-laser beam, e.g. a frequency quadrupled Nd-Yag laser which is focussed on the surface of the sample. In

*) LAMMA is a registered trade mark of Leybold-Heraeus GmbH

the focus a small amount of material is vapourised and ionised. From the resulting plasma ions are extracted and analysed in a time-of-flight mass spectrometer. With this method the spot size can be as small as $0.3 \mu\text{m}^2$ whereas the sampling depth is rather large - up to several μm depending on the laser intensity. The laser intensity also determines the degree of fragmentation of the molecules. It should be mentioned that only one laser shot is needed to obtain a complete spectrum.

Table I summarises the properties of the three methods. It indicates that all three methods are able to supply information on the element composition of a surface. Compounds can be identified with AES via chemical shift in certain cases. SIMS and LAMMA can also detect molecular ions which enables chemical compounds to be determined. Hydrogen and its compounds, e.g. hydrocarbons, can only be detected by SIMS and LAMMA. Whereas AES and SIMS are sensitive to only a few atomic layers at the surface, LAMMA averages over a few μm depth and is therefore more a "bulk" analysis method. Yet its very small spot size enables the investigation of small contaminated regions.

All methods have in common that they need large and sophisticated experimental setups as well as considerable experience for the interpretation of the produced spectra, therefore all analysis were made in specialized laboratories⁵.

Three different wire samples with contaminations on the surface have been used : a CuBe-wire for the comparison of SIMS and LAMMA with AES, and two different samples of gold-plated tungsten wire to explore the analysing potential of LAMMA.

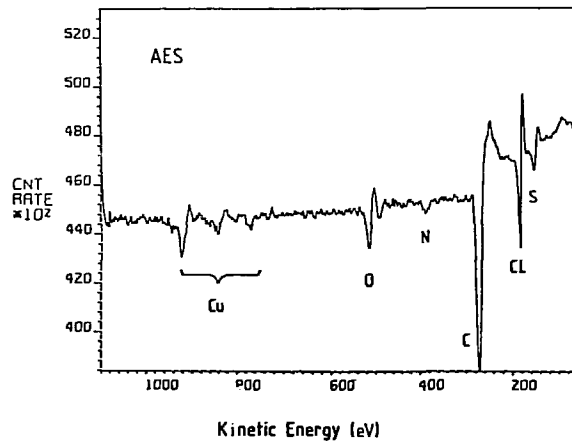
The CuBe-wire (sample 1) had been stored on air for several years and showed coloured spots on its surface already before usage in a chamber. These spots looked blueish black in diffuse light whereas in directed light they appeared white. An oxidation of the surface was suspected. Figs. 1-3 show the AES, SIMS and LAMMA spectra obtained from this wire. Whereas AES produces a spectrum relatively easy to interpret, the spectra of SIMS and LAMMA exhibit numerous peaks. With all methods Cu, O, C and Cl can clearly be identified. LAMMA and SIMS show additional peaks at the mass positions of OH^- and CH^- as well as peaks which can be attributed to organic compounds ($m/e = 26, 42, 63, 79, 81$ and $m/e = 24, 48, 60, 72, 84$, respectively). The contamination film on the surface of this wire contains hydrocarbons and/or other organic substances, but no copper oxide was found.

In addition several peaks in the SIMS spectra can be attributed to compounds consisting of Be, O and H as for example BeO^- ($m/e = 25$), BeO_2^- (41) or BeOH_2^+ (26) etc. These ions can be found in secondary ion mass spectroscopy of oxidized CuBe surfaces⁶. Due to the heat treatment of CuBe the Be concentration is higher at the surface⁶ therefore it can be understood that Be lines are more abundant in the SIMS than in the LAMMA spectra. Due to this Be enrichment at the surface it was not surprising that ion sputtering which removed the surface layers not only reduced the C and O peaks but also the Be peak. This analysis already demonstrates the detailed information obtainable with both SIMS and LAMMA.

TABLE I

Comparison of surface analysis processes

	AES	SIMS	LAMMA
Excitation via	e^-	Ar^+	γ
Analysis of	e^-	I^\pm	I^\pm
Information depth	$\leq 30 \text{ \AA}$	$\leq 10 \text{ \AA}$	$\leq 5 \text{ \mu m}$
Spot size		$\sim 0.1 \text{ cm}^2$	$\sim 1 \text{ \mu m}^2$
Detection of elements	yes	yes	yes
compounds (chemical shift)		yes	yes
hydrogen	no	yes	yes
Quantitative analysis	possible	possible	possible

**Fig. 1** AES spectrum of the contaminated CuBe-wire (sample 1).

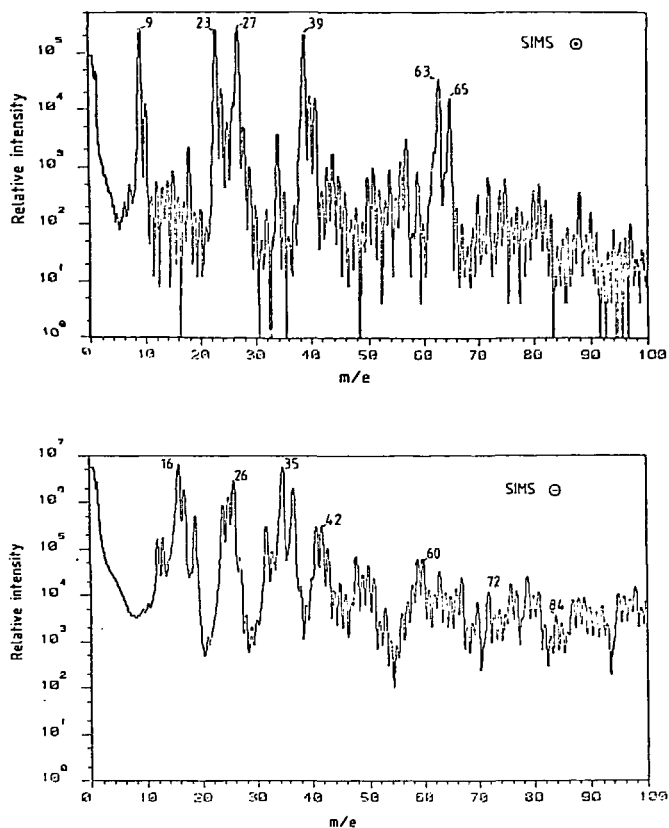


Fig. 2 Positive and negative secondary ion mass spectra of sample 1. Na($m/e = 23$) and K(39) are ubiquitous elements.

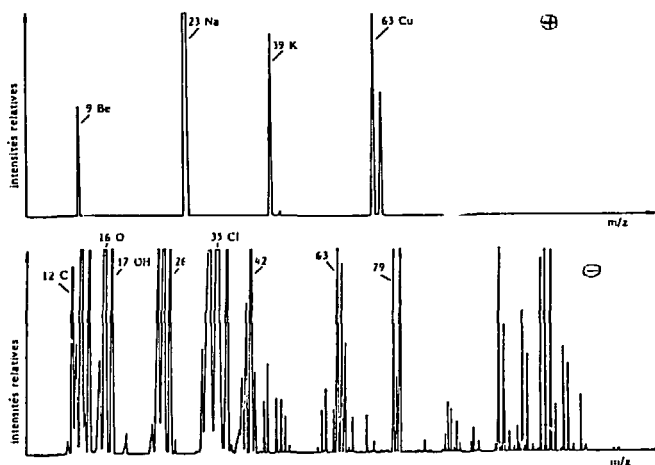


Fig. 3 Time of flight mass spectra for positive and negative ions produced with LAMMA (sample 1).

The potential of LAMMA was further explored with the analysis of contaminated gold plated tungsten wires. One wire (sample 2) had been used in drift chambers of the EMC-experiment at CERN. Near the beam spot the chamber suffered from radiation damage⁷. Fig. 4 shows 2 photographs of the coated area with different magnification. The LAMMA spectra are given in Fig. 5. They show a clear silicon peak in the positive spectrum as well as SiO_2^+ , SiO_3^+ and SiO_3H^+ as secondary ions typical for silicon oxide. In addition mass peaks at the position of Cl, OH and of organic compounds (like $m/e = 26, 42, 48$) are detected. The contamination therefore consists of organic silicon compounds or SiO_2 plus organic compounds.

The other wire (sample 3) was used in a small test chamber which was operated for a short time with reversed bias (i.e. negative high voltage on the sense wires). This resulted in glow discharges which in turn produced black spots on the sense wires. In these spots only hydrocarbon fragments were detected (Fig. 6). The glow discharge obviously resulted in a plasma polymerization of the organic component of the chamber gas ($\text{Ar}/\text{CH}_4, 9:1$), no impurities like silicon were deposited.

For the analysis of surfaces LAMMA and SIMS provide additional information to AES especially on hydrocarbon contaminations and on molecular compositions. LAMMA is well suited for the analysis of small spots. The interpretation and quantitative analysis of the results is difficult but possible.

REFERENCES

- [1] J.J. Lander, Phys. Rev. 91 (1953), 1382
- [2] A. Benninghoven, Surface Sci. 35 (1972), 472
- [3] F. Hillenkamp et al., Appl. Phys. 8 (1975), 341
- [4] A. Benninghoven, Appl. Phys. 1 (1973), 3.
- [5] We are grateful to :
 Dr. H. Klewe-Nebenius, G. Pfennig, Kernforschungszentrum Karlsruhe;
 Dr. H. Fehmer, J. Schwar, Phys. Institut, Univ. Münster;
 Dr. J. Dennemont, Institut d'Hygiene, Genève
 for performing the AES, SIMS and LAMMA analysis, respectively.
- [6] R. Buhl et al., Proc. 2nd Int. Conf. on Solid Surface (1974), 807
 Japan. J. Appl. Phys. Suppl. 2., Pt.2, 1974.
- [7] For details see the information table submitted to this workshop by Dr.
 W. Mohr, Fakultät für Physik, Univ. Freiburg.

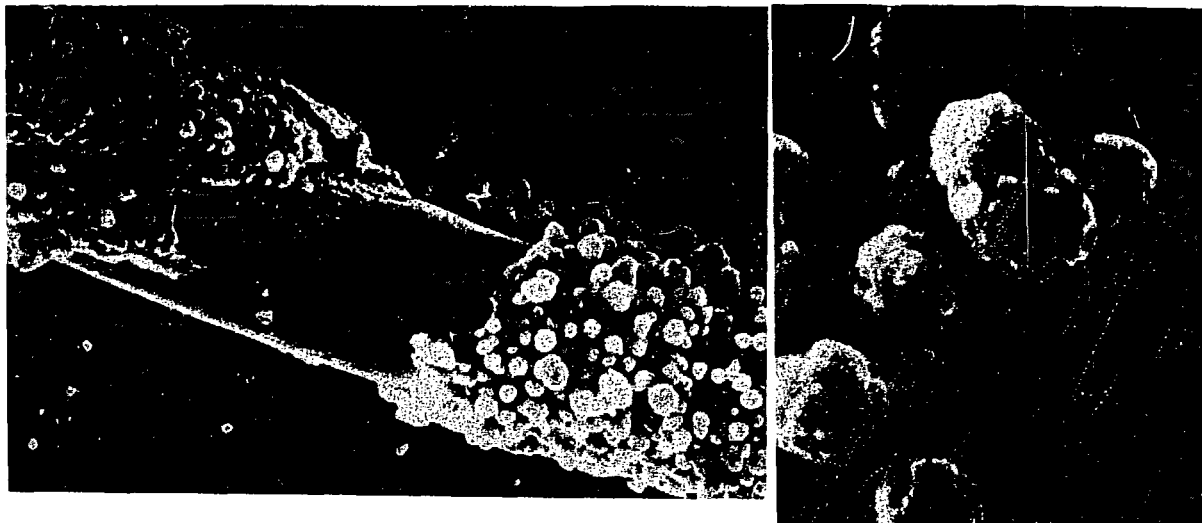


Fig. 4 Coated region of a gold plated tungsten wire (sample 2). The magnification factors are 1480 and 10700, respectively (courtesy of W. Mohr, Phys. Inst., Univ. Freiburg).

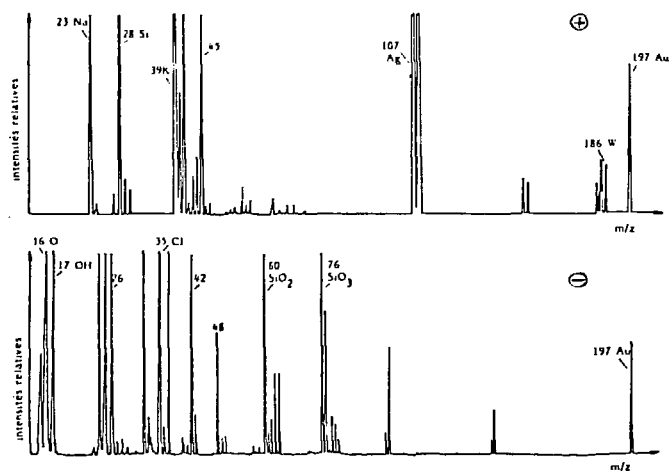


Fig. 5 Positive and negative ion spectra of sample 2 obtained with LAMMA. The Ag-peak is due to an additional silver plating which was used to increase the wire diameter locally.

53, 54

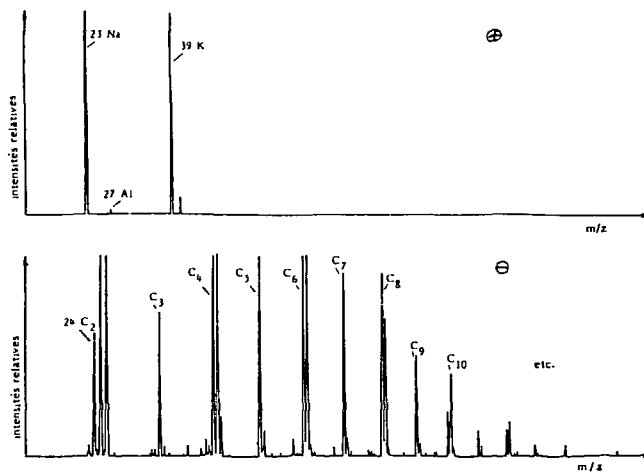


Fig. 6 LAMMA mass spectra of sample 3.

WIRE CHAMBER AGING

Muzafer Atac
Fermi National Accelerator Laboratory^a

ABSTRACT

Wire chamber aging can be due to a variety of reasons. Some of the most commonly known reasons are discussed to some detail. Most chambers live fairly long when glow discharges, edge breakdowns, photoelectric feedback, and field emissions from cathodes are prevented. Polymerization and coating by impurities take substantial integrated charge, larger than 0.03 coulomb per wire per centimeter before observing substantial deterioration in chamber performance with most chamber gases. Tests with 50/50 A-C₂H₆ with 0.5% or more ethanol vapor show that no appreciable damage is observed up to 1 coulomb charge per centimeter wire segment.

INTRODUCTION

Wire chamber aging especially if it is due to polymerization process may be very complicated to predict and understand. During the avalanche process large organic molecules break up several times by collisions with electrons and UV-photon absorption (quenching) processes. These products can be oil and paraffin-like substances coating anode and cathode surfaces. Some of these products form a long chain of molecules, polymers on the surfaces.

It was found by S.S. Friedland¹ that in a counter filled originally with Argon-Methane, the methane (mass 16) will decrease, but masses 27 and 28 were observed to increase, indicating polymerization and formation of such compounds as C₂H₄ and others. In general, it was found that gases in the methane series polymerized more than they dissociated, and that the reverse happened with such compounds as ethyl acetate and alcohols.

Polymerization is undesirable since as soon as the compound combines with more than 5 or 6 carbon atoms, it becomes a liquid or solid at room temperature and is deposited on the solid surfaces.

Contamination in chamber gases could slowly change anode and cathode surfaces. Oxidation can be accelerated during the avalanche process. Contamination of Si, S, Br, Cl, etc... compounds may coat surfaces and change surface characteristics, therefore, gas purity is an important factor in the chamber aging process. For the same reasons dielectric films such as mylar, Kapton, etc. should not be used for covering chamber windows. They permit diffusions of gases into chambers and also slowly alter electric fields as they are charged up. Such windows should be covered with metallic materials on the inside.

Wire chamber aging can be accelerated with any of the following phenomena: Discharges (glow discharges or sparks), edge breakdowns, photoelectric feedback, and

^aOperated by Universities Research Association under Contract with the United States Department of Energy.

field emission from cathode surfaces. Discharges and edge breakdowns may leave scars on the surfaces.

In this paper some suggestions about the design and the operation of the drift chambers and proportional chambers are presented.

EDGE BREAKDOWNS

It is often found that with planar wire chambers that breakdowns at straight cut frame edges leave dark regions on both anode and cathode wires after some usage. Fig. 1a shows a typical frame that is commonly used for making planar wire chambers. Depending upon electric fields, thickness of the dielectric frame, and gas mixture substantial surface electric current flow may occur. The current may increase in time and result in surface corona discharge. A simple way of avoiding this problem is to make the frame as shown in Fig. 1b. With the addition of a ledge surface current path is doubled preventing surface corona.

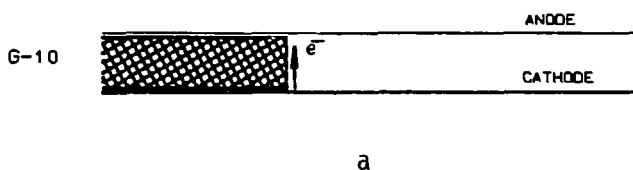


Fig. 1a. Commonly used wire chamber frame with straight edge.

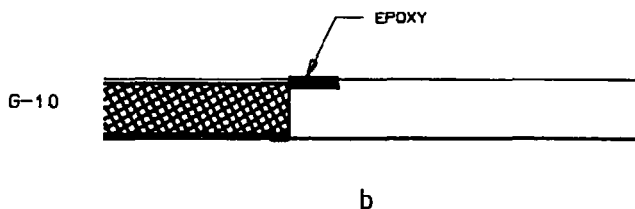


Fig. 1b. Wire chamber frame with ledge.

FEEDTHROUGH DESIGN

Cylindrical drift chambers have become very popular in recent years as colliding beam experiments have gained great importance. An injection molded small dielectric tube, with the help of crimp tube having a very small inner diameter (as small as 75 μm), precisely positions the wire under a required tension.

Figs. 2a and b show two different arrangements. Fig. 2a is a cross section view of a Delrin feedthrough. The main characteristic of this design is that the V-groove precisely positions the wire at the center of the Delrin tube at the innerface of the aluminum plate. The crimp tube stops somewhere within the aluminum plate, leaving the anode wire at a very high electric field since the dielectric surfaces are charged up as indicated

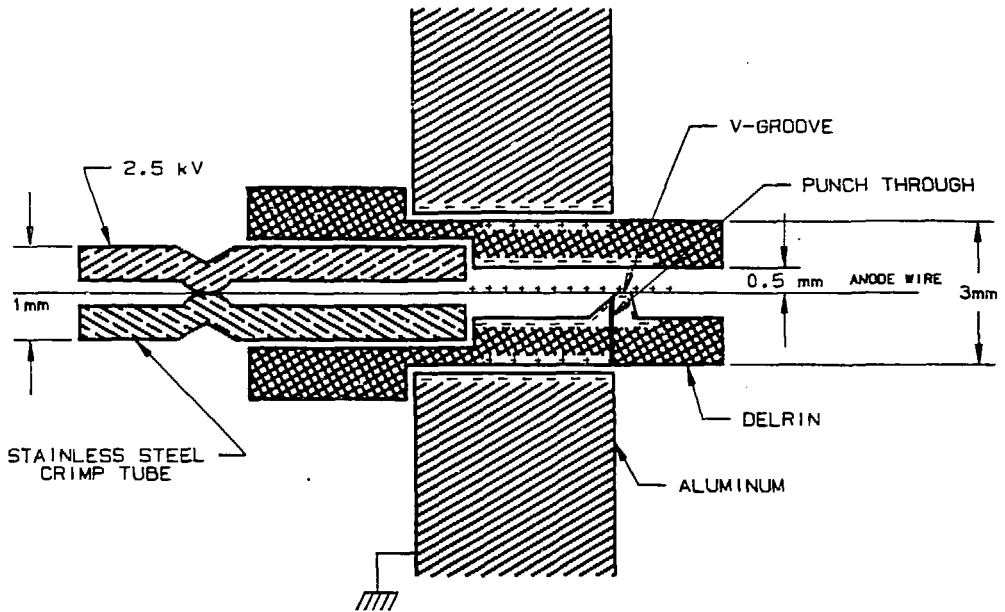


Fig. 2a. Feedthrough arrangement with V-groove which positions wire precisely. The arrangement may cause breakdowns.

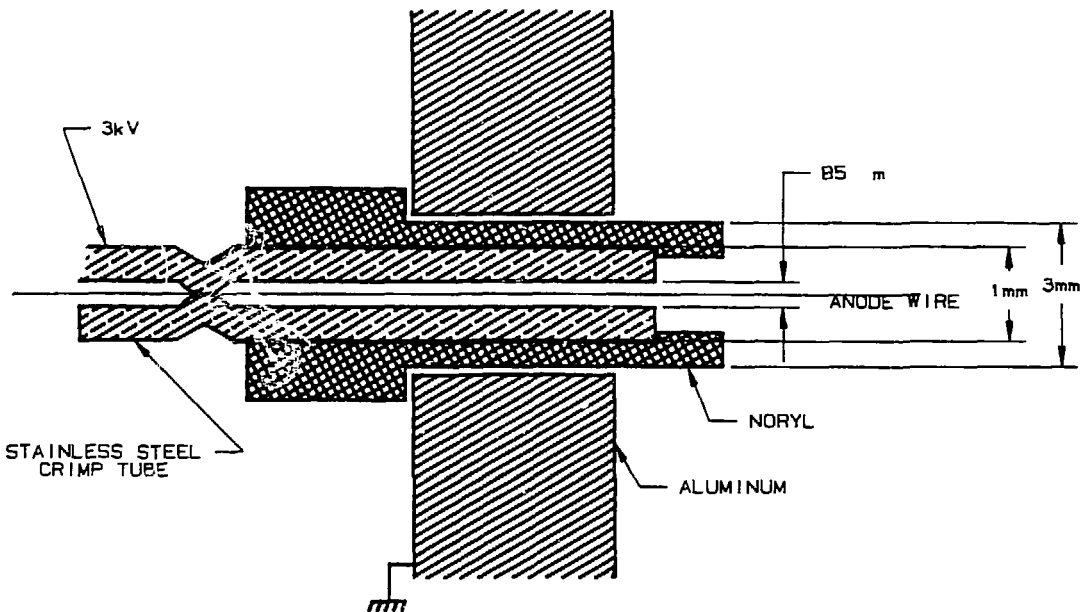


Fig. 2b. Feedthrough arrangement with crimp tube positioning wire precisely. Large enough diameter lowers the electric field.

in the figure. This may result in breakdown through the dielectric in a random way. Dark canals are found in the Delrin around the V-groove regions. The configuration shown in Fig. 2b would prevent the current punch-through by dropping the electric field within the aluminum plate since the crimp tube extends into the chamber volume. A 1 mm thick tube drops the field to a much lower value, and an 85 μm size hole in the tube precisely positions the wire.² Tests done with this feedthrough arrangement using Delrin materials (grades: 100, 500, 900, and 900s) showed considerable noise pulses even without the anode wire with a potential applied between the crimp tube and the aluminum plate. The noise pulses showed up around 2 kV and increased in amplitude as the voltage was increased. Fig. 3 shows such pulses. They are indistinguishable from typical proportional pulses. Magnified cross-sectional cuts showed voids in the injection molded Delrin samples. The most probable cause of the noise pulses is that the surface of the voids slowly charge up, polarize, and discharge producing random pulses which are shaped by the amplifier. The feedthroughs get noisier in time and show currents reaching 1 nA level. In this search of good injection molded dielectric materials polyethylene and Noryl N190 were found to be excellent: no noise pulse up to and beyond 3 kV and the leakage current was less than 10^{-12} A. This limit is due to insufficient sensitivity. Noryl is as rigid as Delrin and very stable, but polyethylene is not sufficiently rigid for the application.



Fig. 3. Noise pulses produced in Delrin material.

FIELD EMISSION FROM CATHODE WIRES

Electrons can be emitted from a cathode wire surface when the electric field exceeds some critical value that is dependent on the surface quality and type of material. The field may be as low as 30 kV/cm. Coated or plated Be-Cu wire surfaces are found to be rather imperfect, full of dark spots. The study was done with a cylindrical tube of 1 cm diameter with a semitransparent window, In-Sn oxide coated mylar film. Photon emission from the region surrounding anode wire was observed when the wire was under a reversed high voltage, negative potential on the wire, and aluminum tube at ground. Conductive transparent window is also kept at ground potential.

Generally under normal operating conditions randomly emitted single electron pulses will not be seen in drift or proportional chambers unless the gas gain is set to be very high, above a few times 10^5 . But these pulses can be there and accelerating the aging process. Fine finished stainless steel wires were found to be better for this effect. Good surface quality and rather thick wires, 150 μ m or thicker, were advisable for the cathode or field wires for eliminating the field emission.

PHOTO-ELECTRONS AND DISCHARGES

Another very damaging phenomenon is glow discharge or spark discharge.³ They occur at a critical gain for a given intensity in a gas mixture when ultraviolet photons are not fully quenched. The phenomenon manifests itself by a continuous current drawn from a high voltage power supply. It starts with an increase in current and after a brief hesitation current goes up again, and it reaches a steady value. The current may vary from a small fraction of a microampere to tens of microamperes.

It may be initiated with photon electron exchange process when UV quenching is insufficient. The most likely way this phenomenon may happen is to create a streamer condition which cannot quench itself and branch streamers. This then feeds itself through successive regeneration of electrons by photons continuously. Details can be found in Ref. 3.

The streamer condition may be reached at high rates with a sufficient gain when a track or tracks are accidentally produced in the vicinity of a fully developed avalanche cone which provides electrons to be multiplied successively at the tip of the cone where the field is high.

The breakdown current was studied using tubes and a small drift chamber each having a semitransparent window (In-Sn oxide coated mylar film). Using an image intensifier video camera described earlier^{4,5} photons emitted from the active area were observed while the average current drawn from the high voltage power supply was recorded. Pulses from the anode wires were also observed to detect streamer transitions when the applied voltage was sufficiently high.

Fig. 4 shows the experimental arrangement. A fairly intense Sr^{90} β -source of $2 \times 10^5/\text{sec-cm}^2$ rate was used for the tests. The gas mixture was 50/50 $\text{C}_2\text{H}_6/\text{A}$ flowing through ethyl alcohol at 0°C , adding 1.4% vapor to the mixture. The flow rate was 200 cc per minute.

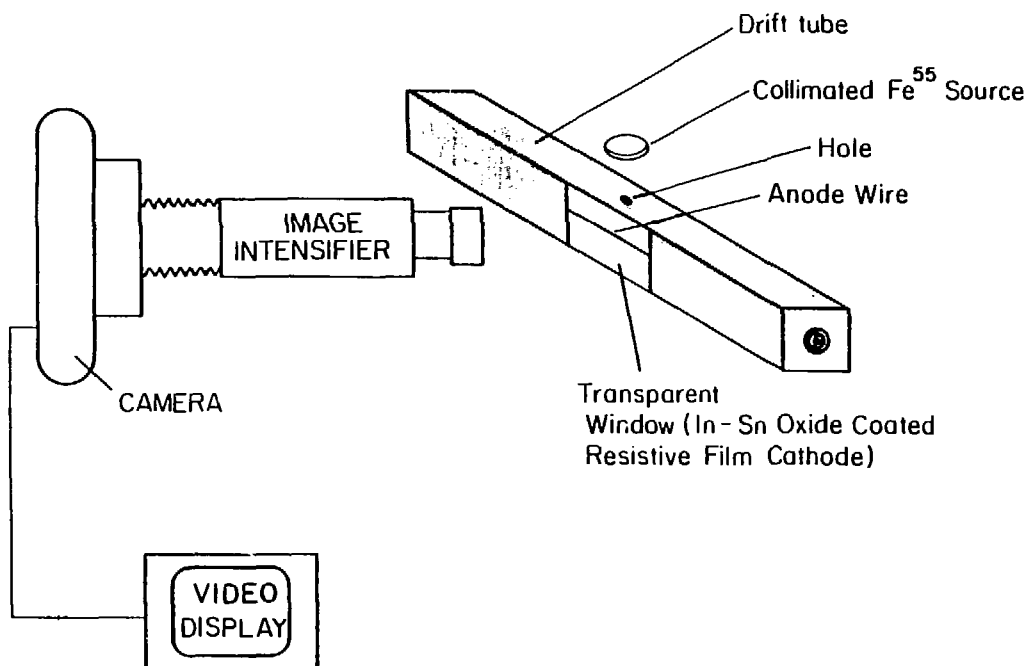


Fig. 4. Experimental arrangement with image intensifier camera for observing photon activity.

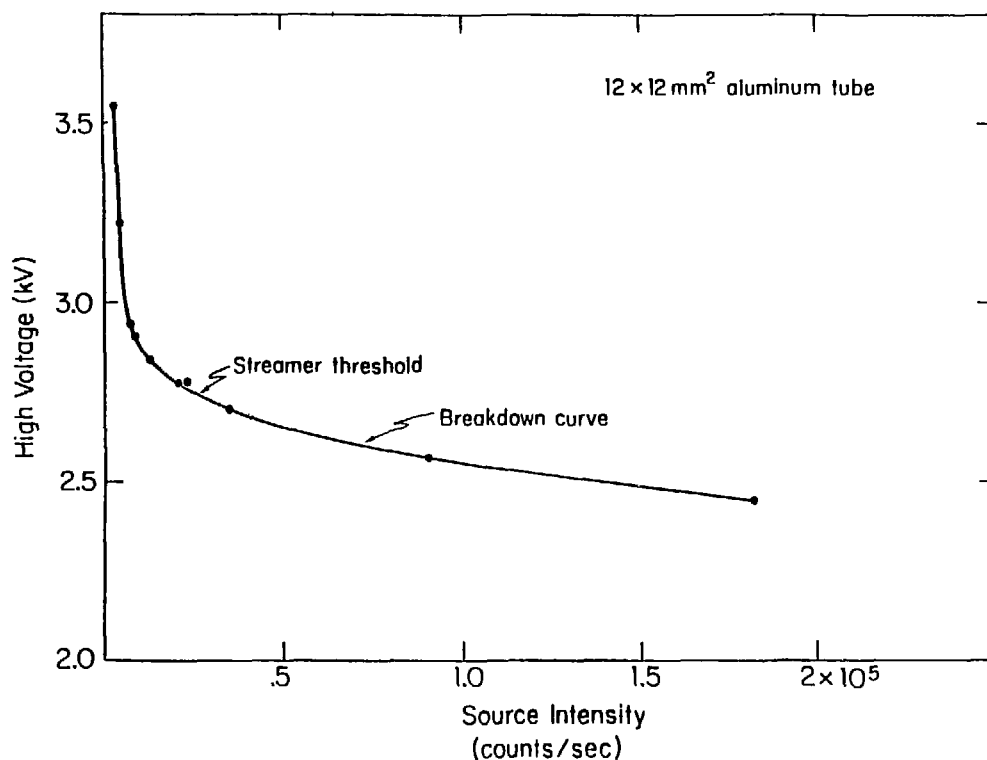


Fig. 5. Breakdown curve for 12 mm \times 12 mm size aluminum tube. Gas mixture 50% A/50% C_2H_6 bubbling through ethyl alcohol at 0°C adding 1.4% vapor.

Fig. 5 shows the breakdown curve for 12 mm \times 12 mm size aluminum tube having 50 mm thick gold plated tungsten wire. As seen in the figure, it is a well-behaved smooth curve all the way to the full streamer operation. Thin aluminum absorbers were used to lower the source intensity. The breakdown occurred at a critical gain and intensity when the average current exceeded 0.5 mA. Without the ethyl alcohol vapor the breakdown current is below 0.02 mA.

For optical observation of the breakdown phenomenon the ethyl alcohol component of the gas mixture was removed, only 50% A/50% C₂H₆ was used. The β -source intensity was about 10^5 counts per wire per cm² per second for the small drift chamber shown in Fig. 6. The photon activity made the anode wires visible at 1.8 kV. Boiling-like activity appeared on the TV monitor at 1.9 kV as shown in Figs. 7a and b. The activity stayed within circles of about 3.6 mm diameter at 2.1 kV. The circles remained when the source was removed as seen in Fig. 7b. The voltage had to be reduced below 1.8 kV for the circles to disappear.

1.4% ethanol vapor was added to the gas mixture, and the photon activity was observed. Figs. 8a, b, and c show that it takes considerably higher voltage for the wires to be visible. At 2.8 kV self-quenching streamers are seen and at 3.1 kV full streamer operation. The fact that branch streamers did not occur, and the breakdown condition was not met with the ethanol vapor in the drift chamber with the wire cathode configuration is a significant clue that breakdown is mediated by photoelectron conversion on the cathode surface. The breakdown occurs with 1.4% ethanol in the tube since it is a continuous coverage of cathode surface as compared to very small solid angle coverage with the wire cathode surface.

Ultraviolet photon transmission curves provided by Dr. Victor Ashford show that ethanol absorb the longer wavelength UV photons quite efficiently (Fig. 9). These are long ranged photons that are capable of knocking out electrons from cathode surfaces, and ethane molecules are very ineffective in quenching them.

Another independent experiment resulted in the attenuation length of $\lambda = 480 \mu\text{m}$ for those photons capable of producing electrons in 50% A/50% C₂H₆ from the cathode wall of the 12 mm \times 12 mm aluminum tube. The attenuation length is reduced to $\lambda = 160 \mu\text{m}$ with the addition of 1.4 ethanol vapor. These numbers were not affected with the same tube after coating the inner wall with colloidal graphite.

No breakdown could be detectable up to 7 mA average current when 4.4% ethanol vapor was added to the gas mixture. Fig. 10 shows breakdown current as a function of ethanol concentration.

AGING

Argon-ethane gas mixture has been very popular because of the good saturation property of electron drift velocity (Fig. 11) thus providing very good spatial resolutions. Long time studies of the gas mixture have shown that the lifetime of wire chambers can be very long since breakdown conditions are prevented with the addition of ethyl alcohol vapor. The table below shows integrated charge for different ethanol concentrations. These are very direct measurements of currents drawn from the high voltage supply

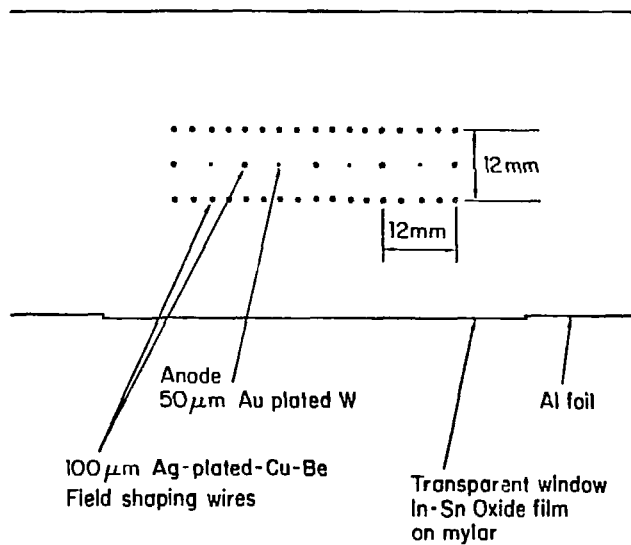


Fig. 6. Cross section view of the small drift chamber for optical observation of breakdown phenomenon.

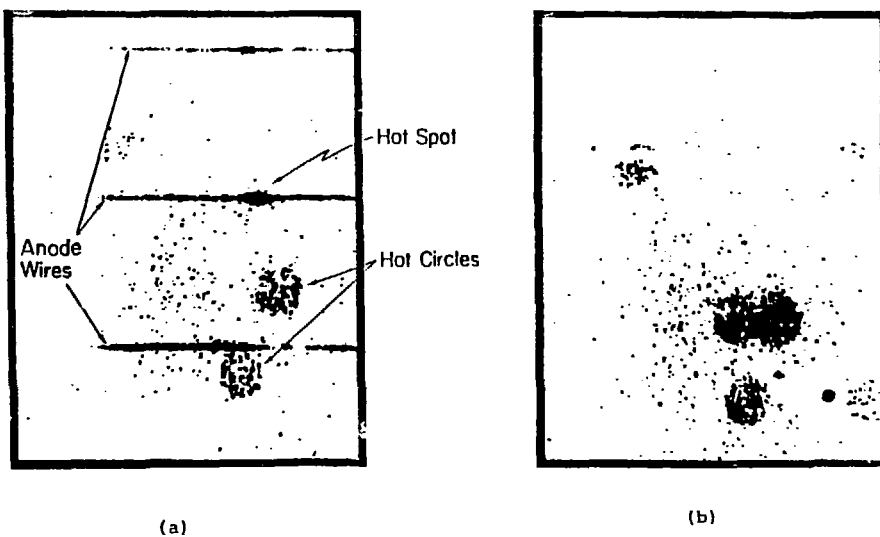
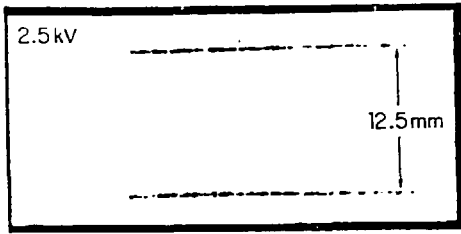


Fig. 7a. Photon activity showing normal operating regions along the anode wires together with breakdown regions, using the Sr^{90} β -source without ethyl alcohol vapor in the gas.

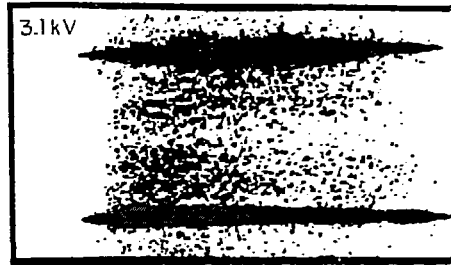
Fig. 7b. Breakdown regions are continuously active even after removing the source.



(a)



(b)



(c)

- Fig. 8a. Ethyl alcohol is added to the chamber gas. Chamber operating in saturated avalanche mode.
- Fig. 8b. Chamber operating in a mixed mode; self quenching streamers appear.
- Fig. 8c. Full streamer operation. Up to full streamer operation with no breakdown activity with the help of ethyl alcohol vapor.

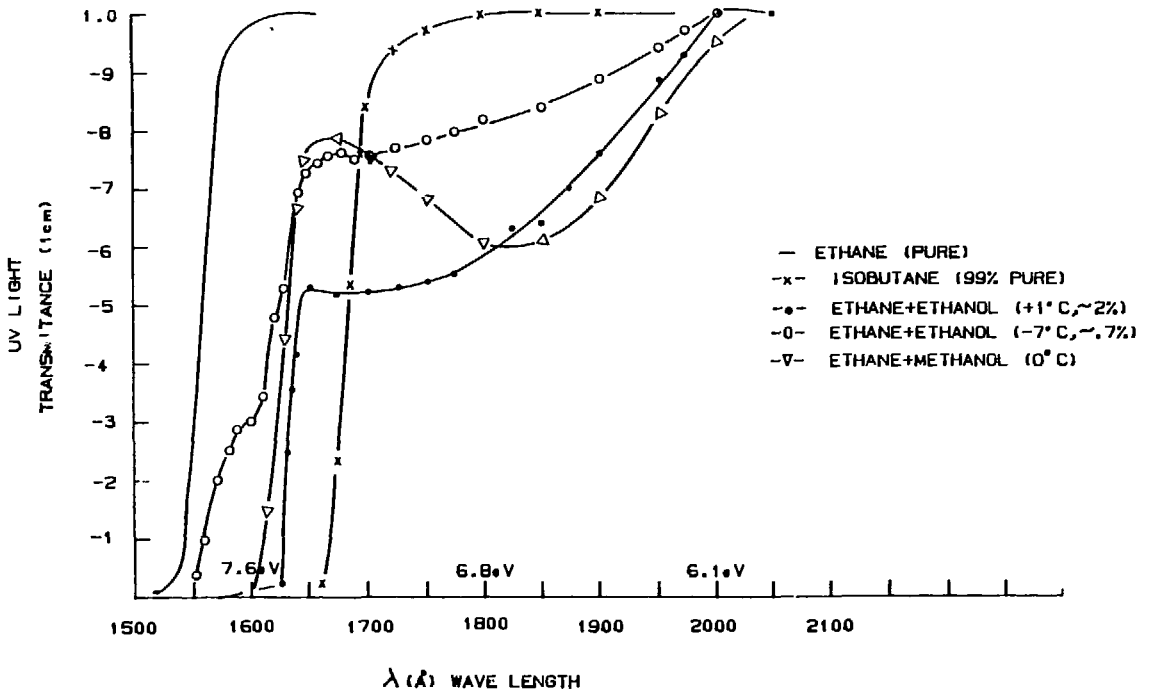


Fig. 9. UV transmission curves through the given gas mixtures (provided by V. Ashford).

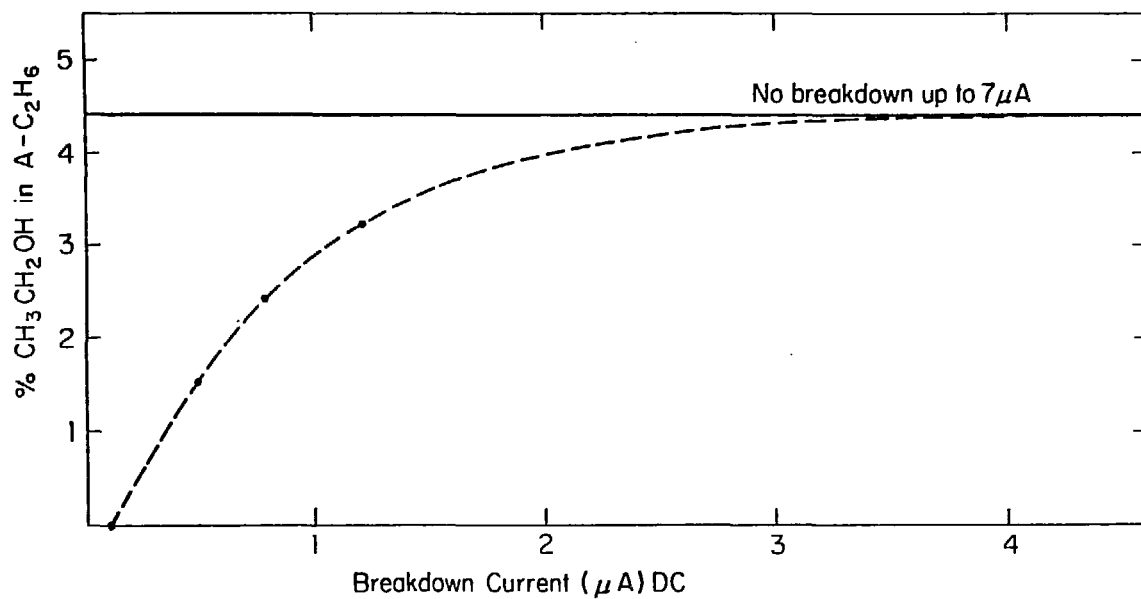


Fig. 10. Breakdown current as a function of ethyl alcohol concentration.

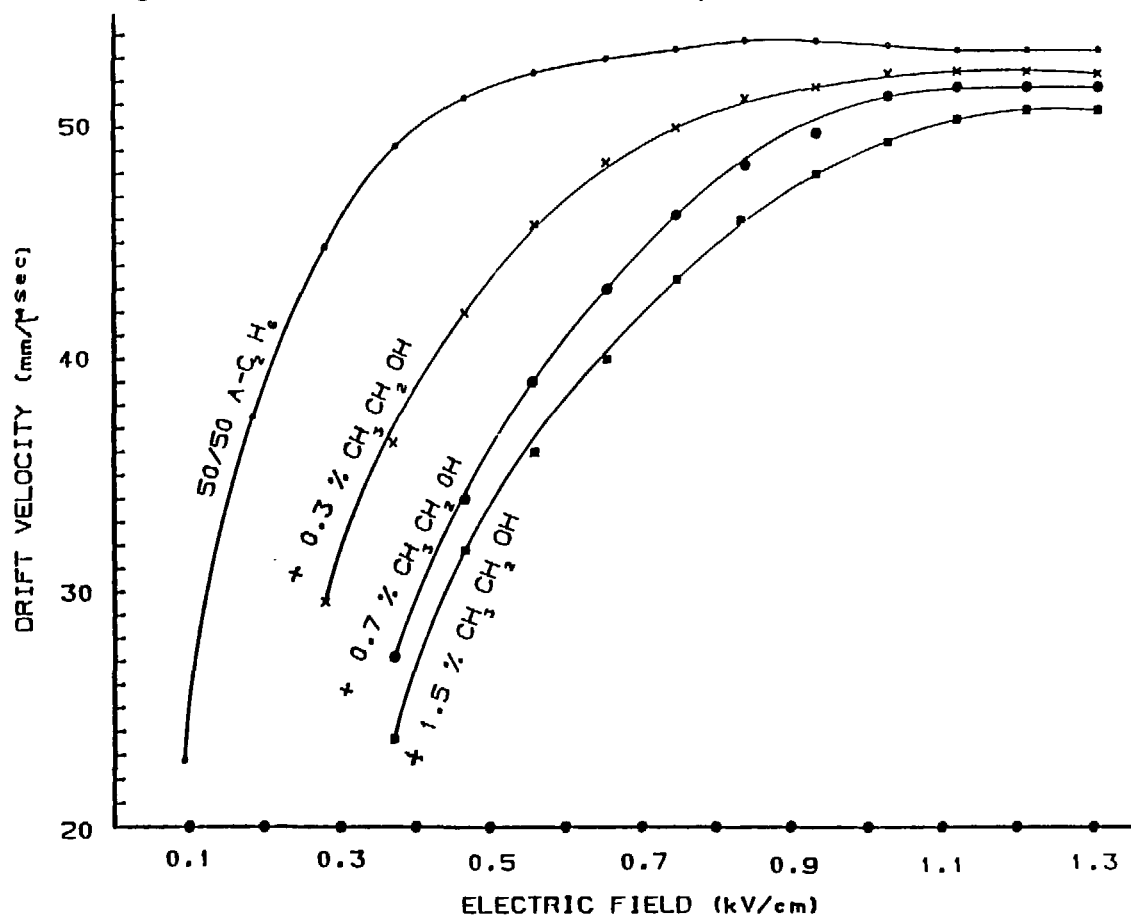
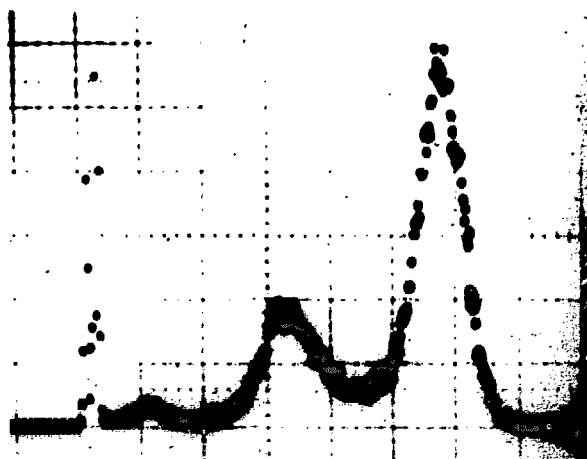
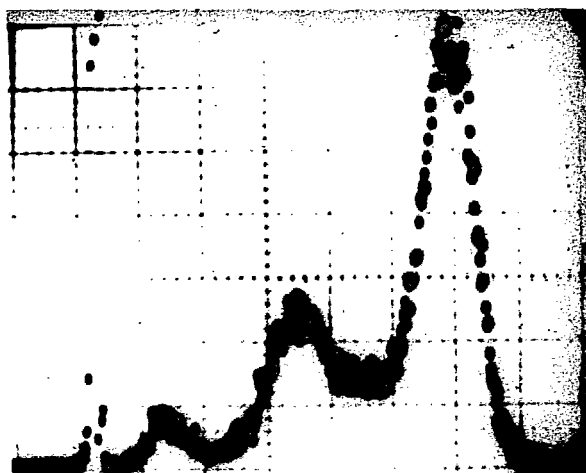


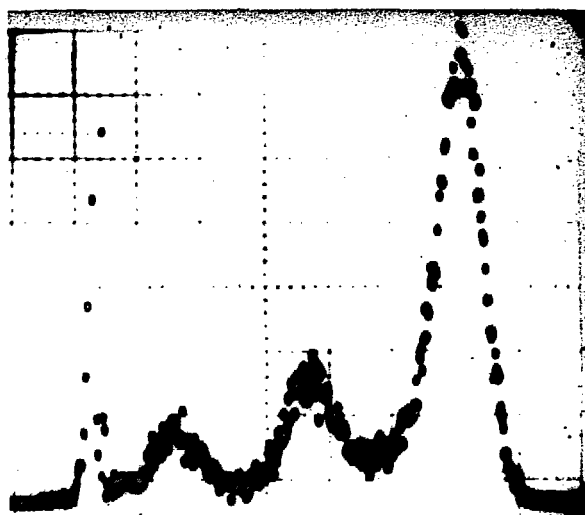
Fig. 11. Electron drift velocity as a function of high voltage for different ethyl alcohol vapor concentration in 50% A/50% C₂H₆ gas mixture.



(a)



(b)



(c)

Fig. 12. Fe⁵⁵ pulse height spectra taken after 1.5 coulomb integrated charge on one wire over a 6 mm full width segment. a. and c.: The spectra taken 6 mm away from the exposed section on either side. b. Fe⁵⁵ spectrum taken on the exposed section of the wire showing slightly worse peak to valley ratio.

running steadily for five weeks or more keeping the current above 0.5 mA with the β -source illuminating a 6 mm length of one wire in the wire drift chamber. The gas gain was kept above 5×10^4 during the runs.

Gas Mixture	Collected Charge (Coulomb/cm ² Wire)
50/50 A-C ₂ H ₆ + 1.5% ethanol	1
50/50 A-C ₂ H ₆ + 0.7% ethanol	2
50/50 A-C ₂ H ₆ + 0.5% ethanol	1.5

During the runs an Fe⁵⁵ source pulse height spectrum was taken periodically to see if the resolution had changed. The most sensitive clue to aging is a reduction of 5.9 KeV peak height to valley (between 3 KeV argon escape peak and 5.9 KeV line ratio). After the above runs there was slight darkening of the anode wire surface. This could be due to coating by impurities. Fig. 12 shows three pulse height spectra of the Fe⁵⁵ source. Fig. 12b is on the aged spot, and Figs. 12a and c are taken at 6 mm distances on both sides of the aged spot. A slightly worse peak to valley ratio is seen in Fig. 12b. This picture was for the 0.5% ethanol case. There was no observable change on the cathode wires.

ACKNOWLEDGMENT

The author would like to express his appreciation to Ayfer Atac for her creative drawings.

REFERENCES

1. S.S. Friedland, Phys. Rev. 74, 898 (1948).
2. M. Atac, T. Hessian, F. Feyzi, IEEE Trans. on Nucl. Sci., Vol. 33, No. 1 (1986) 189.
3. M. Atac, IEEE Trans. on Nucl. Sci., Vol. NS-31, No. 1 (1984) 99.
4. M. Atac and A. Tollestrup, Fermilab Report FN-337 (1981).
5. M. Atac, A. Tollestrup, D. Potter, Nucl. Inst. and Meth. 200 (1982) 345-354.

OUR AGEING EXPERIENCE WITH THE UA1 CENTRAL DETECTOR

Sean Beingessner^{*} , Thomas Meyer⁺ , Vincent Vuillemin⁺ , Michel Yvert^{+,#}

UA1 Experiment

ABSTRACT

The UA1 experiment has been taking data since 1981 and has recorded a total of 770 events/nb. The central detector has now accumulated, in its hottest region, a total charge density of 1 Coulomb per meter without showing any sign of deterioration. A test with a small prototype chamber, which simulates the central detector, is in progress; after a total of 3.8 coulombs per meter no deterioration has appeared. The analysis of a faulty part of this small chamber shows an organic-like deposit on the cathode and a pebble-like deposit containing sulphur on the sense wire.

AGEING STATUS OF THE UA1 CENTRAL DETECTOR

THE IMAGE CHAMBER :

In fig1 and 2 the basic geometry of the UA1 central detector¹ is shown . The 25m³ , 6 meter long cylinder is divided into 6 half cylinders , the 0.7 Tesla magnetic field is horizontal and parallel to the wires (perpendicular to the beam line) . The planes of wires are specially arranged in order to optimize the momentum measurement accuracy (the sagitta being measured as much as possible by the drift time) . The general characteristics of the detector are shown in table 1 . At nominal voltage we have an electric field of 210 kV/cm on the sense wires , 33 kV/cm on the cathode wires and 2.7 kV/cm on the field wires . In fig3 a Megatek display of all the hits of a typical UA1 event is shown . The electronics record for each hit the total charge

* University of Victoria , CANADA

+ CERN , Geneva SWITZERLAND

Annecy (LAPP) , FRANCE

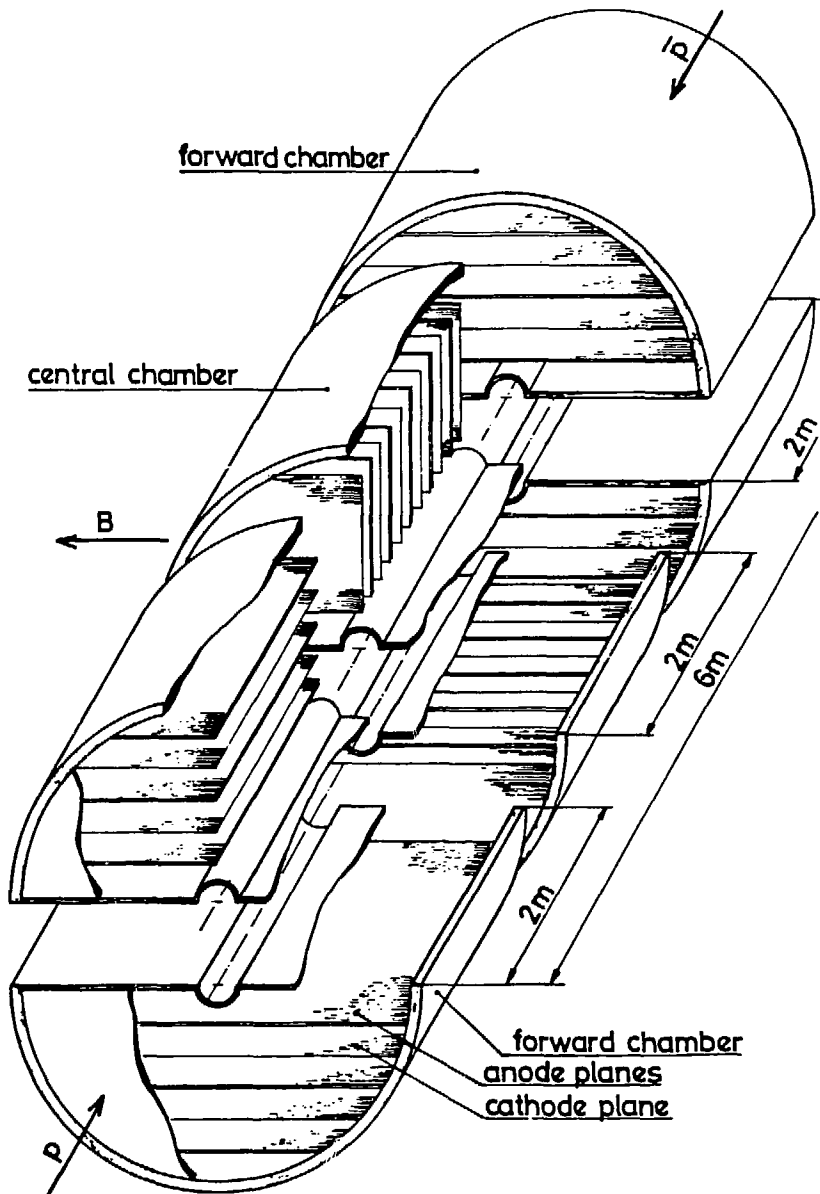


Figure 1
Open , schematic view of the UA1 central detector

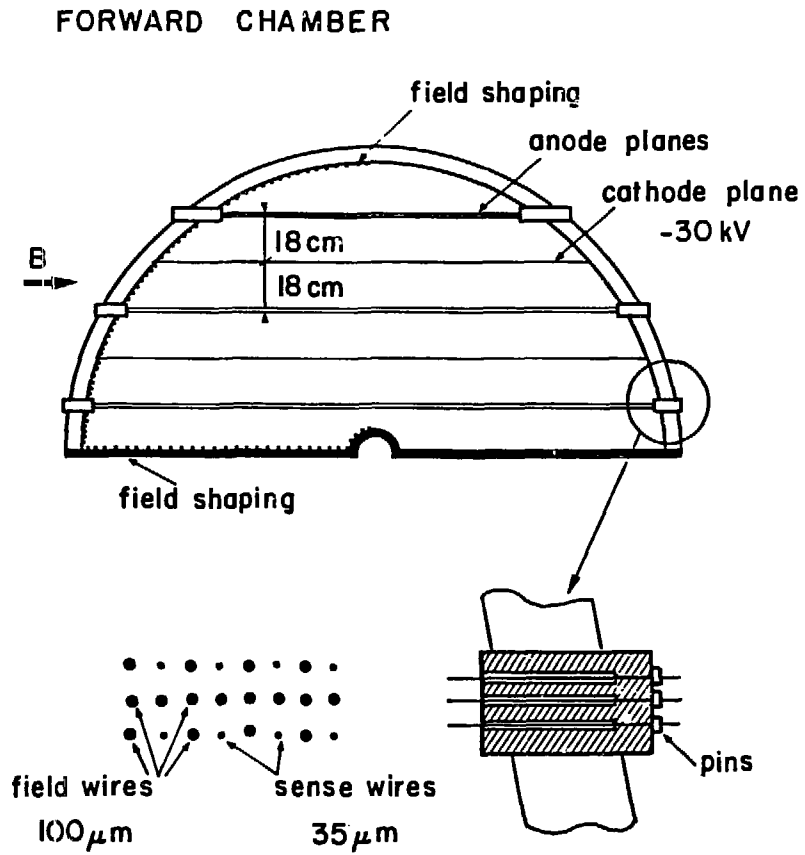


Figure 2
Basic arrangement of the drift cells (UA1 central detector)

General characteristics of the detector

Type	Drift chamber with charge division readout of the second coordinate
Gas mixture	Argon (40%) + ethane (60%)
Drift field and gap length	1.5 kV/cm, 18cm
Drift velocity	5.3 cm/microsec
Drift angle	23^0 at $B = 0.7$ T
Anode plan arrangement	
a) Distance between sense wires	10 mm
b) Wire length	80 cm min., 220 cm max.
c) Sense wire charac.	35 microns Ni-Cr stretched at 80 g
d) Field wire charac.	100 microns gold-plated Cu-Be stretched at 200 g
Cathode plane structure	
a) Distance between wires	5 mm
b) Wire characteristics	150 microns gold-plated Cu-Be stretched at 200 g
Total number of wires	22800
Total number of sense wires	6110

Table 1

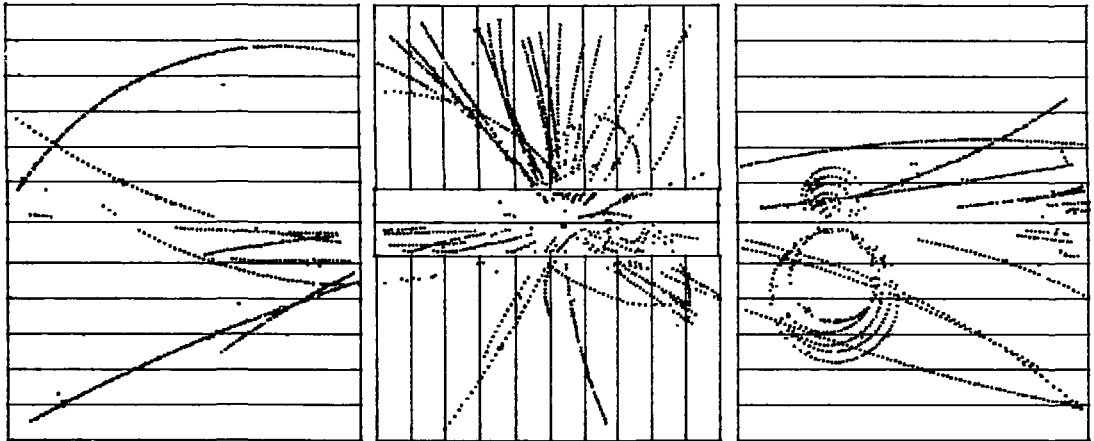


Figure 3
Megatek display of the hits for a typical UA1 event

collected and the 3 space coordinates (wire number , drift time , and position along the wire using the charge division technique) .

CHARGE COLLECTED IN THE HOT REGION :

Since 1981 a large amount of data has been collected , which now amounts (Christmas 1985) to 770 events/nb . At large luminosities we have drawn currents up to $30\mu\text{A}$ in the hottest drift gaps . This has motivated our detailed investigation to estimate the total charge density collected in those parts of the detector.

We observe :

a) The highest currents are drawn in the drift gaps surrounding the beam pipe (not surprising) .

b) The currents are almost linear with the luminosity of fig4; this shows that the beam gas interactions are not the dominant source of current . In the hottest drift gap , which is in the forward chambers , the current is approximately given by

$$I(\mu\text{A}) = 7. \times 10^{-29} \times L$$

where L is the luminosity in $\text{cm}^{-2}\text{s}^{-1}$.

c) Using the hits from min bias tracks we derive the probability for a hit to reach a given wire in the first drift gap of a forward chamber (fig5) , which ranges between 0.6 to 0.7% .

d) The charge division coordinate distribution (fig6) is almost gaussian with a fitted standard deviation $\sigma \approx 0.2\text{m}$ for all forward drift gaps . This width does not change significantly along the beam direction .

From these observations we conclude that the total charge collected from the hottest wires corresponds to a maximum density of $1 \text{ Coulomb m}^{-1}\text{pb}$. Taking the total luminosity recorded and assuming a 20% data taking inefficiency , this correspond to a total collected charge in the hottest forward chamber of about 1 Coulomb per meter (December 1985) . Note that this estimate is accurate within 20% .

SEARCH FOR AN AGEING EFFECT :

Since at this irradiation level , a group has observed very strong ageing effects when using a comparable gas mixture² (we use argon ethane 40 – 60% , they were using argon ethane 50 – 50%) , we have compared the performances of our detector in September 1983 (this is almost at the beginning of the large integrated luminosity runs) with what we observe now (December 1985) . Using the hits from min bias

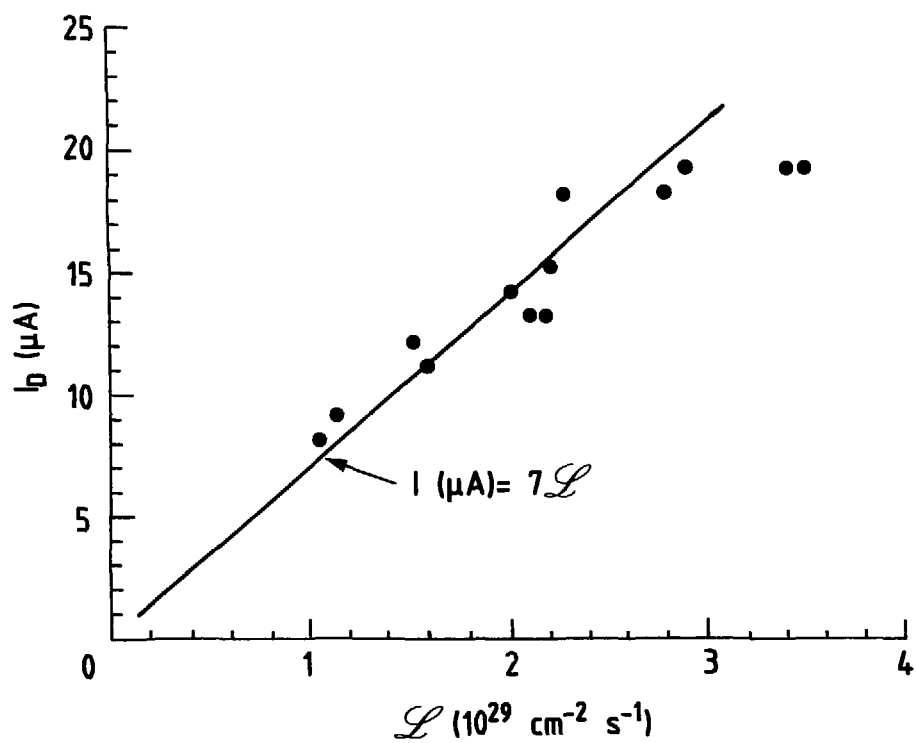


Figure 4
Current in the first drift gap of a forward chamber versus the luminosity

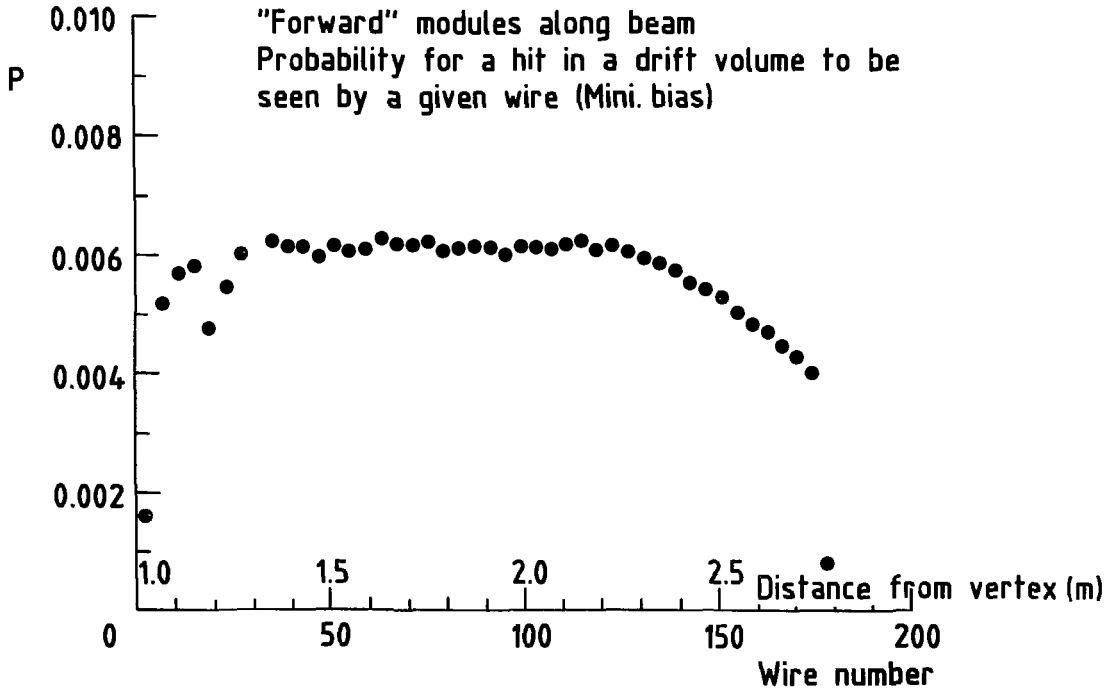


Figure 5

Probability for a hit to reach a given wire in the 1st drift gap of a forward chamber

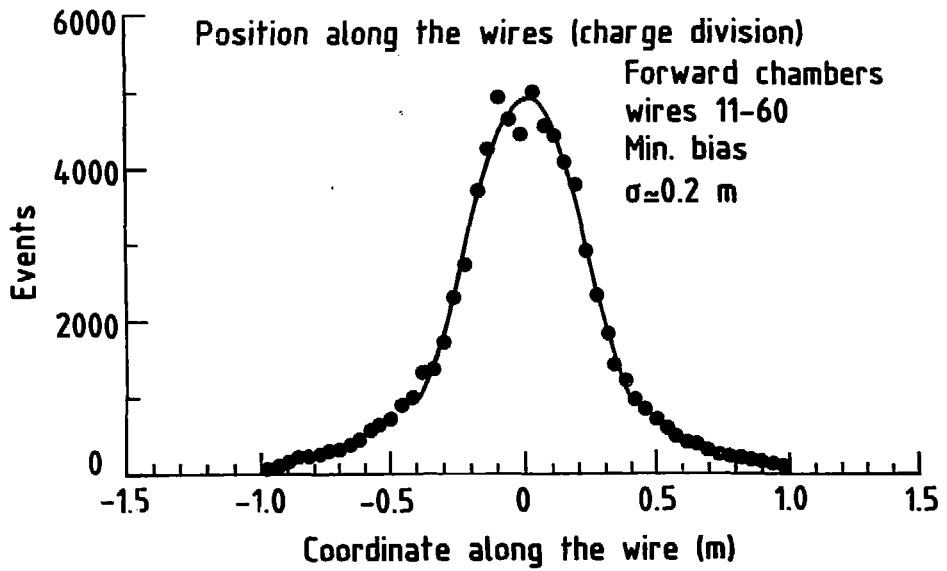


Figure 6
Charge division coordinate (along the wires) in the hottest region

tracks , we select those situated in the hottest region of the detector namely wires 61 to 110 and $|z| < 0.2\text{m}$ (see fig 5 and 6) and plot the charge collected per hit corrected for the track angle (Landau distribution) . In order to compare the two periods , in fig7 we plotted both the September 1983 and December 1985 distributions normalised to the same gain and to one event . In case of serious illness we would expect a deformation of this distribution , that means a change in the width (not in the mean value) . We do not observe any noticeable change .

Another approach is to assume that a possible deterioration of the performances, if any , can be due to very local deposits on the sense wires , a deposit in the immediate vicinity of the avalanche (not a deposit coming from negative ions drifting from far away) . With the magnetic field being directed along the wires the drift direction is tilted 23° with respect to the electric field orientation (see fig8) . Using the fact that since 1981 we ran UA1 with the same field direction , we can expect an eventual deposit not to be uniformly distributed around the sense wires (see fig8) . We have therefore inverted the magnetic field , such that the drift angle becomes -23° and hence we use the "young" part of the sense wires . In fig9 the same distribution as for fig7 but for hard trigger tracks and for normal and inverted magnetic field (december 1985 data) is shown . Again we do not observe any sizable change in the width of these distributions.

Our conclusion from this study is that up to now no noticeable change is observable in the UA1 central detector. Nevertheless since the 1 Coulomb per meter charge density collected up to now has caused trouble to other groups , we are currently artificially ageing a small test chamber in a controlled way in order to better forecast the ageing process in the UA1 central detector .

AGEING A SMALL TEST CHAMBER

EXPERIMENTAL CONDITIONS :

We have built a small test chamber which presents the same features as the UA1 central detector :

- same drift gap of 18cm
- same material whenever possible (we added a mylar window)
- same wire diameter , wire material , and wire configuration
- same potential (i.e. electric field)
- same gas mixture (40 - 60% argon ethane) , not recirculated , non purified

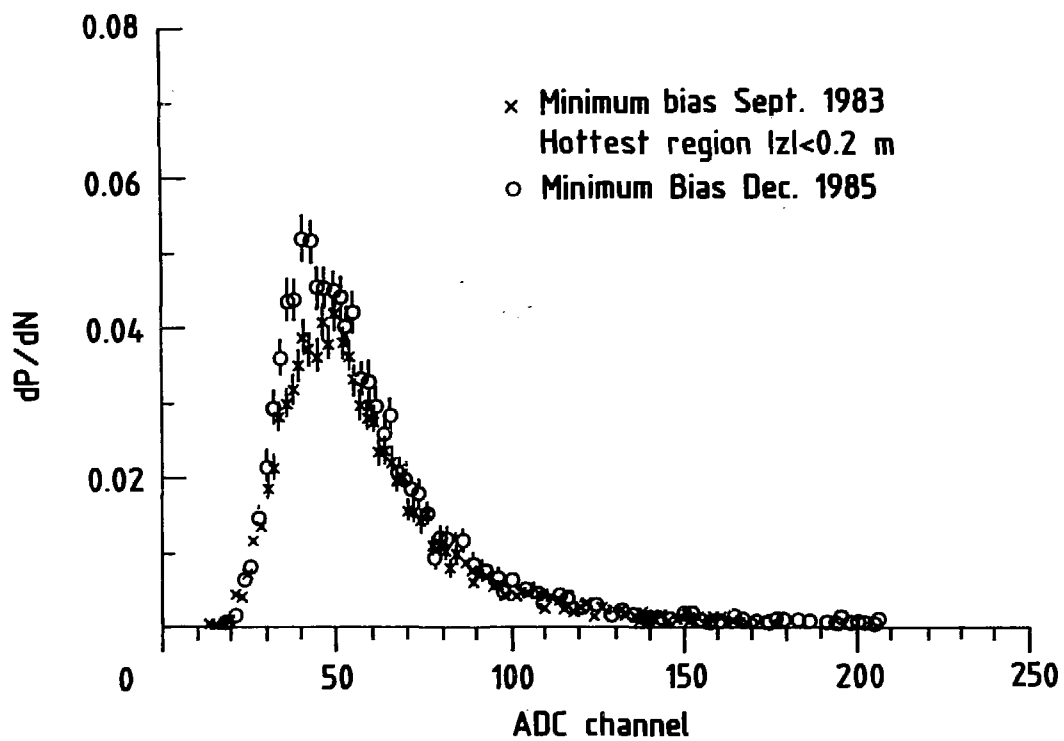
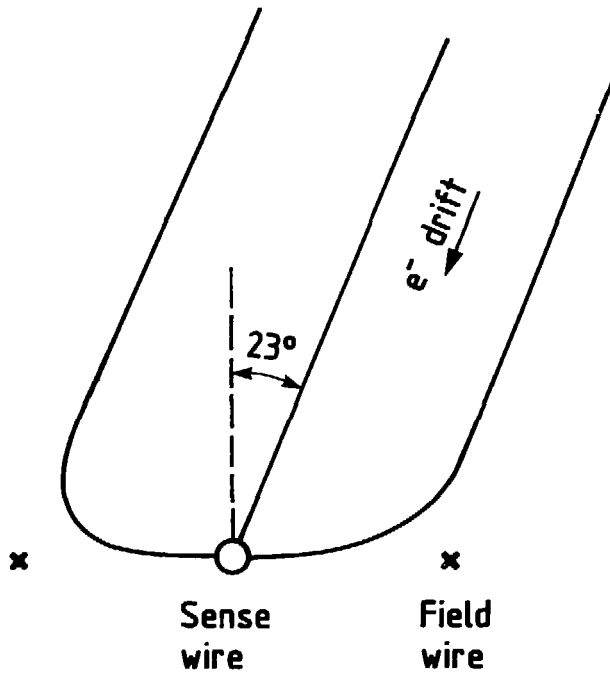
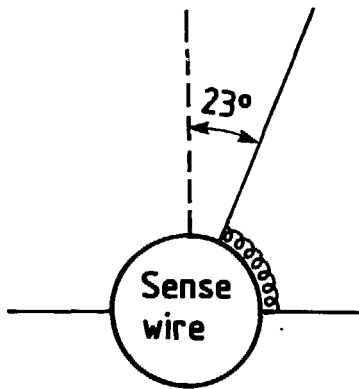


Figure 7
Minimum bias trigger , Landau distribution obtained in sept 1983 and in dec 1985
(hot region)



The sense wires
have not the same
"age" all around



Enlarged view

Figure 8
Sketch of the drift lines in the presence of a magnetic field

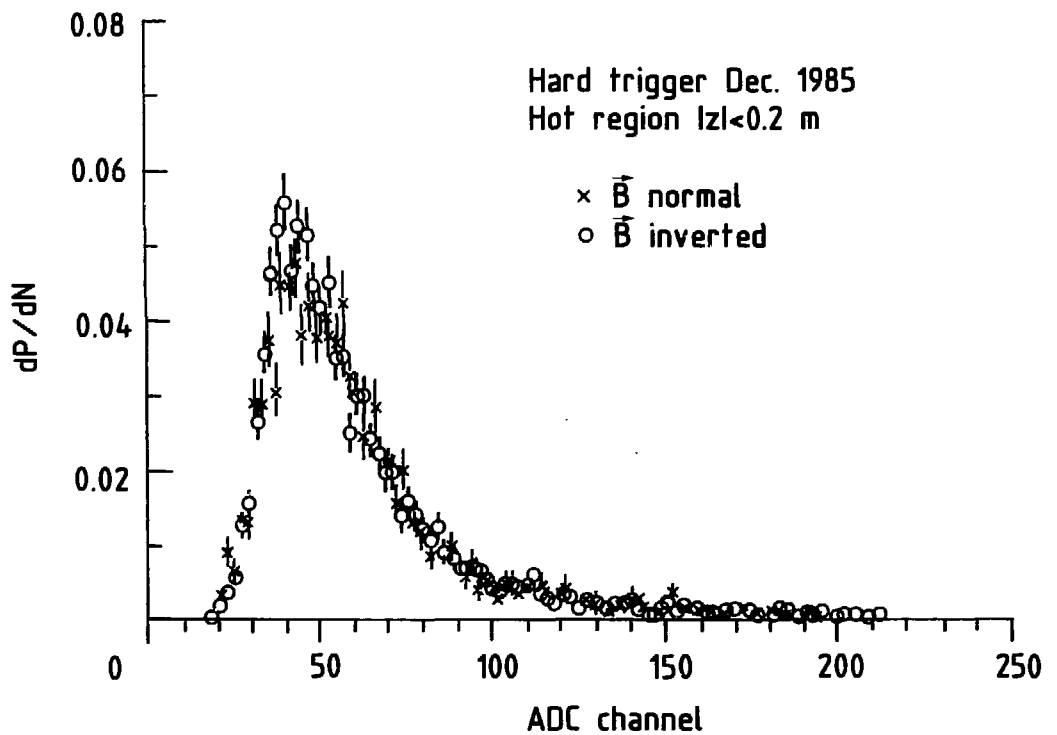


Figure 9
“Hard” trigger, Landau distribution for normal and inverted field (hot region)

The difference lies mainly in the size of the chamber which has only 24 sense wires . To artificially age this test chamber we irradiate it from one side using a Sr^{90} source situated outside the chamber (the source flux is then attenuated by the wall). The schematic layout is shown in fig10 .

In order to control the evolution of the chamber we have:

1) measured the current collected on the sense wires when the Sr^{90} source is active , this measurement is shown in fig11 , we note :

a) the first and last wire have a higher gain than the others . To avoid any edge effect we have grounded the first and last field wire in order to reduce their gain to a negligible value.

b) two wires (9 and 10) were hot , however we left them untouched until they went into discharges and sparks .

2) measured the density of radiation produced by the Sr^{90} source inside the chamber . This profile is shown in fig12 with a gaussian fit of $\sigma = 3.24\text{cm}$

3) from time to time we remove the Sr^{90} source to record a Fe^{55} spectrum (in self trigger mode) on four reference wires (wires 2 , 9 , 16 and 22) . We obtain the peak position and width of the spectrum by fitting a gaussian shape on the points situated around the maximum and containing at least 30% of the maximum value . This procedure is illustrated in fig13.

OPERATIONS :

After 300 hours of irradiation , we had a breakdown on wire 9 , which is far from being the most irradiated one . Since it was hot already from the beginning , we conclude that the breakdown was due to a mechanical defect . We tried to clean the surrounding cathode and field wires without success . Finally we decided to remove the whole cell corresponding to wire 9 for later analysis .

At the time of this presentation , our small chamber is still under irradiation and after a collection of more than 3.8 Coulombs/m does not show any change in resolution as shown in fig14 , where we plot the σ/mean ratio for the Fe^{55} peak as recorded on the most irradiated wire .

ANALYSIS OF THE FAULTY CELL :

We have examined the wires of the faulty cell in a scanning electron microscope without finding any mechanical defect . The field wires do not show any significant

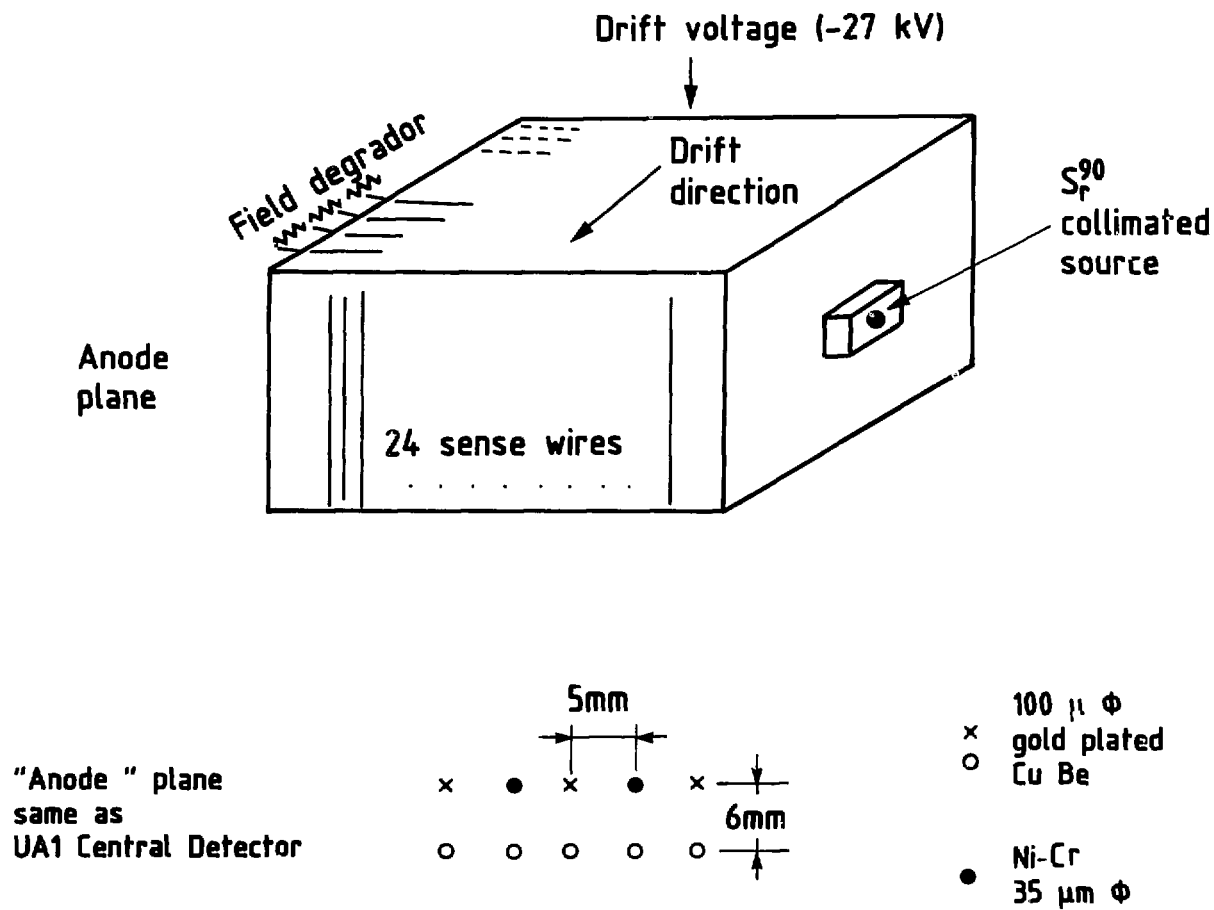


Figure 10
Schematic layout of our small test chamber set up

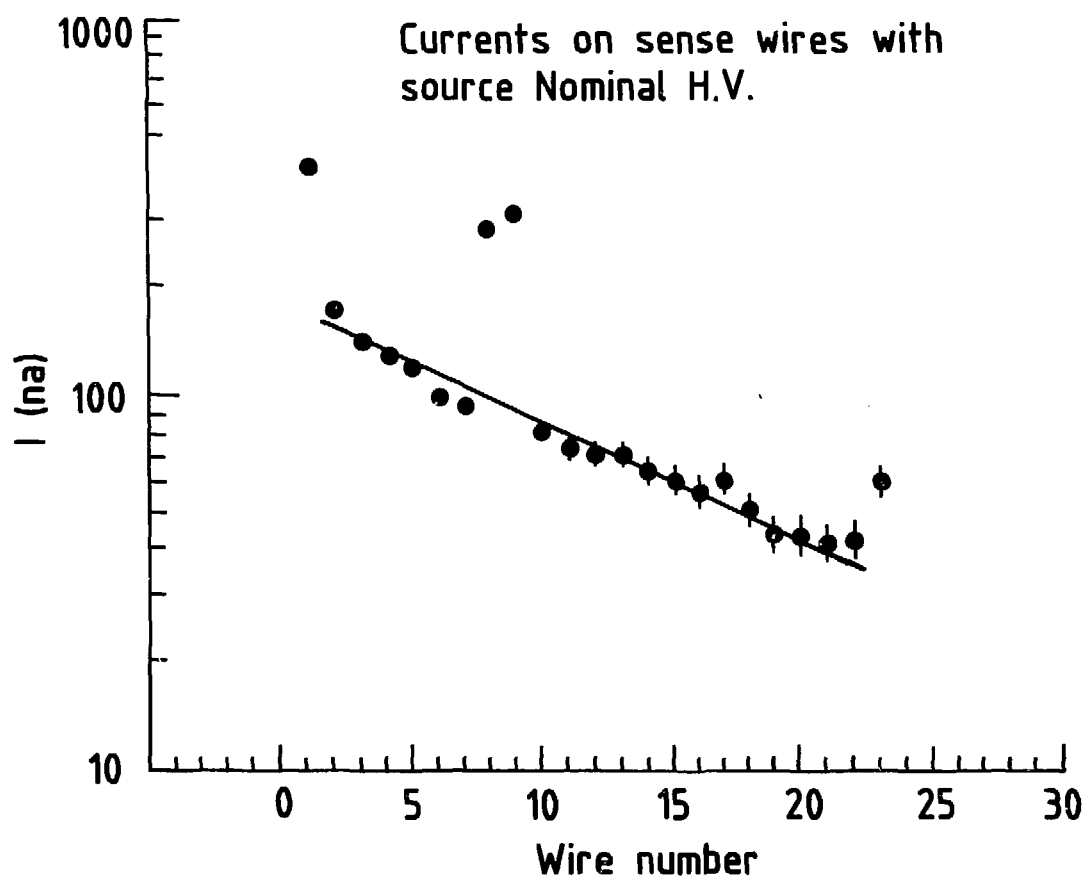


Figure 11
Measured current on the sense wires in the presence of the Sr^{90} source

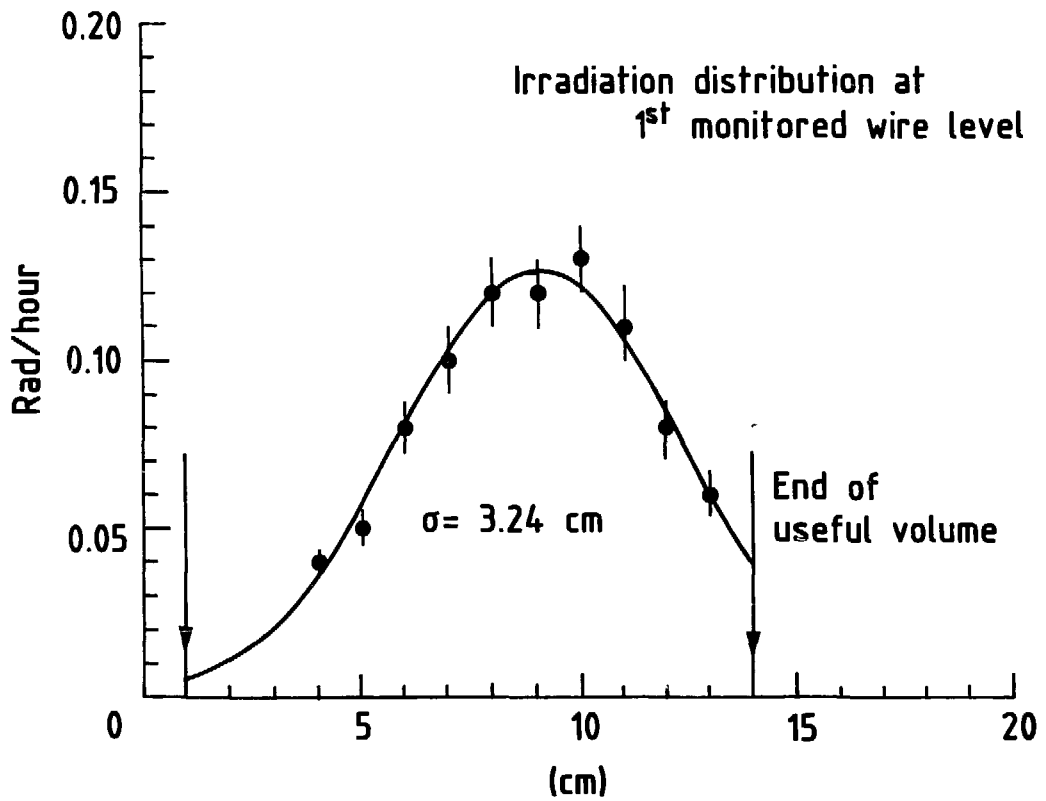


Figure 12
Profile of the Sr^{90} source inside the test chamber
(at the level of the most irradiated wire)

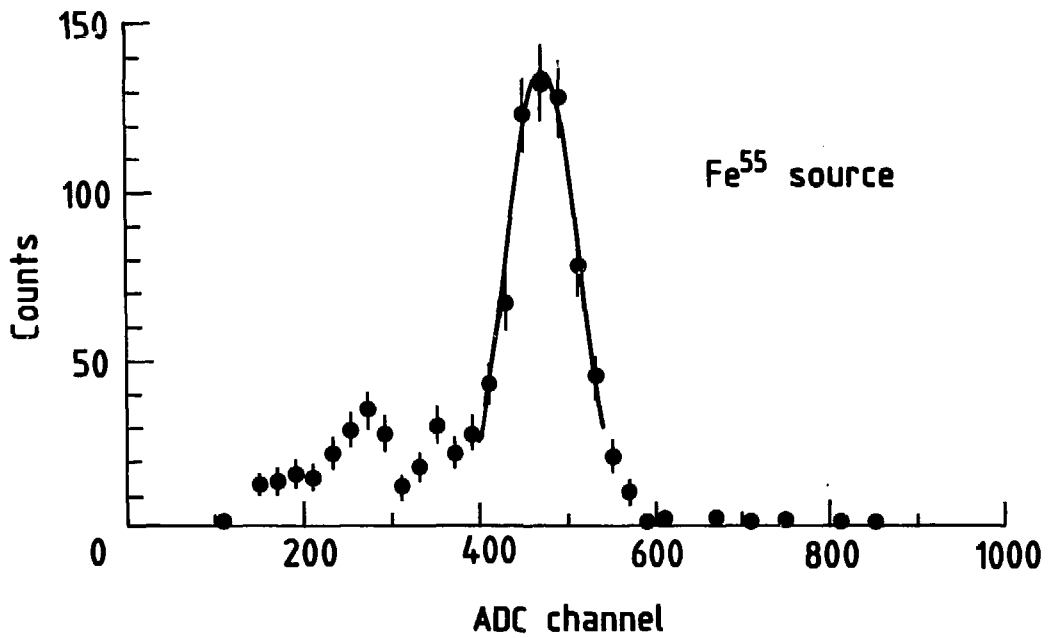


Figure 13
A typical Fe^{55} spectrum and the gaussian fit of the peak

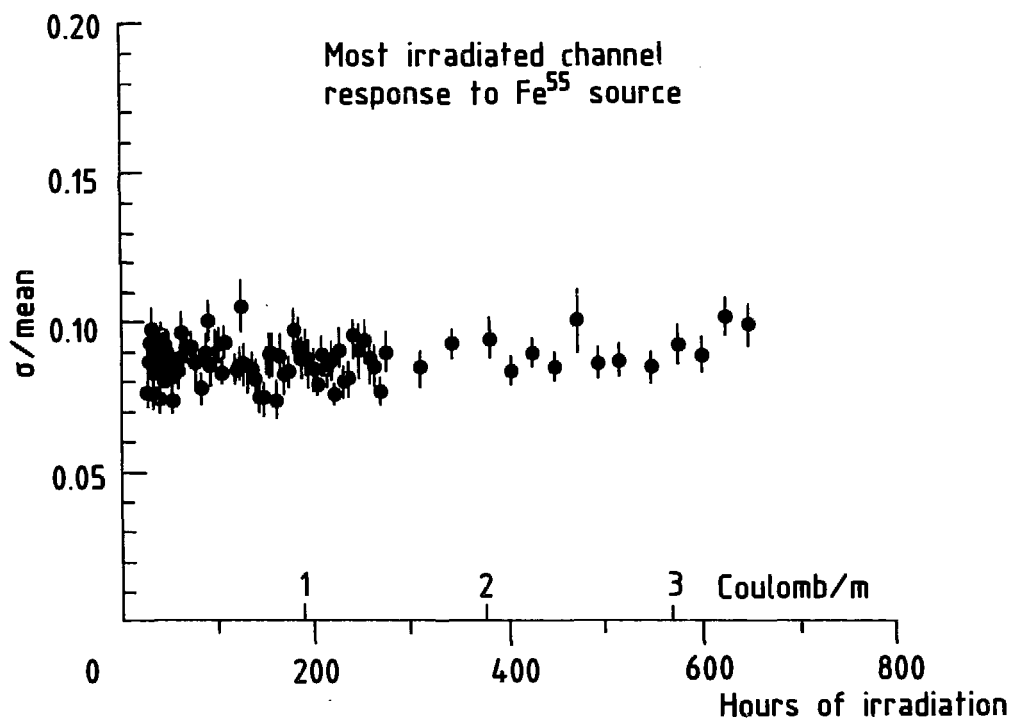


Figure 14
Resolution (σ/mean of the Fe^{55} peak) for wire 2 versus irradiation

deposit , while on the cathode wires we found a rather smooth coating in the vicinity of the breakdown region (fig15) . The X-ray analysis (fig16) of this coating does not show any substance with an atomic number above 9 (which is the detection limit of the analyser we used) and therefore we conclude that the deposit is probably made of carbon containing polymers . The sense wire analysis shows only tiny deposits with a pebble like shape in the breakdown region (fig17) . The corresponding X-ray analysis (fig18) shows clearly the presence of sulphur in this region . The presence of this sulphur is a complete mystery to us , it might be linked to the observation made by Francesco Villa at this workshop that the DELRIN tubes we use contain sulphur , which is a component of an unmolding agent used in the fabrication process of these tubes.

SUMMARY

Our conclusions can be summarized with the following points:

- The UA1 central detector does not show any ageing sign , even if in some hot places the total charge density collected up to now approaches 1 Coulomb per meter.
- A test chamber with the same working conditions as the UA1 central detector is still alive with no significant change in resolution after the collection of a total charge density of more than 3.8 Coulombs per meter .
- The analysis of a faulty region in the test chamber shows :
 - no mechanical defect
 - no deposit on the field wires
 - an organic-like deposit on the cathode wire (in the problem region)
 - a pebble-like deposit (in the problem region) containing sulphur on the sense wire .

The ageing test of the small chamber is still in progress , and we intend to continue it in order to reach a better understanding of the ageing process in the UA1 central detector .

ACKNOWLEDGEMENTS

We highly appreciated the kind cooperation and help of J.D.Adam , whose competence and skill with the CERN electron microscope was found invaluable.

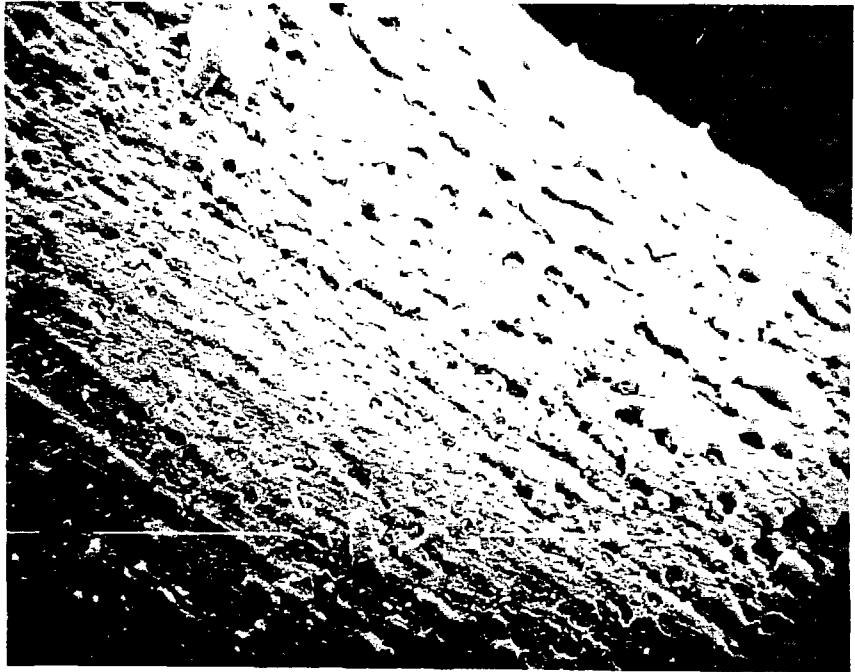


Figure 15
Cathode wire (magnification 2800) in the breakdown region

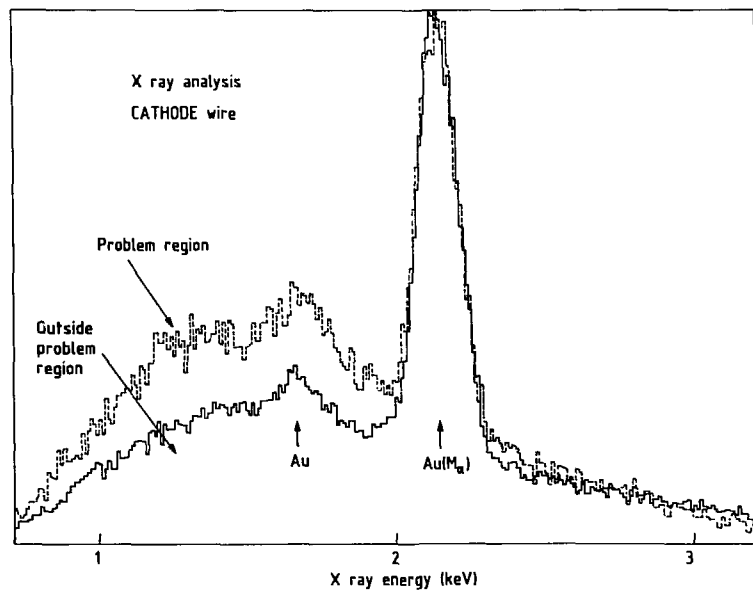
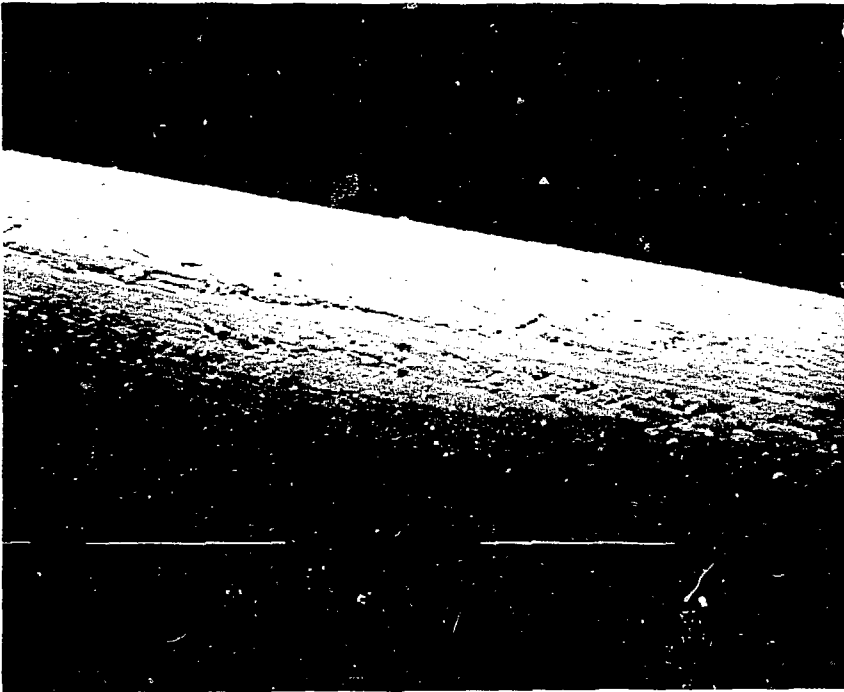


Figure 16
X-ray spectrum analysis of the coating on the cathode wire



Sense wire
breakdown region



Sense wire
outside
breakdown region

Figure 17
Sense wire (magnification 2500) in and outside the breakdown region

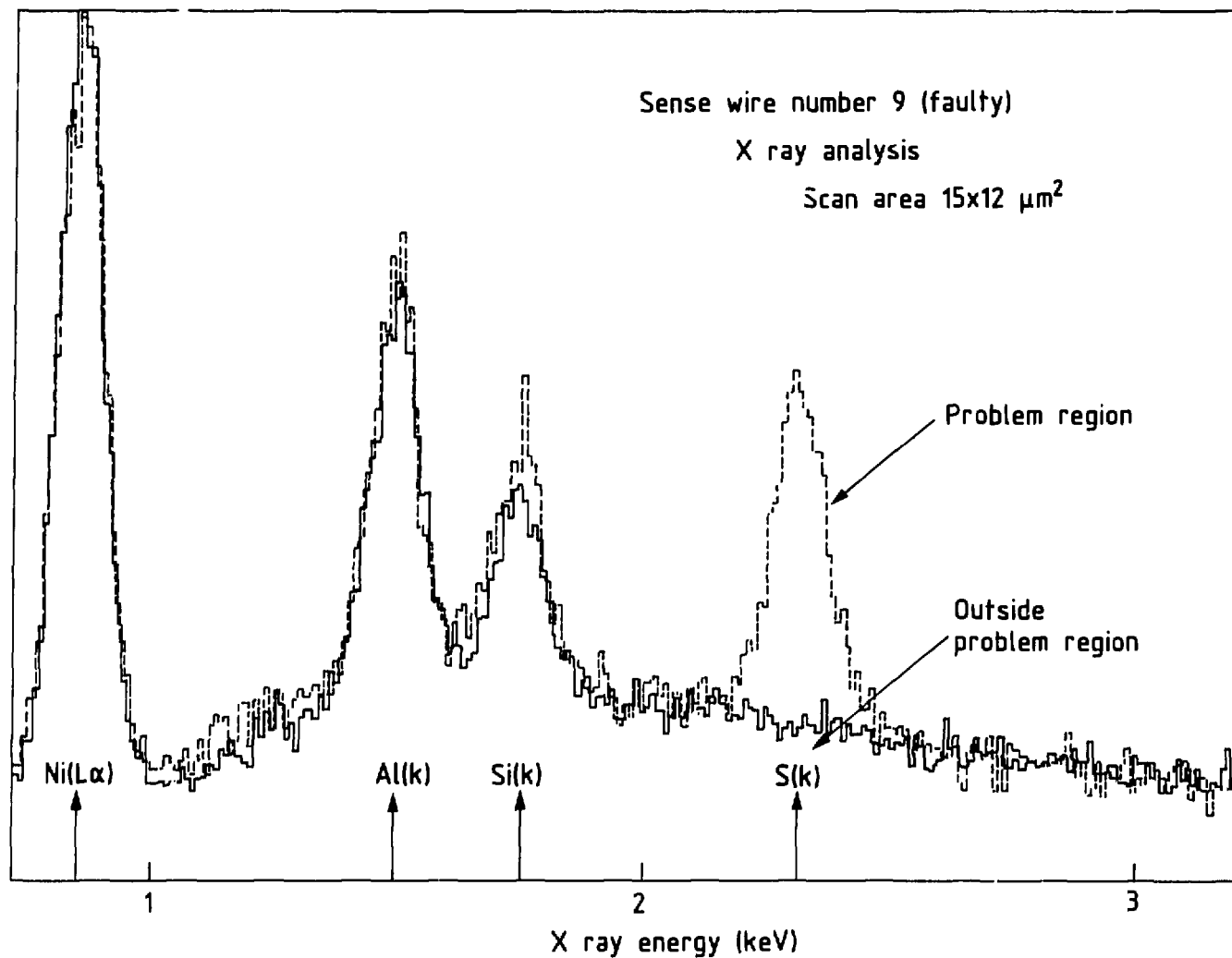


Figure 18
X-ray spectrum analysis of the deposits on the sense wire

REFERENCES

1) For a description of the UA1 central detector and its performances please refer to :

- A.ASTBURY et al , CERN/SPSC/78 – 06 , SPSC/p 92 (30 jan 1978)
- The UA1 central detector
M.CALVETTI et al CERN – EP/82 – 44
Presented by M.CALVETTI at the Int.Conf. on instrumentation for
colliding beam physics
SLAC , 17 – 23 Feb 1982
- The construction of the central detector for an experiment at the CERN $\bar{p}p$
collider
M.BARRANCO et al NIM 176(1980)175

2) J.ADAM et al NIM 217(1983)291

EXPERIENCE WITH THE UA1 MICRO VERTEX DETECTOR IN THE SPS COLLIDER

UA1 Collaboration

presented by

Darrel Smith *
Physics Department
University of California
Riverside, California , 92521

Abstract

The design and operation of a small pressurized drift chamber in the SPS Collider is described. The cylindrical chamber with inner radius of 3 cm is concentric with the beam axis. The chamber received radiation corresponding to 6×10^{-4} C/cm on the sense wires.

INTRODUCTION

The micro vertex detector was designed to tag heavy quark decays in the UA1 experiment at CERN. It was first installed in August 1985 for the Fall 1985 SPS collider run. After one month of running, the detector was removed for modifications. After removal, we made a detailed examination of the chamber. A description of the chamber and the running conditions in the collider are given below.

CHAMBER AND CELL DESIGN

The UA1 micro vertex detector (MVD) is one of a small family of detectors used for heavy flavor tagging¹⁻³. It is a cylindrical jet-style drift chamber mounted inside the UA1 central detector⁴. Details of the micro vertex detector electronics and resolution studies have also been reported⁵.

* Work supported by the U.S. Department of Energy

The wires in the micro vertex detector run parallel to the cylinder axis (i.e. the beam axis) and are strung between two 12 mm thick stesalit plates 80 cm apart. The detector covers 2π in azimuth with an inner and outer radius of 3.0 and 8.3 cm respectively. The chamber was divided into 16 cells in the azimuthal plane (figure 1). The chamber was then enclosed in an aluminum pressure vessel. The parameters of the microvertex detector are listed in table 1.

The geometry of one of the drift cells is shown in figure 2. Each cell contains 16 sense wires alternating with 17 field wires. The sense wires are staggered by $\pm 100 \mu$ relative to the field wire plane. The spacing between field and sense wires and between the cathode wires is 1.58 mm. The innermost sense wire is 33 mm from the chamber axis. The maximum drift length is 16 mm which limits the longitudinal diffusion of drift electrons. The inner and outer racetracks (IRT and ORT) were constructed to degrade the high voltage to ground in the radial direction. The ORT also maintains the wire tension.

OPERATING CONDITIONS

The operating conditions for the micro vertex detector were determined from measurements made on 2 previous chambers. The gas used in the chamber was a mixture of 53%-47% Argon-Ethane. It was supplied from pre-mixed bottles where the purity of the argon and ethane were better than 99.996% and 99% respectively. We do not know the composition of the remaining 1% of ethane. The gas flowed from the premixed gas bottle to the aluminum pressure vessel through 50 m of stainless steel and a few meters of teflon. The volume inside the pressure vessel was 28 liters. The flow rate through the vessel was 20 l/hr and the gas was vented. The gas pressure was 3.0 atmospheres. The chamber was assembled without a provision for evacuating the gas (i.e. no vacuum pump connected). There is also no known source of oils or grease that can be introduced into the chamber.

The electric field between cathode and sense wires was chosen in order to transport the electrons at a saturated drift velocity and still maintain electrical stability. The E/p value of 1.85 kV/cm-atm corresponds to a drift velocity of 51 μ /ns. The electric field at the surface of the sense(anode), cathode, and field wires was 442, 34.8, and 6.0 kV/cm respectively.

The radiation incident upon the chamber was generated by proton-antiproton collisions at a rate of 10^4 interactions/sec. The approximate gain per primary electron was $4-6 \times 10^4$. The gain was determined from integrating the average pulse due to a minimum ionizing particle at the preamp output. The average pulse height for a minimum ionizing particle traversing the middle of the chamber was 80 mV for the running conditions described in table 1. The number of charged particles as a function of angle from the central to the forward region of the chamber varies as $1/\sin\vartheta$ where ϑ is measured from the beam direction. This means that the charge on the wires increases toward the ends of the wires.

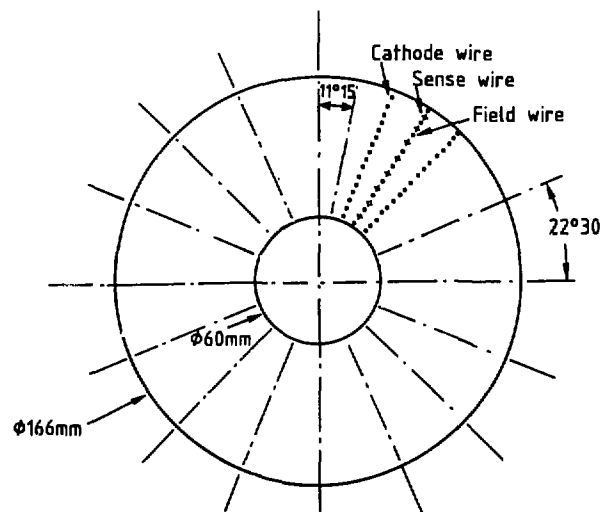


Figure 1 Shows the arrangement of the 16 drift cells on the stesalit endplate. The wire/pin positions are shown for one cell.

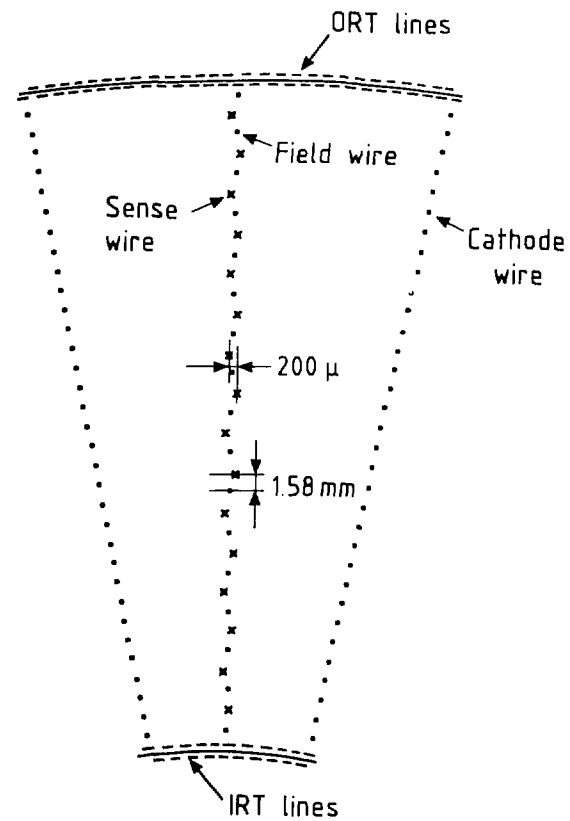


Figure 2 A single drift cell.

Table 1

Parameters of the micro vertex detector

Inner radius	25 mm
Outer radius	89 mm
Wire length	800 mm
Maximum drift distance	16 mm
Number of cells	16
Number of sense wires per cell	16
Total number of sense wires	256
field wires	272
cathode wires	528
Radial position of the first sense wire	33 mm
last sense wire	80 mm
Spacing between field/sense wires	1.58 mm
Staggering	100 μ
Sense wire material	23 μ (Nicotin a Ni-Co-Cr-Mb-Fe alloy)
Field/Cathode wire material	150 μ (Cu-Be)

Running Conditions:

Drift Field	1.85 kV/cm-atm
Field wire voltage	-2.15 kV
Gas mixture	Argon-Ethane (53%-47%)
Pressure	3 atmospheres
Drift velocity	51 μ /ns

The current due to the ions drifting toward the negative high voltage (the cathode wires, ORT and IRT) was monitored as a function of the instantaneous luminosity. Figure 3 shows the current varying linearly from 20 μA to 120 μA as a function of luminosity. In the collider, the luminosity is increased by increasing $I_{\bar{p}}$, the antiproton current. The beam gas, however, is due to I_p , the proton current, because $I_p/I_{\bar{p}} \approx 10$. Since the current is observed to follow the luminosity, it must be due to the $p\bar{p}$ collisions and not the beam gas. It was calculated that we would collect 1 C/m, on the average, for 500 nb^{-1} of data. The chamber operated for 30 nb^{-1} for an average collected charge of 6×10^{-4} C/cm.

OBSERVATIONS

After one month in the SPS collider, the micro vertex detector was removed for modifications and examined. A cathode wire was cut from the chamber and a photograph of the 150 μ diameter wire was made using an electron microscope (figure 4). No growth was observed on the surface of the wire. The wire appeared the same as when it was installed. A sense wire was not cut for a similar test because of the difficulty involved in replacing it. The field and sense wires were also observed to have no growth on their surface.

We did not expect to see any radiation damage for the amount of charge collected (6×10^{-4} C/cm) and this is consistent with what we observed. We also observed that the current monitored by the high voltage system was directly proportional to the rate of $p\bar{p}$ collisions and not due to beam gas.

ACKNOWLEDGEMENTS

The people who have worked on the micro vertex project are L. Bassi, P. Cennini, F. Ceradini, R. Frey, L. Gately, D. Gee, W. Guryn, M. Ikeda, A. Kernan, W. Ko, F. Lacava, K. Ley, J.P. Merlo, K. Morgan, M. Moricca, Th. Muller, G. Piano-Mortari, G. Muratori, D. Pitman, C. Rubbia, I. Sheer, and D. Smith. We thank the CERN technicians M. Delattre, J. Lecoultre, G. Gendre, and D. Lacroix who worked so hard to construct our chamber. We received advice and assistance from our UA1 colleagues; in particular, G. Ciapetti, W. Kozanecki, T. Meyer, Martti Pimia, B. Sadoulet, V. Vuillemin, and M. Yvert. We thank S. Lazic and J.-C. Labbé for their technical support. We appreciate the help of students J. Boudreau, M. Lai, D. Raftery, W. Sweeney.

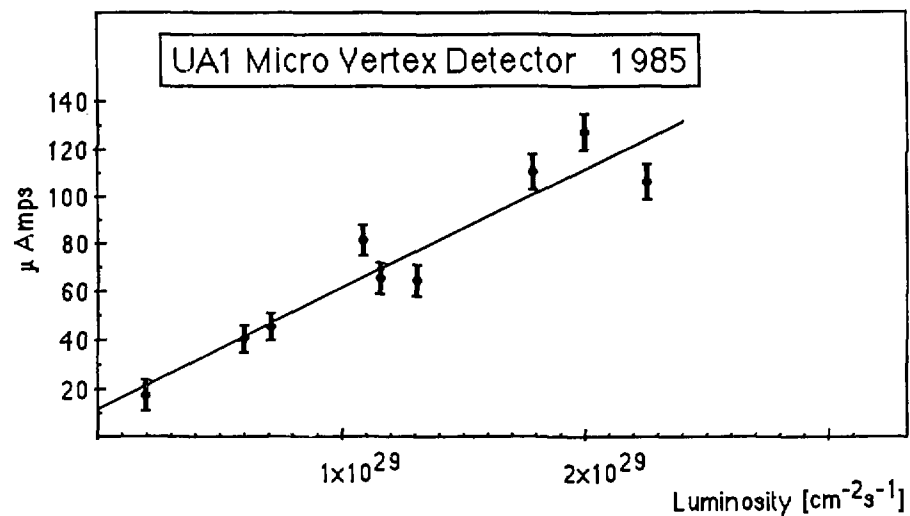


Figure 3 The current, due to drifting ions, as a function of the instantaneous luminosity.



Figure 4 An electron microscope photograph of a 150μ Cu-Be-Au cathode wire near the outer radius after one month in the collider.

References:

- [1] J.A. Jaros, Proc. of the Int. Conf. on Instrumentation for Colliding Beam Physics, Stanford, CA, SLAC Report 250 (1982) 174.
- [2] D.M. Binnie et al., Nucl. Instr. Meth. 228 (1985) 267.
- [3] CLEO experiment. T. Jensen, private communication.
- [4] UA1 Collaboration, G. Arnison et al., Physics Letters 126B (1983) 398.
- [5] IEEE Symposium on Nuclear Science, San Francisco, Oct. 23-25, 1985, in press. CERN EP-Report 85-193.
- [6] Stesalit -- Tradename for Stesalit 4412, a 60% fiberglass and 40% epoxy compound possessing good mechanical and machining properties and low outgassing.

WIRE CHAMBER DEGRADATION AT THE ARGONNE ZGS§

W. Haberichter and H. Spinka

High Energy Physics Division

Argonne National Laboratory, Argonne, Illinois 60439

February 24, 1986

Abstract

Experience with multiwire proportional chambers at high rates at the Argonne Zero Gradient Synchrotron is described. A buildup of silicon on the sense wires was observed where the beam passed through the chamber. Analysis of the chamber gas indicated that the density of silicon was probably less than 10 ppm.

Introduction

A number of multiwire proportional chambers (MWPC's) were constructed at Argonne National Laboratory for use in $\pi\pi$ and pp elastic scattering spin experiments at the Zero Gradient Synchrotron (ZGS). The first few of these chambers were built in 1971 and 1972, and the first major experiment to use them was in 1973.¹ Since that time, they have been used almost continuously in 17 different experiments at the ZGS and the Clinton P. Anderson Meson Physics Facility at Los Alamos (LAMPF), with only minor modifications in the chamber construction or the electronics. An upgrade to the electronic connectors and the electronics for these chambers is currently in progress in preparation for an upcoming experiment at Fermilab.

For most of the ZGS experiments and some of the LAMPF experiments, three $128 \times 128 \text{ mm}^2$ MWPC's were located in the beam, a few meters upstream of the experimental target, to record the incident beam particle trajectories. Long run times were needed in order to collect sufficient elastic scattering events for the spin measurements. Typical beam intensities ranged from 10^4 to 10^6 per second, averaged over the accelerator cycle of several seconds. Instantaneous rates were up to about $5 \times 10^6/\text{sec}$. Experiments usually ran continuously for one to four months with interruptions for maintenance and repair of accelerator and experimental apparatus. Therefore, in a typical experiment, the total number of incident beam particles might be on the order of 10^{12} in an area of about $1\text{-}2 \text{ cm}^2$.

The efficiency of the MWPC's in the ZGS beam was observed to decrease monotonically with time. Areas of the chambers that were not in the direct beam were found to have good efficiency, whereas in the center of the beam it could be 20% or less. When the chambers were disassembled, deposits were seen on both the sense wires and the high voltage (cathode) foils. This paper describes some of our tests to understand the cause of the deposits and our unsuccessful attempts to eliminate the problem. Ultimately, the chambers were moved relative to the beam a number of times, and the sense wires were changed at the end of the experiment in order to decrease the impact of these problems on the spin measurements.

Description of Detectors

The MWPC's located in the ZGS beam were all of identical construction. Each chamber contained both horizontal and vertical sense wires of 20 μm diameter gold-plated-tungsten with a spacing of 2.0 mm. Near each edge of the chamber, three additional wires of increasing diameter were located parallel to the sense wires to prevent electrical breakdown to the G10 frames. Initially, the wires were soldered and epoxied to printed circuit boards that were part of the chamber frames. Later, when the wires were replaced, they were soldered only. A standard lead-tin eutectic, resin-core flux solder was used. The active area of these chambers was $128 \times 128 \text{ mm}^2$, and the total area was $140 \times 140 \text{ mm}^2$.

The G10 chamber frames, and thus the gap spacing between the cathode plane and the anode sense wires, were $0.25" = 6.4 \text{ mm}$ thick. The frames containing the wires consisted of a 1.6 mm thick printed circuit board of G10 epoxied to a 6.4 mm thick frame of G10; then it was machined to the proper thickness. The individual frames were bolted together with nylon threaded rod and nuts. The initial design called for O-rings to make the gas seal. Later, this seal was made with silicon-rubber glue (RTV) outside the O-ring groove.

The outer gas windows were 50 μm mylar covered with nontransparent mylar tape of about the same thickness. The cathode planes were initially aluminized mylar of thickness 50 μm . Early experience with these chambers in the beam showed that the aluminum was eventually etched away near the high voltage connection, presumably from the relatively high currents in these chambers due to the beam. The aluminum was also etched away in isolated spots, probably associated with "hot spots" or sparks. Additional problems were encountered in the area located in the direct beam, as described below. For these reasons, the cathode planes were changed to 50 μm aluminum foil for the beam chambers. NIM high voltage power supplies designed by T. Droegge were used with series protection resistors of $9 \text{ K}\Omega$ on these MWPC's.

Various gases were tried with these chambers. Complexities of the gas mixing systems for the "magic gases" led to the adoption of argon-carbon dioxide mixtures. Based on the length of the high voltage plateau, a 65%-35% mix of Ar-CO_2 was chosen. Problems with chamber sparking and frequent breakage of the sense wires were solved with the addition of 0.4 - 0.5% Freon - 13 B1 (CBrF_3). Research grade gas was ordered in high pressure 1A gas cylinders from commercial vendors. The gas came premixed and chemically analyzed to verify its purity.

The chambers were operated at atmospheric pressure. A gas control panel, containing pressure regulators and flowmeters, was located near the gas bottles about 10m from the chambers. Polyflo tubing was used for most of the distance between the control panel and chambers, with a short ($\sim 10\text{cm}$) length of tygon tubing at the chambers to reduce mechanical stresses. Similar tubing brought the exhaust gas back to the control panel, where it was bubbled through mineral oil before venting. Gas flowed to each chamber separately; they were not connected in series. The total gas volume of each chamber, exclusive of the tubing, was about 900 cc. The gas flow gave a change in this volume on the order of once a day.

The threshold on the electronics² for these chambers was equivalent to 1 mV across a 100 Ω input resistor. Allowing for the fact that the operating voltage was 100-200V above the knee in the plateau curve, the number of collected electrons per beam particle was roughly 10^6 - 10^7 . Estimating the number of primary electron-ion pairs (essentially all beam particles were close to minimum ionizing), then the total gain of the chambers per primary electron was approximately 10^4 . The operating voltage was 4400V at the ZGS and 4200V at LAMPF (from the reduced atmospheric pressure). This gave electric fields of ~ 33 and 0.5 kV/mm at the sense wires and cathode planes, respectively.

Experimental Observations

Soon after the chambers were constructed and tested in the beam, problems were encountered with the efficiency, which decreased with time. When the chambers were disassembled, whitish deposits were observed on both the sense wires and the cathode aluminized mylar planes near the location where the beam had passed through the chamber. Chemical analyses of the wires showed a striking buildup of silicon. Several changes were made at that time. a) The fluid used in the bubbler was changed from a silicon-based oil to mineral oil ($\sim \text{CH}_2$). b) The gas lines were changed from tygon to polyflo with a short length of tygon near the chamber. c) The aluminized mylar cathode planes were changed to aluminum foil planes. d) The wires with the deposits were replaced, although it appeared that the deposits could be removed mechanically. The deposits changed qualitatively, but the drops in efficiency persisted.

Tests were performed by operating two of the beam chambers with the standard gas (Ar-CO₂-Freon 13B1) and the third chamber with magic gas (68% Ar, 28.5% Isobutane, 3% Methylal, 0.5% Freon 13B1). Although detailed studies were not performed, the rate of drop in the efficiency was found to be about the same for the two gas mixtures. (The efficiency dropped about 10% for beam exposures of 10^{10} to 10^{11} particles/cm².) Thereafter, the standard mixture was used.

After these changes and tests, a chemical analysis of the chamber gas was performed with a mass spectrometer. Gas samples were taken, while the chambers were in operation, at five points in the gas system, both upstream and downstream of the chamber. No gross impurities (greater than ~ 100 ppm) were present in the mass range 12 to 250, except those that could be masked by Ar, CO₂ or Freon 13B1 (CBrF₃). The samples were also cooled to LN₂ temperature and the argon pumped off. The resulting samples were tested again. Only CO₂ and CBrF₃ with a trace of H₂O were detected, suggesting that the impurities were probably less than 10 ppm initially. It is possible that ²⁸SiO was present at a low level in one or more of the gas samples, masked by the CO₂. However, the absence of signals from SiO₂ or Si or from ²⁹SiO and ³⁰SiO would limit the presence of SiO to a few hundred ppm.

The tungsten sense wires and the aluminum foil cathode planes were submitted to an ion microprobe mass analysis by D. V. Steidl of the Argonne Chemical Engineering Division. A beam of 20 KeV N₂⁺ of diameter $\sim 3\mu\text{m}$ was obtained from a duoplasmatron source and a mass spectrometer. This beam was used to sample the wires directly, and it was rastered over an area of 80 x

$100 \mu\text{m}^2$ on the foils. The resulting positive ions were measured with a second mass spectrometer. The vacuum in the apparatus was about 10^{-9} Torr, so little of the signal corresponds to beam - gas background. The results are given in Tables 1 and 2 and Fig. 1.

These results can be used to give rough comparisons of the surface compositions of the new and bombarded wires and foils for a given element. Comparisons between elements for a given sample do not give true abundances,

Table 1
Ion Microprobe Analysis of Gold-Plated Tungsten Wires

<u>Ion</u>	<u>Relative Abundance on Irradiated Wire</u>	<u>Relative Abundance on New Wire</u>
$^1\text{H}^+$	3.4	1.3
$^7\text{Li}^+$	---	0.2
$^{12}\text{C}^+$	1.2	0.2
$^{19}\text{F}^+$	0.25	< 0.1
$^{23}\text{Na}^+$	7.4	48
$^{27}\text{Al}^+$	8	1.2
$^{28}\text{Si}^+$	2200	5
$^{39}\text{K}^+$	5	54
$^{40}\text{Ca}^+$	< 0.7	< 4
$^{52}\text{Cr}^+$	0.6	0.15
$^{56}\text{Fe}^+$	< 1.7	0.4
$^{120}\text{Sn}^+$	0.3	< 0.1

Table 2
Ion Microprobe Analysis of Aluminum Foils

<u>Ion</u>	<u>Relative Abundance on Irradiated Foil</u>	<u>Relative Abundance On New Foil</u>
$^1\text{H}^+$	2.8	3.3
$^7\text{Li}^+$	3	1.9
$^9\text{Be}^+$	2.3	2.0
$^{12}\text{C}^+$	4	1.7
$^{19}\text{F}^+$	53	0.2
$^{23}\text{Na}^+$	53	15
$^{24}\text{Mg}^+$	63	30
$^{39}\text{K}^+$	3	0.9
$^{40}\text{Ca}^+$	4	1.2

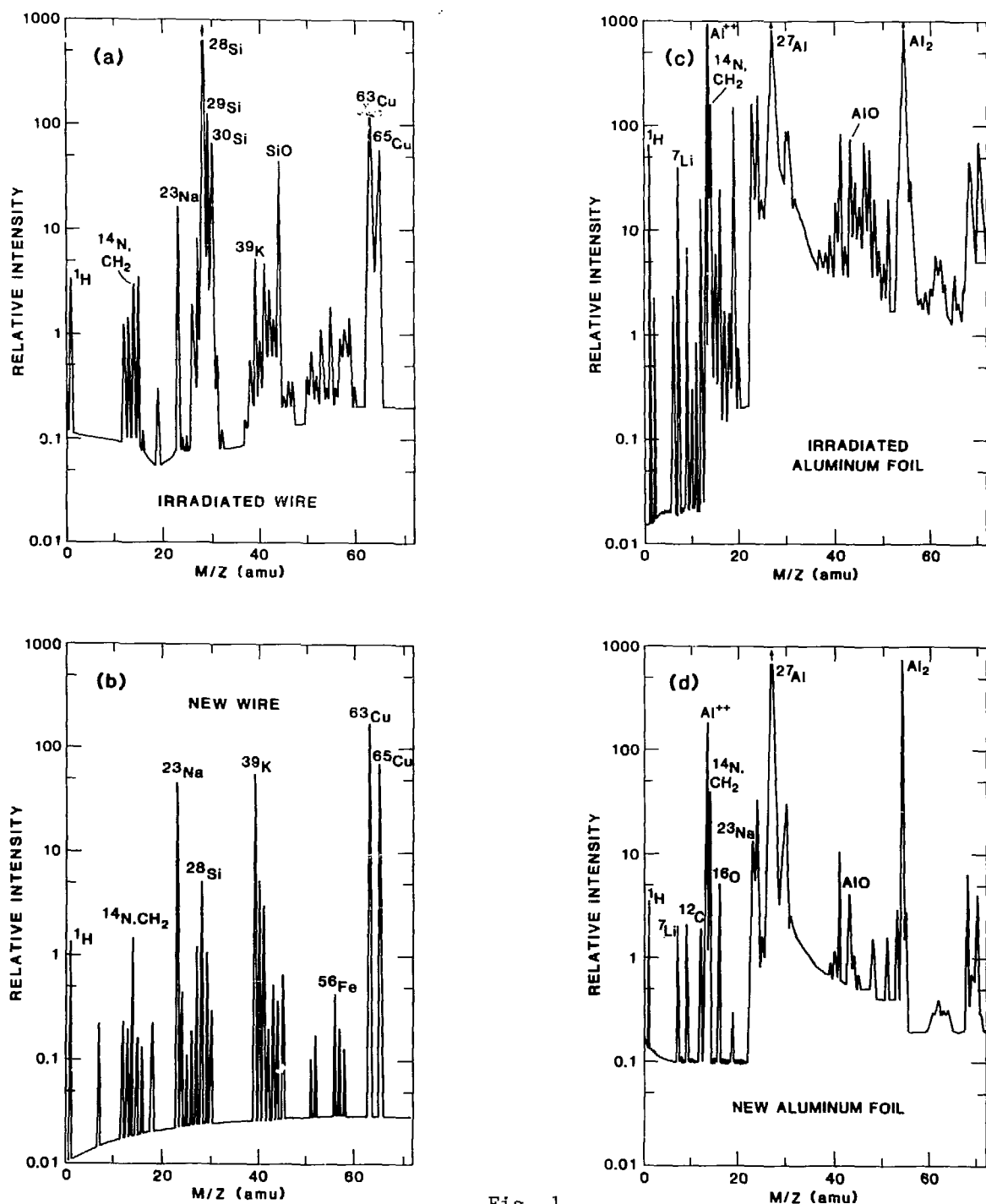


Fig. 1

Results from an ion microprobe mass analysis of tungsten anode wires and aluminum cathode foils from the MWPC's in the ZGS beam. The figures shown are a composite of several spectra with different sensitivities.

a) Irradiated wire. b) New wire. Signals were also seen at much higher masses corresponding to tungsten and gold. A copper holder for the wires was employed, which led to the copper signals. c) Irradiated foil. d) New foil.

efficiency is assumed to occur because the wire diameter is increased by the deposits to give a surface potential about 10% less than the chamber operating voltage. Furthermore, if the deposit is assumed to have a dielectric constant similar to glass (SiO_2 , $\epsilon \sim 3-4$), then the calculated thickness is somewhat larger than 10,000 Å. On the other hand, the silicon spacing would be somewhat larger as well. In both estimates, the deposits were assumed to be continuous, without voids, which has not been demonstrated experimentally.

The material estimated above was deposited in roughly one month at a beam intensity of at least 2×10^6 /pulse with a pulse every 3 seconds. As a result, a lower limit to the amount of silicon per incident proton was

$$\geq 8 \times 10^4 \text{ silicon atoms deposited/incident proton.}$$

This is an enormous number! Even with the assumption of only a single, continuous layer of silicon (3 Å instead of 10,000 Å), the limit is roughly 25 silicon atoms deposited per incident proton. Clearly, the process that deposits the silicon is very efficient.

Such large numbers immediately rule out nuclear reactions of the protons with the gas or tungsten wire, since there is so little material present in the chamber. Nuclear reactions on the mylar ($\text{C}_5\text{H}_4\text{O}_2$) or CO_2 in the gas couldn't lead to silicon in any case. Likewise, sputtering of material from the G10 frames by particles in the beam halo is probably ruled out. With a beam spot size of 1-2 cm diameter, and a distance of greater than 6 cm to the frames, probably less than one part in 10^3 of the beam struck the frame. It seems implausible that on the average $\sim 10^8$ silicon atoms could be ejected from the frame for each particle in the halo that struck the frame.

With an assumed value of 10^7 electrons collected per incident beam particle, then the efficiency of depositing a silicon can also be expressed as

$$\geq 0.008 \text{ silicon atoms deposited/collected electron.}$$

Silicon contamination of the chamber gas was measured to be orders of magnitude smaller than this, on the order of 100 ppm, or perhaps even 10 ppm or less. Furthermore, the ions formed near the anode wire should have a positive charge and thus be repelled. Clearly, chemical reactions are involved in some way with the depositing of the silicon.

Finally, it can be checked that the limits on the gas contamination do not exclude the gas as the source of the silicon. The precise gas flows were not recorded for the chambers. Taking a conservative value of 1 cc/min for the bubbling rate and a 10 ppm contamination of the gas by silicon, then 10^{17} silicon atoms would pass through each chamber in about seven hours. An allowance for the fact that not all the gas went near the beam would increase this estimate by about an order of magnitude to a few days. Therefore, if the gas contained silicon as a contaminant at a low level, whatever chemical processes taking place in the chambers would have to collect it efficiently.

Conclusions

Observations of MWPC's in multi-GeV beams of protons and pions at the ZGS indicated a drop in efficiency for exposures of about 10^{10} - 10^{11} beam particles/cm². Deposits on the sense wires (silicon) and the cathode planes (fluorine) were visible in the area of the chambers where the beam was present. The precise mechanisms for depositing the silicon and fluorine are not understood. The source of the fluorine was likely to be the Freon 13B1 (CBrF₃) in the chamber gas. The silicon was probably present as an impurity in the chamber gas at the level of 10 ppm or less. The source is not known, but may have been the G10 chamber frames, the RTV gas seal, or the commercial gas mixture. Many atoms of fluorine and silicon are deposited for each beam particle and the chemical processes responsible for depositing the silicon are reasonably efficient.

ACKNOWLEDGEMENTS

It is a pleasure to acknowledge the efforts of D. Bridges, J. Caruso, R. Crane, R. Daly, T. Droege, G. Hicks, T. Kasprzyk, K. Nield, A. Rask, W. Rusen, B. Sandler, C. Wilson and the many other members of the polarized target group for assistance with the construction, testing and operation of the MWPC's described in this paper.

REFERENCES

- 1) I. P. Auer et al., Phys. Rev. D24, 1771 (1981).
- 2) K. Nield and R. Daly, Argonne National Laboratory Report ANL-HEP-PR-77-32 (1977), unpublished.

§ Work supported by the U.S. Department of Energy, Division of High Energy Physics, Contract W-31-109-ENG-38.

THE OMEGA AND SFMD EXPERIENCE IN INTENSE BEAMS

OMEGA and SFMD Collaborations

Presented by O. Ullaland

CERN, European Organization for Nuclear Research, Geneva, Switzerland

ABSTRACT

We will report on our experience on radiation induced damage to multiwire proportional chambers at the SFMD [1] and the OMEGA [2] at CERN. Both spectrometers are large detectors with a long lifetime in intense beams. The SFMD detector showed some efficiency loss limited to the high intensity area near to the beams. The effect was observed after four years of operation and an integrated charge of 0.3 C/cm anode wire. This loss of efficiency could be offset by a change in the electric field. The OMEGA spectrometer has been exposed to an integrated beam particle flux of $10^{13}/\text{cm}^2$ in the last seven years. There is no evidence of any radiation induced damage. We will discuss the results separately since the two spectrometers differ in operating condition.

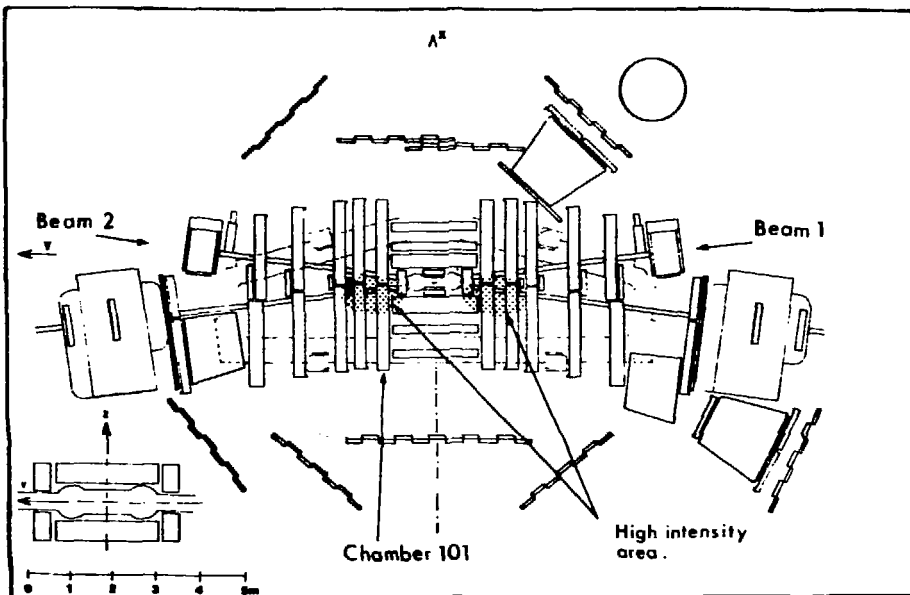
1. THE SPLIT FIELD MAGNET DETECTOR

The Split Field Magnet Detector (SFMD) [1] was a multipurpose multiparticle spectrometer at the ISR. It covered 30 m³ of 1 Tesla magnetic volume with 4 m³ of active detectors (fig. 1).

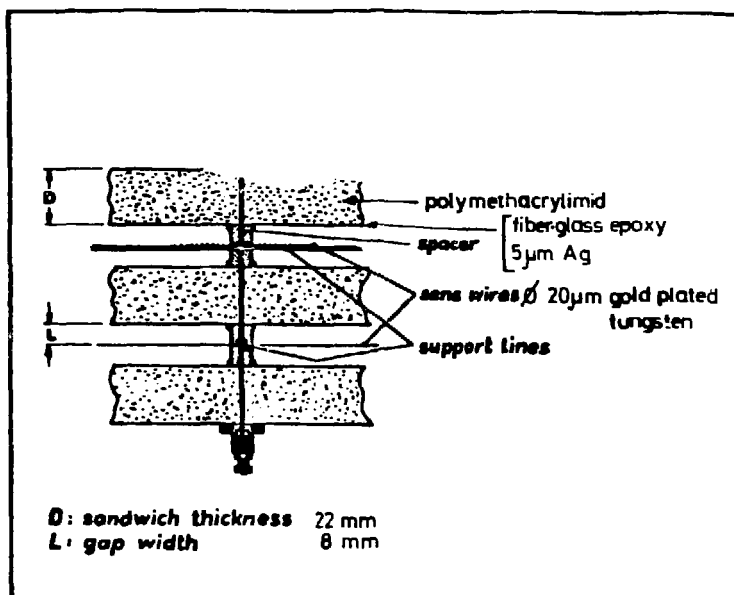
The multiwire proportional chambers are of the frameless self-supporting type (fig. 1(b)). We used polymethacrylimid foam as core material for the sandwich structure. Thin sheets of fiber-glass reinforced epoxy are used as facing material. The HV electrodes are made of a 5 μm silver layer sprayed on this surface. The chamber frames are 5 mm thick fiber-glass epoxy. The half gap of the chambers is 8 mm and the anode wires are 20 μm diameter gold plated tungsten wires with 4 mm wire spacing.

The gas mixture for the chambers was 53% argon, 40% isobutane and 7% methylal. The argon was 99.996% pure while the isobutane was only $(96 \pm 2)\%$ pure. The balance was propane, n-butane and ethane. Air contamination accounts for less than 1000 ppm. The methylal has not been analysed for impurities. The gas feed lines for the chambers were 60 m of stainless steel + 25 m of Rilsan (polyamide 11). The exhaust oil bubblers were placed 25 m from the exit of the chambers.

The SFMD detector had only wire coordinate read-out. The chambers were operated at more than 100 V above the nominal onset of the 100% efficiency plateau. The operation voltage was 3500 V which corresponds to a gas amplification of about 10^5 .



(a) The Split Field Magnet detector.



(b) Cut through a SFM proportional wire chamber.

Fig. 1

We observed an efficiency loss in the reconstruction of the forward jets after 4 years of data taking. The inefficiency was strictly confined to the high intensity spot near the outgoing beam tubes (fig. 1(a)). The integral particle density in this region of the detector was about $2 \times 10^{11}/\text{cm}^2$. The SFM detector system included more than 75000 anode wires. We will, however, only discuss the results from chamber 101 (fig. 1(a)). This chamber covers the forward jet. Efficiency plateau curves were taken on this chamber and the effect is visible near the beam area (fig. 2). There is no difference in the plateau curves taken along the chamber apart from the voltage offset. The effect can therefore be explained by a change in the anode wire diameter produced by a radiation induced deposit on the wire (fig. 3). The wires were examined by a scanning electron microscope. The measured diameter coincides with the calculated one.

The maximum change of the anode wire radius was about $1 \mu\text{m}$ for an integrated charge of approximately 0.3 C/cm anode wire. The deposit could easily be removed by alcohol.

2. THE OMEGA DETECTOR

The OMEGA [2] spectrometer is a detector for fixed target experiments (fig. 4). It is capable of handling intense beams of hadrons, electrons and photons up to 450 GeV/c . It is a multiwire proportional chamber system installed in and around a superconducting 1.8 Tesla magnet at the SPS since 1979.

The proportional chambers are multigap modules built with prestressed glass fiber reinforced epoxy frames (fig. 4(b)). The half gap of the chambers is 8 mm and the anode planes are made with $20 \mu\text{m}$ diameter gold plated tungsten wires with a spacing of 2 mm . The cathode planes are $12 \mu\text{m}$ Mylar (PCTFE) with a $4 \mu\text{m}$ graphite layer on each side. The chamber structure is protected from the outside atmosphere by $50 \mu\text{m}$ thick Mylar with $12 \mu\text{m}$ Al towards the inside.

The gas mixture for the chambers is 65% argon, 35% isobutane and 1.5% isopropyl alcohol in the argon. The alcohol is used in this gas mixture as a substitute for methylal which attacks the Mylar. The argon is 99.996% pure and the isobutane has a purity of 99.5%. The contamination of $\text{O}_2 \leq 100 \text{ ppM}$ and of $\text{H}_2\text{O} \leq 20 \text{ ppM}$. The purity of the alcohol is 99.7% where water is the main impurity. The gas tubings to the chambers are 50 m of copper + 10 m of Rilsan (polyamide 11). The gas exit from the chambers is controlled by an electronic pressure regulation. This system avoids therefore any active oil bubblers in the gas system.

The chambers in OMEGA have been in the beam since 1979. They have operated with a gas amplification of about 6×10^4 . The beam intensity which has been used over the last 3 years is about $1.5 \times 10^{17}/\text{cm}^2/2 \text{ s}$ beam spill time. This gives a total particle density in the beam of about $10^{13}/\text{cm}^2$, or an integrated total charge dose to approximately 3 C/cm anode wire. The beam region of the chambers is not deadened but does not respond above about $10^5/\text{cm}^2/\text{s}$ due to space charge. This could lower the charge dose in the beam region to approximately 0.03 C per cm of anode wire.

No trace of deposit has been observed on our anode wires.

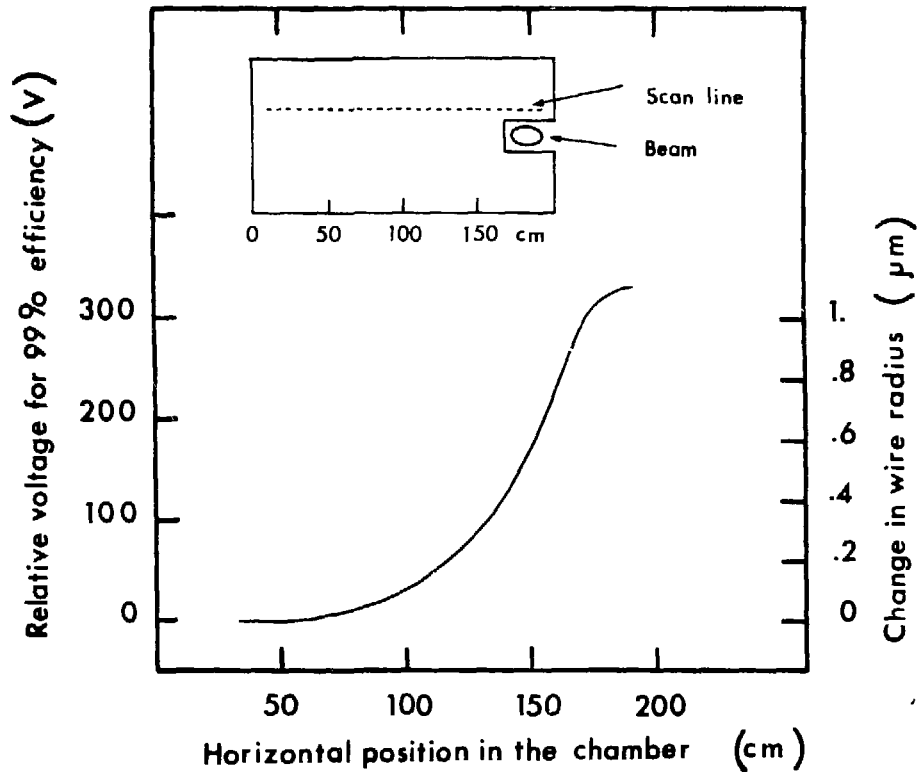


Fig. 2 Relative voltage setting for 99% efficiency as a function of the position in the chamber.

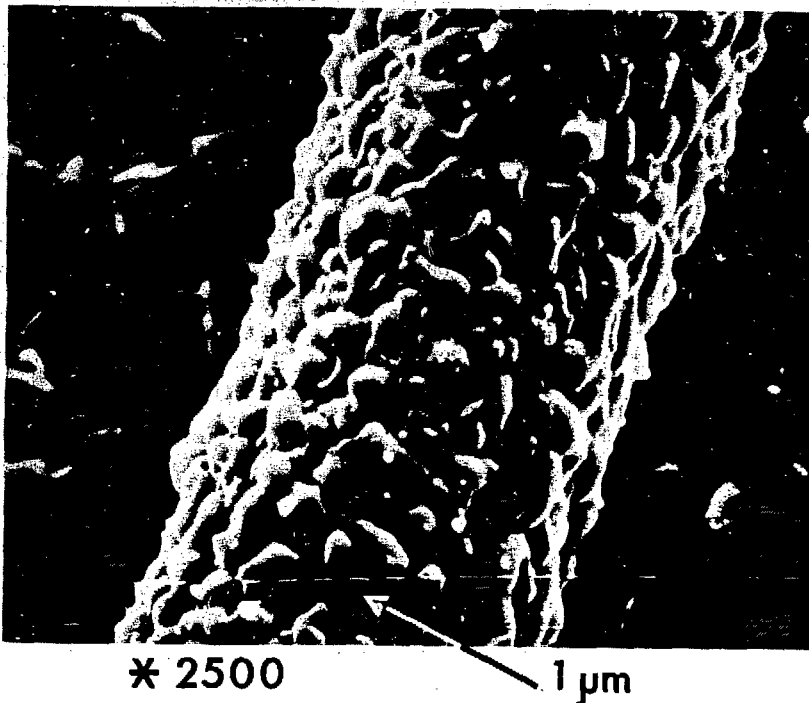
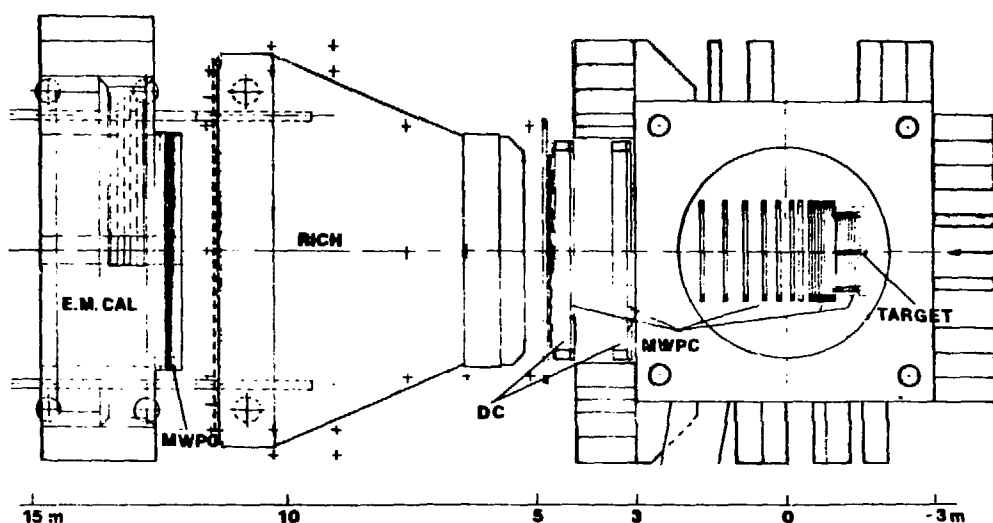
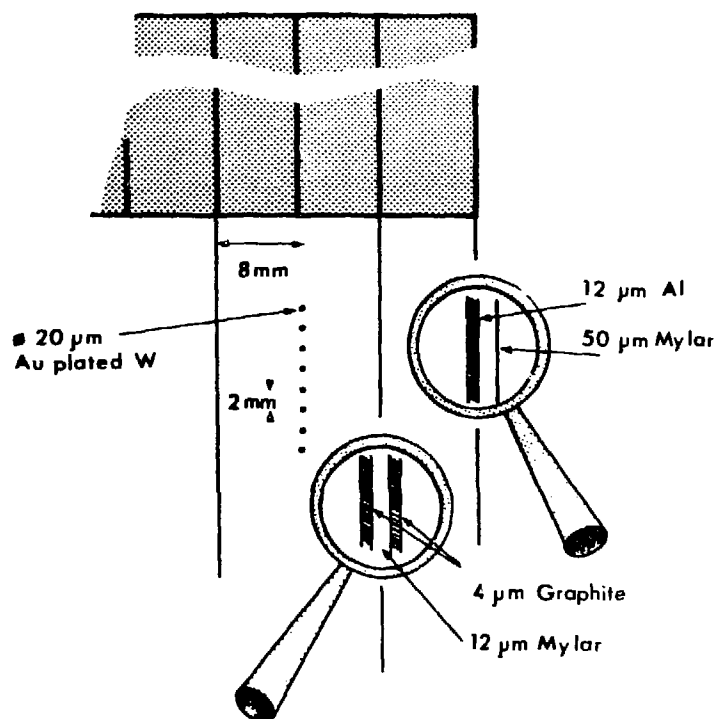


Fig. 3 A picture with a scanning electron microscope of an anode wire with deposit.



(a) The layout of the OMEGA spectrometer.



(b) Cut through an OMEGA proportional wire chamber.

Fig. 4

REFERENCES

- [1] W. Bell et al., A system of multigap proportional wire chambers, Nucl. Instr. Meth. 156 (1978) 111.
- [2] W. Beusch, OMEGA Prime, A project of improving the OMEGA particle detector system, CERN/SPSC 77-70 (1977).

AGEING EFFECTS IN GASEOUS DETECTORS AND SEARCH FOR REMEDIES

A. Dwurazny, Z. Hajduk and M. Turala*

Institute of Nuclear Physics, Krakow, Poland

NA11/NA32 at CERN

Abstract

Wire ageing effects observed in the chambers of the ACCMOR spectrometer at CERN SPS are described, as well as results of laboratory tests performed to find solutions to this problem. In 50:50 Argon-Ethane gas mixture the loss of efficiency began after accumulating about 0.02 C/cm of anode wire, but the tests indicated that this limit can be extended to at least 0.1 C/cm by adding 0.1% iso-propyl alcohol. Analysis of wire deposits showed silicon, even with the alcohol added. Using sealed proportional counters searches for nonpolymerising gases were made including Argon-Nitrogen and Argon-CO₂. With these two gases the lifetime is significantly improved, to about 0.1 - 1.0 C/cm, depending upon the gain or resolution requirements.

Introduction

The ageing effects in proportional counters were noticed a long time ago¹. In the wire chambers the first studies of ageing were performed by Chrapak and collaborators². They have observed the increase of the leakage current in MWPCs and the shrinkage of their plateaux after some dose of irradiation. These effects were explained as being caused by deposits on the cathodes and were cured by the addition of "methylal". Last year many groups also faced a different problem, namely a severe reduction of the gas amplification factor as a result of the accumulation of some deposits on the anode wires, which grew in the regions of intense irradiation (discharges)³⁻⁵. The composition of the deposits, their formation and origin were not well understood.

To satisfy the needs of our experiments (NA11/NA32 at CERN SPS) as well as to understand better the phenomena of ageing and trying to find a more permanent solution to this problem we have performed a series of laboratory tests of small wire chambers and proportional counters. Some of the results of these tests were already mentioned in our earlier papers on this matter^{3,6}, but we present here more details in view of general interest.

* Visitor at the University of California at Santa Cruz, USA

Test chambers and proportional counters

For all of our laboratory tests we have used small drift chambers of the sensitive area of about $20 \times 20 \text{ cm}^2$ which had the construction and the geometry of the cell similar to the large drift chambers of the ACCMOR (Amsterdam-Bristol-CERN-Cracow-Munich-Rutherford) spectrometer⁷. The geometry of an individual cell of such chamber is presented in Fig. 1a. The frames of these chambers were machined out of fiberglass. The chambers had thin mylar-polyethylene windows of a total thickness of about $50 \mu\text{m}$. The chambers were easy to open for cleaning or for exchanging a wire. The sealing was done with soft rubber O-rings and a small amount of silicone grease. The chambers were flushed with commercially available gases of technical purity; for mixing them we used a "standard CERN gas rack" equipped with a refrigerator (it allowed us to keep liquid admixtures at constant temperature). The gas was distributed using "tygon" tubes and the outlet was via a bubbler filled with silicone oil.

The construction of the proportional counters used for tests is presented in Fig. 1b. The counters were kept under vacuum (0.01 Pa) during about 10 days to reduce the possible outgassing and then filled with selected gas mixtures using a special clean set-up for their preparation (constructed mainly out of glass and kept under vacuum). Gas mixtures were prepared out of spectroscopically pure gases. The counters were sealed by melting of glass capillaries.

Prevention of leakage currents caused by deposits on cathodes

For the drift chambers of the ACCMOR spectrometer we have chosen 50:50 Argon-Ethane gas mixture because of its saturated drift velocity at moderate strength of electrical field. In some of our chambers filled with this gas mixture we have observed the growth of whiskers or substantial leakage current after some irradiation; in many cases the current persisted even after the removal of a radioactive source. We interpreted this effect as being caused by emission of electrons from the cathode wires which were covered by some deposits (Malter effect) and we tried the solution suggested by others, namely addition of a small quantity of an admixture (e.g. "methylal") which has ionization potential lower than hydrocarbons and which does not polymerize². The effect of such treatments on the efficiency and current curves is shown in Fig. 2. We have verified that the extra alcohol had a small effect on the drift velocity. The addition of about 0.2% of "methylal" has changed the average drift velocity by less than 2%.

Deposits on the anode wires and extension of the lifetime of wire chambers

The drift chambers of the ACCMOR spectrometer were originally running with 50:50 Argon-Ethane gas mixture. After two years of operation we have noticed a severe drop of efficiency in the beam region of these chambers. We have found that it was caused by deposits on the anode wires which have formed in the beam region and this effect became significant after the accumulation of about 0.02 C/cm of an anode³. Some

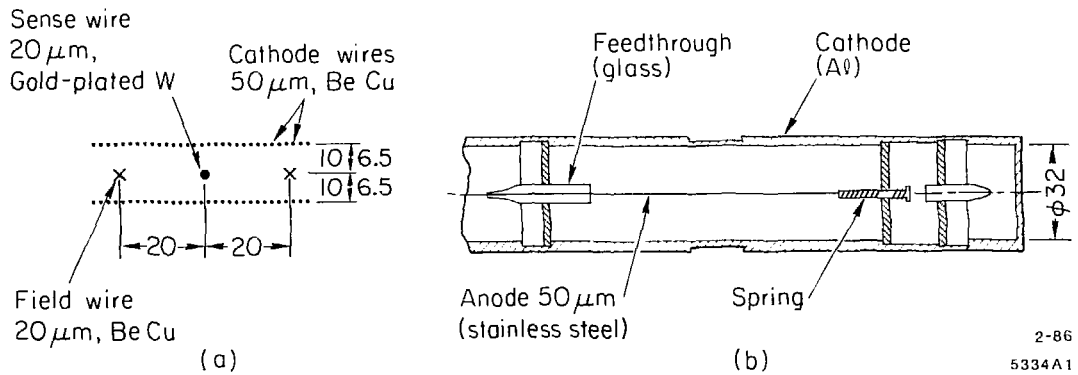


Fig. 1. Geometry of an individual cell of test drift chamber (a) and the construction of proportional counter (b).

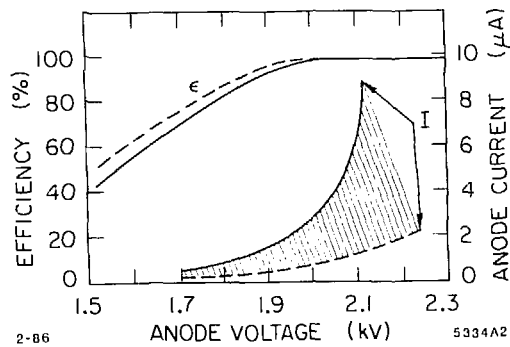


Fig. 2. Efficiency and current curves for the test chamber flushed with gas mixtures with (broken line) and without "methyral" (solid line). The shaded area shows the excess of the leakage current.

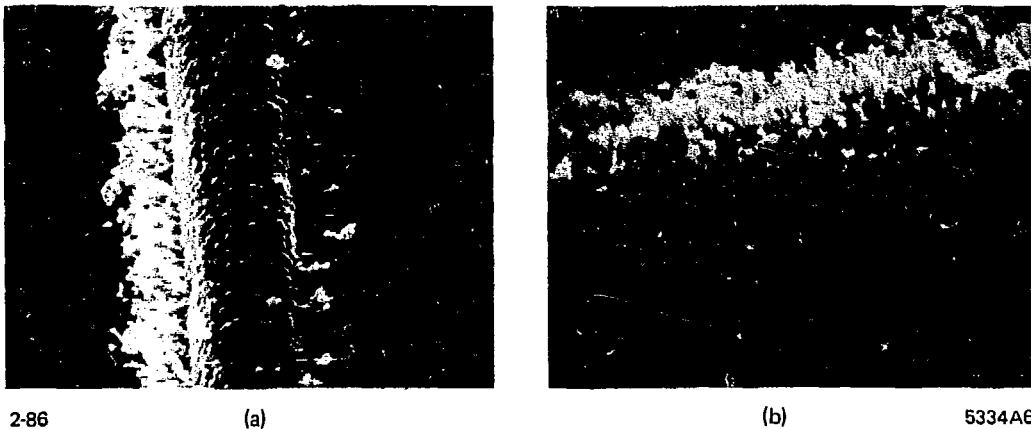


Fig. 3. Deposits on the anode wires from the ACCMOR drift chambers which operated with 50:50 Argon-Ethane gas mixture; (a) gold plated tungsten wire, 20 μ (ESM, magnification X1250), (b) stainless steel wire, 25 μ (ESM, magnification X2500).

of the photographs of these deposits, taken under the scanning electron microscope (SEM) are presented in Fig. 3. The fluorescent analysis of these deposits has shown the presence of silicon, in addition to the other elements which were expected as the components of the wire. See Fig. 4. (The apparatus could not detect such elements as Hydrogen and Carbon.)

Our laboratory tests of small drift chambers flushed with the same gas mixture and irradiated by β source confirmed the formation of anode deposits after the accumulation of a certain number of pulses. In particular we have performed ageing tests of small drift chambers flushed with 50:50 Argon-Ethane gas mixture, one of which contained also a small addition of iso-propyl alcohol. For ageing a small region of these chambers was illuminated with β particles over the extended period of time. (The total anode current was about $4\mu\text{A}$ but the distribution of this current was poorly known.) Each day the efficiency curve was measured. The sets of such curves taken for gas mixtures with and without the alcohol are shown in Fig. 5. By comparing the results from these two kind of mixtures we could estimate that the limit of unaffected operation of a drift chamber flushed with 50:50 Argon-Ethane gas mixture with addition of 0.1% of iso-propyl alcohol is higher than 0.1C/cm.

One of the anode wires of the small drift chamber operating with the gas mixture with a small addition of alcohol was examined under the SEM. The deposits on this wire (see Fig. 6) have a structure different from the one observed on the wires from the large drift chambers filled with Argon-Ethane mixture. But as in the other case the fluorescent analysis of these deposits has shown the presence of silicone (Fig. 7).

The obtained results suggest strongly that the small addition of alcohol extends significantly the lifetime of wire chambers. This phenomenon could be partially explained by slowing down the polymerization processes with the presence of Oxygen coming out of broken molecules of alcohol⁸. On the other hand some questions still remain: how do the charges get collected on the anode wire which seems to be uniformly covered by thin layer of deposits? is it a conductive layer? (of what kind?) or it is porous? Besides us a few other groups have observed the efficient registration of particles in spite of deposits formed on the anode wires when operating with gas mixtures with the addition of alcohols⁹.

The results of tests were encouraging and, as a consequence, the drift chambers of the ACCMOR spectrometer during the last two years are running with 60:40 Argon-Ethane mixture with 0.1% iso-propyl alcohol. The average drift velocity changed by about 2% but the spatial resolution remained unchanged. Up to now the anodes of these chambers, which are in the beam region, have accumulated about 0.02C/cm. So far no deterioration of performances were observed.

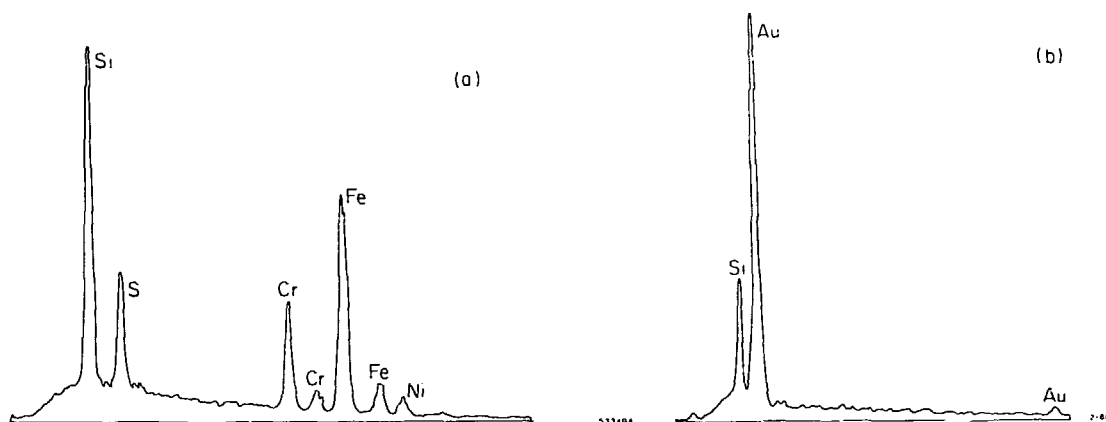


Fig. 4. The fluorescent analysis spectra of anode deposits of ACCMOR drift chambers flushed with 50:50 Argon-Ethane gas mixture, (a) on stainless steel wire, $25\ \mu$, (b) on gold plated tungsten wire, $20\ \mu$.

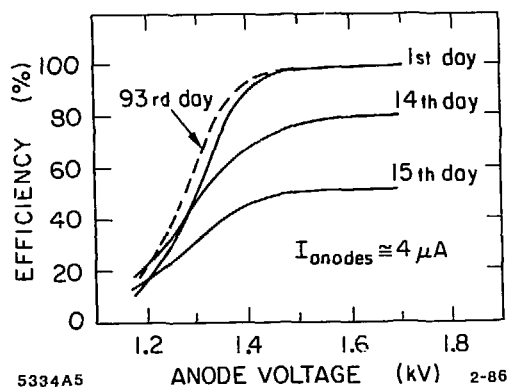


Fig. 5. The efficiency curves from the test drift chamber flushed with 50:50 Argon-Ethane gas mixture with (0.1%) and without iso-propyl alcohol taken during the time of its operation with strong β source.

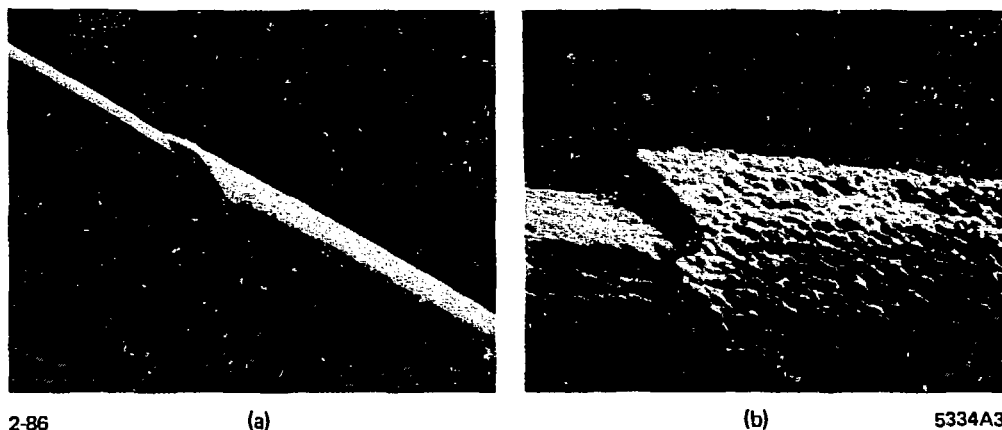


Fig. 6. Deposits on the anode wire of the test drift chamber which was operated with 50:50 Argon-Ethane gas mixture with addition of 0.1% of iso-propyl alcohol; (a) ESM magnification X1250, (b) ESM magnification X10000.

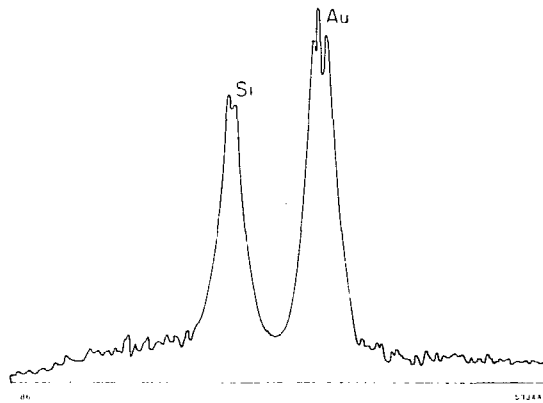


Fig. 7. The fluorescent analysis spectrum of the deposits on the anode wire of the test chamber flushed with 50:50 Argon-Ethane gas mixture with addition of 0.1% of iso-propyl alcohol.

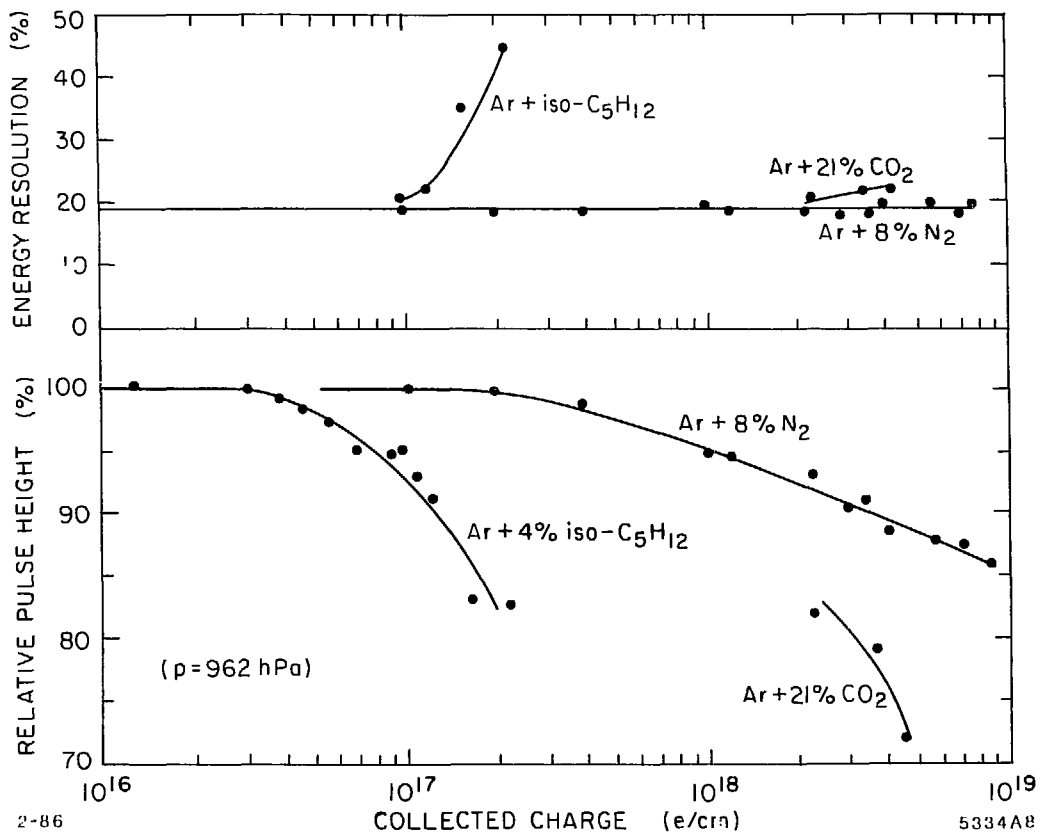


Fig. 8. Energy resolution and relative pulse amplitudes vs. charge collected on the anode wire of test proportional counters for different gas mixtures.

Lifetime of proportional counters

To look for longer term solutions we have studied a number of nonorganic gas mixtures from the point of view of their usefulness in wire chambers. For example, we tested such parameters as gas amplification factor, drift velocity, ease of use, cost, and ageing^{6,10}.

One of the most promising parameters had a family of Argon-Nitrogen mixtures in which the gas gain of up to 10^5 could be obtained. The drift velocity of electrons in these gas mixtures has been measured also and has shown, approximately, linear dependence up to the strength of the electrical field equal to 1.5kV/cm and a slow rise to saturation (at about 5cm/ μ s) at higher values. We have tried to use one of these mixtures (Ar+8%N₂) for proportional and drift chambers but we could not get a stable operation of these devices at gas amplification higher than $3-5 \times 10^3$, which was necessary from the point of view of sensitivity of our electronics. We attribute this problem to long range photons, which in narrow gap chambers liberated electrons from cathodes and subsequently caused breakdowns.

The Argon-Nitrogen gas mixture and the several others have been tested for ageing. For this purpose we have used proportional counters described at the beginning of this paper. The counters were irradiated with a strong ⁵⁵Fe source and periodically we measured the position and the width of the peak of the ⁵⁵Fe source at low intensities. The summary of the results is presented in Fig. 8.

The gas mixture with iso-pentane has shown a lifetime typical of the mixtures with organic quenchers, e.g. about 0.02C/cm of an anode. The examination of the anode wire under SEM has shown the uniform, rather smooth, layer of deposit.

The Ar+21%CO₂ gas mixture has shown a lifetime on the order of 0.5C/cm of the anode. In this case we have noticed that the gas amplification factor started to change much sooner than the energy resolution of the counter.

A similar effect was observed for the counter filled with Ar+8%N₂ mixture. A slow decrease of the pulse height was observed starting from the accumulation of about 0.1C/cm of the anode wire, but the energy resolution was stable up to 1.6C/cm. So far we have no explanation for this effect. The anode wire of this counter examined under the microscope has shown no deposits.

We have also checked the effect of Hydrogen and alcohol on the ageing of sealed proportional counters. For this purpose the counters were filled with the mixture of Ar+10%iso-pentane and 0.5%H₂ or 0.5% of C₂H₅OH. Then the standard ageing and test procedures were performed. The counters have shown approximately the same lifetime as the one without extra additions. The lack of the effect can be attributed to the exhaustion of the limited amount of admixtures in the process of polymerization of iso-pentane.

Acknowledgements

The constant interest of our colleagues from the ACCMOR collaboration presented a great stimulus for our work. M. Cerrada, J. Michalowski and T. Zeludziejewicz helped us to run some of the tests at CERN, and K. Jelen, E. Rulikowska and K. Ostrowski provided a lot of help and advice during tests in Krakow. The beautiful photographs of deposits are due to J. Adams of CERN. N. Rogers from UC Santa Cruz polished the final version of this paper.

References

1. A.J.F. den Boggende et al., J. Sci. Instr. 2 (1969), 701
2. G. Charpak et al., Nucl. Instr. Meth. 99 (1972), 279
3. M. Turala and J.C. Vermeulen, Nucl. Instr. Meth. 205 (1983), 141
4. J. Adam et al., Nucl. Instr. Meth. 217 (1983), 291
5. Workshop on Radiation Damage to Wire Chambers, Berkeley, Jan. 1986
6. A. Dwurazny et al., Nucl. Instr. Meth. 217 (1983), 301
7. G. Blunar et al., CERN/SPSC/78-14
8. D. Hess, these proceedings
9. O. Ullaland, these proceedings
10. A. Dwurazny, Ph.D. thesis, in preparation

INVESTIGATION OF BREAKDOWN CONDITIONS OF DRIFT CHAMBERS*

HARTMUT F.-W. SADROZINSKI
Santa Cruz Institute for Particle Physics

MARK III Experiment

Abstract

Breakdown phenomena characterized by large currents in multiwire chambers were simulated and measured in a small multiwire cell. A variety of breakdown tests were performed, using different gas mixtures, gains, and wire diameters. It was found that the breakdown was well described by the product of the separate anode and cathode wire gains exceeding 10^7 . Cathode wire coating due to breakdown was absent when the CH_4 content was $\leq 4\%$ in $\text{Ar}/\text{CO}_2/\text{CH}_4$ mixtures, and gain lifetime measurements were made for two such mixtures. Experience with excessive current in the MARK III drift chamber, and the subsequent cure with addition of 0.2% of water vapor, are described.

Theory

Breakdown occurs if the gain on the wires is too large. We recognize that gas amplification can occur at both the sense wire *and* the field wire and we define an overall breakdown gain g_t as the product of the gain on the sense wires g_s and field wires g_f :

$$g_t = g_s g_f . \quad (1)$$

Following Sauli,¹ the gain g is determined by the integrated Townsend coefficient α :

$$g = \exp \left(\int_a^{r_c} \alpha \, dr \right) \quad (2)$$

where a is the wire radius and r_c is the radius at which amplification starts. As in Ref. 1, we assume that the Townsend coefficient is a function of the electric field E :

$$\alpha = \sqrt{kNE} \quad (3)$$

where $k = 1.8 \times 10^{17} (\text{cm}^2 \text{V}^{-1})$ for Argon and N is the number of Argon atoms

* Work supported in part by the U.S. Department of Energy

per cm^3 , which yields

$$g = \exp \left(2\sqrt{kN}\sqrt{\lambda'}(\sqrt{\lambda'/E_c} - \sqrt{a}) \right) , \quad (4)$$

with $\lambda' = \frac{\lambda}{2\pi\epsilon_0}$ the linear charge density. Thus the gain on a wire with radius a is a function of the charge per unit length λ' alone if the cutoff field E_c is known. The cutoff field E_c is the lowest field strength at which amplification occurs.

In Ref. 2 we have shown that we can determine the cutoff field as a function of the wire diameter using single wire proportional tubes and that spontaneous breakdown occurs if the gain $g = 10^7$ (i.e., $\int \alpha dr = 17$).

In Table I we show the scaled linear charge density λ'_b and the fields $E_b = \lambda'_b/a$ on the surface of the wires at breakdown for several wire diameters $2a$ for both the sense (anode) wire and field (cathode) wire configurations. Note that for equal wire diameter, breakdown occurs at lower fields when the wire is the cathode. Electron emission could explain this effect. We also show the cutoff fields E_c : while E_c is constant at 50 kV/cm for the cathode wires, we see a slight dependence of E_c on the anode wire diameter. This could be due to our assumption about the dependence of α on E or effects of saturation of the gain.

Breakdown in Multiwire Cells

To study the interplay of gain on sense and field wires to produce breakdown, the small test chamber sketched in Fig. 1 was built. As above, a mixture of 89% A, 10% CO_2 , and 1% CH_4 was used. From electrostatic simulation, the scaled linear charge density λ'_f on the field wires and λ'_s on the sense wires were determined. Using the values for E_c from Table I for field and sense wires, the gains on the wires were calculated with Eq. (4). Fig. 2 shows the gain on the field wire, g_f , vs. the gain on the sense wire, g_s , at breakdown for sense wire diameters of 20, 30, 50, 100, and 178 μm . The data shows the correlation between the gain on the sense wires and the field wires, and suggests that breakdown occurs when the overall gain $g_t = g_s g_f$ is of the order 10^7 . For large wire diameter, the calculation of the gain using Eq. (4) becomes less reliable because it involves the difference of large numbers. Local field emission might also become more important. We are not surprised to see deviation from the simple behavior for diameters $> 100 \mu\text{m}$.

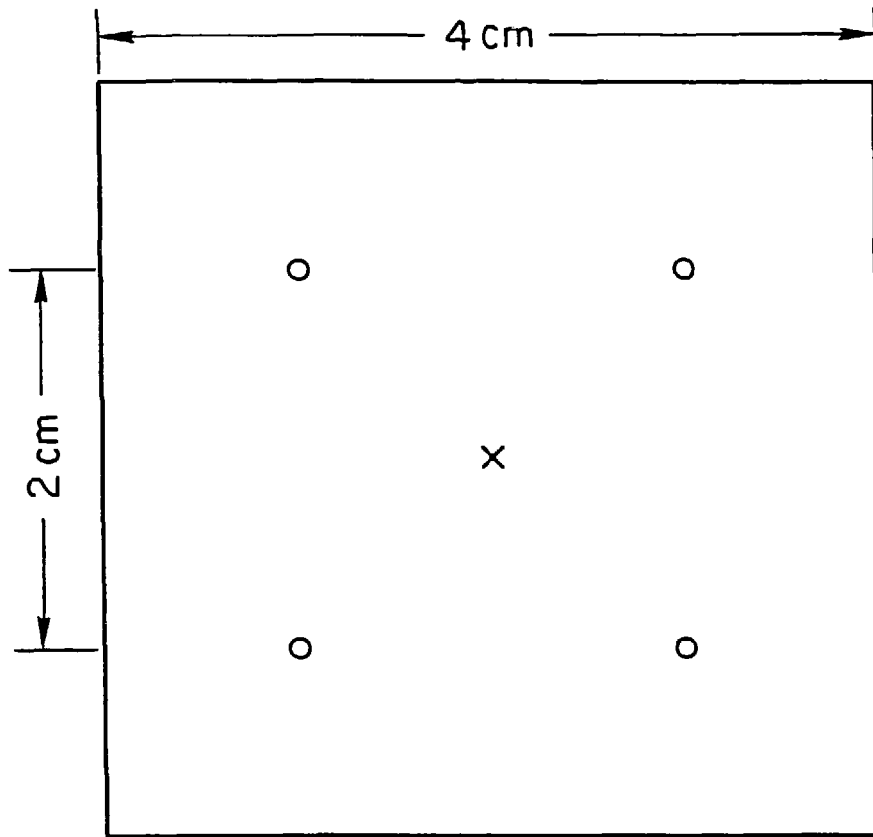
Deposits of Polymers at Breakdown

In order to study the growth of polymers ("whiskers") on the wires, we studied breakdown with different gases, mainly with A/ CO_2 / CH_4 mixtures with more

Table I. Breakdown conditions in a 3/4" diameter tube (Ref. 2)

FIELD WIRE				SENSE WIRE			
Diameter (μm)	λ'_b (kV)	E_b (kV/cm)	E_c (kV/cm)	Diameter (μm)	λ'_b (kV)	E_b (kV/cm)	E_c (kV/cm)
20	.19	190	51	20	.28	280	89
30	.22	147	50	30	.33	220	88
50	.30	118	55	50	.39	154	77
100	.42	83	51	100	.50	98	62
178	.61	69	50	178	.62	70	51
304	.82	54	43				

(Gas: 89% A, 10% CO₂, 1% CH₄)



1-85

5007A1

Fig. 1. Endview of the multiwire cell used to test breakdown. The replaceable sense wire of varied diameter (X) is at ground, the field wires (O) of $178\text{ }\mu\text{m}$ diameter are at high voltage V_f , and the outside conducting box is at high voltage V_0 . The length of the wires is 25 cm.

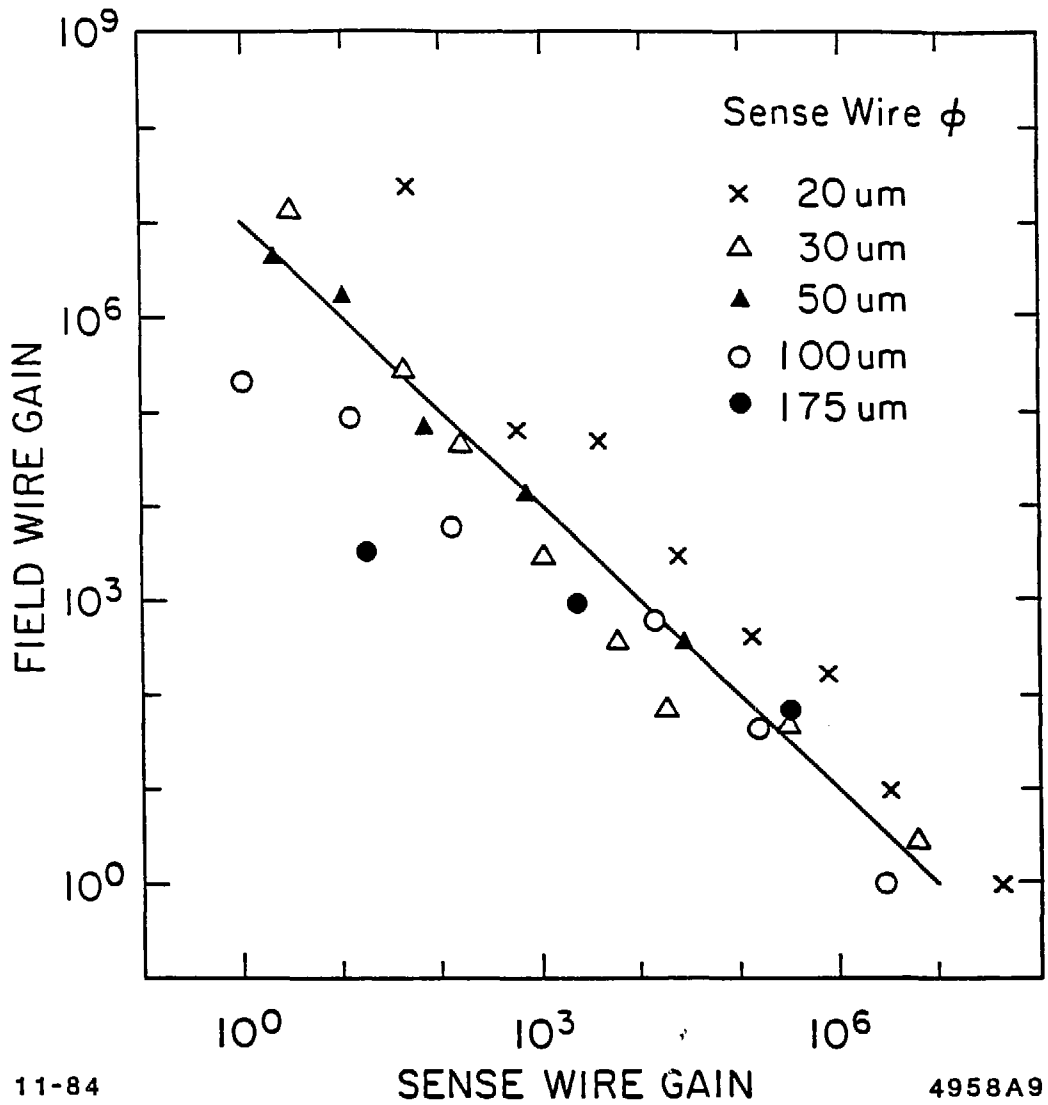


Fig. 2. Field wire gain, g_f , vs. sense wire gain, g_s , at breakdown in a mixture of 89% A, 10% CO_2 , 1% CH_4 for different sense wire diameters. The straight line, to guide the eye, corresponds to a total gain of 10^7 .

than 85% A, and also 50% A/ 50% C₂H₆. The assumption is that in many new chambers we are faced with local breakdown problems which we can study by forcing the chamber to discharge for a long time, and thus examine the gas stability. We can also simulate part of the plasma processes present in environments with large radiation doses. A chamber similar to the one shown in Fig. 1, but with Lucite walls to facilitate visual observation of gas discharges and growth of polymers, was left at the breakdown voltage with a current of 50 μ A for extended periods of time. Within less than 5 minutes, very long "whiskers" were observed in 50% A/ 50% C₂H₆, and 89% A, 10% CH₄, 1% CO₂. Both gas mixtures are known to grow polymers under extreme conditions in drift chambers. Other mixtures fall into two categories (Table II): If the CH₄ admixture was >4%, polymerization was observed within 15 minutes, independent of the CO₂ content (between 1% and 10%). On the other hand, if the CH₄ content was \leq 4%, no polymerization was detected, and no changes in gain were observed even after the chamber was held at breakdown for several hours.

To be more quantitative we subjected two gas mixtures, which did not grow whiskers and which are candidate gases for the new MARK II drift chamber, to continuous large currents (50 μ A) in our test chamber shown in Fig. 1. Every few hours the gain was monitored by measuring the pulse height produced by the photon from a ⁵⁵Fe source. Fig. 3 shows the relative gain in 89% A, 10% CO₂, 1% CH₄, and 93% A, 3% CO₂ and 4% CH₄ as a function of the duration of breakdown at 50 μ A. As can be seen, the two gases are degraded at different rates: the mixture with 93% A, 3% CO₂ and 4% CH₄ seems to survive about 7 times longer, possibly due to better quenching. The time at which the gain is reduced to 50% of its original value corresponds to an integrated charge of 0.28 Coulomb/cm for the 89% A, 10% CO₂, 1% CH₄ mixture and to 1.9 Coulomb/cm for the 93% A, 3% CO₂, 4% CH₄. The cathode wires were extremely clean and the anode wires showed fuzzy deposits.

Experience of the MARK III

The MARK III has been operating at SPEAR since 1981 at energies mostly below 4 GeV. The chamber uses HRS gas with one exchange per day. The gain is high ($>10^6$): $\lambda' = 0.266$ kV on a 20 μ m anode wire where we had determined spontaneous breakdown at $\lambda'_b = 0.28$ kV. The field on the cathode wires is 37 kV/cm—below spontaneous breakdown at 50 kV/cm, but still relatively high.

No problems were noticed in the first 4 years. Then large currents were drawn in the outermost layer distributed over many wires with currents $i \sim 1\text{--}5 \mu\text{A/m}$. In two other layers a few distinct locations were affected. The problem persisted with beams on and off and became 2 \times worse with the magnet off. This points to

Table II. Degradation of cathode wire during breakdown ($i > 5\mu\text{A}$)

	% CO ₂									
	1	2	3	4	5	6	7	8	9	10
1					N					N
2				N						
3			N							
4	N	N	N	N			N			
5	N		W		W					
6	C		W		W					
7	C			W						
8	C									
9										
10	W									

N = no whisker;

W = whisker in < 20 min;

C = charred cathode

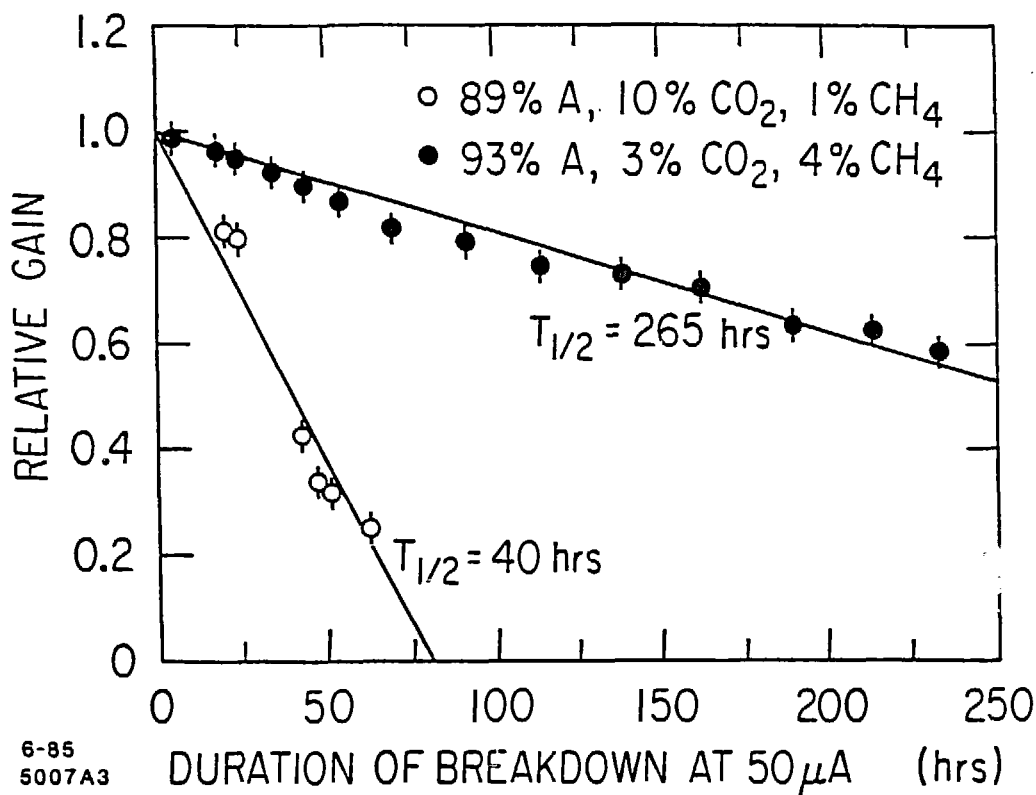


FIG. 3. Relative gain for two different gases as a function of the duration of breakdown at a current of 50 μ A. The 50% points are 40 hours (corresponding to an integrated charge of 0.28 Coulomb/cm) for the 89% A, 10% CO₂, 1% CH₄ mixture and 265 hours (corresponding to an integrated charge of 1.9 Coulomb/cm) for the 93% A, 3% CO₂, 4% CH₄ mixture.

a feedback mechanism between field and sense wires which is partially eliminated when electrons and ions have different Lorentz angles. The current on the anode wires was entirely due to a high rate of fast pulses of 25 ns lengths, consistent with being caused by single electron emission.

Pulled wires were spot checked and anode wires were found pitted, cathode wires looked clean. The problem is believed to be inside the chamber because it disappeared when N_2 was let into the chamber, and also when the outside HV panels were at lower voltage.

In late fall 1985, the CH_4 content was increased from 1% to 2%. The expected lower gain was observed, but no cure.

In December 1985, water was added (10^{-3}) and the chamber quieted down for 20 days. Then it started to draw currents again and the water admixture was increased to 2×10^{-3} .

We are running now with H_2O admixture of 2×10^{-3} for a month and have not seen the reappearance of large currents.

Acknowledgments

We thank Paulo Giubellino, Bill Rowe, Jeff Scala, and Daria Walsh for their help during data taking.

References

1. F. Sauli, CERN 77-09 (1977).
2. P. Giubellino *et al.*, SCIPP 84/37; to be published in *Nucl. Instr. & Methods*.

LIFETIME TESTS FOR MAC VERTEX CHAMBER

Harry Nelson, SLAC/Stanford University

MAC Experiment

A vertex chamber for MAC was proposed in fall 1983 to increase precision in the measurement of the B hadron and τ lepton lifetimes. The chamber had to be placed within the existing central drift chamber, making access for repairs difficult and costly. We therefore used for detector elements thin-walled aluminized mylar drift tubes ("straws") because of their simplicity and robustness.^{[1],[2]} The diameter of the drift tubes was 6.9 mm.

The radial extent of the proposed chamber was from 3 cm to 10 cm, the inner wall of the central drift. It was clear that radiation levels, from synchrotron x-rays and overfocussed electrons, were potentially high. Since the drift distance is short in the straws, we wished to operate them at the highest possible gas gain, to achieve the best spatial resolution. There was a likelihood of drawing large currents in the chamber and thus causing radiation damage. We therefore undertook a study of radiation hardness under the conditions of our proposed design.

Tests were conducted in the vessel illustrated in Fig. 1. One face of the cubical vessel had a Lucite window, through which we could illuminate the straws within. A list of materials in the chamber is in Table I. To correspond to final operating conditions tests were conducted at 4 atma* without gas circulation. Table II contains a list of gases used and operating conditions.

We have observed that pulses from the 5.9 keV x-rays from Fe^{55} remain relatively saturated for pressurized, highly quenched Argon-Hydrocarbon mixtures. However, the pulses from single primary electrons, generated by the photoelectric effect on the thin aluminum cathode, undergo a characteristic "jump" into the streamer mode with pulse heights comparable to those observed for Fe^{55} (Fig. 2). Presumably the large (from ~ 240 primary electrons) avalanche from Fe^{55} occupies or screens the spatial region of streamer growth. The high voltages in Table II correspond, whenever possible, to this "single electron streamer" mode.

Argon-Hydrocarbons typically had a plateau of 300-500 volts for the single electron streamer mode. The large pulses associated with drift chamber operation in this mode should provide optimal spatial resolution and require modest electronics.

It was expected that predominantly Argon- CO_2 mixtures would give good lifetimes. However for such mixes there was no clear single electron streamer plateau; the mixtures are underquenched. Addition of Xenon provides a well quenched gas, without organic additives. This gas mix, 6 in Table II had a plateau of 900 volts.

The ^{55}Fe proportional pulse height spectrum was monitored at intervals throughout

*4 atmospheres absolute pressure

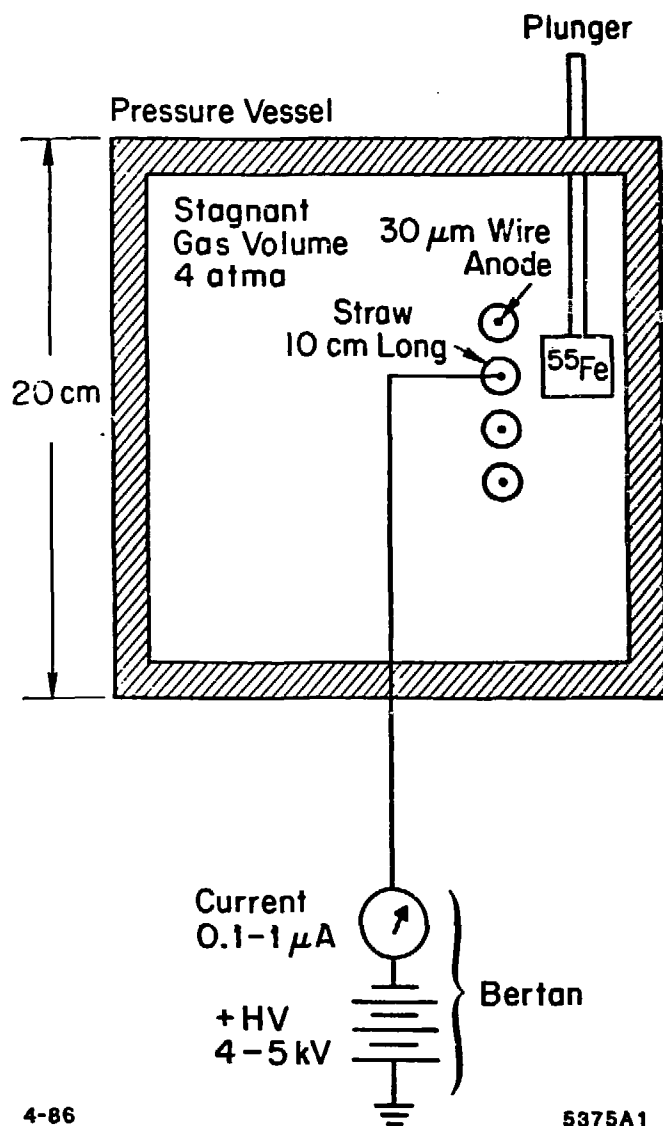


FIG. 1. Test vessel used for lifetime tests. One face of the cubical vessel had a lucite window, through which light could be shined to eject electrons from the straw cathodes via the photo-electric effect. The source had a diameter of 1 cm and gave an event rate of 25 kHz.

TABLE I

1. Aluminized mylar straw, 6.9 mm diameter, 100 μm wall, 0.6-0.8 ohms/sq. surface resistivity. 10 cm long.
2. Virgin Delrin 500 HV insulators.
3. Gold Tungsten anode wire, 30 μm diameter.
4. Teflon insulated coaxial cable and wire.
5. High voltage ceramic capacitors and 5% resistors.
6. Epoxy.
7. Butyl O-rings and vacuum grease.
8. Lucite window.
9. Polyflow tubing.
10. Aluminum.

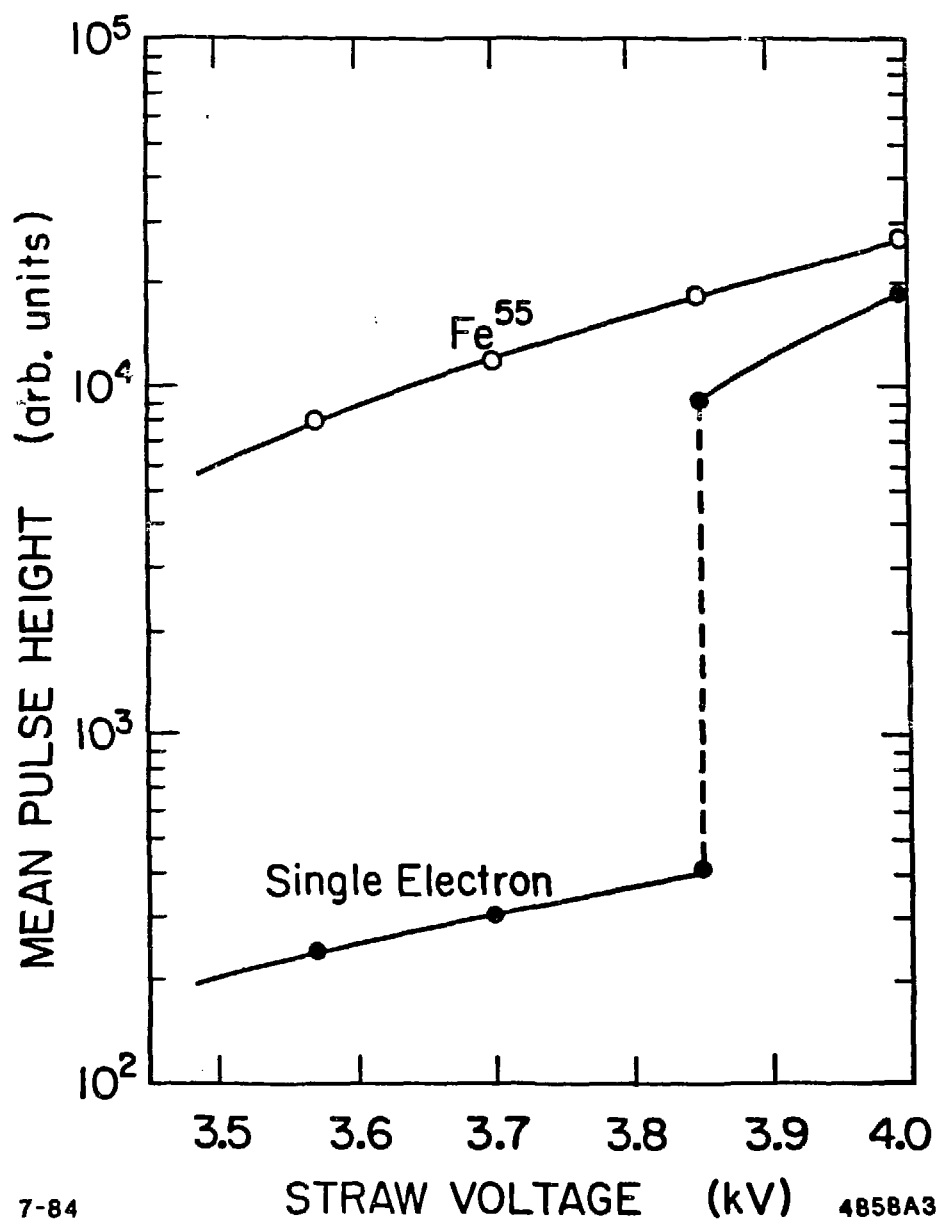


FIG. 2. Mean pulse height as function of voltage in Argon-Ethane at 4 atm.

TABLE II

Gases and Operating Conditions

Number	Mixture	Initial Impurities (ppm)	High Voltage (kV)	Gas Gain (^{55}Fe)	Current Drawn (μA)
1	50% Argon 50% Ethane	< 20	4.5	2×10^6	0.8
2	70% Argon 30% Isobutane	< 100	4.5	2×10^6	0.5
3	49.5% Argon 49.5% Ethane 1.0% H_2	< 20	4.6	3×10^6	1.3
4	50% Argon 50% CO_2	< 100	4.2	2×10^6	0.7
5	49.5% Argon 49.5% CO_2 1.0% CH_4	< 100	4.2	3×10^6	1.5
6	50% CO_2 40% Argon 10% Xenon	< 100	4.6	3×10^6	1.3

the lifetimes studies. In the first three Argon-Hydrocarbon mixtures, a broad continuum developed under the direct 5.9 keV and escape 3.2 keV peaks. This degradation was associated with buildup of deposits on the anode wire. At ~ 0.05 C/cm, there was an abrupt transition to a continuous discharge. Replacing the anode wire restored operation. We concluded therefore that a discharge point had built up on the anode wire. We could not test the addition of alcohol as this dissolved the glue used to bond the drift tubes' mylar walls.

For mixtures 4-6 in Table II, the predominately Argon-CO₂ mixtures, no broad continuum appeared under the characteristic ⁵⁵Fe spectrum. In fact, the 5.9 keV peak narrowed as charge collected, compared with a control straw in the same gas volume. It is likely that the anode wire became cleaner. At 0.15 C/cm, the width of the 5.9 keV peak became rate dependent; by 0.25 C/cm, the pulse height spectrum was permanently broad, even for low rates. Inspection of the inside aluminized mylar wall revealed that aluminum near the source had disappeared; a transition region of greyish aluminum bordered this neighborhood; the normal shiny aluminum surrounded this. We speculate that the positive ions attack the aluminum layer when they neutralize at the cathode. It is to be noted that the cathode in our straws was a thin (.6-.8 ohm/sq surface resistivity) evaporated layer that could be relatively easily removed. CH₄ and Xe have lower ionization potentials than CO₂, so they should cause less damage when they neutralize. However, addition of these molecules did not clearly decrease the rate of cathode removal. By using a thicker aluminum layer, or perhaps by using a metal other than aluminum, one might achieve longer working lifetimes for gas mixtures limited by the cathode damage.

An end view of the MAC vertex chamber is shown in Fig. 3, a side view with shielding configuration in Fig. 4. Gas mixture 4, 49.5% Argon - 49.5% CO₂ - 1% CH₄ was chosen for use in the vertex detector. Operation began in November 1984. The operating pressure is 4 atma; the high voltage on the anode wire +3900 volts, giving 6.5 pC collected for the 5.9 keV x-ray, 3 pC in the first 10 ns.

After injection of beams 4-6 nA/cm are drawn in the inner two layers; current drawn in the outermost pair is almost a factor of 3 less. Typically two random hits per beam crossing are recorded in the chamber, and is due to synchrotron radiation from the beam halo photoconverting in the gas. This background and not the "signal" event tracks were the main source of the current drawn by the chamber.

The charge collected by the vertex detector to January 16, 1986, is given in Table III. No aging phenomena has been observed. Indeed, we are far from the regime of damage for Argon-CO₂ type gases.

CONCLUSIONS

In our tests, Argon-Hydrocarbon mixtures consistently became unusable at ~ 0.05 C/cm collected charge, due to anode buildup. Argon-CO₂ mixtures, while underquenched,

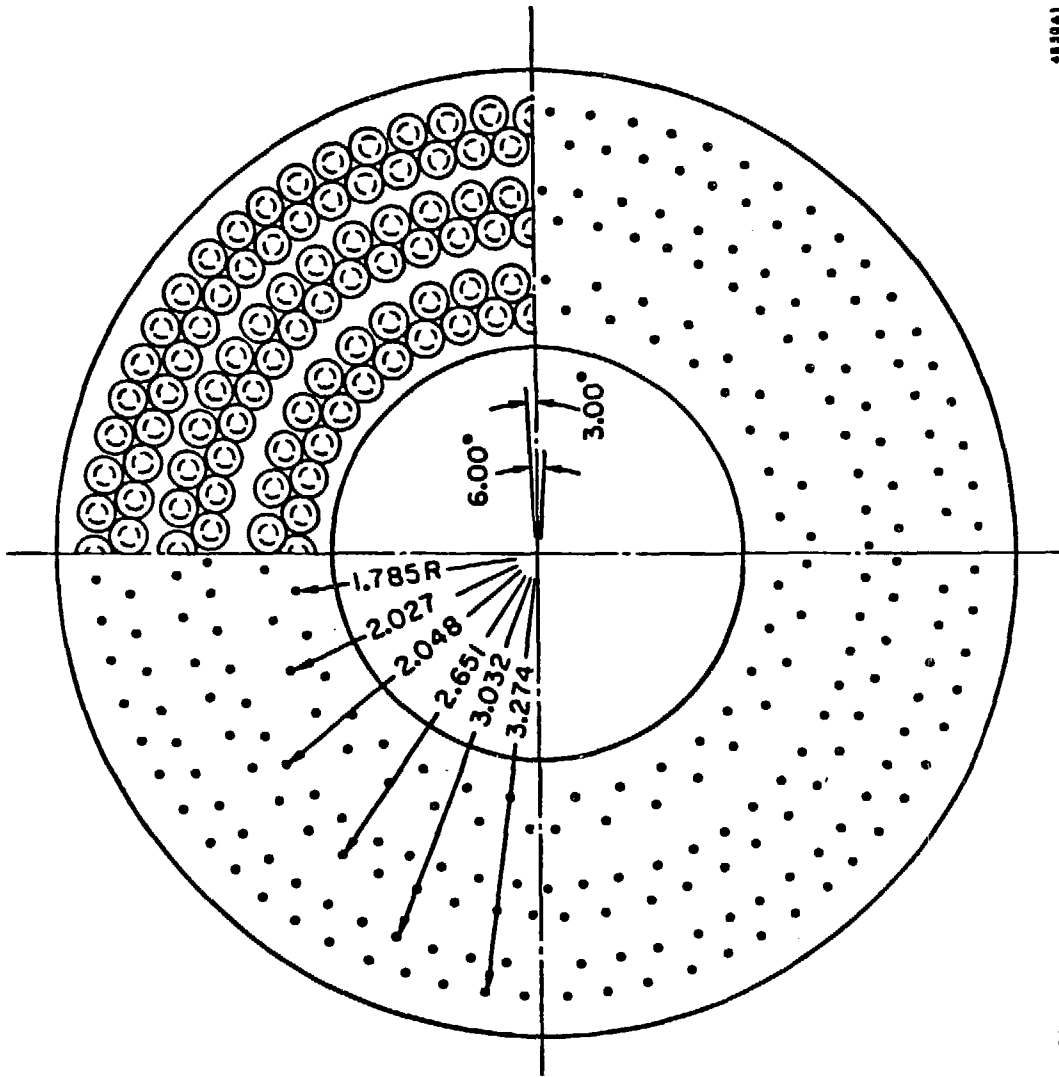
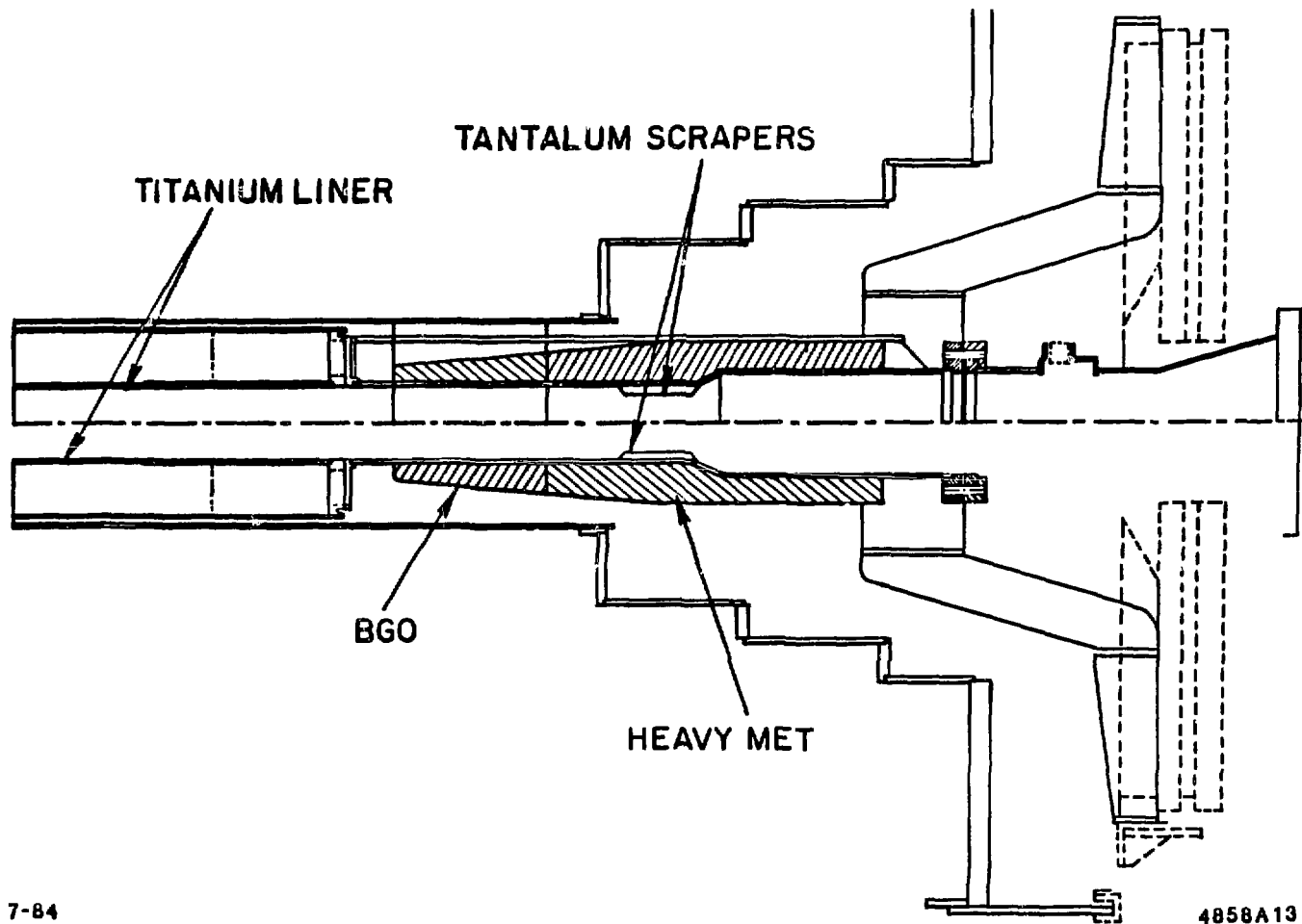


FIG. 3. Layout of the vertex chamber end-plate showing the arrangement of the 6 layers of tubes. Dimensions are in inches.



7-84

4858A13

FIG. 4. Cross section of the MAC Vertex Chamber, shielding and beam pipe assembly, showing the tantalum scrapers, heavy-met absorbers, and titanium liner.

TABLE III

Layer	Radius (cm)	Dose (C/cm)
1	4.58	0.025
2	5.20	0.017
3	6.18	0.014
4	6.81	0.010
5	7.79	0.0093
6	8.41	0.0081

were operational to 0.25 C/cm, at which point loss of cathode material became intolerable. Argon-Xenon-CO₂ proved to be quenched as well as Argon-Hydrocarbons, but was limited by cathode damage. The MAC vertex chamber has operated at a distance of 4.6 cm from the e^+e^- interaction point at PEP for two years and has shown no aging effects.

REFERENCES

1. D. Rust, SLAC-PUB-3311, April 1984.
2. E. Fernandez, et al., SLAC-PUB-3390, August 1984.

RESULTS FROM SOME ANODE WIRE AGING TESTS*

Ivanna Juricic and John A. Kadyk
Lawrence Berkeley Laboratory
University of California
Berkeley, California 94720

ABSTRACT

Using twin setups to test anode wire aging in small gas avalanche tubes, a variety of different gas mixtures were tried and other parameters were varied to study their effects upon the gain drop, normalized to charge transfer: $-\frac{1}{Q} \frac{dI}{I}$. This was found to be quite sensitive to the purity of the gases, and also sensitive to the nominal gain and the gas flow rate. The wire surface material can also significantly affect the aging, as can additives, such as ethanol or water vapor. Certain gas mixtures have been found to be consistent with zero aging at the sensitivity level of this technique.

I. INTRODUCTION

Anode wire aging effects resulting in loss of gain and gain non-uniformities have been observed for many years.^[1] However, the widespread use of gas avalanche counters and chambers, with increasingly challenging requirements, has demanded a more concerted effort be made toward understanding and curing these problems. The present set of tests were begun in an attempt to quantify the gain loss for a particular device, a gas sampling calorimeter, and has broadened to explore the effects of a number of parameters which result in gain loss. The technique makes use of small aluminum tubes of the same type used for the calorimeter, and exposes the tubes to γ radiation from an Fe^{55} source through a thin window. The gain region explored is in the vicinity of the operating region of our calorimeter, but also extends to higher and lower values of gain, covering a range used by many wire chambers. A variety of gas mixtures have been tested, and anode wires of two different compositions have been used. Other parameters that have been investigated include gas flow rate and source intensity. The results are parameterized in terms of the fractional gain loss per coulomb of charge transfer. No attempts were made to study breakdown processes resulting in large currents being drawn, and this phenomenon only rarely happened during the tests. This is relatively easily understood since breakdown processes appear to be initiated by deposits on the cathode, which in the tube geometry are spread over large areas of the cathode, which has, moreover, a small electric field at the surface compared to wire chambers. A large variety of deposits have been found on the anode wires during these tests, but these haven't been analyzed chemically. There are two equivalent test setups, having twin sources, which could be used to run two tests simultaneously.

*This work was supported in part by the Department of Energy under contracts DE-AC03-76SF00098 and DE-AC03-76SF00515.

II. PROCEDURE AND SETUP

The experimental test device used is shown schematically in Fig. 1. Each test counter was used only for one test, and then saved for later photographs and other studies. The aluminum tubes were prepared using a multi-step chemical cleaning procedure, followed by a final alcohol (ethanol) rinse shortly (a few days) before use. The feed-through insulators were made of molded fiberglass-epoxy, and these fit tightly into the ends of the tubes. Small residual leaks were eliminated using RTV in the early tests, and Sicomet 40 ("wicking" viscosity) for later tests, after it was found that the RTV had some influence on the results for certain tests. At the same time, the nylon inlet and outlet tubes for gas flow were also changed to short copper tubes (there was no evidence of problems due to the nylon tubes, however). The 0.6 mC Fe^{55} source illuminated about 6 mm of wire through a window of 0.5 mil mylar sheet, aluminized on the side toward the wire (see Fig. 1). The gas seals made in this fashion were excellent in the later tests (using Sicomet), but also generally very good with the RTV, but with some detectable leaks occasionally.

The anode wires were crimped into stainless steel capillary tubes at each end under 150 g tension. The wires tested were all of 50 μm diameter, and were made either of gold-plated tungsten, or Stablohm 800 (75% Ni, 20% Cr, balance of Al and Cu, according to manufacture^[2]).

The plumbing systems consisted of all copper or glass tubing upstream of the test counter and a short (~ 1 m) section of tygon tubing to a bubbler on the exhaust side. All copper and glass tubing was cleaned with ethanol before installation. Part or all of the gas could optionally be diverted through a glass system designed to bubble the gas through a liquid at a controlled temperature. A sparging device was used to ensure complete saturation of the vapor at the preset temperature. The high voltage was supplied by a Bertan 1739P supply and monitored with a Hewlett-Packard model 3465B 4-1/2 digit VTVM. This power supply was stable to less than ~ 1 volt out of ~ 2 -4 kV. The currents were monitored with electrometers (Keithley models 410 and 610B), with the tubes at ground potential. The HV was set so that the gain was approximately in the desired range, and the current was monitored over the duration of the test, which was generally about 1 week, but ranged from ~ 3 -15 days. Corrections for temperature and pressure changes were made to determine the relative gain. This was done by deducing the dependence upon gas density from the fluctuations in barometric pressure over short periods of the test during which time the drop in gain due to aging was negligible or could be corrected out. Such short-term barometric changes were as large as 1.5%, allowing an accurate determination of $\alpha_p = -(dI/I)/(dp/p)$, where I is the observed current, and p is the gas density. The gas flow and voltage were kept constant during a given run, and the rate of gain drop per coulomb was determined from the corrected current readings.

A "standardized" set of conditions was established corresponding to a 400 nA current, and an estimated gain of about 2×10^4 .^[3] The standard gas flow was ~ 60 cm^3/min and the effective source strength reduced to about 0.25 mC by inserting a 0.001 inch aluminum absorber. The standard wire was gold-plated tungsten, and the standard gas mixture was 50% argon + 50% ethane. The goal for the integrated charge in a given test was at least 0.2 Coulombs. Tests were performed with variations on these standard conditions in order to determine the effects of the various parameters. To be more specific, the gain has been varied corresponding to currents between 90 nA

EXPERIMENT SETUP

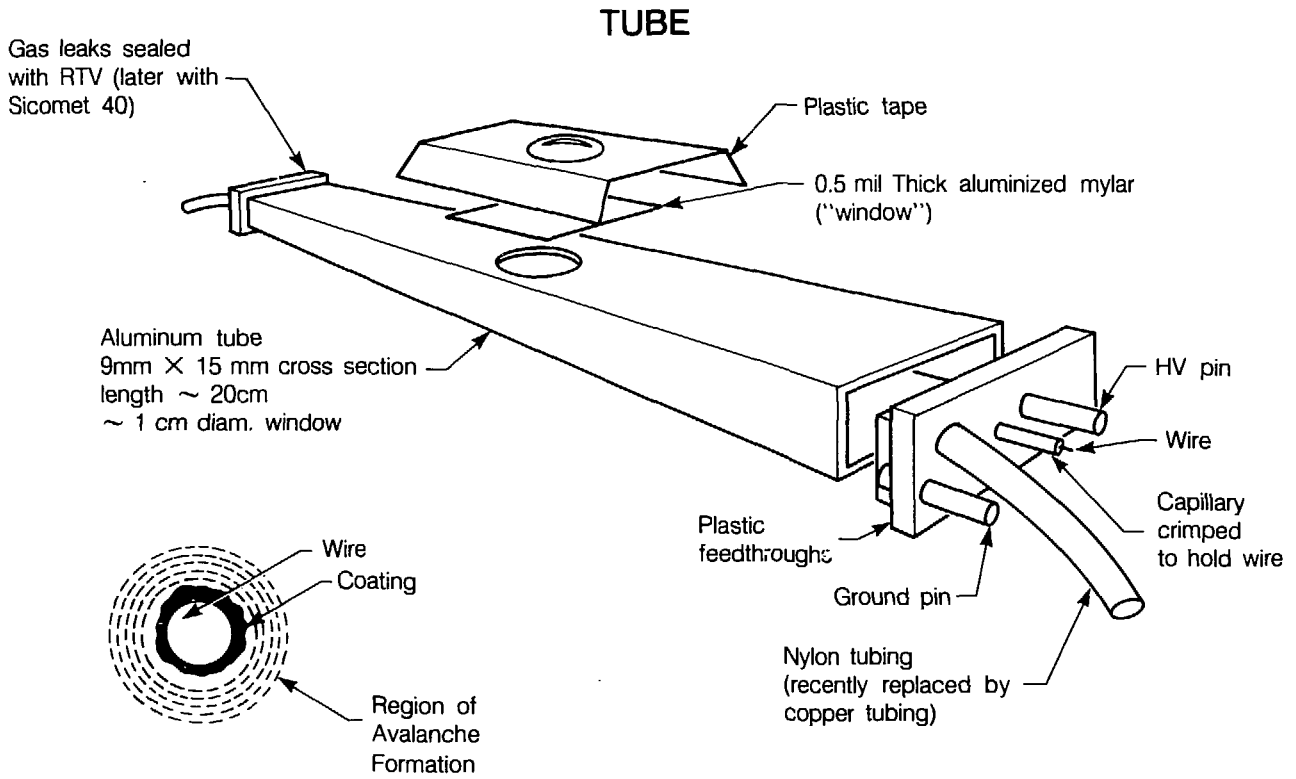


Fig. 1. Sketch of aluminum tube and fittings used for wire lifetime tests. A simple representation of wire, coating, and equipotential lines.

and 2 μA , the gas flow has been varied between about 12 and 380 cm^3/min , and the effective source strength between about 40 and 600 μCi . The principal tests have been made using five primary gas mixtures, plus a variety of additives intended to reduce the rate of wire aging.

III. DISCUSSION OF RESULTS

Table I contains the measurements of the rate of relative gain drop, $R = -\frac{1}{Q} \frac{\Delta I}{I}$ ($\%/\text{Coulomb}$), for the various conditions shown. Results are listed according to initial current values, which are proportional to the initial gain. Some of the tests, however, were done with the full source strength, i.e., no absorber (denoted by the values enclosed in parentheses) or with a reduced effective source strength (using 0.003 inch aluminum absorber). For these tests, a comparison of gain can be made relative to tests done at "standard" source strength (0.001" Al absorber) by using the factor ≈ 0.4 for reduction in intensity of 5.9 keV γ -rays for each 0.001 inch of Al absorber. Since there is evidence that gas flow has a significant effect, the results are also grouped by flow rate. All results in Table I are corrected for gain variations due to ambient temperature and barometric pressure, and residual errors from these sources are negligible, as are voltage variations. The largest effects causing differences between otherwise similar tests are surmised to be due primarily to minor impurity differences in the gas. Some uncertainty could also be due to the stochastic nature of coatings on the wire. For certain of the tests, especially high purity gases were used (UHP argon, CP ethane, etc.) to test the effects of gas purity. These effects can be seen in several instances in this table (for gold-plated tungsten): (1) There are six tests listed for the "standard" condition (Ar/ethane), and it is noted that those with the higher purity gas and/or tubes sealed with Sicomet rather than RTV, give considerably lower values of R . (2) A similar conclusion is reached by comparing two other gases: (80% Ar + 20% CH_4) and (89% Ar + 10% CO_2 + 1% CH_4). In the former case, R is quite large (63) for the less pure gas, and consistent with zero for the purer gas (-6). In the latter case, there is about a factor of 10 between the values of R being very low for the purer gas (147 vs. 15). An intermediate value of $R = 36$ was also obtained with a different gas cylinder of lower purity specification, and this may have been simply a cylinder with fortuitously high purity. (3) Several tests with dimethyl ether clearly show the correlation between small amounts of freon 11 impurity, at the few parts per million level, and the gain drop rate, giving dramatic differences between results having apparently only these very small differences in purity. There are results shown from three different bottles of DME which have been analyzed using the gas chromatography/mass spectrometry technique.^[4] The most recent test was for a bottle having $\lesssim 1$ ppm initially, and (14 ± 7) ppm at end of the test, due to concentration of freon 11 as the DME was used up. The 6-day long run was arbitrarily divided into two parts, and results shown are averages for these parts. The effect of concentrating the freon 11 is quite evident.

Another feature that is evident in Table I is the variation in R with current or "gain": when other conditions are fixed, the value of R decreases with increasing current. This same dependence has been noted by others.^[5] We see also a dependence on gas flow rate, which is explicitly shown in Table II. In three of the comparisons shown, there appears to be a quite significant increase in R for smaller flow rates. In the fourth gas listed, having a 1% H_2 additive, there appears to be a reversal of this rule,

Table I.

$$R = - \frac{1}{Q} \frac{\Delta I}{I} \text{ (\%/Coulomb) for Principal Gas Mixtures}$$

(on ~0.6 cm wire length)

Notes and Symbols: () Used to denote non-standard source intensity (Zero shims, except d)

- a - "Purer" gas
 b - Sicomet seal
 c - RTV seal, Cu tubes on counter
 d - 3 shims (.001" Al absorber)
 e - Very low gas flow (12 cc/min)

- f - Tube breakdown after .007C
 g - "Pure" DME
 h - "10-20 ppm" CFCI_3
 i - ≤ 1 ppm CFCI_3 , 1st half run
 j - ≤ 1 ppm CFCI_3 , 2nd half run

[] Collection of runs all at
 400 nA initial current

() Simultaneous runs

Gas	Wire/flow (≤ 100 cc/min)	Current (nA) (~gain)						
		2000	1000	700	400	200	100	60
50% Ar + 50% C_2H_6	>100			(33)				
	Au/W				[66.42 ^a 17 ^{ab} , 45 ^{ac} 28 ^{ab} , 6 ^b]			
	<100	28		(69)		99		(23) ^{bd}
	>100 Stablohm		(79), (96)					
80% Ar + 20% CH_4	<100	-2		(237)	130 336 ^{ab}			227
	Au/W <100				[63 73, 6 ^{ab}]			
	>100 Stablohm		96					
	<100							
89% Ar + 10% CO_2 + 1% CH_4	>100	16				203		
	Au/W				[36, 15 ^{ab} , 147 ^b]			
	<100							
	>100 Stablohm		55					
93% Ar + 4% CH_4 + 3% CO_2	<100				22 54 ^e			
	Au/W <100							
	>100 Stablohm		10		(26)			
	<100							
Dimethyl Ether	Au/W				[(-12) ^j (11) ^g (108) ^y (732) ^h]			
	60 cc/min							
92% CO_2 +8% iC_4H_{10}	Au/W 60 cc/min				~1800 ^f			

Table II.
Effect of Gas Flow Rate on Gain Loss

Comparison of rate of gain drop vs. flow rate, with other conditions the same (gain, wire, gas):

$$R = \text{Gain Drop Rate} = - \frac{1}{Q} \frac{\Delta I}{I} \frac{\%}{\text{Coulomb}}$$

Shim refers to 0.001" Al absorber: ϕ (absent), 1 (present)

GAS	WIRE	HIGHER FLOW		LOWER FLOW	
50%Ar + 50% C ₂ H ₆	Au/W	105 $\frac{\text{CC}}{\text{min.}}$ ϕ Shim	R = 33 680 nA	50 $\frac{\text{CC}}{\text{min.}}$ ϕ Shim	R = 69 550 nA
50%Ar + 50% C ₂ H ₆	Stablohm	137 $\frac{\text{CC}}{\text{min.}}$ ϕ Shim	R = 90 750 nA	25 $\frac{\text{CC}}{\text{min.}}$ ϕ Shim	R = 237 680 nA
93%Ar + 4% CH ₄ + 3% CO ₂	Au/W	62 $\frac{\text{CC}}{\text{min.}}$ 1 Shim	R = 22 400 nA	13 $\frac{\text{CC}}{\text{min.}}$ 1 Shim	R = 54 300 nA
49.5% Ar + 49.5% C ₂ H ₆ + 1.0% H ₂	Stablohm	137 $\frac{\text{CC}}{\text{min.}}$ ϕ Shim	R = 96 810 nA	20 $\frac{\text{CC}}{\text{min.}}$ ϕ Shim	R = 70 765 nA

although in this case the difference is not so large, and may not be due solely to the effect of the gas flow (e.g., there may be an effect due to the H_2 additive).

As for the tests using Stablohm 800 wire, there appears to be a significantly higher value of R for Stablohm wire than for Au/W. This difference becomes much larger when ethanol or water vapor is used, as can be seen in Table III. However, for other gases there is not such strong evidence for higher R values with Stablohm, though there are not many results on this point.

Table III is concerned only with the effect of certain additives to the standard gas, 50% Ar + 50% ethane. Certain features seem to be rather clear in comparison to corresponding values of R for the standard gas without additives, as given in Table I. As observed by others, the effect of adding a low level (~ 0.5 -1.5%) of ethanol vapor appears to reduce dramatically the value of R in the case of Au/W wire, and within the precision of these tests perhaps even to zero for 1.5% ethanol. However, the effect of ethanol seems to have the reverse effect in the instance of Stablohm wire, as can be seen from the several results in Table III. Comparison with Table I shows that even without additives, Stablohm seems to have higher values of R with Ar/ethane, but this value is dramatically increased with the addition of ethanol. M. Atac, FNAL, has recently obtained evidence confirming this effect, based upon tests showing rapid degradation of pulse height resolution under similar conditions.^[6] Observation of the affected wires under a microscope shows a "clean" Au/W wire, but a striking surface structural and color changes for the Stablohm wire. (See Fig. 2.) It is plausible that certain metallic

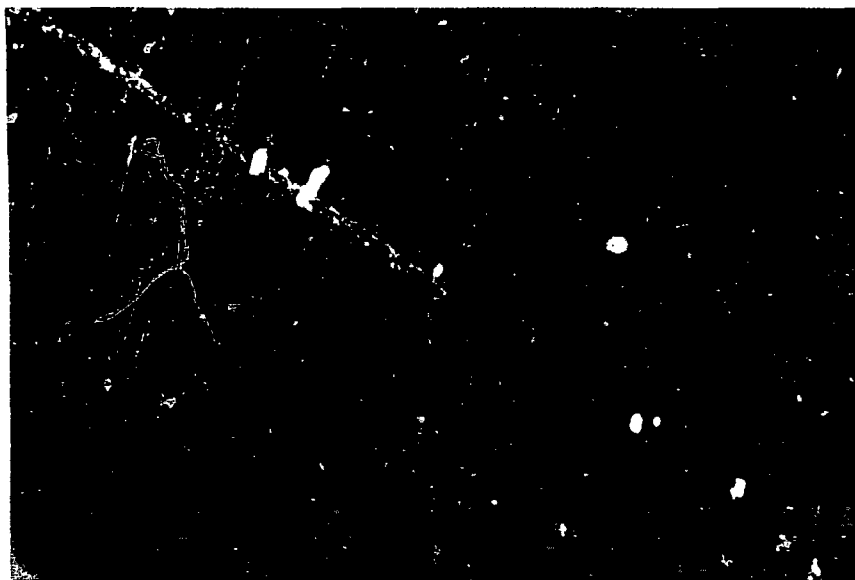


Fig. 2. Photograph of anode wire used in test with test with [Ar (50) + Ethane (50)] + 1.5% ethanol. Wire is made of Stablohm 800, and surface growths (and color change) have occurred after 0.2 Coulombs charge transfer. 400 μ A initial current.

Table III.

$$R = - \frac{1}{Q} \frac{\Delta I}{I} \text{ (%/Coulomb) for [50\%Ar + 50\% Ethane] + Additives}$$

Notes and Symbols: () Used to denote non-standard source intensity (no shims)

a - "Purer" gas

c - Premixed cylinder of [Ar(50) + Ethane (50)] + 1.5% Ethanol

b - Sicomet seal

d - ~0.5% Ethanol

[] Collection of runs all at 400 nA initial current

Gas	Wire/flow (≤ 100 cc/min)	Current (nA) (~gain)						
		2000	1000	700	400	200	100	60
1.5% Ethanol (190 Proof)	Au/W >100	(-12) (2)	19 ^d	(-1)		15 ^d		
	Au/W <100				9, 2 ^{ab}			
	Stablohm >100			(43.9)	[363 ^d , 500 ^d] [1123, 1200]			
	Stablohm <100				938 ^{ab}			
	Au/W <100				35 ^c 11			
1.5% Ethanol (200 proof)	Stablohm <100				245 ^c			
1.0% Hydrogen	Au/W <100			(62)	128			
	Stablohm >100 <100			(96) (70)				
0.2% Hydrogen	Au/W >100 <100	(10)(5) (4), (8)		(86) (32)	82	122		
~0.5% Water	Au/W >100 <100	(3) (72)						
~0.15% Water	Au/W <100 <100				27 65			

elements of the Stablohm are reacting chemically with the gas plasma while for the Au/W wire, the gold coating is chemically inert. Later entries in Table III also suggest enhanced reactivity with Stablohm when water vapor is present, though the effect is less than with ethanol vapor. Surface color changes are also seen in this case. There does seem to be some improvement for Au/W wire using water, but not as much as with ethanol. Finally, there appears to be no evidence of improvement through addition of hydrogen, at either the 0.2% or 1.0% level. This is *not* inconsistent with improvements observed in other gases, however.^[7]

The variations between results seen in these tables for tests done under nominally similar conditions is thought not to be due to intrinsic errors in the technique, but due mainly to variations in gas purity from different gas cylinders. In several comparison tests, the *same* gas was used in parallel runs with only one parameter (source strength, gas flow, additive, etc.) being varied to establish its dependence. Errors due to relative current measurement are estimated to be $\lesssim 0.1\%$. The error due to the stochastic nature of deposits on wires is not known, but could be large in the case of some wires having impressive isolated growths (e.g. on Stablohm wire, as shown in Fig. 2). However, because of the observed sensitivity to trace impurities, it is surmised that the principal deviations are from this source. Some of these impurities are in the gas as received from the supplier, and some were evidently due to the use of RTV for tube seals in the earlier runs. The effect of specific impurities can also be different with different gases, of course. Since there is evidence at this workshop that some gas contaminants can have long-lasting residual effects even after the source of contamination has been removed,^[8] it is possible that the plumbing of the present test apparatus can be vulnerable, since there is no provision for cleaning it after each test. However, such effects cannot be dominant or seriously alter most results, since many of the later tests, using a variety of gases with and without admixtures, have shown very low values of R , and some are consistent with zero.

The wires were photographed after testing. The structural and color changes were frequently found to be quite different for different gas mixtures, or even for the same gas but with some other difference in conditions. Examples of these are shown in Figs. 3 and 4 which are examples of growths on Au/W wire in Ar/ethane, but tested in different gain regions, and having different purity specifications.

IV. CONCLUSIONS

The rate of deterioration of anode wire gain, R , has been found to depend significantly, and in some cases dramatically, on additives, and trace contaminants, in the various gases tested, as well as on the type of wire. In particular, high purity gases yield values of R typically at least ten times smaller than gases of technical grade purity when used with gold-plated wire. On the other hand, even the lower purity gases can be improved by adding water or ethanol vapor, and 1.5% ethanol in Ar (50%) + ethane (50%) has yielded results consistent with $R = 0$. However, Stablohm wire appears to be attacked by use of either of these two vapors in Ar/ethane but especially in the case of ethanol. A most conspicuous example of the sensitivity to contamination is for dimethyl ether, where nearly two orders of magnitude difference in R appears to result from a

elements of the Stablohm are reacting chemically with the gas plasma while for the Au/W wire, the gold coating is chemically inert. Later entries in Table III also suggest enhanced reactivity with Stablohm when water vapor is present, though the effect is less than with ethanol vapor. Surface color changes are also seen in this case. There does seem to be some improvement for Au/W wire using water, but not as much as with ethanol. Finally, there appears to be no evidence of improvement through addition of hydrogen, at either the 0.2% or 1.0% level. This is *not* inconsistent with improvements observed in other gases, however.^[7]

The variations between results seen in these tables for tests done under nominally similar conditions is thought not to be due to intrinsic errors in the technique, but due mainly to variations in gas purity from different gas cylinders. In several comparison tests, the *same* gas was used in parallel runs with only one parameter (source strength, gas flow, additive, etc.) being varied to establish its dependence. Errors due to relative current measurement are estimated to be $\lesssim 0.1\%$. The error due to the stochastic nature of deposits on wires is not known, but could be large in the case of some wires having impressive isolated growths (e.g. on Stablohm wire, as shown in Fig. 2). However, because of the observed sensitivity to trace impurities, it is surmised that the principal deviations are from this source. Some of these impurities are in the gas as received from the supplier, and some were evidently due to the use of RTV for tube seals in the earlier runs. The effect of specific impurities can also be different with different gases, of course. Since there is evidence at this workshop that some gas contaminants can have long-lasting residual effects even after the source of contamination has been removed,^[8] it is possible that the plumbing of the present test apparatus can be vulnerable, since there is no provision for cleaning it after each test. However, such effects cannot be dominant or seriously alter most results, since many of the later tests, using a variety of gases with and without admixtures, have shown very low values of R , and some are consistent with zero.

The wires were photographed after testing. The structural and color changes were frequently found to be quite different for different gas mixtures, or even for the same gas but with some other difference in conditions. Examples of these are shown in Figs. 3 and 4 which are examples of growths on Au/W wire in Ar/ethane, but tested in different gain regions, and having different purity specifications.

IV. CONCLUSIONS

The rate of deterioration of anode wire gain, R , has been found to depend significantly, and in some cases dramatically, on additives, and trace contaminants, in the various gases tested, as well as on the type of wire. In particular, high purity gases yield values of R typically at least ten times smaller than gases of technical grade purity when used with gold-plated wire. On the other hand, even the lower purity gases can be improved by adding water or ethanol vapor, and 1.5% ethanol in Ar (50%) + ethane (50%) has yielded results consistent with $R = 0$. However, Stablohm wire appears to be attacked by use of either of these two vapors in Ar/ethane but especially in the case of ethanol. A most conspicuous example of the sensitivity to contamination is for dimethyl ether, where nearly two orders of magnitude difference in R appears to result from a

~ 20 parts per million contamination of freon 11.

There is a systematic trend toward larger values of R when the current, or average gain, is decreased. There also seems to be a dependence of R upon flow rate so that larger flows are preferable. Some evidence exists, based upon only one test, however, that R increases for smaller source intensity.

There are several examples among the tests of very small rates of aging, consistent with zero within the sensitivity of this technique ($R \gtrsim 15$). It is both encouraging that such good results do exist, and stimulating to find the causes of poorer results so that aging possibly may be controlled over a wider range of options.

ACKNOWLEDGMENTS

Most of the plumbing system and the aluminum tubes was built by Doug Shigley, and his very expert assistance was absolutely essential. Valuable (and often beautiful) color microphotographs were taken of each wire after testing by Bill Love, and some are shown here (unfortunately not in color). Amos Newton performed a careful and thorough analysis of an already depleted bottle of DME to search for all manner of contaminants at the few parts per million level, helping greatly our understanding of the behavior of this gas.

REFERENCES

- [1] A partial bibliography has been included as an appendix to this Proceedings.
- [2] Wire used was supplied by California Fine Wire Co. Stablohm is a trade name of this company. The present gold plated tungsten wire was also obtained from them.
- [3] This has some degree of uncertainty, perhaps as much as a factor of two, due to perturbation of the electric field by the positive ion space charge.
- [4] These analyses were done by Amos Newton of the LBL Chemistry Department. Two of the DME bottles ("pure" and "10-20 ppm") were courtesy of Dave Nygren, LBL.
- [5] See, for example, the paper by R. Kotthaus in this Proceedings, Section 3a.
- [6] Private communication with Muzaffer Atac. He has observed a complete degradation of pulse height resolution after only 0.07 C of charge. Furthermore, he has found that the degradation was *not* localized to the irradiated region, but occurred along the entire length of the wire, 10 cm, and also on the adjacent wire, spaced 12 mm away. His work is still in progress on this phenomenon.
- [7] H. Sipila, M. Jarvinen, Nucl. Inst. and Methods **217**, 298 (1983).
- [8] R. Kotthaus, this Proceedings, Section 3c and Fig. 9.

SUMMARY OF AGING STUDIES IN WIRE CHAMBERS BY AFS, DELPHI AND EMC GROUPS

H.J. Hilke

CERN, European Organization for Nuclear Research, Geneva, Switzerland

ABSTRACT

Ageing rates have been measured in Ar/C₂H₆, Ar/C₂H₆/methylal, Ar/CO₂ and Ar/CH₄/H₂. Deposits were observed on the anode wires only: they were insulating and contained silicon and oxygen in most cases. Impurities from the gas supply, presence of G10 and oil bubbler and geometry of cathodes are shown to affect ageing. Addition of water vapour reduced ageing while addition of hydrogen had no effect.

We summarize studies on radiation damage of wire chambers carried out at CERN by groups involved in the jet chamber for Axial Field Spectrometer (AFS) [1], the TPC and RICH for DELPHI [2], the EMC Muon Spectrometer [3] and a common DELPHI/EMC effort [4].

1. AFS RESULTS

The central detector of the AFS was operating at high luminosities at the ISR (10^{31} – 10^{32} /cm² sec). After one year of operation, a sense wire broke and examination indicated a smooth coating containing mainly Si, and some S in the first atomic layers. At this time, the wire — operating with gas amplification around 4×10^4 — had accumulated $\sim 3 \times 10^{-3}$ C/cm.

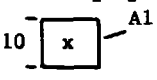


In order to study this damage, tests were started in small chambers of similar geometry. The ISR jet chamber continued operation without major problems for a total of 4 years, accumulating about 0.02 C/cm: no wire broke and the operating voltages were kept constant, except for preventive gain reductions in some runs at highest luminosity. Due to possible long term shifts, e.g. in the gas composition (the percentage of recirculated gas being changed several times), some gain variation — about 20% — cannot be excluded.

The test chamber results are summarized in table 1 (a) to (f). We shall only briefly comment on them; for details see ref. [1].

The test set-up is shown in fig. 1. It contained similar materials as the jet chamber: G10, oil bubbler, etc. The Stablohm sense wire was 30 μ m in diameter, and consisted roughly of 72.5% Ni, 22.5% Cr and 5% Al, Si and others. Always, 2 wires were irradiated by a 100 mCi Fe⁵⁵ source over about 1 cm (typ. 100 nA) and low-intensity spectra (with 1 mCi source) compared to those on a control position (not irradiated).

Typically, the main peak starts broadening, then a second peak forms and slowly outgrows the original peak. The movement of this second peak with respect to the value

TABLE 1

GAS	DEPOSIT	$\frac{1}{Q} \frac{\Delta PH}{PH_0}$ %/C/cm	Instability threshold C/cm	COMMENTS
(a) Ar/C ₂ H ₄ 50/50	Si + 20 (-30 ?) < 0.5% C Smooth layer	(240-) → 1200 (> 0.03 C/cm)	~ 0.025 - ~ 0.035 ^(*)	Nothing on cathodes, + potential w. (*) at > gain (x 2) (= 6 x 10 ⁴)
(b) ≡ (a) + cold trap (-79°C)	Si, S Fibres	400	0.16	
(c) Ar/C ₂ H ₄ /Methylal 60/35/5	Si + 20	~ 300 → 1000	> 0.05	Double peak after 0.01 C/cm (0.02-0.04 <u>w.o.</u> Methylal)
(d) Ar/CO ₂ 50 50	Si, Cl	~ (a)	0.025	1 test only!
(e) Ar/C ₂ H ₄ "PERSPEX Ch"	S, Cl, O <u>soft</u>	≡ (a)	(0.03) -0.13	No G10 No oil bubbler Deposit easily removable
(f) Ar/C ₂ H ₄ 10  Al	+ ?	(<< 150) Consistent w. ~ 0	<u>0.3</u>	4 tests
(g) Ar/C ₂ H ₄ Flat cath.	Si, S 	180	> 0.05	$\frac{fwhm_{irr}}{fwhm_{new}} =$ ~ 2 at 0.025 C/cm 3 at 0.05 C/cm
(h) + 1% H ₂	Si, S	~ 180		≤ (g)
(i) + 500 ppm H ₂ O	Cl, S, Si 	~ 100	> 0.2	~ 1 at 0.2 C/cm
(j) + 1500 ppm H ₂ O	Si	~ 100 (20°C) > 200 at 10°C?	> 0.1	T effect ? (1 test only!)

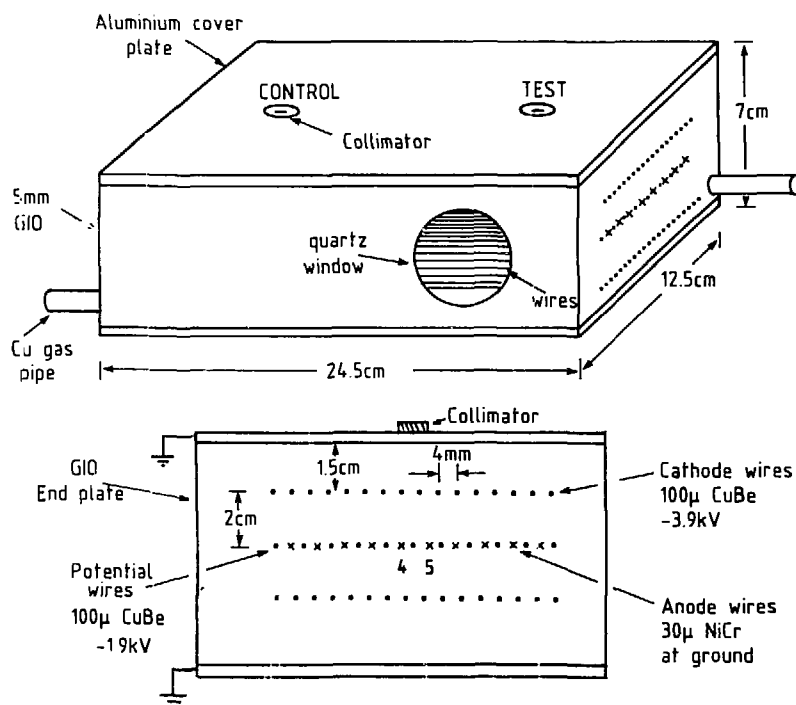


Fig. 1 G10 Test Chamber [1].

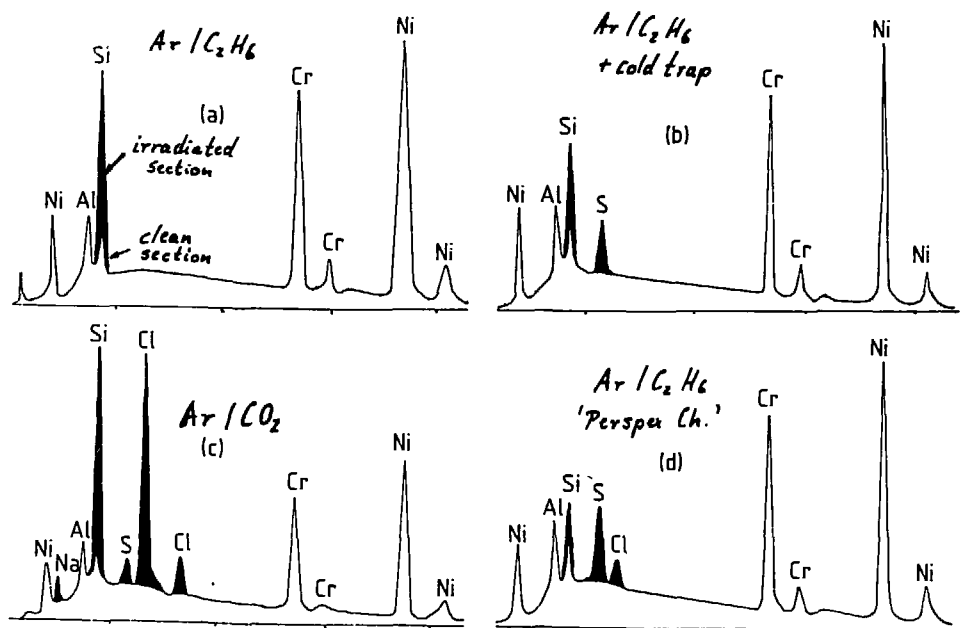
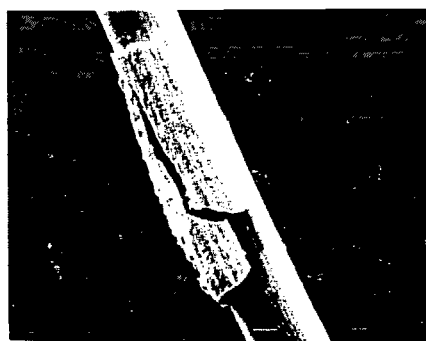


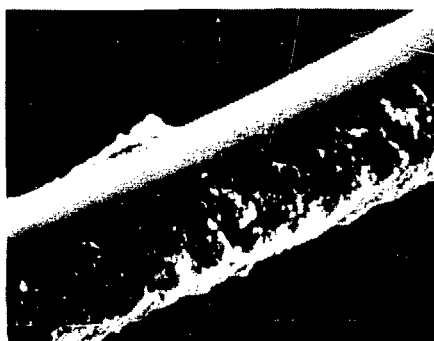
Fig. 2 Fluorescence Spectra [1].



(a)



(b)



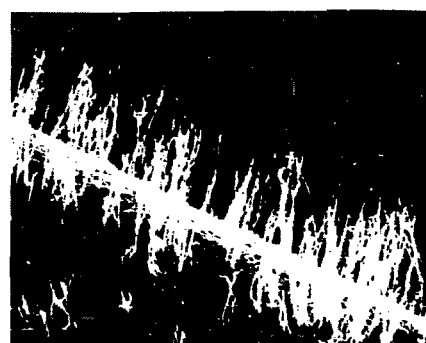
(c)



(d)



(e)



(f)

Fig. 3 Deposits on the anode wire [1]. (a) $\text{Ar}/\text{C}_2\text{H}_6$, 0.02 C/cm; Si + O deposits; (b) $\text{Ar}/\text{C}_2\text{H}_6$ + Methylal, 0.05 C/cm; Si + O; (c) Ar/CO_2 ; Si + Cl; (d) Perspex Chamber, $\text{Ar}/\text{C}_2\text{H}_6$, 0.13 C/cm, S + Cl + O, soft layer; (e), (f) G10 chamber, with cold trap (-79°C) on input line, $\text{Ar}/\text{C}_2\text{H}_6$, Si + S.

from the control position is given in table 1 as $\Delta PH/PH_0$. Several tests with the standard gas Ar/C₂H₆ (50/50) showed rather consistent results (see (a)). Deposits were only observed on anodes, never on cathode or potential wires. Normal fluorescence analysis, permitting detection of elements as low as sodium, showed Si as the major component.

Only in a few cases, wires were also analysed for carbon and oxygen: a strong oxygen signal (oxygen/silicon ratio of 2 to 3) was found but only < 0.5% carbon.

A cold trap was added to suppress possible silane impurities. The threshold for instability (high currents, often persisting after removal of source) improved substantially, and the ageing rate was somewhat reduced. The gas composition was changed (c,d): little effect. A new chamber was constructed out of perspex and aluminium, without the G10 and oil bubbler: the ageing rate was similar, but the deposit was very different: mostly S and Cl, little Si. In an attempt to remove gas impurities before they entered the main chamber, a small, rectangular proportional chamber was connected in front of the bigger test chamber: no effect on the ageing of the big chamber was observed. Then, when inserted directly in front of the oil bubbler, little or no ageing was observed in the rectangular chamber up to 0.3 C/cm (f). Thus, cathode geometry and/or gas flow (flow around sense wire was about 80 times than in the bigger test chamber) seem to affect ageing drastically.

Fig. 2 shows results from the fluorescence analysis and fig. 3 shows electron microscope photos of some deposits.

2. DELPHI RESULTS

The cathode wires in the bigger test chamber were replaced by flat cathodes (the potential wires remained): Ageing appeared to be slower ((g) in Table 1) and the deposit somewhat different, still containing a strong Si component.

Addition of H₂ (1%) hardly changed the results (h).

Addition of H₂O (500 ppm) reduced the ageing rate and increased the threshold for instabilities to > 0.2 C/cm (fig. 4(a)).

3. DELPHI/EMC RESULTS

A new test chamber was built. The 30 μ m Stablohm sense wires were replaced by 20 μ m W(Au) wires: the ageing rate was similar to the standard Ar/C₂H₆ mixture (\approx g). Addition of 1500 ppm of H₂O again slowed down the ageing rate (j). A first test indicated a higher ageing rate at 10 °C than at 20 °C. The test is being repeated. With the fluorescence method, only Si was detected (fig. 4(b)). Auger analysis showed C, but only in the top 100 Å and the same result for an unused wire.

(a)



(b)

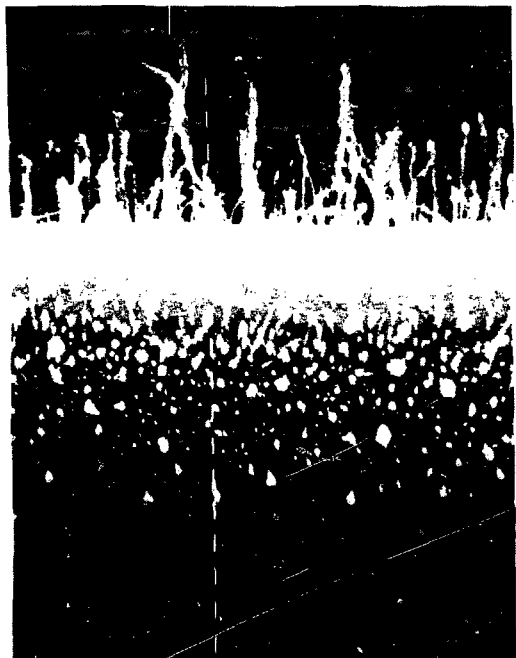
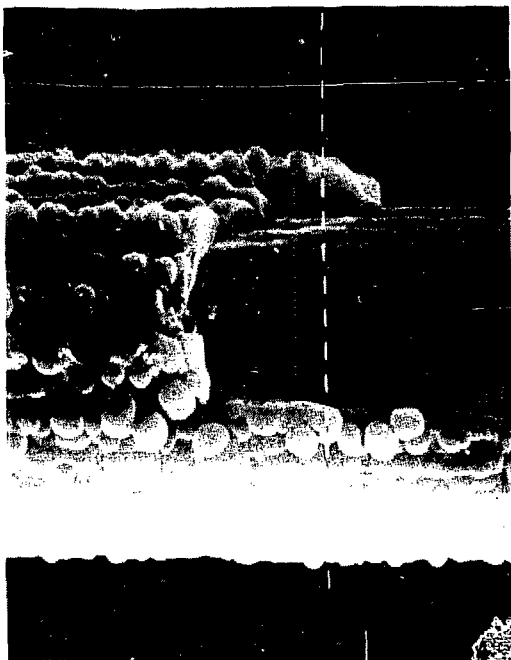


Fig. 4 Deposits on the anode wire. (a) $\text{Ar}/\text{C}_2\text{H}_6 + 500 \text{ ppm H}_2\text{O} + \text{Cl} + \text{S} + \text{Si}$ [2], (b) $\text{Ar}/\text{C}_2\text{H}_6 + 1500 \text{ ppm H}_2\text{O}, \text{Si}$ [4].

(a)



(b)



Fig. 5 Deposits on the anode wire of EMC muon chamber [3]. (a) near beam spot, (b) at 1.5 m from beam spot.

4. MUON CHAMBERS OF EMC (NA2/37)

Big drift chambers are operated with $\text{Ar}/\text{CH}_4/\text{H}_2$ (79.5/19.5/1%). The chambers are not very tight, so that H_2O and oxygen content is likely to be high (walls are Mylar/Aclar foils). Wires are $20\ \mu\text{m}$ W (Au), $50\ \mu\text{m}$ Cu/Be and $100\ \mu\text{m}$ Cu/Be. The chambers experience a high particle flux near the centre of the beam: $50\ \mu\text{A}$ are drawn per plane, originating from a surface of $< 60\ \text{cm}$ diameter. After 60 days, the efficiency drops to 30% near the beam spot and after 100 days, operation is stopped. Near the beam spot, the accumulated charge is around $0.25\ \text{C}/\text{cm}$.

Analysis of the sense wires shows a deposit in the form of a dense packing of "stalactites" near the beam spot and a rather smooth layer far away (fig. 5). Everywhere, a strong Si signal is detected.

5. CONCLUSIONS

Typical ageing rates of $\Delta\text{PH}/\text{PH}_0 = 100\text{--}1000\%/ \text{C}/\text{cm}$ are observed in $\text{Ar}/\text{C}_2\text{H}_6$, $\text{Ar}/\text{C}_2\text{H}_6/\text{Methylal}$, Ar/CO_2 and $\text{Ar}/\text{CH}_4/\text{H}_2$. A cold trap reduced the ageing and changes the appearance of the deposit: thus, impurities from the gas bottle probably contribute to the ageing but are not the only cause. Addition of H_2 (1%) had little effect. Addition of 500-1500 ppm of H_2O reduced ageing rate and especially the threshold for instabilities. It is supposed that H_2O increases the surface conductivity of the insulating deposits and thus decreases the danger of discharges due to surface changes.

Deposits were observed only on anode wires. They mostly showed a strong Si signal.

Suppression of G10 and oil bubbler changed the deposit: strong S, Cl and O signals were observed but hardly any Si. This is a strong indication that outgassing from the G10 and back diffusion from the oil bubbler contribute to the Si deposit. A possible mechanism is the deposition and adhesion of large oil molecules (via thermal movement and/or attraction via an electric dipole moment) on the anode wire and subsequent cross-linking under electron bombardment. This process has been observed under bombardment of a flat anode by $50\ \text{eV}$ electrons [5]: Film formation proceeded with high efficiency when the vapour pressure of the oil (DC 704) was only 2×10^{-9} Torr. We, therefore, conclude that a similar process may be responsible for the formation of the Si-compound deposits observed on the anode wires: the measured rate of deposition ($\leq 1\ \mu\text{m}$ for $\sim 0.1\ \text{C}/\text{cm}$) indeed requires a high efficiency for cross-linking, of the order of a percent per electron.

REFERENCES

- [1] J. Adam, C. Baird, D. Cockerill, P.K. Frandsen, H.J. Hilke, H. Hofmann, T. Ludlam, E. Rosso, D. Soria and V. Vaughan, NIM 217 (1983) 291-297.
- [2] R. Cirio, H.J. Hilke and E. Rosso, unpublished.
- [3] Communicated by D. von Harrach.
- [4] R. Cirio and A. Staiano, unpublished.
- [5] R. Christy, J. Appl. Phys. 319 (1960) 1680; see also ref. [11 16] in ref. [1].

A LABORATORY STUDY OF RADIATION DAMAGE TO DRIFT CHAMBERS

Rainer Kotthaus

*Max-Planck-Institut für Physik und Astrophysik,
Werner-Heisenberg-Institut für Physik, München, W.-Germany**
and

*KEK, National Laboratory for High Energy Physics,
Oho-Machi, Tsukuba-Gun, Ibaraki-Ken, 305, Japan*

ABSTRACT

A laboratory study of aging effects under intense radiation in Ar/C_2H_6 and $Ar/CO_2/CH_4$ filled drift chambers was carried out in order to establish detector lifetimes. In both gas mixtures stable operation in proportional mode and for Ar/C_2H_6 also in the limited streamer regime was possible up to total collected charges of several times $10^{17} e^-$ per mm of anode wire. Gain reductions were observed at rates between 0 and 1% per $10^{16} e^-/mm$ for Ar/C_2H_6 depending on the test conditions. At conditions, where gas amplification was stable in Ar/C_2H_6 , gain losses in $Ar/CO_2/CH_4$ ranged between 1.3 and 3.4% per $10^{16} e^-/mm$. Gain nonuniformities were inferred from broadenings and distortions of the Fe^{55} 5.9 keV γ line. These gain variations are caused by typically less than 100 nm thick deposits on the aged anode wires of poorly conductive material containing O, Si and C. Admixtures of H_2O did not halt the aging processes, but smoothed local gain variations. Contaminations with organic vapor from soft PVC surfaces initiated and accelerated radiation damage. Spark and glow discharges in Ar/C_2H_6 within minutes led to growth of grains and flakes of material containing C as the only detectable element on anode and cathode wires. In contrast discharges in $Ar/CO_2/CH_4$ did not result in any detectable deposits.

*permanent address

1. Introduction

An investigation of radiation damage to small wire chambers operated with $Ar/C_2H_6(1:1)$ and $Ar/CO_2/CH_4(90:9:1)$ gas mixtures was carried out under controlled laboratory conditions both at KEK* in 1984 and at MPI in 1985. The studies were motivated twofold:

- by the occurrence of instabilities in the inner central drift chamber of the CELLO detector¹ after about 2 years of operation at PETRA
- by the desire to establish a lifetime for the track detector² of the 4π magnetic spectrometer VENUS³ presently being prepared at KEK to study e^+e^- physics at the TRISTAN storage ring.

A 1 : 1 mix of Ar and C_2H_6 is a saturated, low diffusion drift gas allowing for high gas gain ($> 10^5$) in proportional mode and is therefore commonly used as count gas in high precision drift chambers.

However, recent reports^{4,5,6} and observations⁷ clearly indicate premature aging of Ar/C_2H_6 filled wire chambers exposed to intense radiation. The radiation damage is due to deposits on anode (and in some cases cathode) wires of poorly conductive material sometimes containing Si^4 as a major component. Similar aging effects due to deposits usually containing C as a major element have been observed in chambers using Ar/CH_4 mixtures^{8,9}. The surface coating of the electrodes results in electric field distortions. As a consequence elevated dark currents, gain reductions and nonuniformities and finally instabilities leading to selfsustaining discharges have been experienced.

Promising behaviour for longterm storage ring operation has been observed for a 10 : 1 mixture of Ar and CO_2 with 1% of CH_4 added for improved quenching. This mixture is used by the HRS and MARK III collaborations¹⁰ at PEP and in contrast to Ar/C_2H_6 seems to resist the growth of "whiskers", i.e. needles of presumably hydrocarbon polymers, under electrical discharges⁶.

*The study at KEK was done in collaboration with: N. Ishihara, T. Kohriki, T. Kondo, K. Kubo, S. Nakamura, S. Odaka, F. Suekane and Y. Watase (VENUS Drift Chamber Group)

We have carried out a comparative aging study of Ar/C_2H_6 and $Ar/CO_2/CH_4$ filled drift chambers operated in proportional mode at gas amplification between 5×10^4 and 3×10^5 , in the limited streamer mode (Ar/C_2H_6 only) and under glow and spark discharge conditions. Furthermore the effect on aging rates of controlled additions of H_2O to the chamber gas and of vapor outgassed from soft PVC surfaces was studied quantitatively. Using collimated Sr^{90} sources, irradiations were carried to total charge doses of up to $4.4 \times 10^{17} e^-$ per mm anode wire corresponding to more than a decade of typical e^+e^- storage ring operation¹¹.

The radiation damage was probed by recording Fe^{55} 5.9 keV γ spectra. After the end of each test, which typically took 10 days, wire specimens were taken for surface microanalysis using scanning electron microscopes (SEM) and a scanning Auger microprobe (SAM)*.

In section 2 the experimental setups and methods are described. In section 3 we present the results on gain variations. In section 4 the results of the morphological and chemical microanalysis are given and discussed. Section 5 summarizes the results of both studies.

2. Test Setup and Procedure

Table I summarizes details of the two setups used at KEK and MPI and lists some of the relevant operating parameters.

The test chambers used at KEK (fig. 1a) are *Al* boxes ($L \times W \times H = 20 \times 12 \times 7.5 \text{ cm}^3$) housing 5 rectangular drift cells of the open grid type (fig. 1b) selected for the VENUS central drift chamber. The removable top and bottom covers are sealed using flat rubber profiles. A glass bottom facilitates visual inspection. The insulating wire feedthroughs are made of polyoxymethylene (DELRIN) hav-

*SEM analysis at: Nat. Research Institute for Metals, Niihari-Gun,
Ibaraki-Ken, 305, Japan
Dr.-Ing. H. Klingele, Institut für Raster-Elektronen-
Mikroskopie, Adelgundenstr. 8, D-8000 München 22

SAM analysis at: Bundesanstalt für Materialprüfung (BAM)
Unter den Eichen 87, D-1000 Berlin 45

Table I Parameters of test setups

Parameter	KEK	MPI
Test chamber volume ($L \times W \times H$)	$200 \times 120 \times 75 \text{ mm}^3$	$150 \times 160 \times 20 \text{ mm}^3$
Number of cells	5	7
Cell size ($W \times H$)	$20 \times 17 \text{ mm}^2$	$20 \times 10 \text{ mm}^2$
Anode wire (at pos. pot.)	$30 \mu\text{m } W/Re, Au \text{ plated}^*$	$20 \mu\text{m } W/Re, Au \text{ plated}^*$
Cathode wire (at ground)	$140 \mu\text{m } Mo, Au \text{ plated}^{**}$	$128 \mu\text{m } Cu/Be, Au \text{ plated}^{***}$
Distance of Al cover to anode wire	24 mm	10 mm
Windows	mylar foil	Al coated mylar foil
Chamber seals	flat rubber profiles	rubber O rings
Wire feedthroughs	DELTRIN	HOSTAFORM
Feedthrough seals	silicone rubber (RTV)	epoxy
Gas mixtures (atmospheric press.)	$Ar/C_2H_6(1:1)$	$Ar/C_2H_6(1:1)$ $Ar/CO_2/CH_4(90:9:1)$
Gas purity	research grade purity	$Ar :> 99.996\%$ $C_2H_6 :> 99.95\%$
Gas flow rate	$50 \text{ cm}^3/\text{min}$	$100 \text{ cm}^3/\text{min}$
Time / vol. exchange	20 min	5 min
Gas lines	plastic hoses	stainless steel tubes (for special test: soft PVC hose)
Gas system seal (downstream of ref. chamber)	H_2O filled bubbler	buffer volume filled with chamber gas
Modes of operation	proportional and limited streamer mode glow and spark discharge	proportional mode
Gas amplification in prop. mode	5×10^4	$(2 - 3) \times 10^5$
El. field at cathode surface	10 kV/cm	11 kV/cm
Max. charge dose (e^-/mm)	3×10^{17}	4.4×10^{17}

* Manufacturer: LUMALAMPAN, Kalmar, Sweden

** Manufacturer: PLANSEE, Reutte, Austria

*** Manufacturer: LITTLE FALLS, Paterson, N. J., USA

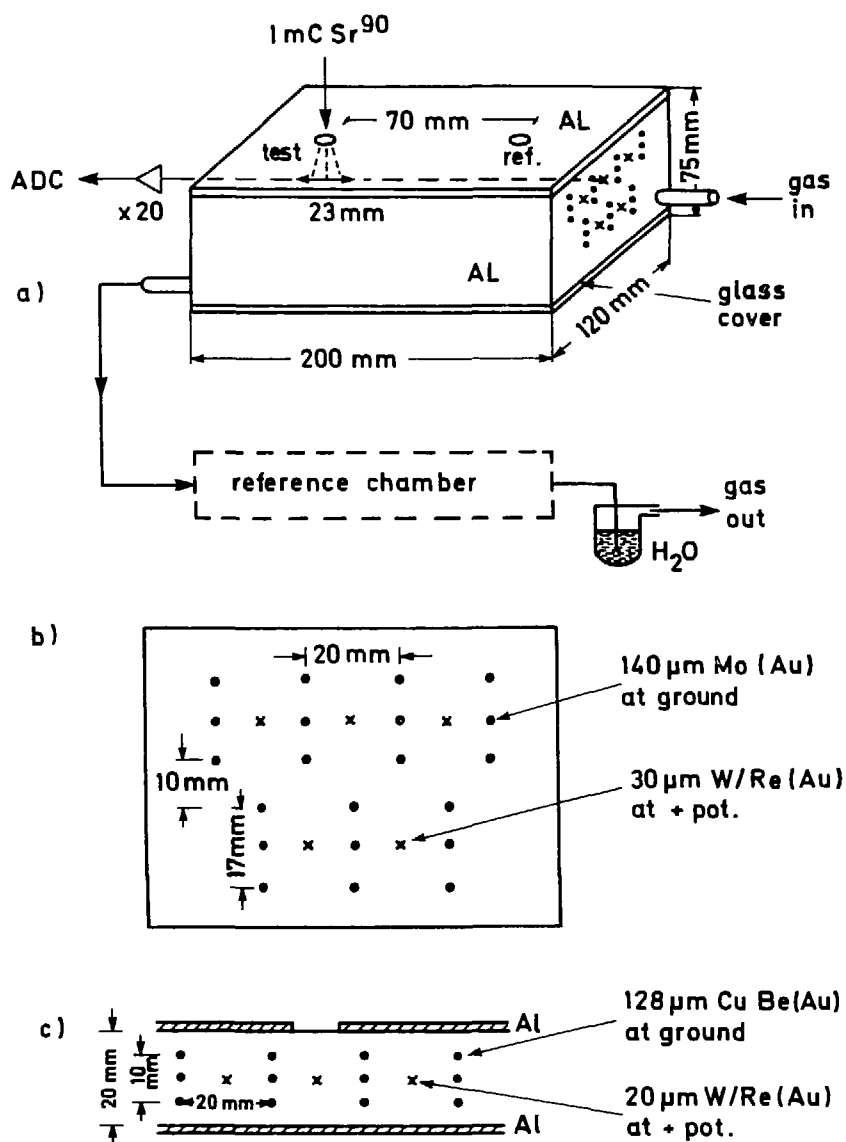


Fig. 1: Experimental set up:

- a) schematics of KEK test set up
- b) drift cell arrangement used in KEK tests
- c) drift cell arrangement used in MPI tests.

ing cylindrical brass inserts for precise positioning and soldering of the wires. The feedthroughs are sealed with silicone rubber (RTV). The sense (anode) wires are *Au* coated *W/Re* (3%) wires of 30 μm diameter. The potential (cathode) wires are 140 μm diameter *Au* coated *Mo* wires kept at ground potential. Thick potential wires had been chosen deliberately in order to keep the electric field at the cathode surface below 15 kV/cm for operation in proportional mode. There are indications ⁶, that higher cathode surface fields cause instabilities under intense radiation. In a special test to study the effect of the cathode field on the aging process the 140 μm *Mo* wires were replaced by 30 μm *W/Re* wires.

In the MPI tests a somewhat different chamber and cell geometry (fig. 1c) was used. A single row of 7 rectangular wire cells strung inside an *Al* frame is sandwiched by flat *Al* covers 20 mm apart. The only nonmetallic inner chamber surface materials were wire feedthroughs machined of polyoxymethylene (HOSTAFORM) and rubber O ring seals.

Two ports (10 mm diameter, 70 mm apart) in the top *Al* cover (fig. 1a) define test and reference positions on the same sense wire. A collimated 1m C Sr^{90} source was positioned at the test port such that β rays were emitted in a radiation cone of 23 mm diameter at the sense wire plane. The radiation profile along the wire direction was measured by moving a narrow (1.1 mm diameter) collimator across the radiation cone and measuring the anode current. The measured width is 23 mm FWHM as expected from geometry and was used to determine the total dose per mm wire. The degree of aging was determined quantitatively by comparing Fe^{55} spectra measured at the test and reference positions of the same sense wire using the same electronics chain thus minimizing systematic errors. The Fe^{55} probing source was collimated such that its radiation cone covered the same solid angle as the Sr^{90} source. We would like to stress, that quantitatively the measured gain change at the aged spot depends on the collimation of the probing source, which averages over the Sr^{90} radiation cone. In order to be able to monitor the gain stability at the reference position of the irradiated sense wire a reference chamber was connected downstream of the test chamber to the same gas line. At KEK plastic hoses were used. Typically the chambers were flushed at a flow rate of 50 cm^3 / min corresponding to one volume exchange per 20 min. The gas system

was sealed with a distilled H_2O bubbler at the reference chamber outlet. At MPI all gas lines were made of stainless steel. The flow rate was typically $100 \text{ cm}^3/\text{min}$ (5 min per volume exchange) and no liquid filled bubblers were used to seal the gas outlet. All gases used were premixed and of research purity grade as typically used in high energy physics experiments.

The total collected charge was determined by integrating the continuously recorded anode current. For irradiations in proportional mode the anode current was around $1 \mu\text{A}$. The Fe^{55} spectra were recorded using a current sensitive amplifier and a multichannel analyzer (LRS qVt , model 3001). The qVt calibration was monitored in regular intervalls using a calibration pulse of known charge.

Atmospheric pressure (p) and ambient temperature (T) were recorded with each measurement. The gain variations observed at the reference position are clearly related to the gas density changes $\frac{\delta \rho}{\rho} = \frac{\delta p}{p} - \frac{\delta T(K)}{T(K)}$ due to p and T variations. Figure 2 shows the time dependence of the observed Fe^{55} peak position and of the gas density due to p and T changes over a period of 180 h during the course of the first aging test with Ar/C_2H_6 at KEK. After correcting for the observed density changes using the empirical relation $\frac{\delta G}{G} = -9.3 \frac{\delta \rho}{\rho}$ the peak position measured at the reference point is stable to within $< \pm 2\%$ though the total charge collected at the test position of the same wire increases from 5 to $20 \times 10^{16} e^-/\text{mm}$. It should be emphasized, however, that our results do not depend on the ability to do these density corrections, since the aging effect is determined by comparing measurements done at the test and reference positions under identical conditions.

3. Measurements of Gain Variations

a) Dependence on mode of operation:

At KEK two tests were carried out with Ar/C_2H_6 at different gas gains G :

in proportional mode: $G = 5 \times 10^4$, total collected charge: $21 \times 10^{16} e^-/\text{mm}$

in the limited streamer mode: $G > 10^6$, total collected charge: $33 \times 10^{16} e^-/\text{mm}$

Figure 3 shows the ratio of the Fe^{55} peak positions as measured at the test and reference spots versus the total charge accumulated at the test spot. In both cases a monotonously decreasing gain is observed at the test position. The pulse

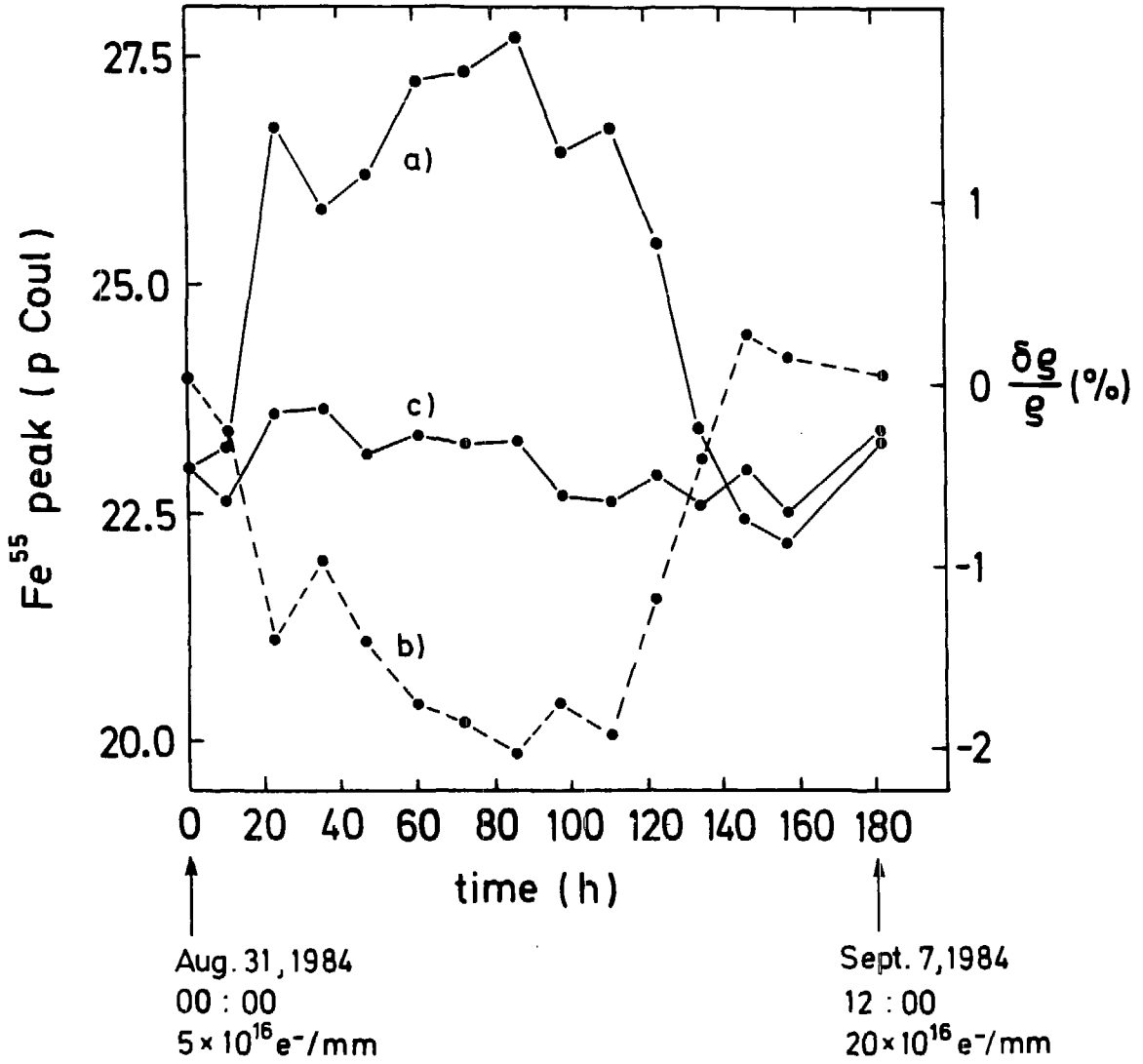


Fig. 2: Reference pulse height and density variations during first Ar/C₂H₆ test:

a) measured Fe⁵⁵ peak position

b) relative gas density variation $\frac{\delta \rho}{\rho} = \frac{\delta p}{p} - \frac{\delta T(K)}{T(K)}$

c) Fe⁵⁵ peak position after density correction.

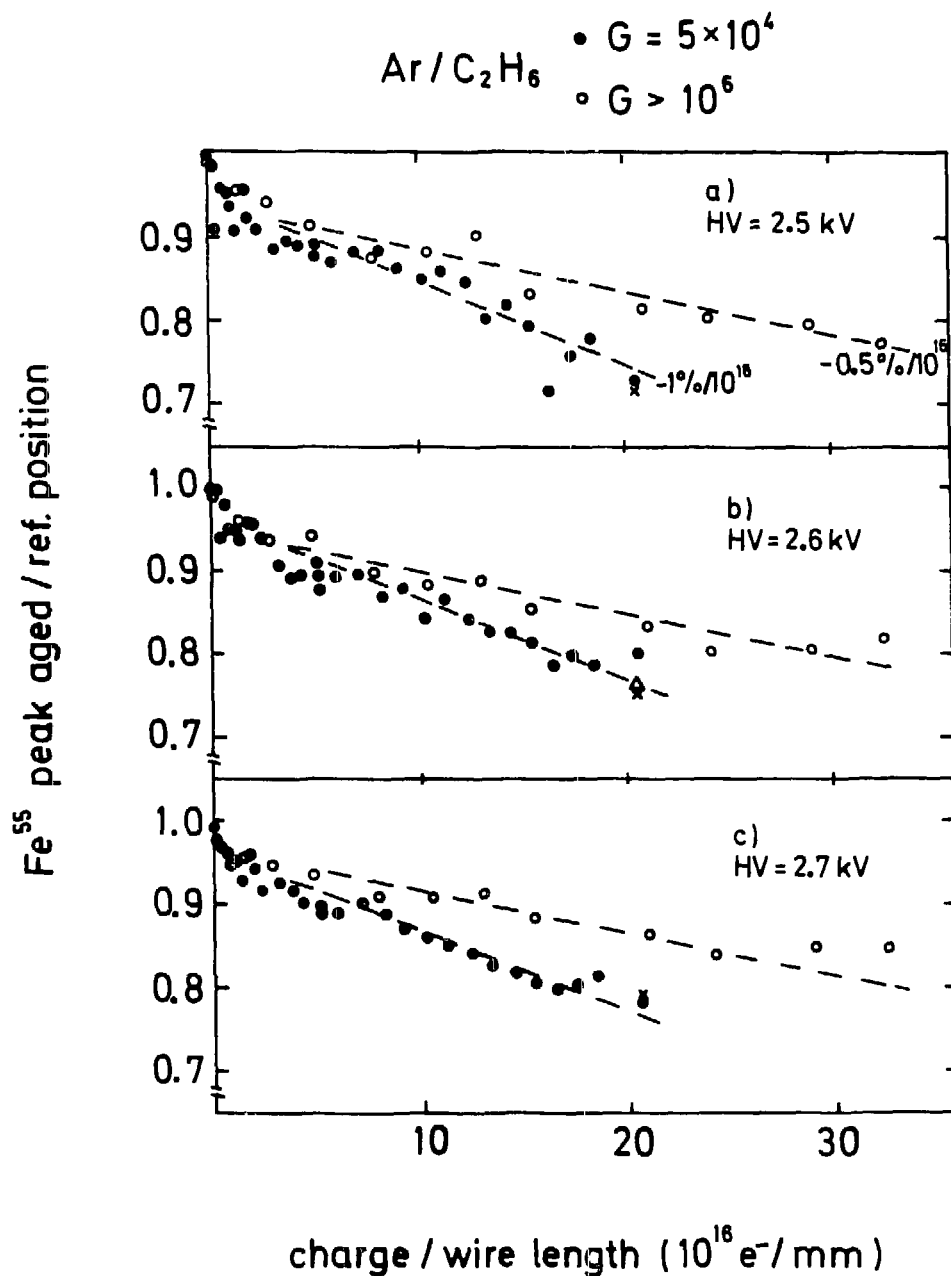


Fig. 3: Relative gain as function of total collected charge for proportional and limited streamer modes in Ar/C₂H₆ (KEK test). Graphs a) - c) refer to different gas gains for the Fe⁵⁵ pulse height measurements. The symbols x and Δ mark remeasurements within 2 days after terminating the irradiation.

height measurements are done at 3 different gas gains between 1.8 and 6.5×10^4 (figs. 3 a,b,c) in order to be sensitive to potential space charge effects. All three measurements are consistent with each other, demonstrating, that the observed loss of gas amplification at the irradiated spot is not affected by the probing conditions. The drop off for aging in the limited streamer mode is significantly smaller than for proportional gain. After an initially somewhat larger rate of gain reduction, for doses exceeding a few times $10^{16} e^-/\text{mm}$ the gain decreases linearly at rates of $\simeq 1\%/10^{16} e^-/\text{mm}$ and $\simeq 0.5\%/10^{16} e^-/\text{mm}$ for $G = 5 \times 10^4$ and $G > 10^6$ respectively. These rates of gain reduction are about an order of magnitude smaller than those reported from similar tests done at CERN⁴. The comparison of irradiations in proportional and limited streamer modes shows, that aging effects for a given accumulated charge dose depend on the mode of operation, being larger for smaller gas amplification. A similar observation was made in recent tests carried out at LBL¹².

The tests were stopped, when the gas gain at the aged spot had dropped to approximately 75% of the gain at the reference position, which remained constant throughout the tests (fig. 2). After the end of the aging test in proportional mode gain measurements were continued for 2 days with *HV* kept on for the first day. No significant further gain shift, in particular no recovery, was observed (fig. 3).

In addition to the overall gain decrease a strong distortion and significant broadening of the Fe^{55} line was observed to develop gradually with increasing total dose. Despite these degradings the chambers could be operated in a stable manner up to the end of the tests at 21 and $33 \times 10^{16} e^-/\text{mm}$ not showing any signs of elevated dark currents or selfsustaining discharges, which had been observed in the tests at CERN⁴ starting at doses of 2 to $3 \times 10^{16} e^-/\text{mm}$. The CERN test chambers were operated at considerably higher electrical fields at the potential wire surface (typically $\simeq 40$ kV/cm according to our field calculations). In order to investigate the effect of the cathode field strength on the aging processes we replaced the $140 \mu\text{m}$ *Mo* potential wires of the irradiated cell by $30 \mu\text{m}$ *W/Re* wires thus raising the electric field at the potential wire surface to $\simeq 40$ kV/cm at a gas gain of 5×10^4 . The rate of gain reduction ($\simeq 1\%/10^{16} e^-/\text{mm}$) and qualitatively the Fe^{55} line distortions were unaffected by this change of cathode

wires. But – in qualitative accord with the observations at CERN⁴ – high anode dark currents (few 100 nA), which could only be quenched by reducing the *HV* to very low values, occurred at a collected charge of $6 \times 10^{16} e^-/\text{mm}$.

b) Comparison of Ar/C_2H_6 and $Ar/CO_2/CH_4$

At MPI aging rates in the Ar/C_2H_6 and $Ar/CO_2/CH_4$ gas mixes were compared under identical conditions using *Al* chambers (fig. 1c) and carefully cleaned stainless steel gas pipes avoiding liquid filled gas bubblers and gas exposure to nonmetallic surfaces as far as possible (see table I). Figure 4 shows the results of these measurements. Whereas for the C_2H_6 mix no significant gain drop is observed ($|\delta G/G|/Q < 0.2\%/10^{16} e^-/\text{mm}$) up to $Q = 17 \times 10^{16} e^-/\text{mm}$ 3 irradiations of $Ar/CO_2/CH_4$ filled chambers showed gain losses with test to test variations between 1.3% and 3.4%/10¹⁶ e⁻/mm (see also table II). Gain variations of up to $\pm 10\%$, which occurred both at the test and the reference spots of the irradiated sense wire in the early stages of CO_2 tests ① and ② (fig. 4), were not seen in test ③, when gain measurements were done at very narrow charge increments. Though we do not have a definite explanation for these initial gain changes*, we can not think of a mechanism, which could have affected the slope of the linear gain drop observed at later stages of the irradiation.

Our conclusion is, that under the MPI test conditions there is a definite difference in gain loss rates for Ar/C_2H_6 and $Ar/CO_2/CH_4$, the C_2H_6 mixture being more resistant¹³.

The difference in radiation hardness between the 2 gases is also clearly reflected by Fe^{55} line shapes measured both at the aged and reference wire spots (fig. 5). The spectrum measured in Ar/C_2H_6 at the aged position after $Q = 31 \times 10^{16} e^-/\text{mm}$ (fig. 5a) does not show any degrading compared to the reference spectrum (fig. 5b). Figures 5c–e show overlays of spectra measured at both wire spots at the respective ends of the three $Ar/CO_2/CH_4$ tests. The spectra at the irradiated spots are clearly degraded. In addition to a downward shift of the main

*A possibility for relative gain changes at the test and reference wire spots may be space charge effects due to conductivity changes of the aluminized Mylar window. After the end of the irradiations we found the *Al* coating at the aged spot partially sputtered away.

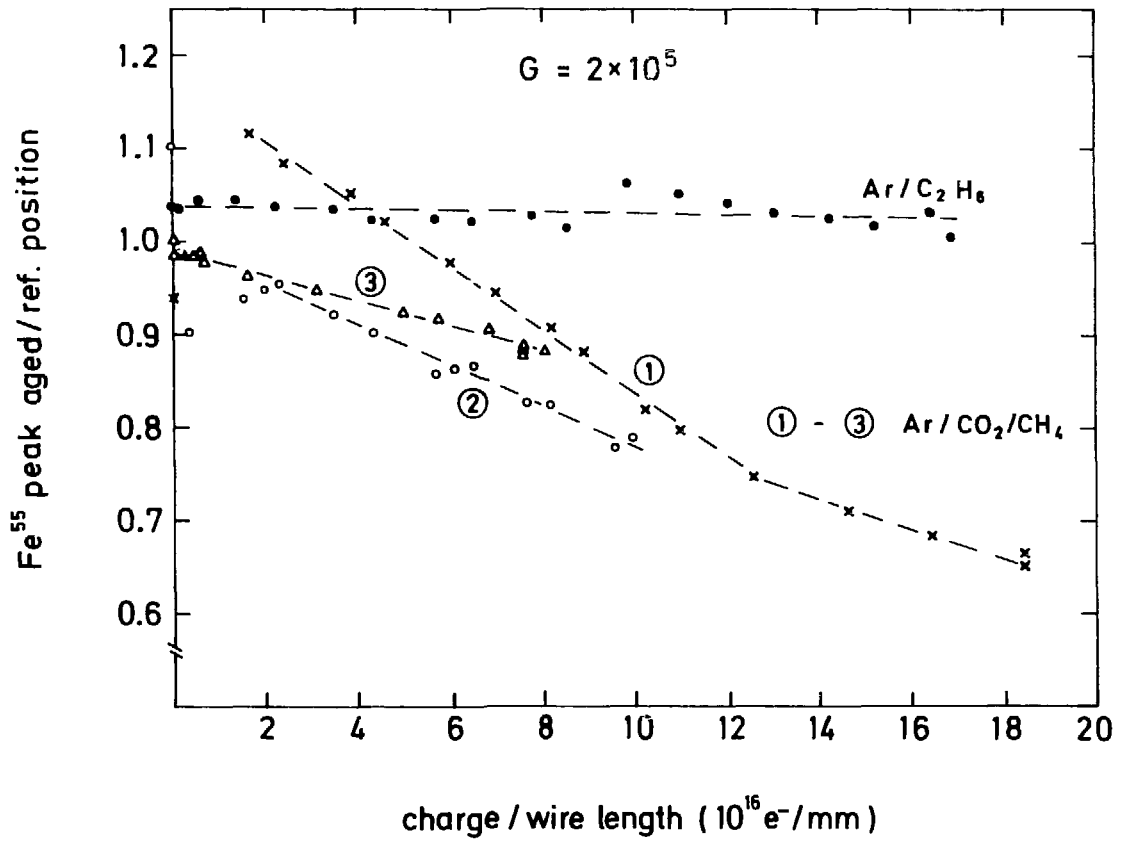


Fig. 4: Relative gain as function of total collected charge (MPI test); comparison of aging in $\text{Ar}/\text{C}_2\text{H}_6$ and $\text{Ar}/\text{CO}_2/\text{CH}_4$ (tests ① to ③) for proportional mode ($G = 2 \times 10^5$).

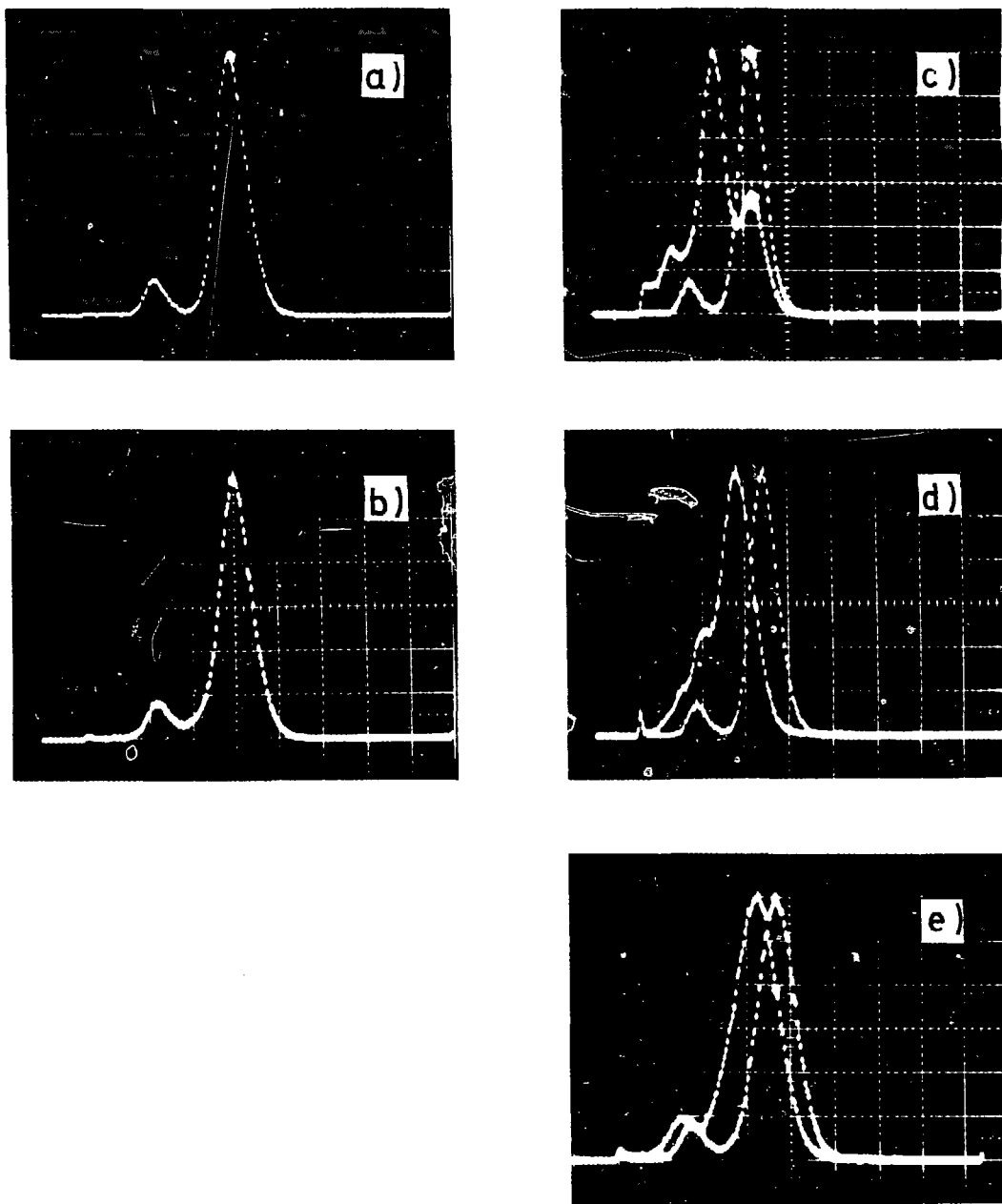


Fig. 5: Comparison of Fe^{55} pulse height spectra measured at aged and reference positions:

- a) $\text{Ar}/\text{C}_2\text{H}_6$, aged pos., $Q = 31 \times 10^{16} \text{ e}^-/\text{mm}$, b) $\text{Ar}/\text{C}_2\text{H}_6$, ref. pos.,
 c) - e) $\text{Ar}/\text{CO}_2/\text{CH}_4$, aged and ref. position, tests ① to ③,
 c) $Q = 18 \times 10^{16} \text{ e}^-/\text{mm}$, d) $Q = 10 \times 10^{16} \text{ e}^-/\text{mm}$, e) $Q = 8 \times 10^{16} \text{ e}^-/\text{mm}$.

peak due to a general loss of gas amplification at the aged spot significant line distortions reflect local gain inhomogeneities as a result of the irradiation: a double peak in test ①, a build-up between the main and the Ar escape peak in ②, and a line broadening in ③. The distortions emerged gradually with increasing total dose.

c) Effects of gaseous contaminants

The effect on aging rates of H_2O and organic vapor outgassed from soft PVC surfaces was studied by

- bubbling the incoming chamber gas through a temperature controlled bath of distilled H_2O contained in a Cu vessel
- introducing 10 m of soft PVC hose into the input gas line

The influence of the additives on aging rates was studied in a comparative way: Irradiations were started with uncontaminated gases and after significant charge doses continued with H_2O or PVC plasticizer vapor mixed in.

Figures 6 and 7 show the effect of adding 0.67% of H_2O to $Ar/CO_2/CH_4$. At $Q = 10^{17} e^-/mm$ the Fe^{55} spectrum at the test spot was clearly degraded (fig. 7a): the relative gain had dropped to less than 80% of the starting value and the line width had increased by more than 50%. With the admixture of H_2O the spectrum improved instantaneously (compare figs. 7a and b): the amplification at the irradiated spot went up and the line width shrunk to almost the initial value. When the irradiation was continued, the gain variations progressed much the same as before H_2O was added. In particular the rate of gain loss was not significantly reduced. At the end of the test ($Q = 25 \times 10^{16} e^-/mm$) the Fe^{55} spectrum at the aged spot was strongly distorted (fig. 7c).

The role of H_2O in smoothing local gain variations presumably by positive action on the electrical conductivity of wire coatings was also observed with Ar/C_2H_6 in a test, which was started on a wire most likely contaminated at the test position (fig. 8). The gas amplification at the test spot is definitely lower and the width of the Fe^{55} line substantially broader than at the reference posi-

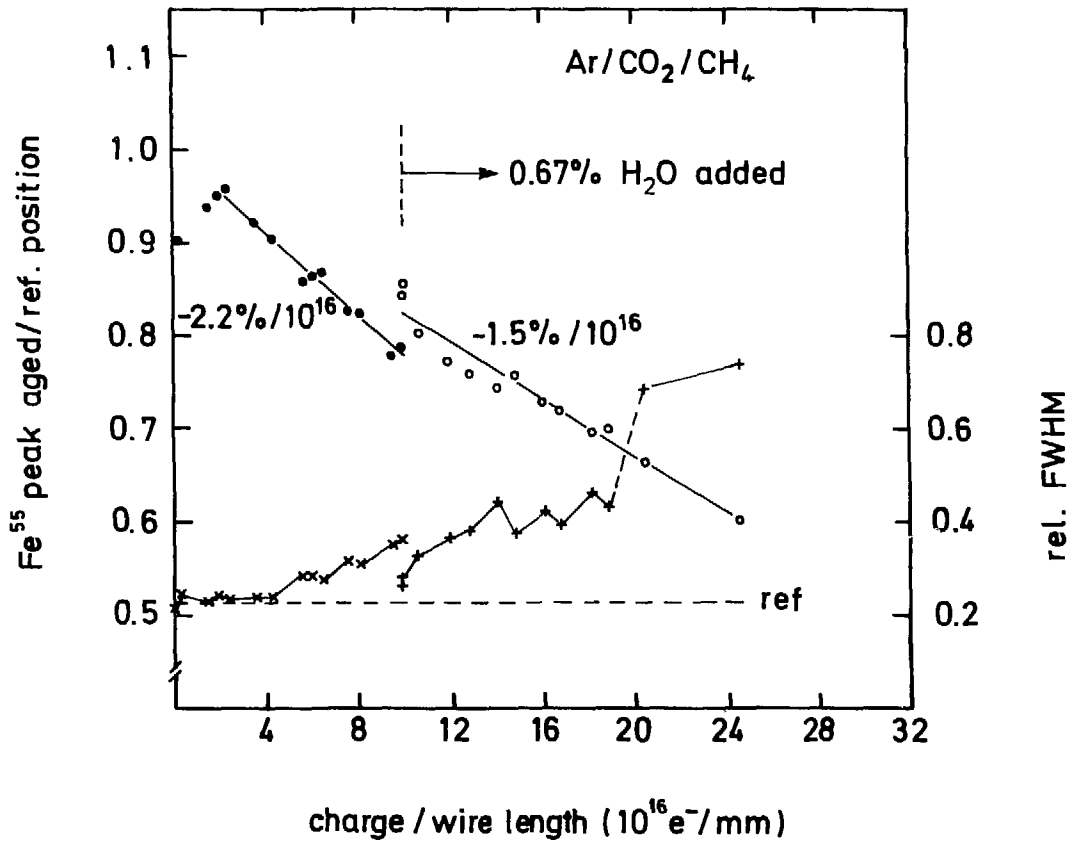


Fig. 6: Effect of H₂O admixture to Ar/CO₂/CH₄ on aging rates. Dots and circles mark measured Fe⁵⁵ peak ratio. Crosses and the dashed line refer to rel. FWHM of Fe⁵⁵ spectra at aged and reference positions, respectively. The break in the line broadening at 20×10^{16} e⁻/mm occurs, when the secondary structure in Fig. 7c exceeds half height.

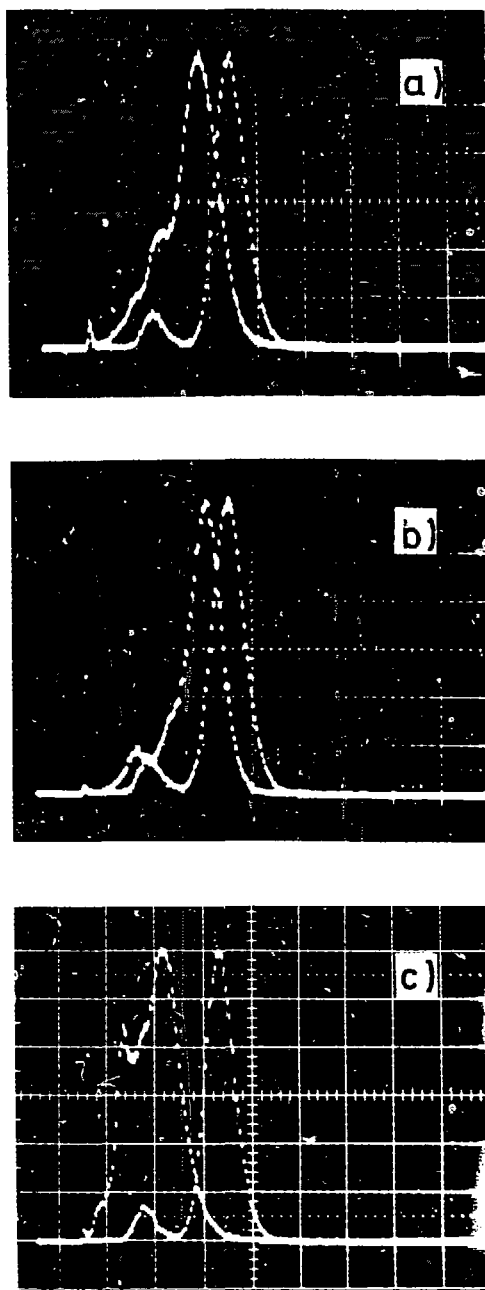


Fig. 7: Effect of H_2O admixture to $\text{Ar}/\text{CO}_2/\text{CH}_4$ on Fe^{55} pulse height spectra measured at aged and reference positions:

- a) $Q = 10 \times 10^{16} \text{ e}^-/\text{mm}$, before adding H_2O
- b) $Q = 10 \times 10^{16} \text{ e}^-/\text{mm}$, after adding 0.67% H_2O
- c) $Q = 25 \times 10^{16} \text{ e}^-/\text{mm}$ (end of test).

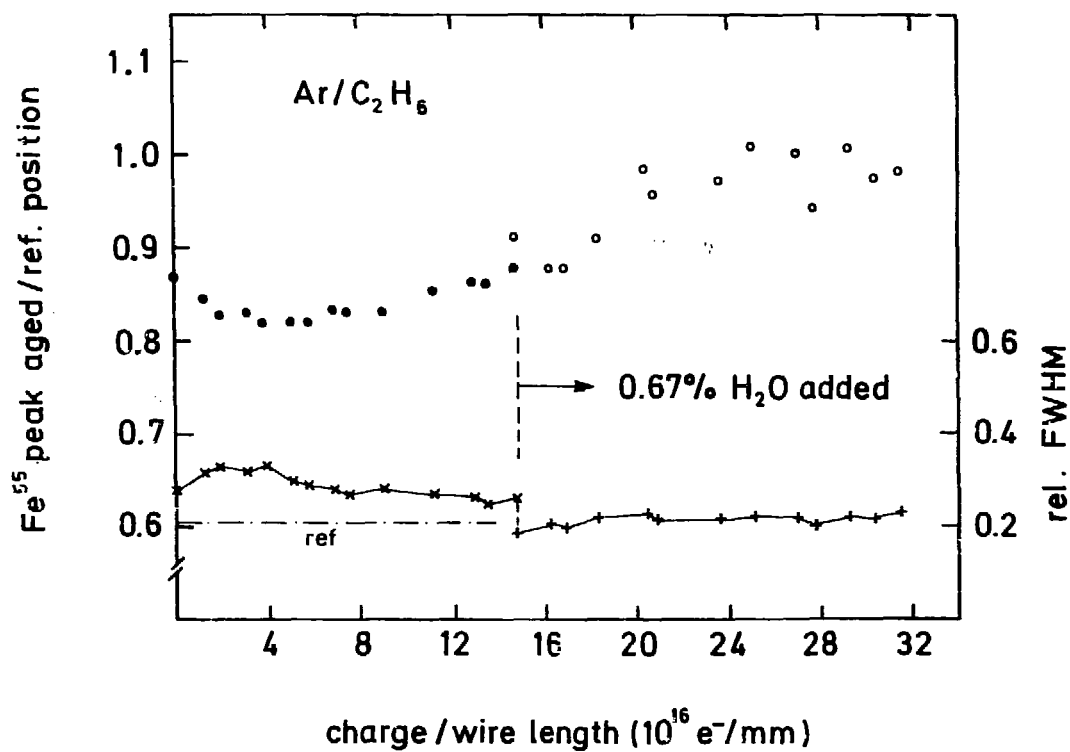


Fig. 8: Effect of H_2O admixture to $\text{Ar}/\text{C}_2\text{H}_6$ on local gain differences. Reduced gain (dots) and large width (crosses) of Fe^{55} line at the aged position, probably due to wire surface contamination, are positively affected by adding 0.67% H_2O .

tion*. After adding H_2O the gain ratio approaches 1 and the relative FWHM immediately shrinks to 20%, the value measured at the reference spot.

To summarize our experience with 0.67% H_2O added to the two gas mixes: Local gain differences are efficiently reduced. Aging rates in $Ar/CO_2/CH_4$ under intense radiation are at the most only marginally slowed down.

The effect of vapor outgassed from new, soft PVC hoses is twofold: Aging rates are definitely accelerated (fig. 9,10). For Ar/C_2H_6 no loss of gain was observed with the use of steel gas pipes (fig. 9). After inserting a 10 m PVC hose (at $Q = 17 \times 10^{16} e^-/mm$), the gain at the aged spot started to drop at a rate of 2.4%/10¹⁶ e^-/mm . Moreover, even after removing the PVC hose and returning to steel tubes (at $Q = 31 \times 10^{16} e^-/mm$), the gain kept falling at a not much reduced rate. It appears, that the exposure of the chamber gas to PVC surfaces had initiated lasting aging processes, which were not at work before. In $Ar/CO_2/CH_4$ the use of the same PVC hose more than doubled the gain loss rate observed in test ③ to 2.8%/10¹⁶ e^-/mm (fig. 10).

The second, more surprising effect of soft PVC vapor admixed to Ar/C_2H_6 was an immediate, drastic loss of resolution at the reference position, where the wire was not irradiated (fig. 9). A quantitatively much less pronounced line broadening of the reference spectrum was also observed in $Ar/CO_2/CH_4$ (fig. 10). In contrast to the permanent loss of performance at the aged spot, the line broadening at the reference position disappeared, when the PVC hose was removed from the gas system.

The gain reduction rates measured in the various tests described are collected in table II.

*There is a mild, but quite definite, interesting tendency for "improvement", both of gain and width, during the irradiation before H_2O was added ($Q \leq 14 \times 10^{16} e^-/mm$).

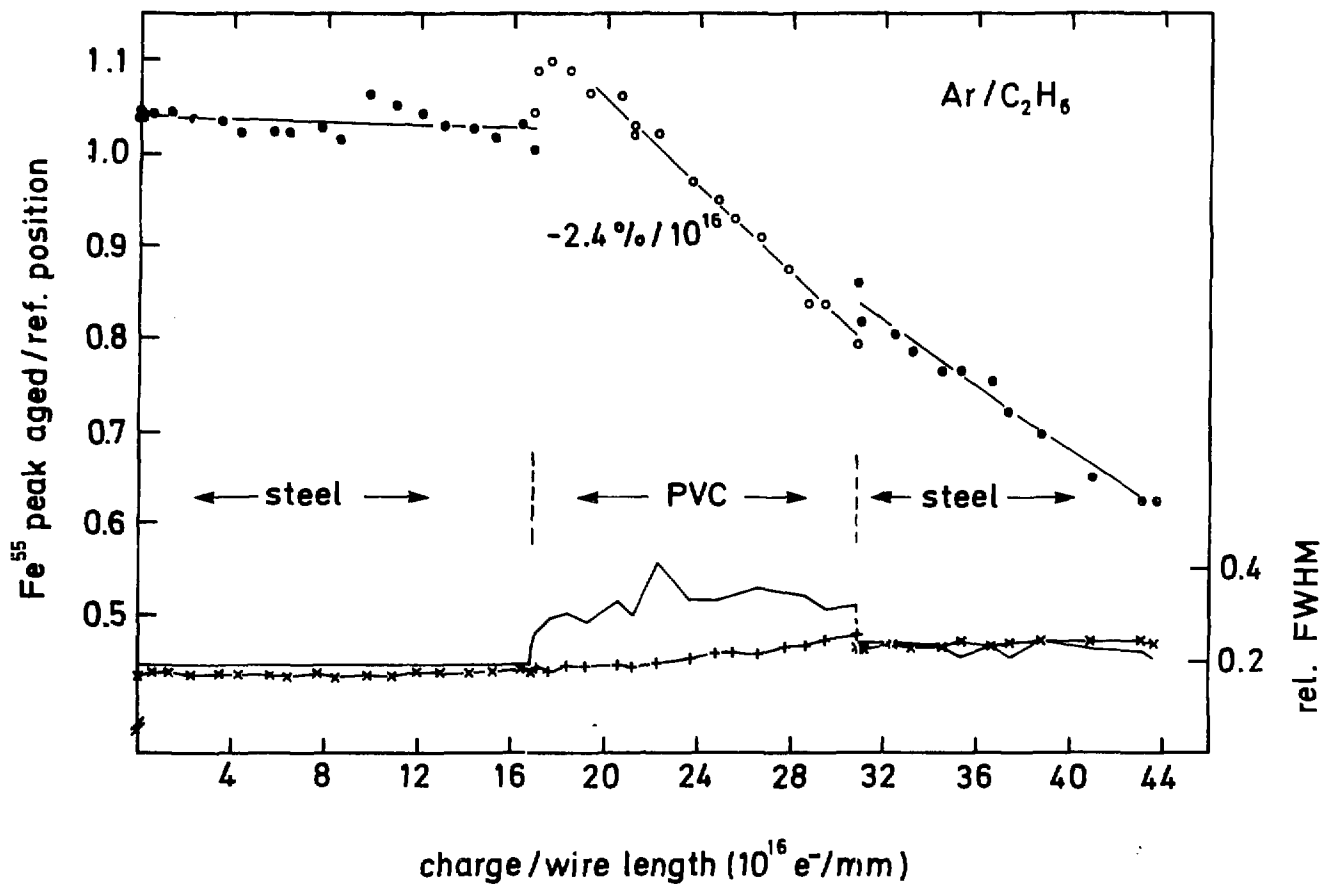


Fig. 9: Effect of soft PVC gas hose on aging rates in Ar/C₂H₆. Outgassing of the PVC surface causes a loss of gain (dots and circles) at the irradiated position and a temporary line broadening (solid curve) at the reference spot. The gain continues to fall with increasing charge dose even after removing the PVC hose.

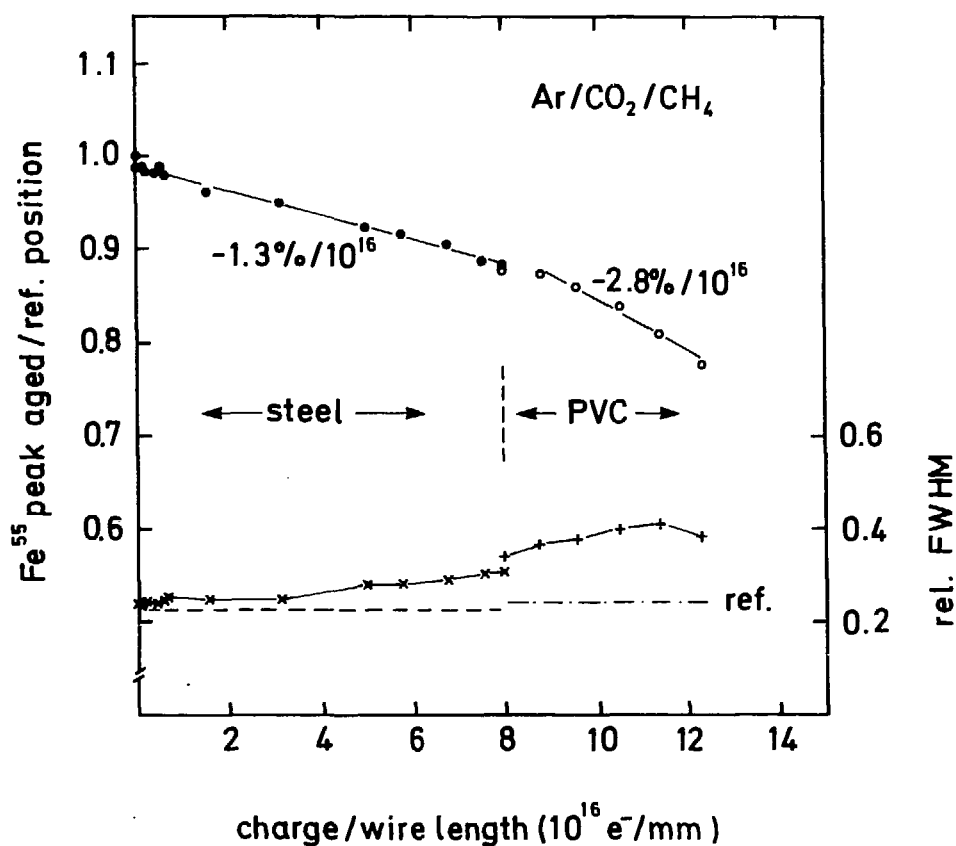


Fig. 10: Effect of soft PVC gas hose on aging rates in Ar/CO₂/CH₄. Outgassing of the PVC surface causes the gain loss rate at the aged position to increase by more than a factor of two.

Table II Gain reduction rates($|\frac{\delta G}{G}|$ per $10^{16} e^-/\text{mm}$)

Test condition	Ar/C_2H_6 (1 : 1)	$Ar/CO_2/CH_4$ (90 : 9 : 1)
1984 KEK set up $G = 5 \times 10^4$ (table I) $G > 10^6$	1% 0.5%	
1985 MPI set up $G = 2 \times 10^5$ (table I)	< 0.2%	1.3% – 3.4%
0.67% H_2O added	no effect seen	2.2% → 1.5%
vapor from PVC plasticizers admixed	< 0.2% → 2.4%	1.3% → 2.8%

4. Surface Microanalysis

Specimens of aged wires were taken for surface microanalysis at scanning electron microscopes (SEM). SEM analysis was also done for sense and potential wires, which were forced to discharge for about 30 min both in Ar/C_2H_6 and in $Ar/CO_2/CH_4$ ("whisker growing test") by raising the HV such that glow and spark discharges could be observed.

The SEM analysis yields information on the morphology of the wire surface by imaging with scattered and secondary electrons and on the atomic composition of the surface material by X ray fluorescence spectroscopy.

Surfaces of wires from tests carried out at MPI were also chemically analyzed by Auger Electron Spectroscopy (AES), which is a particularly well suited method for low Z materials. Whereas the SEM probing depth is on the order of $1\mu m$, AES is a genuine surface method, probing depths of a few nm only (limited by the Auger e^- range in the surface material). AES combined with Ar ion beam sputtering allows to take profiles in depth of chemical element composition. Moreover, due to the superior energy resolution compared to X ray spectroscopy, AES provides some information on molecular bonds.

All anode wires aged in proportional and limited streamer modes, including those from Ar/C_2H_6 tests not having shown gain reductions, have deposits at the test positions. Cathode wire surfaces are clean and not distinctly different from those of virgin wire specimens. Figure 11 shows examples of SEM photographs of $20\mu m$ W/Re sense wires from Ar/C_2H_6 (figs. 11a,b) and $Ar/CO_2/CH_4$ (fig. 11c) tests done with the use of gas lines made of steel tubes (fig. 11a) and PVC hoses (figs. 11b,c). The least coated wire (fig. 11a, Ar/C_2H_6 and steel tubes) is the one not having shown gain changes. The thickness of the surface film is well below $1\mu m$. Compared to the two Ar/C_2H_6 specimens, the coating on the $Ar/CO_2/CH_4$ aged wire (fig. 11c) is less uniform and complete. Both specimens from tests using PVC hoses, in particular the one aged in Ar/C_2H_6 (fig. 11b), show very fine needles of a few μm lengths attached to the general surface coating. These needles are not grown with the use of steel tubes.

Figure 12 shows differential Auger e^- spectra of sense wire deposits from a)

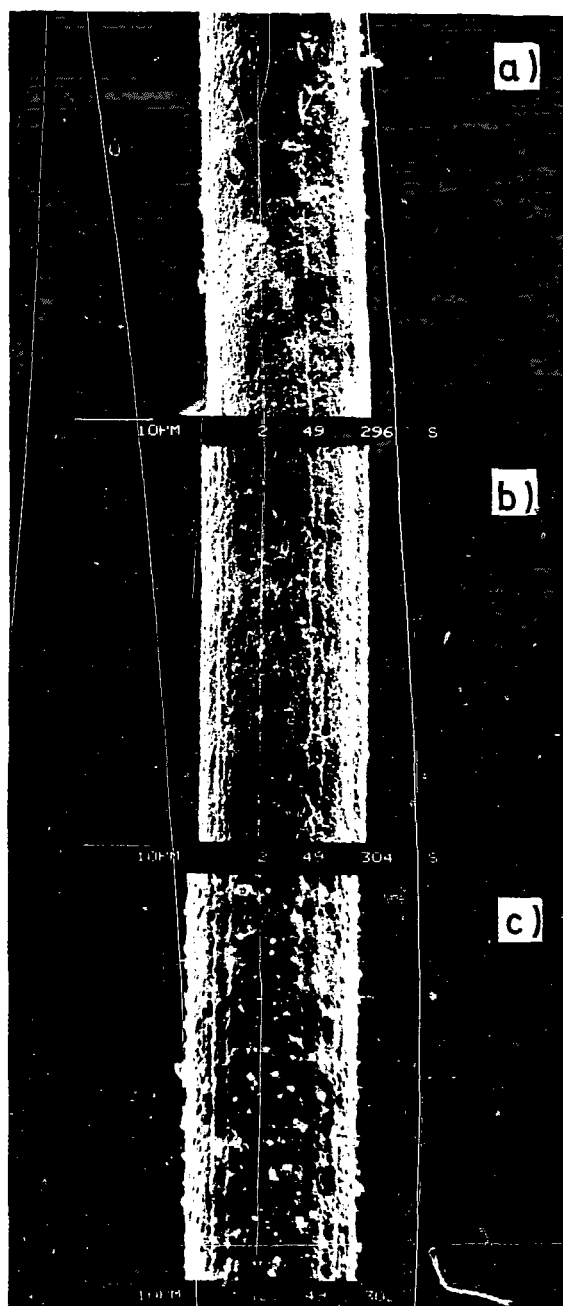


Fig. 11: Scanning electron micrographs of aged sense wire specimens:

- a) $\text{Ar}/\text{C}_2\text{H}_6$, $Q = 17 \times 10^{16} \text{ e}^-/\text{mm}$, steel gas tubes
- b) $\text{Ar}/\text{C}_2\text{H}_6$, $Q = 44 \times 10^{16} \text{ e}^-/\text{mm}$, steel and PVC gas tubes
- c) $\text{Ar}/\text{CO}_2/\text{CH}_4$, $Q = 12 \times 10^{16} \text{ e}^-/\text{mm}$, steel and PVC gas tubes.

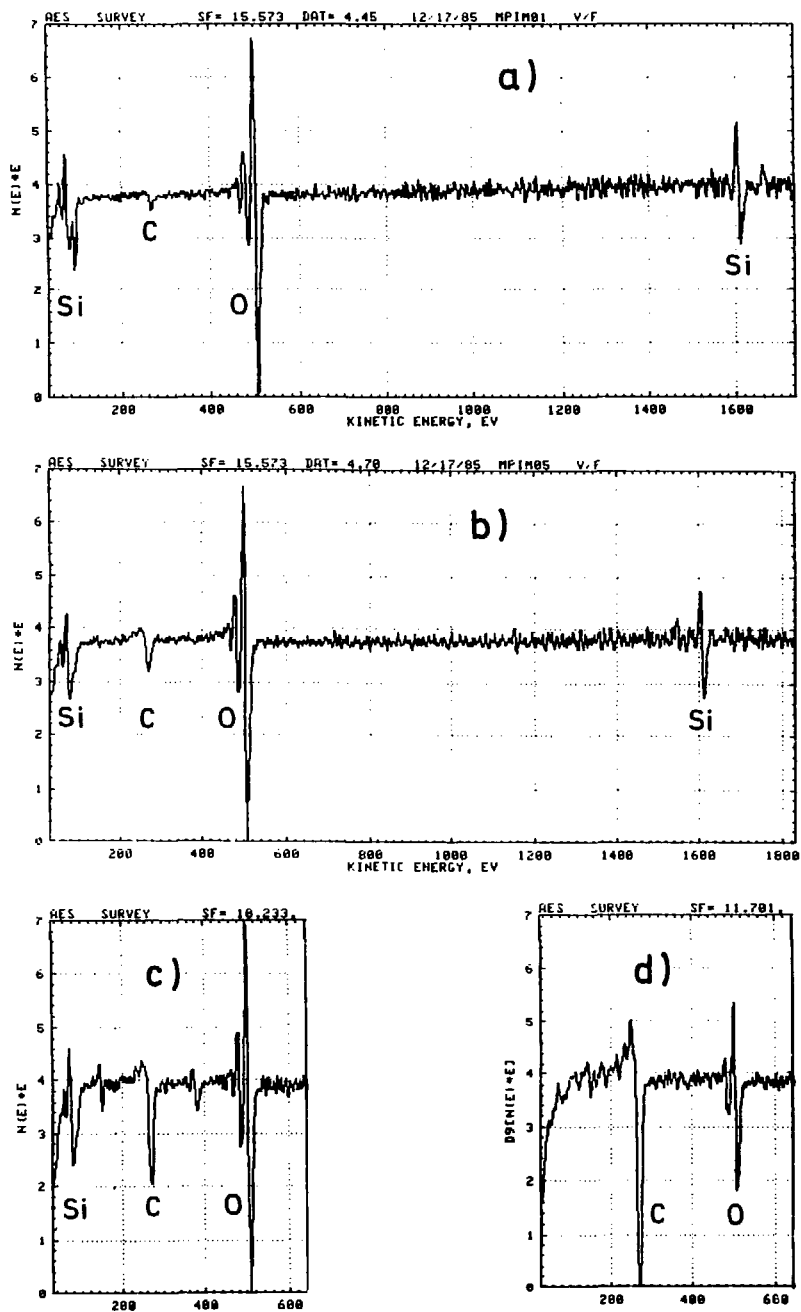


Fig. 12: Auger electron energy spectra:
 a) integrated over typical surface element of sense wire specimen aged in $\text{Ar}/\text{CO}_2/\text{CH}_4$, $Q = 18 \times 10^{16} \text{ e}^-/\text{mm}$
 b) same for $\text{Ar}/\text{C}_2\text{H}_6$, $Q = 17 \times 10^{16} \text{ e}^-/\text{mm}$
 c) and d) spectra taken at distinctive spots (c): light, d): dark of surface element analyzed in b).

$Ar/CO_2/CH_4$ and b) Ar/C_2H_6 aging. O and Si are the most abundant elements and there is surprisingly little C in both cases. A comparison of the many spectra taken for Ar/C_2H_6 and $Ar/CO_2/CH_4$ consistently showed a 2 to 3 times larger C to O ratio for the C_2H_6 mix. This is qualitatively as expected from the vastly different hydrocarbon contents of both mixes. The spectra have been taken by integrating over surface areas of typical appearance in SEM photographs. Selecting distinctive surface spots can result in drastically different element abundances as is shown in figs. 12c and d, where much more C and less or even no Si (fig. 12d) is present. In all spectra the position and shape of the Si peaks (in particular the LMM peak below 100 eV) strongly indicate, that Si is bound to O rather than being elementary. This is further supported by the relative abundance of O and Si^* .

AES combined with Ar ion beam sputtering allows to take profiles in depth of atomic composition. Examples of such profiles are given in fig. 13. Shown as a function of sputtering time (i.e. depth) is the peak to peak ratio of the dispersive Auger e^- lines of O, Si, C, Au and also W taken from energy spectra such as shown in fig. 12. Qualitatively, all profiles show a surface film containing O and Si , the relative amounts of which stay approximately constant over the full layer thickness. After this material has been sputtered away, the Au plating and finally the W base of the sense wire show. C is not particularly abundant in the surface film. The coatings grown in $Ar/CO_2/CH_4$ (figs. 13a,b) are definitely thicker (by a factor of 2 to 3) than the ones resulting from aging in Ar/C_2H_6 (figs. 13c,d). This is in accord with the observed differences in gain changes. Based on an etching rate of 130 nm / min, as measured for a Ta_2O_5 reference specimen, we estimate the thicknesses of the Si and O containing films to 50 nm (20 nm) for $Ar/CO_2/CH_4$ (Ar/C_2H_6). The distribution of elements in deposits grown in Ar/C_2H_6 using PVC hoses (fig. 13d) differs from the case, where steel tubes were used (fig. 13c), in that the abundance profiles are less steep. In particular the O intensity in fig. 13d extends out to very long sputtering times, reflecting a very nonuniform layer thickness within the surface area, over which the depth profile

*Though AES line intensities are not easily converted into element abundances, the spectra of figs. 12a and b are consistent with an $O : Si$ ratio of 2 : 1

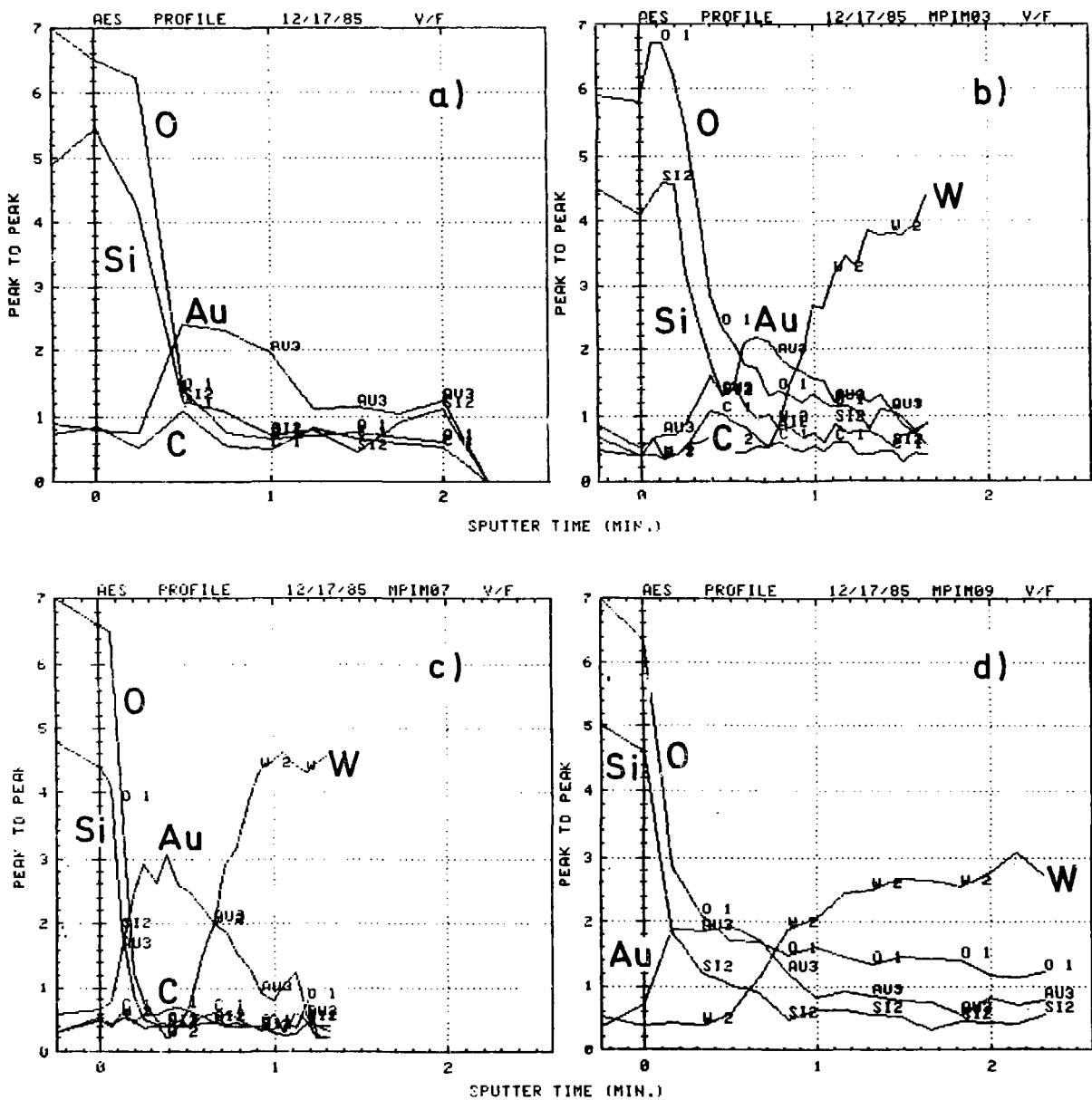


Fig. 13: Profiles in depth of O, Si, C, Au and W abundance in surface material of aged sense wire specimens. The profiles were taken by combining AES with Ar^+ beam sputtering. Etching rates depend on the surface material. For a Ta_2O_5 reference specimen the rate is 130 nm/min.

a) and b) $\text{Ar}/\text{CO}_2/\text{CH}_4$ specimens, $Q = 18 \times 10^{16} \text{ e}^-/\text{mm}$

c) and d) $\text{Ar}/\text{C}_2\text{H}_6$ specimens: c) $Q = 17 \times 10^{16} \text{ e}^-/\text{mm}$, steel gas tubes

d) $Q = 44 \times 10^{16} \text{ e}^-/\text{mm}$, steel and PVC gas tubes.

has been integrated. This may be expected from SEM photographs (fig. 11).

Chemical analysis of anode wire specimens from KEK tests with Ar/C_2H_6 was done by energy and wave length analysis of X ray fluorescence at a SEM. The results differ quantitatively from those of the AES analysis of MPI specimens: C was found to be the major element. O appeared in varying, but generally large amounts. Si showed up in typical quantities of less than 10% of a pure Si reference target. A direct and detailed comparison of the KEK and MPI results is not possible, since different methods of analysis were used.

Our results from MPI tests are in qualitative agreement with those of ref. 4 for deposits grown on $NiCr$ anode wires in Ar/C_2H_6 and Ar/CO_2 mixtures, also showing large amounts of Si .

With respect to glow and spark discharges the two gas mixes differed strikingly: Whereas electrical discharges with visible and audible sparks for about 30 min did not lead to any detectable wire coatings in $Ar/CO_2/CH_4$, the same treatment in Ar/C_2H_6 resulted in heavy deposits both on anode and cathode wires (figs. 14a,b) of a more or less complete layer of grains and flakes of electrically poorly conductive material. On the anode wires every few mm one finds isolated "towers" of material typically several μm high and surrounded by ringshaped deposits (fig. 14a). Most likely, these structures developed at spark discharge spots. C is the only detectable element in both the anode and cathode coatings. A lateral abundance profile taken by X ray wave length analysis across the discharge spot of fig. 14a is shown in fig. 14c. Sweeping through the structure, the C intensity rises to a maximum of about 80% of a pure C reference. The Au intensity from the wire plating and also the weak O signal are obscured, demonstrating, that the O is a general surface contamination rather than a major element in the C containing material. The Si intensity is insignificant ($\leq 1\%$ of a pure Si reference).

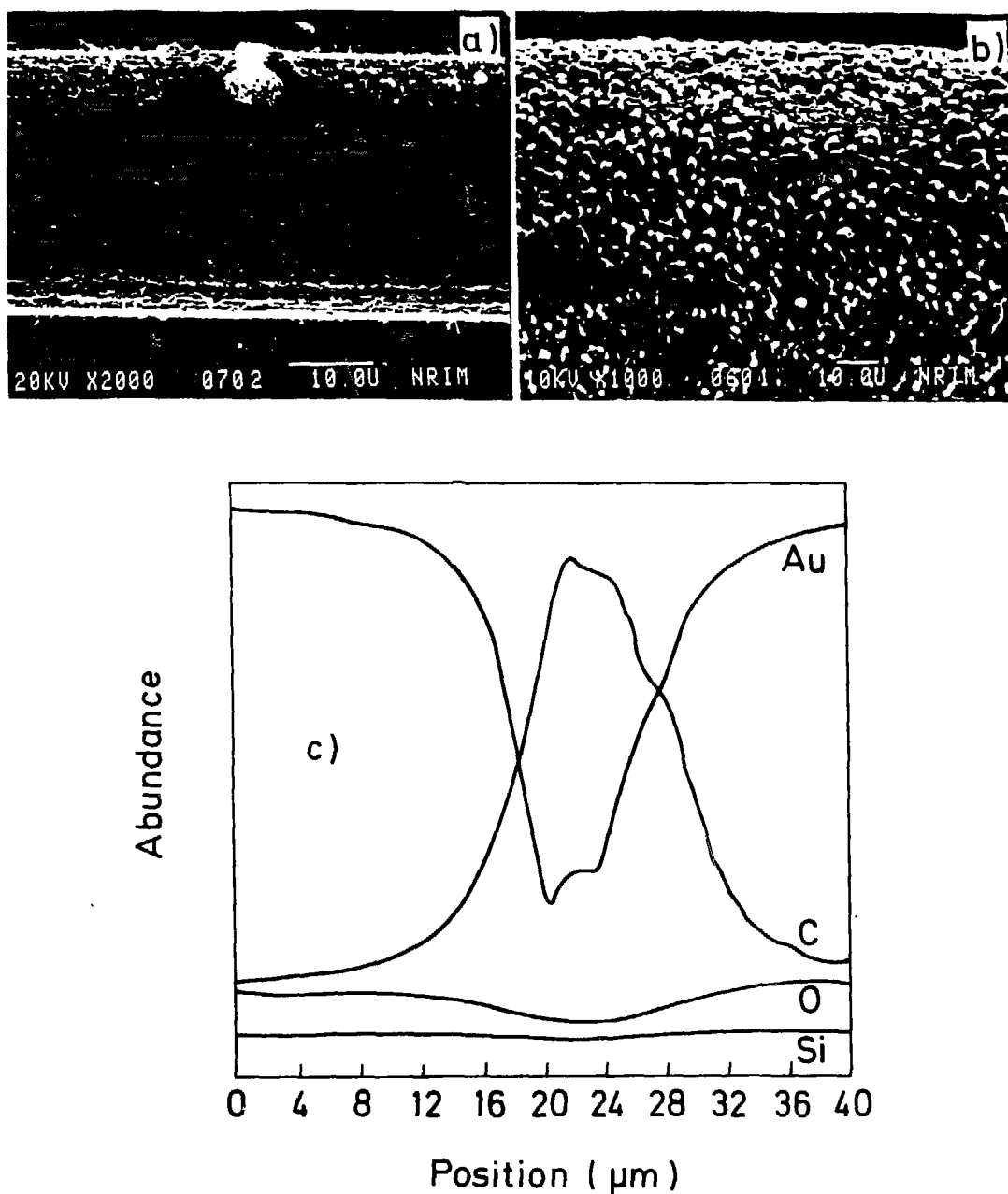


Fig. 14: Results of spark discharges in Ar/C₂H₆:

- a) and b) scanning electron micrographs of a) anode and b) cathode wire specimens after spark discharges for 30 min.
- c) lateral Au, C, O and Si abundance profiles across the discharge spot in micrograph a) taken by X ray wavelength analysis.

5. Summary and Discussion

Ar/C_2H_6 (1 : 1) and $Ar/CO_2/CH_4$ (90 : 9 : 1) filled drift chambers equipped with thick (128 and 140 μm) potential wires have been exposed to Sr^{90} sources to study radiation damage under controlled laboratory conditions. For both gas mixtures irradiations in proportional mode ($G = 5 \times 10^4$ to 3×10^5) and for Ar/C_2H_6 also in the limited streamer regime were carried to total collected charge doses of up to $4.4 \times 10^{17} e^-/mm$ corresponding to more than a decade of typical e^+e^- storage ring operation. Instabilities, i.e. enhanced dark currents and selfsustaining discharges, which occurred in earlier, similar studies by the AFS group at CERN⁴ at charge doses as low as a few times $10^{16} e^-/mm$, were not observed. The suppression of such instabilities is most likely due to the use of thick cathode wires and correspondingly low electrical field at the cathode surface reducing ion impact energies and field emission. The occurrence of instabilities in a special test with thin cathode wires and the AFS experience, that chambers with flat cathodes did not appear to age⁴, support this view.

The growth of anode wire surface films containing O , Si and typically small amounts of C was observed for both gas mixtures. For Ar/C_2H_6 we could find operating conditions (see table I), where deposition rates were sufficiently reduced to not affect the gas amplification even at the highest charge doses. Under the same conditions for $Ar/CO_2/CH_4$ gain reductions at rates of 1.3 to 3.4% per $10^{16} e^-/mm$ and nonuniformities were inferred from Fe^{55} spectra (see table II). This result is somewhat surprising at first sight. Usually hydrocarbon plasma polymerisation is considered the most important aging process under intense radiation. Therefore one would expect lower deposition rates and correspondingly slow aging for the CO_2 mix containing 1% of CH_4 only. The presence of large amounts of O and Si in the anode coatings, however, and the generally low aging rates suggest, that hydrocarbon polymerisation is not the dominating aging process under the conditions prevailing in our tests. Therefore it may not be the hydrocarbon contents of the count gas, which determines the aging rate, but rather the concentrations of O and Si and the conditions, under which these elements react to form solid chemicals. Although some candidate sources of Si , like $G10$ and Si oil, had been avoided in our tests and others, like heavy silanes accompanying

the hydrocarbon component of the chamber gas, had been excluded previously⁴ as contributing sources, there still remain various possibilities for *Si* contamination. As in previous analyses^{4,9}, the origin of *Si* found in the anode films remains undetermined. The fact, that at least a large fraction of *Si* appears to be bound to *O*, may mean, that in order to suppress “*Si*-aging”, it is equally important to eliminate *O* sources.

From AES depth profiles the thickness of the *O* and *Si* containing anode wire coatings after exposure to $1.8 \times 10^{17} e^-/\text{mm}$ is estimated to be 20 and 50 nm for *Ar/C₂H₆* and *Ar/CO₂/CH₄* respectively. These layers are by far too thin to explain the loss of gas amplification measured for *Ar/CO₂/CH₄* by the field reduction due to the increased anode wire diameter. A conductive layer of a few μm would be necessary to cause the observed gain drop. We conclude, that the deposit is insulating and that negative surface charges are responsible for the observed gain variations. SEM photographs clearly showed charge up of coated wire specimens under electron bombardment. Also, the instantaneous positive effect on *Fe*⁵⁵ line position and width of *H₂O* additions to the chamber gas (figs. 6-8) is most naturally explained by enhanced anode wire surface conductivity after attachment of the polar *H₂O* molecules to the surface film.

The reduction of local gain variations both in *Ar/C₂H₆* and *Ar/CO₂/CH₄* was the only significant effect of *H₂O* on preaged wires. There was at the most only a marginal slow down of aging rates in *Ar/CO₂/CH₄*, when 0.67% of *H₂O* was added (fig. 6). Thus, *H₂O* additions may be a good remedy to counteract performance losses in dE/dx chambers, but do not promise to protect against longterm radiation damage. In this respect our measurements do not confirm an observation by the CHARM Collaboration¹⁴, who succeeded to halt gain losses under low intensity radiation in *Ar/C₃H₈*(95 : 5) by adding 0.5% of *H₂O*.

The exposure of both gas mixes to soft PVC surfaces definitely accelerated aging (figs. 9,10 and table II) and led to changes in the morphology of anode wire deposits (fig. 11). The coatings are less uniform and covered with fine needles. These nonuniformities are also seen in atomic abundance profiles in depth (fig. 13d). A significant signal even after long *Ar*⁺ sputter times of *O* not accompanied by *Si* suggests the contribution of qualitatively different deposition processes

not present without vapor from organic plasticizers.

Two remarkable consequences of using soft PVC hoses with Ar/C_2H_6 are shown in fig. 9: The gain drop induced by the use of PVC hoses continued even after removing the hoses from the gas system. The pulse height resolution at the reference position was strongly degraded as long as the PVC tubes were in use. Though we do not have explanations for these observations, our experience with soft PVC gas hoses clearly shows, that it is important for lifetime and performance, to avoid contact, even if only temporary, of chamber gases to material containing high vapor pressure commercial plastics. This is in qualitative accord with experience on the effect of outgassings of plastic cable insulation⁹.

The most striking difference between the 2 gas mixtures is the behaviour under spark discharges. In Ar/C_2H_6 discharges very quickly (within min) lead to heavy deposits on anode and cathode wires whereas continuous sparking in $Ar/CO_2/CH_4$ for 30 min did not leave any detectable deposits. The nature of the deposits caused by discharges in Ar/C_2H_6 (fig. 14) is different from the ones grown in proportional and limited streamer modes in that they consist of grains and flakes of material containing almost exclusively *C* and possibly light elements (e.g. *H*), which the *X* ray analysis was not sensitive to.

Our conclusion concerning the relative radiation hardness of the 2 gas mixtures is:

- For unperturbed operation in proportional mode even at high gas gain ($2 - 3 \times 10^5$) both mixtures provide a lifetime sufficient for a typical, general purpose e^+e^- storage ring experiment. For stable longterm operation thick potential wires and correspondingly low electric fields (~ 10 kV/cm) at the cathode surface are crucial.
- The fact, that chambers filled with $Ar/CO_2/CH_4$ aged faster than with Ar/C_2H_6 , and the presence of large amounts of *O* and *Si* compared to *C* suggest, that hydrocarbon plasma polymerisation had been suppressed to an extent, that it was not the limiting process. Whereas for next generation experiments the observed "*Si-O*—aging" rate appears tolerable, with a view to far future experimentation, e.g. at the extremely intense radiation backgrounds expected for SSC, an understanding and possibly further

suppression of the processes involved is clearly desirable.

- Spark and glow discharges have disastrous consequences in Ar/C_2H_6 and have to be avoided carefully. In this respect $Ar/CO_2/CH_4$ is a safe gas mixture and therefore is a good choice for running-in phases of new detectors, in particular, when there is no in situ experience with radiation backgrounds.

ACKNOWLEDGEMENTS

I am grateful to Prof. G. Buschhorn for encouragement and granting a leave of absence from Max-Planck-Institut für Physik, to Prof. T. Kondo and the VENUS drift chamber group for the enjoyable collaboration and the very pleasant stay at KEK. K. Furuya, National Research Institute for Metals, Niihari-Gun, carried out the SEM analyses of the KEK wire specimens. I also thank him, Dr. H. Hantsche, Bundesanstalt für Materialprüfung, Berlin, and Dr. H. Klingele, Institut für Raster-Elektronen-Mikroskopie, München, for educating me on the intricacies of surface microanalysis, W. Erbe, W. Pimpl and L. Reindl for their contributions to the MPI test set up, and Rita Heininger and Elisabeth Loskutow for their expert drafting and editing.

REFERENCES

1. CELLO Coll., H.-J. Behrend et al., *Physica Scripta* 23 (1981), 610
2. R. Arai, et al., *Nucl. Instr. and Meth.* 217 (1983), 181
3. VENUS Coll., J. Iwahori et al., Proposal for Study of e^+e^- Reactions with a Large Aperture Spectrometer, KEK Report TRISTAN - EXP - 001 (1983)
4. J. Adam et al., *Nucl. Instr. and Meth.* 217 (1983), 291
5. M. Turala and J.C. Vermeulen, *Nucl. Instr. and Meth.* 205 (1983), 141
6. H.F.W. Sadrozinski, Santa Cruz Institute for Particle Physics Report SCIPP 84/28 (1984)
7. Several groups, in particular at the SLAC and DESY storage rings, have observed a degrading of their Ar/C_2H_6 filled drift chambers, which was counteracted by adding "protective" vapors like C_2H_5OH , H_2O or O_2 .
8. A.J.F. den Boggende et al., *Journal of Scient. Instr.* 2 (1969), 701
A. Smith and M.J.L. Turner, *Nucl. Instr. and Meth.* 192 (1982), 475
9. K. Kwong et al., *Nucl. Instr. and Meth.* A238 (1985), 265
10. J. Roehrig et al., *Nucl. Instr. and Meth.* 226 (1984), 319
11. e.g. the inner layers of the CELLO track detector have collected an average total charge of $\simeq 2 \times 10^{16} e^-$ /mm per year of operation at PETRA energies above 40 GeV.
12. J. Kadyk, these proceedings
13. In a recent test at KEK, after carefully optimizing the gas system, the gain loss rate in $Ar/CO_2/CH_4$ could be reduced to $0.4\%/10^{16} e^-$ /mm (private communication by T. Kondo).
14. A.N. Diddens et al., *Nucl. Instr. and Meth.* 176 (1980), 189

LONG TERM BEHAVIOUR OF THE JET CHAMBER AT JADE

K. Ambrus, J. Heintze, P. Lennert, H. Rieseberg, A. Wagner

Physikalisches Institut, Universität Heidelberg

Abstract

The long term behaviour of the jet chamber of the JADE detector is analysed in order to determine to what extent radiation damage has occurred. A total charge of 0.02 C/cm has been collected per wire on the innermost 32 layers (ring 1 and 2), about half that charge on the outermost 16 layers (ring 3). Only in the innermost ring a change of amplification as function of the accumulated charge of $-(11 \pm 2) \% / 0.01 \text{ C/cm}$ has been observed. The radial dependence of the aging suggests radiation damage accumulated during filling of the storage ring rather than aging of the sense wires as a possible cause of the observed amplitude decrease.

1) Introduction

The JADE detector ¹ at the e^+e^- storage ring PETRA is in operation since 1979. Its central tracking device is a drift chamber of the jet chamber ² type. The drift chamber is used to provide a picture of the event topology, to measure the momenta of charged particles and to help in particle identification by multiple sampling of the ionisation loss. The chamber is exposed to an intense machine induced background of synchrotron radiation. The continuous measurement of the chamber current caused by this radiation and of the gas gain of the individual wires provides detailed information on long term aging effects in the chamber. In the following chapters first the structure of the jet chamber together with its relevant parameters is summarized. Then the characteristic features of the radiation are described to which the chamber is exposed. Effects of radiation damage are then searched for in an analysis of the time dependence of the amplitudes.

2) Structure and Parameters of the Jet Chamber

The jet chamber is a pictorial drift chamber operating inside a solenoidal magnetic field of 4.8 kG. A detailed description of this chamber has been given previously ². Here only those features of the detector are summarized which are of relevance for the present analysis.

The sensitive volume of the jet chamber is a cylinder surrounding the beam pipe. The outer diameter is 1.6 m, the inner diameter 0.4 m, the length 2.4 m. The chamber is subdivided into 24 sectors, shown schematically in Fig. 1. Each sector of 15 degrees contains 4 cells with 16 anode wires each. In this way the 96 cells are arranged in three concentric rings, where rings 1 and 2 contain 24 cells each, while ring 3 is made of 48 cells. Up to 48 points are measured along each track. In the further discussion all wires having the same radial distance from the beam line are called a "layer". The chamber body is mounted inside a pressure vessel to allow for operation at elevated pressure.

At each point three coordinates, r , ϕ and z are given by the wire position, drift time and charge division measurement. The charge division method requires the measurement of the integrated charge for each hit at both ends of the anode wire. The ratio of these amplitudes determines z and the sum of both amplitudes measures the energy loss dE/dx of the particle in the chamber gas. This measurement of the total charge, determined up to 48 times along each track, is used for particle identification by multiple sampling. A genuine multihit electronics ³ is connected to each of the 1536 wires of the detector, which consists of preamplifiers on both ends of each wire, a discriminator-integrator, and fast analog and time memories with a capacity of 8 hits per wire. The preamplifiers are mounted onto the pressure vessel.

In Table 1 the characteristic parameters of the anode and potential wires and of the cathode structure are given, as well as the voltage settings. In the case of the cathodes, the voltages quoted are those at the points of largest drift distance. The resulting electric field in each cell is 940 V/cm.

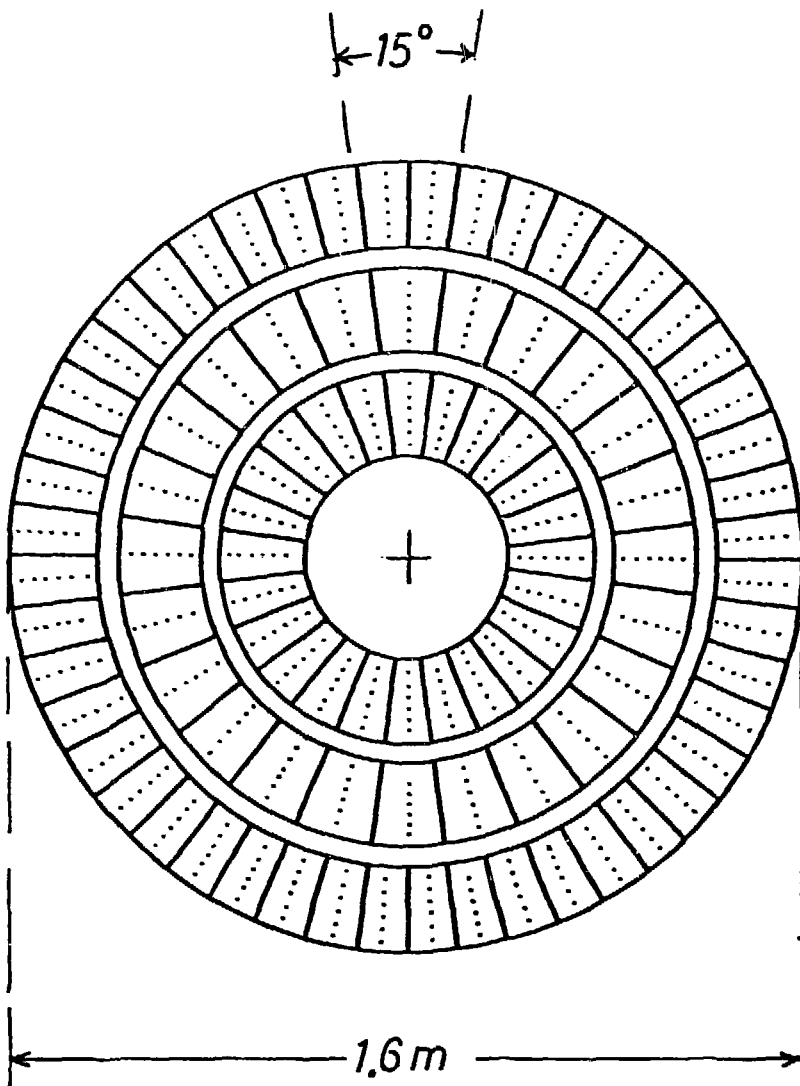


Fig. 1 Cross section through the jet chamber.

Table 1

element	dimension	electric field at surface [kV/cm]	voltage	material
anode wire	20 μm	340.0	0	W(Au)
potential wire	100 μm	14.6	-2.26 kV	CuBe
cathode	18 mm x 0.5 μm	0.94	-6.03 kV (R1) -8.66 kV (R2) -6.38 kV (R3)	Cu on Kapton

In order to monitor the currents in the chamber, all 16 anode wires of each cell are connected through resistors (44 k Ω) to a bus leading to a current meter. The individual currents of all 96 cells are continuously monitored and recorded at a rate of 30 μs per measurement. The typical dark current drawn when the storage ring is not in operation is < 10 nA per wire and is mainly due to cosmic rays. This current increases to 60-180 nA per wire when beams are stored in the machine, the current being proportional to the intensity of the stored beam.

The chamber is operated with a gas mixture of Ar / CH₄ / i-C₄H₁₀ (0.885/0.089/0.026) at 4 bar pressure. The gas (20 m³) is sealed in the detector and circulated at a flow rate of 10 l/s. The chamber volume has been thoroughly evacuated at the start up of the experiment and refilled with fresh gas 18 times since. The error in reproducibility of the gas mixture is estimated to be 0.1 % out of 10 % for C₂H₄ and 0.2 % out of 3 % for i-C₄H₁₀. No additional purification of the gas takes place during circulation, however the partial pressures of H₂O and O₂ are carefully monitored. Fig. 2 shows the amount of H₂O in the chamber as function of time. The chamber was re-opened once at the end of 1980 which explains the rerise of water to a level of 1000 ppm. Since then, the water level has dropped with each refill to the present level of 300 ppm. The error bars in

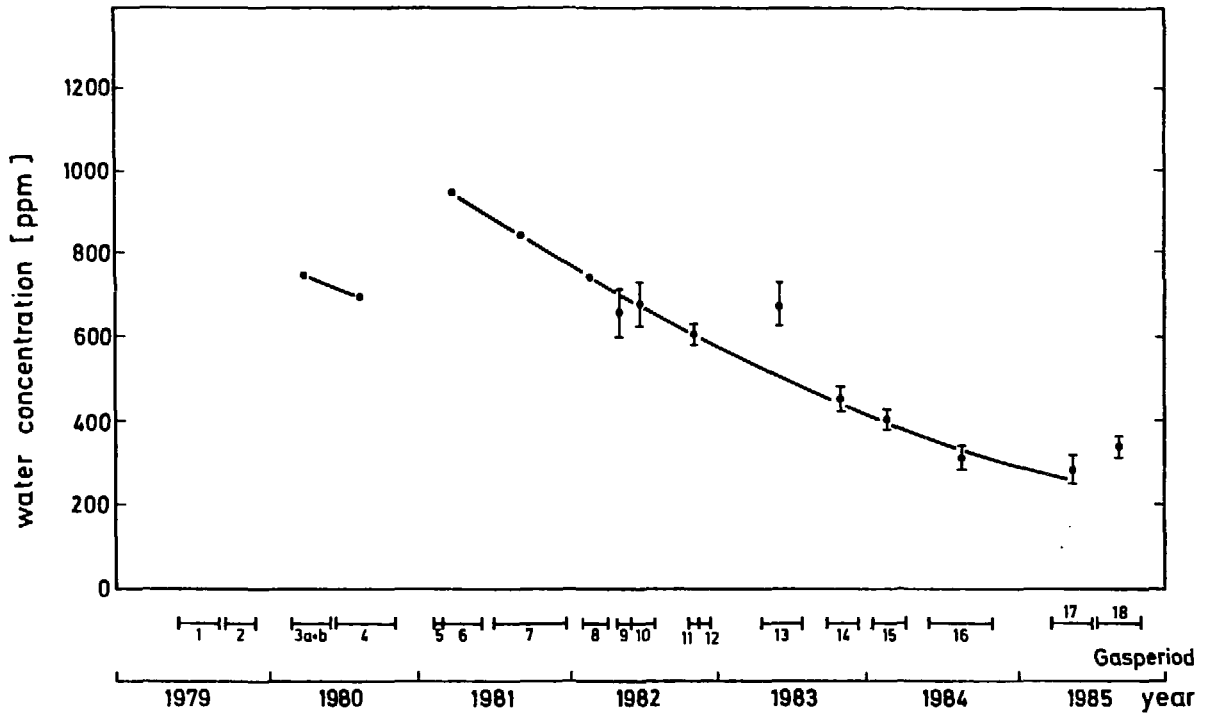


Fig. 2 Water concentration as function of time. In 1979 no measurements were made, at the end of 1980 the detector was reopened. Period 13 corresponds to a hot summer, in period 18 a small amount of water was added. The error bars reflect the variation with temperature.

Fig. 2 reflect the variation in humidity due to changes in temperature. The high point in period 13 is due to a very hot summer. During period 18 a small amount of water was added to the gas in order to stabilize the drift velocity which is a strong function of the water content of the gas ⁴. The mean oxygen content of the gas is 30 ppm, raising from 5 ppm at the beginning of a fill to 60 ppm at the end.

The chamber is operated at a gas gain of $(3-4) \cdot 10^4$. Only one quarter of the total charge is collected during the integration time of the electronics (120 ns).

3) Radiation Exposure of the Drift Chamber

During injection the radiation exposure at an e^+e^- storage ring can reach values of 30 krad per month near the beam pipe. This number is derived from a measurement taken at a distance of 4 m from the interaction point, at a beam energy of 22 GeV and integrating over 5 months ⁵. In this phase the high voltage of the chamber is turned off. During data taking under stable beam conditions the radiation deposited in the gas is about 2 rad per month and is predominantly due to synchrotron radiation, causing compton scattering and photo effect.

Information about the spatial distribution of the radiation and the released charge can be obtained either through the current measurement described above or through the analysis of those hits in the chamber which are not correlated with tracks. It has been found that the chamber current and the number of hits due to synchrotron radiation are proportional to the stored beam current, where the proportionality factors are a function of energy. In Fig. 3a and 3b the spatial distribution of the synchrotron radiation hits is shown, first as function of the distance from the beam (layer number) and second as function of the azimuthal angle (cell number), shown separately for each ring. These data are taken at a center of mass energy of 45 GeV and an average current of 4.2 mA per beam. While the number of hits is a function of beam energy and current, the shape of these distributions remains nearly always the same. Only occasionally, in the case of a badly aligned beam, the background in ring 1 increases slightly due to off-momentum electrons which are scattered into the chamber. From Fig. 3a it becomes evident, that the synchrotron radiation due to its high energy has an attenuation length which is large compared to the chamber radius, and that therefore the radiation exposure is the same for each layer. In azimuthal direction the radiation distribution shows an

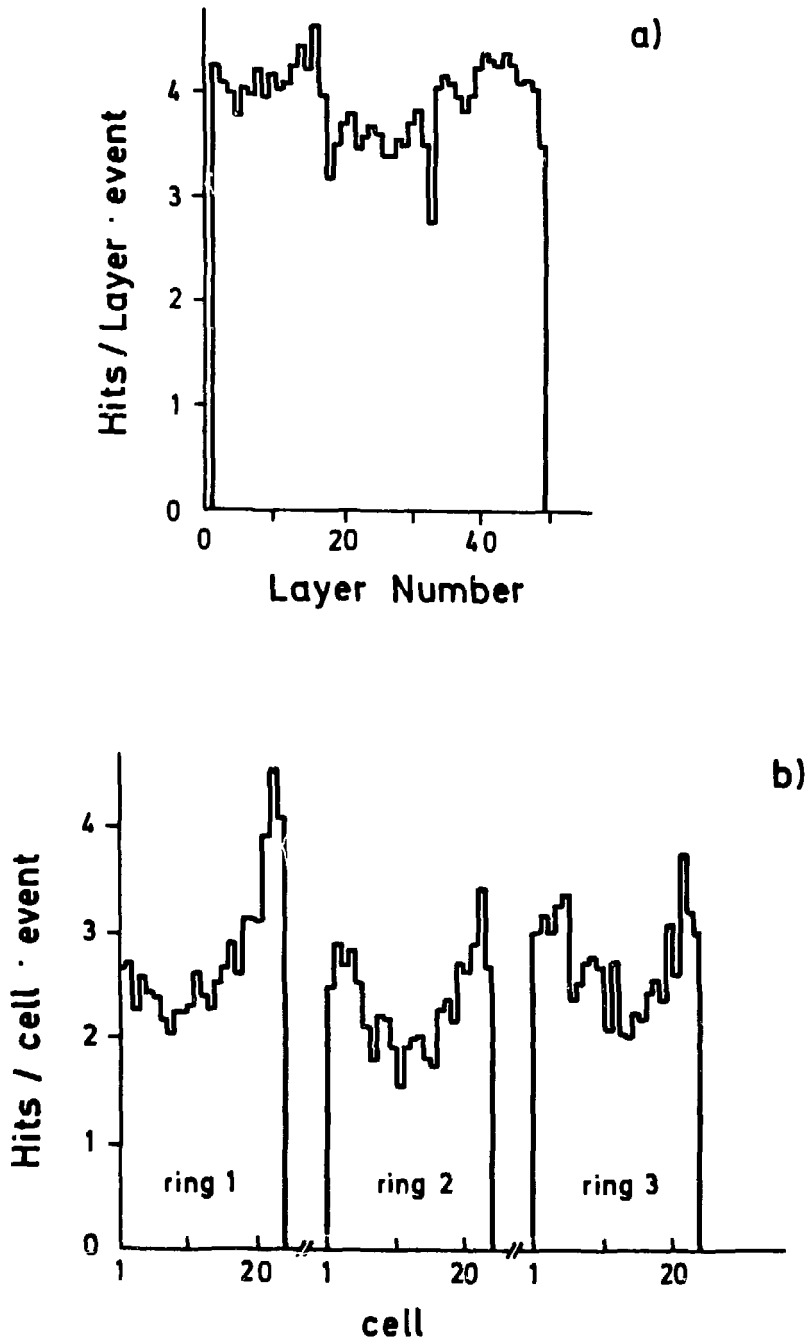


Fig. 3 The radial and azimuthal distribution of hits due to synchrotron radiation: (a) hits per layer, (b) hits per segment, shown separately for rings 1, 2 and 3. The data are taken from runs at a center of mass energy of 42 GeV.

increase in the horizontal plane towards the inside of the storage ring, typically in the order of 25 %.

Through charge division also the distributions of the radiation along the wires can be measured. One finds that the distributions in all three rings are similar in shape and that 70 % of all hits lay in the region of $|z| < 60$ cm, and 30 % in $60 \text{ cm} < |z| < 120$ cm.

The energy deposited per hit by the synchrotron radiation exhibits an exponentially falling spectrum with a mean energy of 15 keV, and extending up to 60 keV. These values can be compared with the mean energy loss of 7 keV for a minimum ionising particle.

Starting from this energy spectrum one can now check to what extent the chamber current is due to synchrotron radiation. The mean energy deposit of 15 keV corresponds to a total charge of 3.7 pC deposited per wire. For a typical run at 40 GeV center of mass energy one observes 2.5 hits per cell and bunch crossing. With $2.5 \cdot 10^5$ bunch crossings per second the anode current due to synchrotron radiation is 2.3 μA . The current measured under these conditions with the anode current monitor is 2 to 3 μA . One can therefore conclude that the chamber current and the radiation exposure is entirely due to synchrotron radiation.

In Fig. 4 the mean accumulated charge per wire is plotted as function of time for the wires of ring 1. The integrated charge in ring 2 is approximately (10 - 15) % less than in ring 1 with few exceptions during early running, where the radiation level at the innermost wires was higher. Since ring 3 is subdivided into twice as many cells as ring 1 and 2, and since the number of hits per layer is the same in all rings, the charge accumulated per wire is only half that of ring 2. This is indicated also in Fig. 4.

4) Search for Radiation Damage

During the more than six years of operation of the chamber at the PETRA storage ring, no increase in dark current, no breakdown of the high voltage or any other defect has occurred which could be attributed to a serious radiation damage. In order to search for aging effects due to radiation, the amplitude spectra of cosmic ray muons were analysed. The data used for this were taken at the beginning of 1981 and 1985, during periods where the storage ring was not in operation.

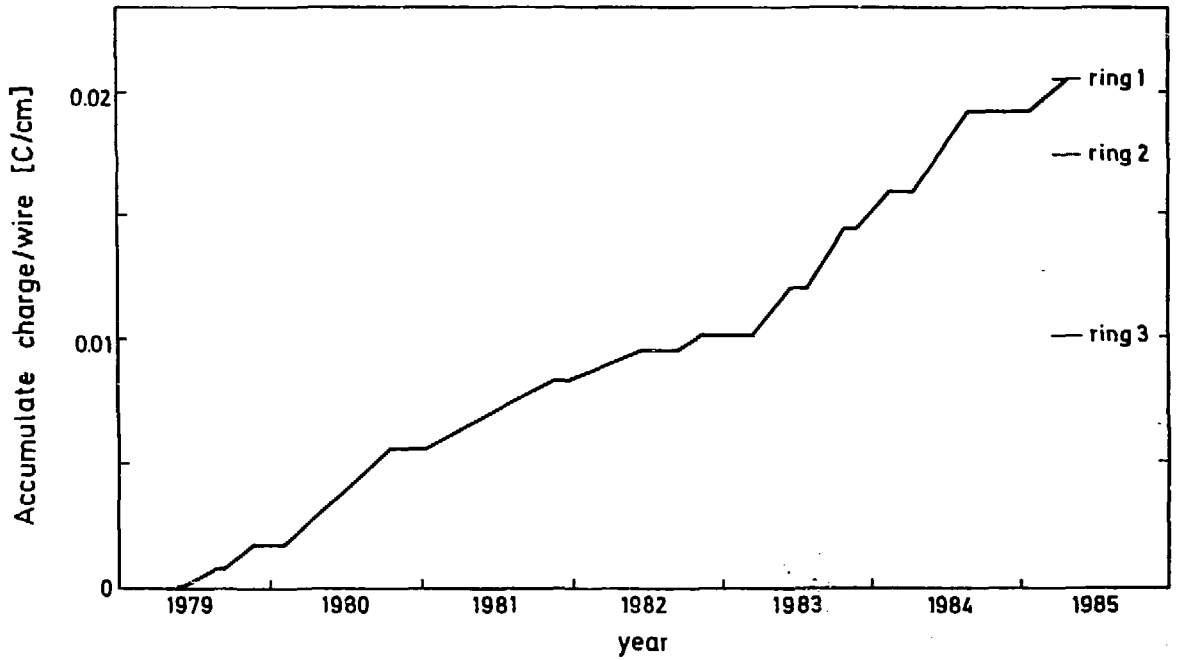


Fig. 4 Mean accumulated charge per wire of ring 1 as function of time. The integrated charge in rings 2 and 3 is also indicated.

After determination of the mean signal charge per cell, the average amplitude per ring is calculated. It is then assumed that the wires of ring 3 have been unaffected by radiation during the time period considered here, since the accumulated charge per wire is less than 0.005 C/cm. Making this assumption allows to eliminate small effects of variations in pressure, gas composition and voltage settings on the amplitudes by normalizing the data taken in 1981 and 1985 in such a way that the mean amplitudes in ring 3 are equal.

The results for the decrease in amplification with time and accumulated charge in rings 1 and 2 are summarized in table 2, where A is the mean amplitude.

Table 2

		ring 1	ring 2
$\frac{A(1981) - A(1985)}{A(1981)}$	[%]	15 ± 3	2 ± 3
accumul. charge Q	[C/cm]	0.014	0.011
dA / A·dQ	[% / 0.01 C/cm]	$-(11 \pm 2)$	$-(2 \pm 3)$

The analysis of cosmic ray data taken at the end of 1985 confirms this result⁶.

The observed decrease in amplification per unit of accumulated charge is considerably bigger in ring 1 than in ring 2. While in ring 2 only a small effect is observed, which within its error is compatible with zero, (and which also justifies the assumption made above that ring 3 shows no aging), a small yet significant decrease of 11 % / 0.01 C/cm is seen in ring 1.

Since both rings have experienced approximately the same irradiation during the time where the chamber was under voltage, this decrease in ring 1 is probably not (only) due to aging of the chamber (sense wires). Another interpretation could be radiation damage to the preamplifiers

caused by the significant particle flux near the beam pipe during injection, as mentioned in chapter 3. However, no quantitative estimate can be made of such an effect, since neither the total radiation dose at the location of the preamplifiers is monitored nor are the effects of the radiation on the preamplifiers exactly known.

5) Conclusion

After more than six years of operation of the jet chamber of JADE, the mean collected charge per wire in rings 1 and 2 amounts to 0.02 C/cm, in ring 3 to 0.01 C/cm. No increase in the dark current of the chamber has been observed. Using cosmic ray muons as calibration tool the dependence of the amplification on the accumulated charge has been determined. A decrease in amplitude of 20 % during the entire period of operation of JADE has been seen in ring 1 while no significant effect has been observed in ring 2, inspite of the same accumulated charge. In conclusion, no clear indication of aging of the chamber itself has been seen, but small radiation effects in the amplifiers close to the beam pipe could be the reason for the observed drop in amplification.

Acknowledgement

We would like to thank Prof. G. Heinzelmann for his contribution to this analysis. This work was supported by the Bundesministerium für Forschung und Technologie.

References:

- 1) W. Bartel et al., JADE collaboration, Physics Lett. 88 B, 171 (1979)
- 2) H. Drumm et al., Nucl. Instr. and Meth. 176, 333 (1980)
- 3) W. Farr et al., Nucl. Instr. and Meth. 156, 283 (1978)
- 4) B. Schmidt, PhD thesis, University of Heidelberg 1986, to be published
- 5) P. Hill, JADE collaboration, private communication
- 6) An earlier determination of aging effects in the chamber which was based on the analysis of events collected during normal data taking has been abandoned, since it was too much depending on beam conditions (the results presented at the workshop were obtained using this method).

PERFORMANCE OF THE JADE VERTEX DETECTOR

H. Kado, II. Inst. f. Experimentalphysik der Univ. Hamburg

JADE¹ Experiment

Abstract

The design of the JADE Vertex Chamber is described. After half a year of successful operation part of the chamber showed significant standing and sometimes fluctuating anode currents. The history which probably led to this effect and the means by which it was cured are reported.

Introduction

The JADE Vertex Detector is a pictorial drift chamber (Jet Chamber type) with 166 sense wires, arranged in 24 cells. The layout of the chamber is shown in figure 1. The chamber operates with a gas mixture of Ar[89.1%] + CO₂[9.9%] + CH₄[1.0%] at ~1.15 bar and constant density. The total chamber volume is $4 \cdot 10^4 \text{ cm}^3$ and the gas is vented with a flow of 15 l/h. Sense wires and cathode wires are maintained at opposite high voltages, whilst the potential wires are grounded. Figure 2 shows the calculated electric field in the chamber. All important mechanical and electrical parameters of the chamber are summarised in table 1.

The read-out system is based on 100 MHz FADCs² in a CAMAC environment. Pedestal-determination and hit-finding are performed by fast microprocessors within the CAMAC crates. With preliminary calibration constants an R-Phi resolution of 120 μm has been achieved.

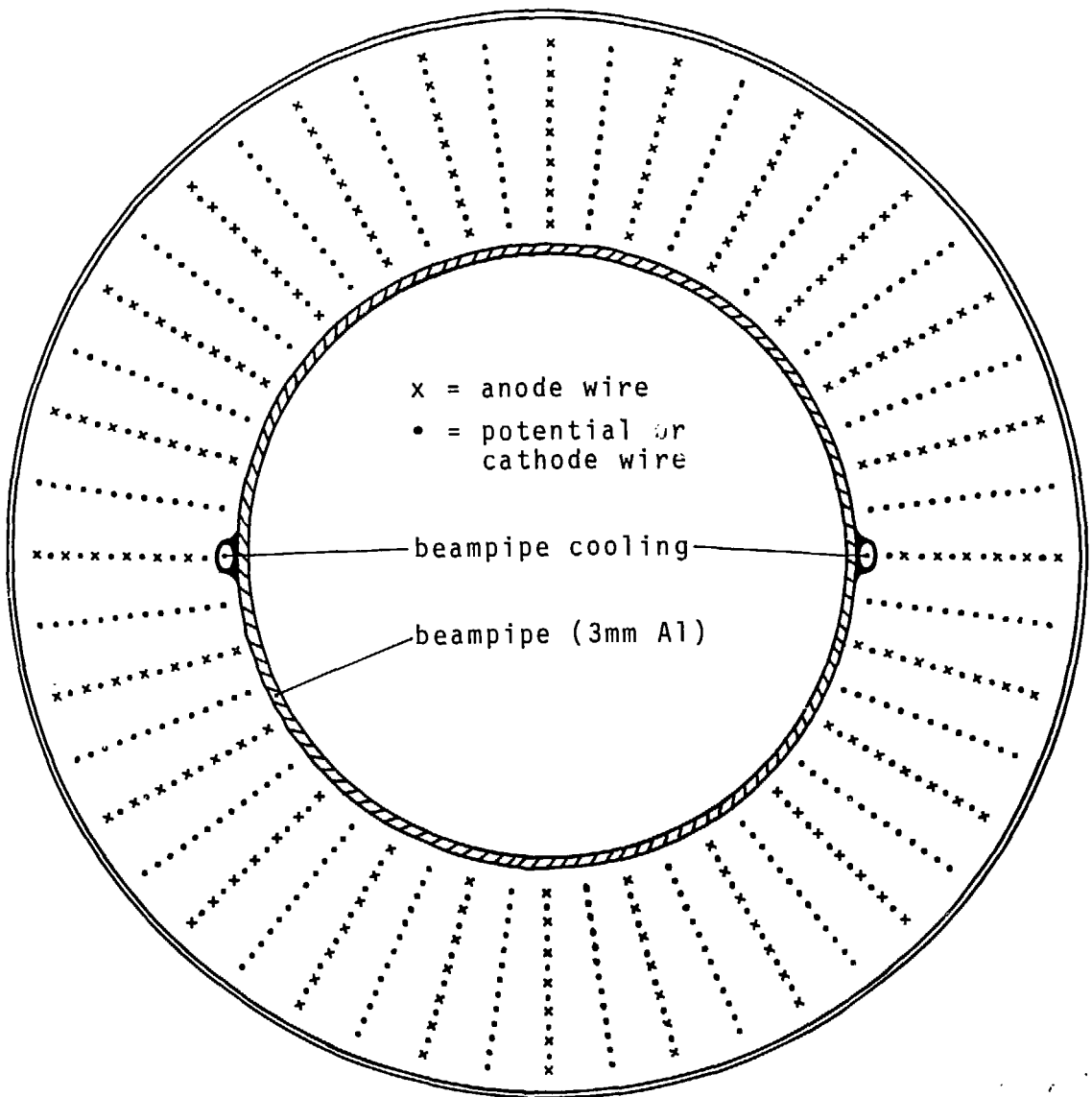


Figure 1 : The JADE Vertex Detector, viewed along the direction of the colliding beams.

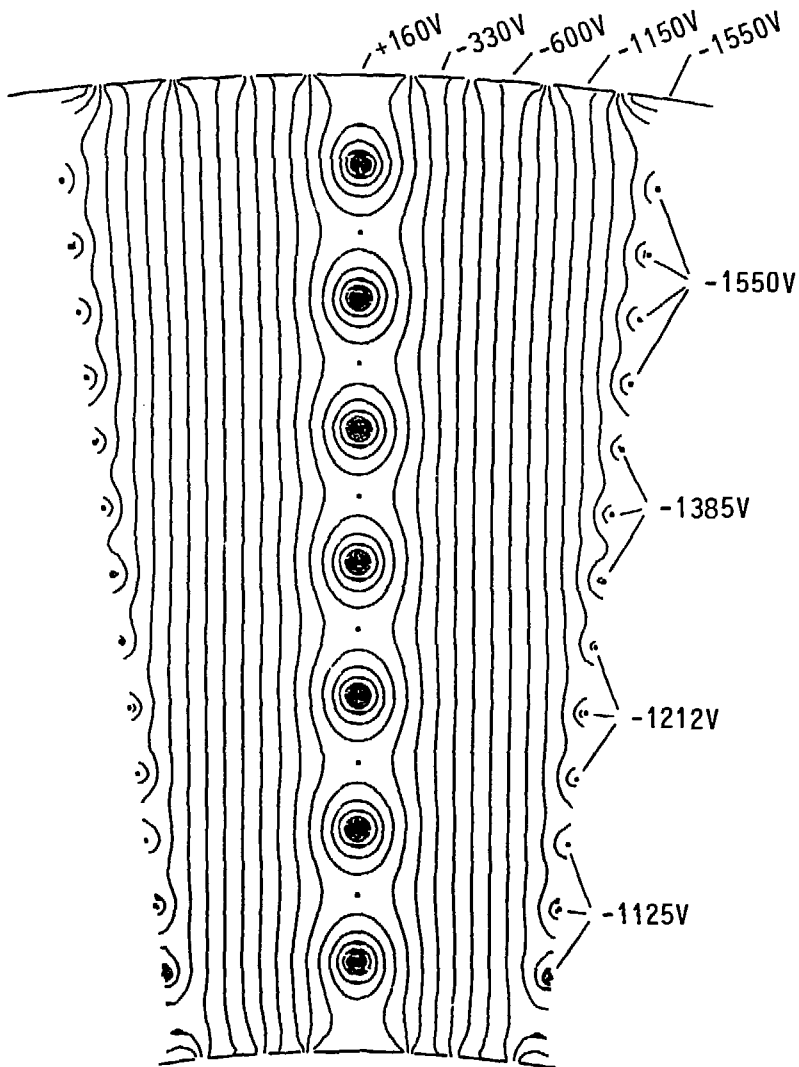


Figure 2 : One cell of the Vertex Chamber, with calculated equipotential lines.

Table 1 : Mechanical and electrical parameters of the chamber

Length of chamber	760 mm
Inner diameter of chamber	186 mm
Outer diameter of chamber	320 mm
Distance of first sense wire layer from vertex	99 mm
Drift distance in layer #1	13 mm
Drift distance in layer #7	20 mm
Spacing between anode and potential wires	4.5 mm
Spacing between cathode wires	4.5 mm
Diameter of anode wires	20 μ m
Diameter of cathode and potential wires	100 μ m
Material of anode wires	W(Re)
Material of cathode and potential wires	Cu Be
Stretching force of anode wires	0.4 N
Stretching force of cathode and potential wires	6.4 N
Mechanical staggering of anode wires	None
Potential of anode wires	+1475 V
Potential of cathode wires	-1125 ... -1550 V
Potential of potential wires	GND
Electric field at surface of anode wires	240 kV/cm
Electric field at surface of cathode wires	20 ... 26 kV/cm
Electric field at surface of potential wires	4 ... 5 kV/cm
Resistance of anode wire (760mm)	153 Ω
Input impedance of preamplifier	25 Ω
Coupling capacitor	10 nF

Observations

Construction and assembly of the Vertex Chamber was finished in spring 1984. During first tests before installation a large signal was found coming from two adjacent cells. The signal consisted of very clear and regular pulses - resembling a pulse generator. The frequency, but not the amplitude, was dependent on both anode and cathode voltage. Unusually high currents were not observed. The source of this phenomenon was traced to lie inside the chamber in the region of the end flange; but because of a tight time schedule it was not possible to reopen the (sealed) chamber to repair this. Thus it was decided to provide the chamber with an independent supply for the affected cathode plane.

When the Vertex Chamber became operative, it turned out that the effect could be suppressed by a slightly reduced voltage at this single cathode plane. The chamber then worked for half a year without major problems. After that time it became obvious that the currents in the region next to the specially supplied cathode plane began to grow. This effect was not limited to the anode or cathode wires; even the field shaping copper strips on the chamber walls showed significant standing currents. In summer 1985 these currents reached more than a factor of 4 above the normal values.

In general the following behaviour was observed :

- * Immediately after the high voltage was applied to the chamber, all currents were normal.
- * With circulating beams in PETRA, the currents in the affected region began to grow and reached their unusually high values within a couple of minutes.
- * Without beams everything was fine. The currents were where they should be - almost at zero.

In spite of the high currents, no differences were observed when comparing data from the "ill" sections of the chamber with data from the "healthy" parts; so the effect was ignored for the rest of the running period.

Nevertheless a device was provisionally installed to add small amounts of water to the gas. In the last week of the running period 1985 the device was brought into operation and the effect was astonishing : with about 0.3% H₂O-vapour the parasitic currents vanished within two days! Apart from the slightly different drift velocity (5% less than before), this seems to have no adverse effect on the data. Thus we plan to run with about 0.1% H₂O in 1986.

Conclusion

The large standing currents observed in part of the JADE Vertex Chamber after six months` running, might be interpreted as a kind of "premature ageing" initiated by a mechanical imperfection in this area inside the chamber. The parasitic currents could be eliminated by adding a small amount of water to the chamber gas.

Additional observations

With a test chamber it was observed that a slightly different gas mixture (Ar[89%] + CO₂[10%] + CH₄[1%] --> Ar[90%] +CO₂[5%] + CH₄[5%]) leads to carbon filaments ("whiskers") growing from the cathode wires in field direction. The effect was reversed when using the original gas again: the whiskers shrank and finally disappeared.

References

- [1] JADE collab., W. Bartel et al., Phys. Lett. 88B, 171 (1979)
- [2] W. Farr et al., IEEE Transac. Nucl. Sci. NS-30.1, 95 (1983)

EXPERIENCE WITH THE TASSO CHAMBERS

DAVID M. BINNIE, IMPERIAL COLLEGE LONDON

TASSO Experiment

Abstract : In several years of generally satisfactory operation the TASSO drift chambers have accumulated total charge densities in excess of 0.2/cm on the innermost wires.

There are two TASSO drift chambers close to the beam. I am grateful for Dr. Hartmann's help with this summary of our experience with them.

Cylindrical Drift Chamber

The main cylindrical drift chamber¹ (CDC) has 2340 identical drift cells. The fundamental pattern consists of four wires, a triplet of field wires and a sense wire. See Fig. 1a. The field wires are of 120 μ m diameter molybdenum and the sense wires 30 μ m diameter tungsten, both gold plated. There is a 0.5T solenoidal field. Wires are either paraxial or at a small stereo angle. All field wires are at the same potential; the sense-field potential difference is 3.0KV, which results in fields of 230 and 18-20 KV/cm at the surfaces of the sense and field wires respectively.

The chamber is operated at atmospheric pressure, and apart from an initial year with 90/10 Argon/Methane has been filled with a 50/50 Argon/Ethane mixture, initially alone and later modified by the addition of Ethanol. (Mixture bubbled through alcohol at 2⁰C). Total volume is 15m³ and the gas flow corresponds to one filling a day.

Through the years of operation there has been almost continuous apprehension not only as to the lifetime of the chamber but also as to what would happen with the next planned increase in PETRA beam energy. In 1982, it was decided to bubble through alcohol, primarily to reduce the total ionisation current collected by the sense wires, in particular that produced in the low field regions away from the cells. With this and changes to collimator masks and shielding, the total chamber current at the start of a fill slowly crept up, with increasing PETRA energy, to about 1.4ma. The total chamber charge is approximately 1ma x 6 months/year x

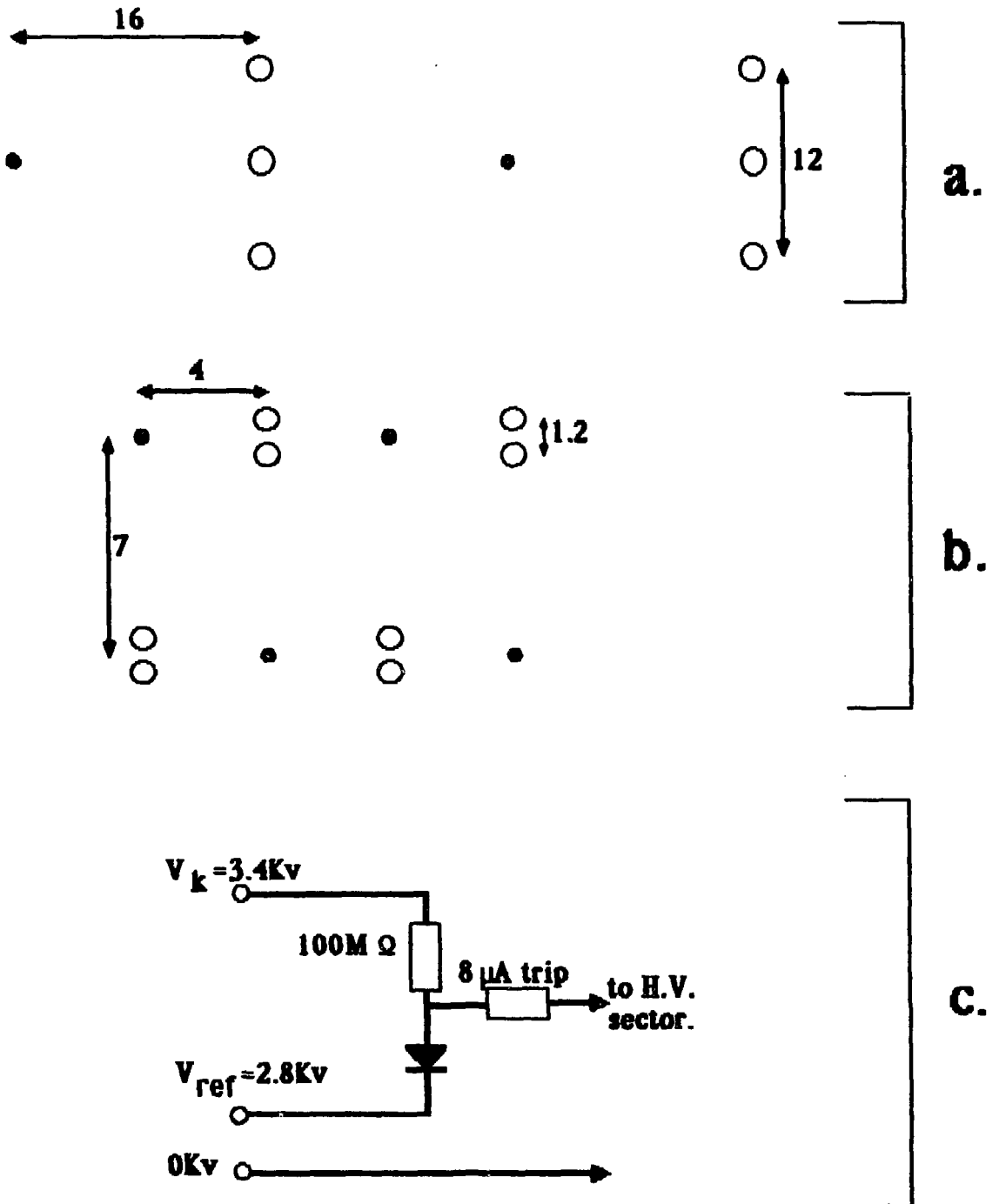


Figure 1 a) and b). The basic wire configuration in the main TASSO drift chamber and vertex detector respectively. Dots are sense wires, open circles are field wires. All dimensions are in mm. c) Outline of the scheme used to distribute chamber high voltage to each of 48 sectors. Voltages refer to normal operation.

6 years - 9×10^4 coulombs. The average charge/wire is therefore about 40C, or 0.12C/cm. From the distribution of currents we estimate a total charge of 0.2 - 0.4C/cm towards the middle of the innermost wires. After about two years there was a definite loss of gain, necessitating a 100v increase in operating voltage. A year later no further change had been seen. There has been no explicit test for degradation for the last year but no sign of further deterioration, eg. of the inner compared to the outer wires. No wires have broken and no examination of wires has therefore been made since installation.

We don't know why the chamber has lasted so well. The argon used is very pure (from the liquid argon calorimeter). After the degradation a fine and an ultra-fine filter were inserted in the gas line, and more attention was paid to minimising the oil known to have been in the Ethane. (The composition of this oil was unknown). Insufficient information is available to allow us to deduce which if anything was the important change.

Vertex Chamber

A description of this chamber and its first year or so of operation has been published² and most of what I say will be covered in more detail in this paper. I will however refer to a further effect that has become clear since that time and which could be of interest.

The chamber is of all-wire construction; 20 μ m diameter gold-plated tungsten-rhenium sense wires and 100 μ m diameter, silver-coated, beryllium copper field wires. Space was very tight and there are only two field wires/sense wires and no other guard or potential wires. The arrangement of wires is shown in Fig. 1b.

The chamber was originally designed for operation at 4 bar 50/50 Argon Ethane and encouraging results had been obtained with a small prototype. During the short time available to test the chamber (using cosmic rays) prior to the installation in TASSO it quickly became apparent that to run this chamber, which would be quite inaccessible once installed, would with such a gas mixture be too risky. Firstly there was evidence for possibly three whiskers - which I define as fine strands of conducting material which grow spontaneously from field wire to sense wire - in as many weeks. This rate corresponded to one/year in our prototype so it is

not surprising that there was no evidence of such whiskers in the original chamber. I find the low rate very puzzling - what is it that takes so long? The second problem was that in deliberately trying to bring out electrical weaknesses in the chamber by taking up to 5Kv (4.2Kv being a more normal voltage with this gas), one sense wire broke close to a feed-through and others showed melting or charring of epoxy in this region.

Tests showed (see also B. Foster's report in this proceeding) that Argon/CO₂ mixtures not only appeared to be very much safer but could even destroy fragments of whiskers grown in Argon/Ethane. With a 95/5 Argon/CO₂ mixture at 3 bar we could keep the operating voltage down to 2.8Kv. At this voltage incidentally we get 350Kv/cm and 35Kv/cm at the surfaces of the sense and field wires respectively. (It will be noticed that with Argon/Ethane at 4.2Kv, the field at the field wire is 52Kv/cm or 13Kv/cm/bar, the first clearly very high, the second thought possibly low enough to be safe). The low concentration of CO₂ kept both the voltage and the drift velocity low, nevertheless at 3 bar there was enough quenching for stable operation of the chamber.

In operation with PETRA on, total radiation induced chamber current could be up to about 200 μ A even at an operating voltage barely on the plateau. The distribution was peaked in the horizontal plane towards the inside of the PETRA ring, suggesting that the major contribution came from lower energy particles that started to spiral inwards. For wires in this region of the chamber the total accumulated charge was estimated at 1/3 μ A for 18 months, i.e. 0.25C/cm (wires 60cm long).

High voltage is supplied to 48 separate sectors of the chamber. The circuit is similar to that used in the CDC¹. The essentials are shown in Fig. 1c. The 'keep alive' voltage V_K is set 600v above the reference or normal chamber voltage. The effective impedance is therefore very low up to 6 μ A, 100M Ω above this. A sector is set to trip at a nominal 8 μ A.

After 10 weeks of satisfactory operation with PETRA, currents in some sectors started to increase rather than decrease during a run, and would persist and continue to grow slowly even with PETRA off, eventually causing a trip. These currents were very much less sensitive to a drop in the applied voltage than is normally the case, so the effect was

not just in the gas; only partial recovery was achieved by leaving the chamber off for some hours, the currents were not associated with large pulses. Mark II at PEP had experienced a rather similar effect and following a suggestion of Atac³ had eliminated the problem by introducing Ethanol vapour. To avoid Ethanol, and the possibility of whiskers, and noting that of course the gas is very dry, we thought to try water vapour, imagining either that it might allow surface charges on an insulator to leak away, 'damp', or would in some manner hide them by adhering as a polar molecule to the surface of the insulator, or both. There was very little scope for experimentation; at first we thought that water alone was working; later we found that this was not so. However if we bubbled the Argon through water and the CO₂ through Ethanol, both at 7.5°C, this proved and has continued to prove satisfactory. We have not tried to turn off the water. (The chamber volume is 0.06m³, the flow corresponds to 2 changes/day).

Turning now to the more recent experience, a visitor to TASSO would commonly find 1 or possibly 2 sectors switched off. These nearly always lie close to the horizontal plane, but on the outer side of the PETRA ring, where the normal chamber current is a minimum. It is now known that this problem is certainly sometimes and can possibly always be associated with a sudden loss of the PETRA beam. If the magnetic field in PETRA falls, the beam moves outwards, hence producing the observed pattern of damaged sectors. We have no information on the nature of the damage apart from an interesting and happy observation. In all but the innermost sector we have found it possible to make a cure by deliberately allowing the sector to draw current. The 'keep alive' voltage is lowered and the reference voltage raised so that the diode is always off (Fig.1c). The 100MΩ resistor 'protects' the sector. After maybe half an hour, with a few μa flowing, the sector will start to recover and eventually normal voltage settings can be restored.

It will be interesting to examine the chamber closely when PETRA ceases operation at the end of this year.

References

1. H. Boerner et al, Nuc. Instr. & Methods 176 (1980) 151.
2. D.M. Binnie et al, Nucl Instr. & Methods 228 (1985) 267.
3. M. Atac, Fermilab preprint FN-376 (1982).

RADIATION DAMAGE CONTROL IN THE BNL HYPERNUCLEAR SPECTROMETER DRIFT CHAMBER SYSTEM

P. H. PILE, BROOKHAVEN NATIONAL LABORATORY

Abstract

A high rate drift chamber system has been in use at the BNL hypernuclear spectrometer system for the past three years. Some of the chambers have accumulated charge doses up to about 0.2 C/cm-wire without showing external signs of aging. The system design and performance will be discussed as well as the results of some laboratory drift chamber aging tests.

1. INTRODUCTION

Hypernuclear research at the Brookhaven National Laboratory AGS requires drift chambers to be used in kaon beams which are accompanied by 10^6 to 10^7 pions and muons per 1.2 second beam spill. A schematic representation of the hypernuclear spectrometer system¹ is shown in Fig. 1. The pion plus muon rate at the D1 drift chamber position is about 10^7 /spill over a 2×12 cm area while at D2 through D7 the rates are about 1.5×10^6 over a 2×4 cm area. We have operated drift chambers in this beam line spectrometer for the past three years and have accumulated, in about 3400 hours of AGS beam time, from 0.1 to 0.2 C/cm-wire (0.5 to 1.0×10^{12} minimum ionizing $\pi^- + \mu^-$ /cm-wire) in some of the chambers without signs of chamber aging. The design of these chambers will be discussed as well as the results of laboratory aging tests using a ^{90}Sr source and two different gases.

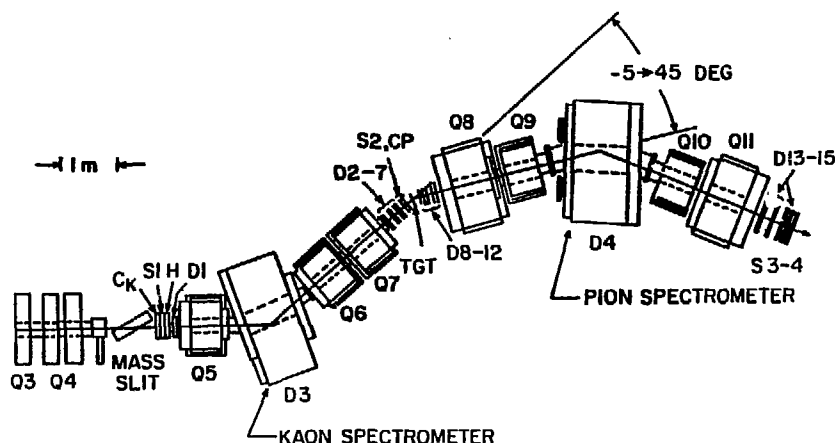


Fig. 1. Schematic representation of the BNL hypernuclear spectrometer system. The kaon spectrometer is actually the last few magnetic elements of the LESB-I beam line.

2. DRIFT CHAMBER CONSTRUCTION

The basic cell structure of the drift chambers is shown in Fig. 2(a). The left-right ambiguity of the particle track in the chamber is removed by using two planes per coordinate measured with the second plane offset by one drift distance with respect to the first. Figure 2(b) shows a partial side view of a chamber and illustrates the close proximity of the preamplifier² to the chamber. The small cathode foil to wire distance was achieved by avoiding the use of o-rings. The design allows the chamber to operate in beams with intensities up to about $3 \times 10^5/\text{s-mm-wire}$ without space charge problems. Table 1 lists some of the chamber parameters. Additional chamber electronics include LeCroy 2735 amplifier-discriminator cards followed by CAMAC multi-hit TDC's³. A more detailed discussion of the chamber design is contained in Ref. 4.

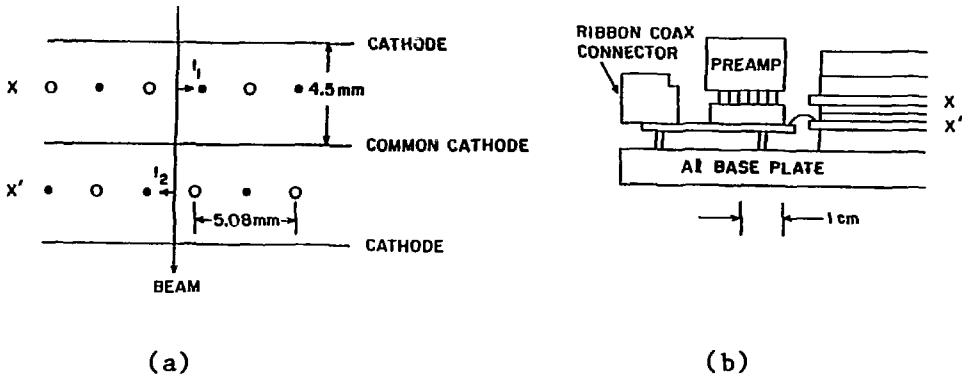


Fig. 2. (a) High rate drift chamber basic cell structure. (b) A partial side view of a high rate drift chamber showing the close proximity of the preamplifier to the gas volume of the chamber.

3. CHAMBER PERFORMANCE AND AGING TEST

After about 200 hours of exposure to the hypernuclear kaon beam (about .01 C/cm-wire) some of the chambers developed a severe aging problem. The symptoms of the aging were a localized drop in efficiency and the presence of a 10 to 200 nA chamber dark current. The localized drop in efficiency is illustrated in Fig. 3 which shows the ^{55}Fe pulse height as a function of chamber wire number. In this case the pion beam was localized on the central two wires of the chamber. An examination of the wires showed whiskers growing on the anode wires and deposits on the cathode wires (Figs. 4(a) and 4(b)). The chamber gas at the time was argon-ethane (50-50). The problem was traced to a soft urethane adhesive which was used in the affected chamber to secure the cathode foils to the G-10 frames. The aging problems did not reappear after the adhesive was covered with a hard 5-minute epoxy.

Table 1

BNL Hypernuclear Spectrometer High Rate Drift Chamber Parameters

Active Area:	5x12 cm and 17x12 cm
Frame Material:	G-10
Sealing Method:	Paraffin-Rosin-Beeswax (10-40-50%)
Cathode Foil Material:	2000 Å Cu Evaporated on 1-mil Kapton
Common Cathode Material:	2000 Å Cu Evaporated on Both Sides of 1-mil Kapton
Potential Wires:	63.5 Micron Cu-Be
Signal Wires:	10 Micron Au-W
Drift Distance:	2.54 mm
Cathode Foil to Wire Distance:	2.2 mm
Number of Signal Wires:	24 per Plane, 2 Planes per Chamber
Gas Mixture:	20% Isobutane, 4% Methylal, Bal Ar
Operating Voltages:	-1100V Cathode Foils -1300V Potential Wires
Gas Gain:	3×10^4
Double Pulse Resolution/Wire:	45 ns
Approximate Space Charge Limit:	3×10^5 /s/mm/wire
Position Measurement Accuracy:	150 Microns rms

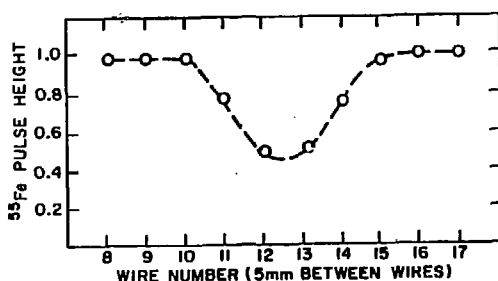


Fig. 3. Pulse height with a ^{55}Fe source as a function of wire number in a radiation damaged chamber.

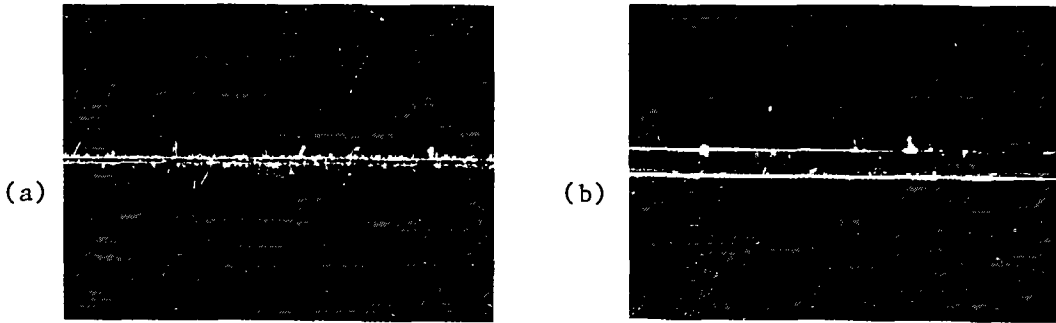


Fig. 4. (a) and (b) Photomicrograph of a portion of a 10 μm anode wire (a) and a 63.5 μm cathode wire (b) from a radiation damaged chamber.

Following the aging problem discussed above, a laboratory test of chamber aging was conducted using a 5 mCi ^{90}Sr source collimated to 1 cm. The source strength was concentrated on 2 wires. The results of one of the tests are shown in Fig. 5. The figure shows the localized pulse height (^{55}Fe source) as a function of ^{90}Sr exposure in days. The maximum exposure resulted in an accumulation of about .02 C/cm-wire-day by the anode wires for a total of about 0.6 C/cm-wire. For the worst case the pulse height reduction was 50% over the 30-day period. We thus would expect to have noticeable aging with our drift chambers with about 0.2 C/cm-wire or about 3 years of AGS beam time. A visual inspection of the wires showed visible growths on both the anode or cathode wires.

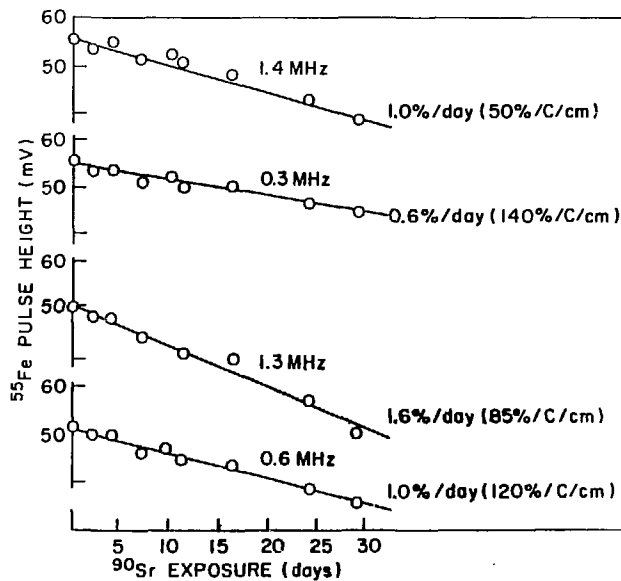


Fig. 5. Chamber #1 aging test using a collimated ^{90}Sr source. The equivalent charge is about .02 C/cm per day for the highest rate case. The gas was argon-ethane (50-50%).

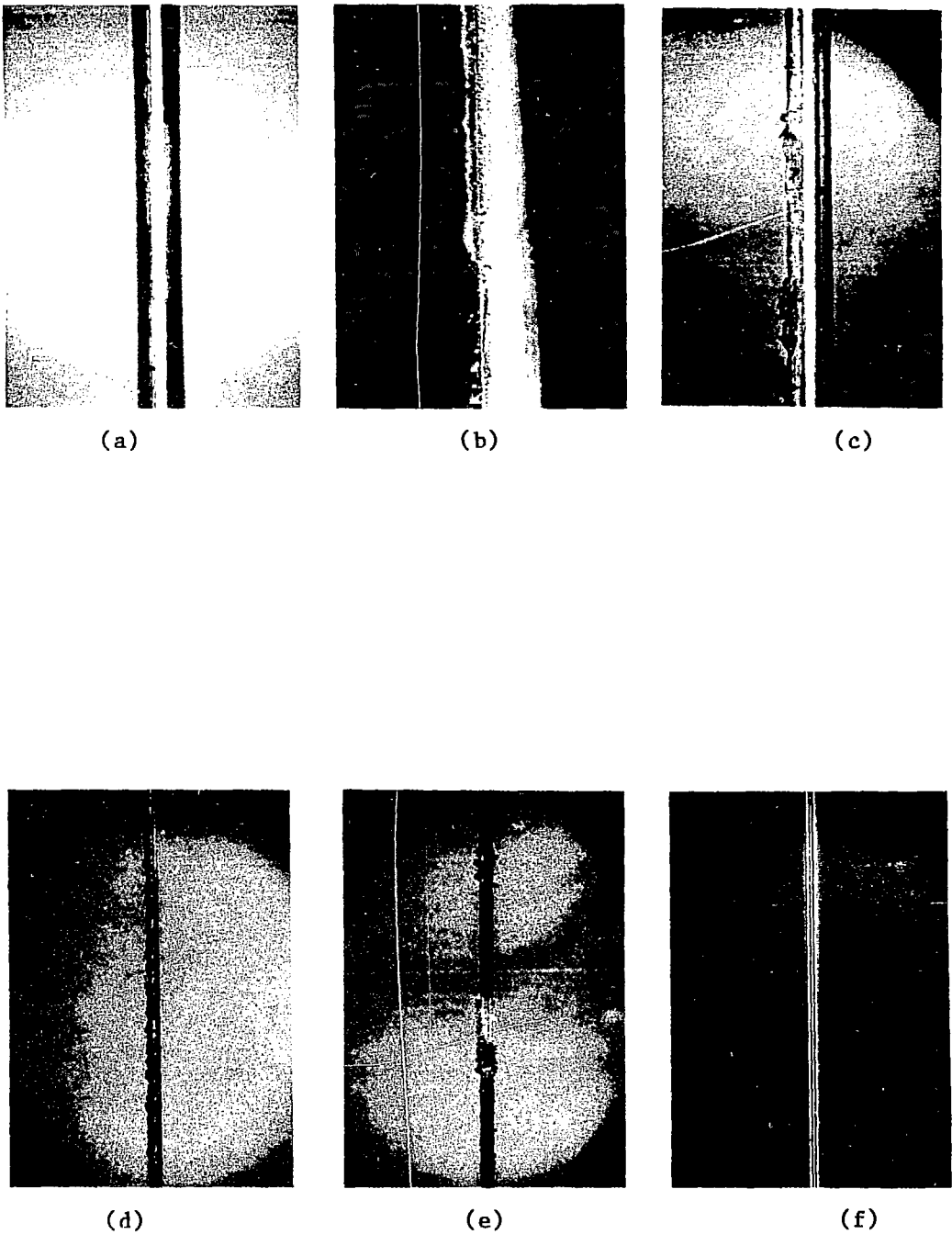


Fig. 6. (a-c) Radiation damage to 63.5 μm anode wires, (d-e) Radiation damage to 10 μm cathode wires, (f) Undamaged cathode wire. The gas was argon-ethane (50-50%) and the source ^{90}Sr . The photomicrographs were made by W. Marin of BNL.

Figure 6(a) shows a photomicrograph of a portion of a radiation damaged anode wire. The deposit forms a thin non-conducting coating on the wire and is easily seen when contrasted with the undamaged wire surface surrounding the deposit. The deposit shown on this photograph was in a region at the edge of the primary ^{90}Sr source strength. A higher magnification of the deposit is shown in Figure 6(b). The photograph shows both the deposit and the undamaged wire. A damaged anode wire directly in line with the source is shown in Figure 6(c). The wire, in this case, was gently scraped with a razor blade to show the texture of the deposits. The cathode wire deposits are shown in Figures 6(d) and (e). Figure 6(f) shows a portion of an undamaged cathode wire. The portions of wire shown in Figures 6(d) and (e) were in line with the ^{90}Sr source. The deposits on the cathode wire are not as smooth or as thin as the anode wire deposits but, like the anode deposits, are non-conductive. The deposits do not have the same whisker-like structure of those in Figure 4(a) and, therefore, apparently have a different origin.

A second test with the argon-ethane gas was performed using another chamber and three different chamber gains, and the results are shown in Fig. 7. The results are plotted both in terms of % loss in ^{55}Fe pulse height per day and per C/cm. A higher gas gain then may lead to a smaller percentage loss per C/cm but not necessarily to a chamber which will live longer in terms of actual beam time. Finally, a lifetime test was done with a argon-isobutane-methylal (75-20-5%) gas mixture. The results are shown in Fig. 8. As can be seen, the argon-isobutane-methylal gas mixture did not show evidence of aging after an exposure of about 0.2 C/cm-wire. The non-polymerizing methylal is understood⁵ to charge exchange with the migrating isobutane molecules, thus removing them as a potential source of polymers at the potential wires.

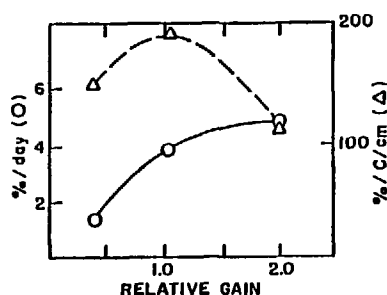


Fig. 7. Chamber #2 aging test showing the loss of ^{55}Fe pulse height/day and loss/C/cm as function of chamber gain. Gas is argone-ethane.

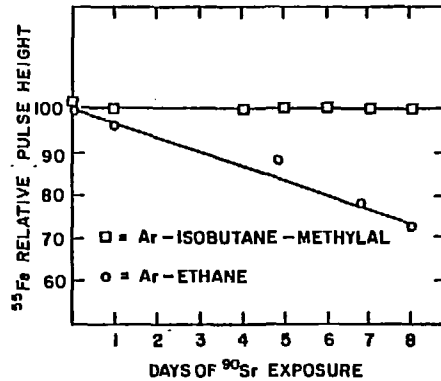


Fig. 8. Chamber #2 aging tests with two different gases.

The effect of the methylal concentration on the avalanche size in the argon-isobutane gas mixture was also studied. Figure 9 shows the results of the test. The relative pulse height obtained with a ^{55}Fe source is shown as a function of methylal concentration. As can be seen, there is a sharp decrease in pulse height with concentration above 4%. The concentration must, however, be kept high enough (3-4% according to ref. 5) to insure full efficiency for the charge exchange mechanism discussed in the preceding paragraph. A 4% concentration of methylal seems to be a sensible choice. No aging tests, however, were done as a function of methylal concentration.

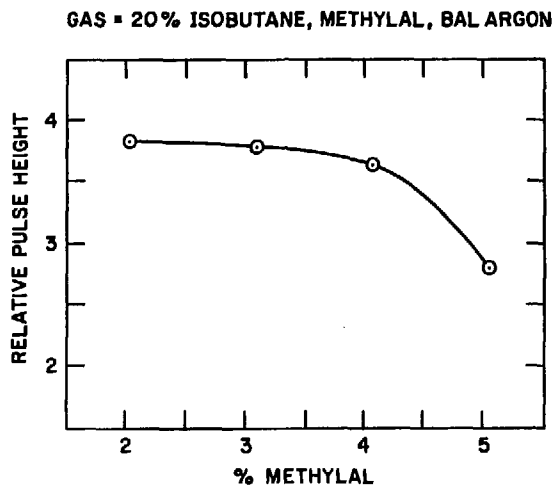


Fig. 9. Effect of methylal concentration on pulse height (^{55}Fe) with a 20% isobutane, methylal and the balance argon gas mixture.

3. CONCLUSIONS

The hypernuclear spectrometer drift chambers have been operating for the past two years with the argon-isobutane-methylal gas mixture without external evidence of chamber aging. During the first year of use the chamber gas was argon-ethane. The total dose accumulated by the chambers range from about 0.05 to 0.2 C/cm-wire during the past three years.

The principal design features of these chambers which we believe have contributed significantly to their long life are:

- (1) Low gas gain--achieved by the use of a preamplifier on each sense wire.
- (2) Small avalanche size--achieved by low gas gain and small (4.5 mm) cathode foil to cathode foil separation.
- (3) Clean chamber and gas handling system--only hard, low vapor pressure epoxies are used. All machined G-10 surfaces are coated with epoxy. No PVC tubing is used in gas systems.

Although we expect aging problems to develop in the chambers at some point, we believe that by adhering to the above design principles and by using a non-polymerizing gas, such as argon-ethane-ethanol or argon-isobutane-methylal, drift chambers can be expected to survive in intense beams and accumulate charge doses in excess of 0.2 C/cm-wire.

REFERENCES

1. P. H. Pile. "BNL Hypernuclear Spectrometers and Instrumentation, Present and Future." AIP Conf. Proc. No. 123, Steamboat Springs, Colorado (1984), p. 813.
2. The preamplifier was developed by the BNL Instrumentation Group under V. Radeka and is available through Rel-Labs, Inc., Hicksville, New York, Model RL-723.
3. Farr and Wiskat. Nucl. Instrum. & Meth. 190 (1981) 35.
4. P. H. Pile. "Instrumentation for Handling High-Intensity Separated Beams." Proc. of the Third LAMPF-II Workshop, Los Alamos, New Mexico, LA-9933-C, Vol. II (1983), p. 875.
5. F. Sauli. "Principles of Operation of Multiwire Proportional and Drift Chambers". CERN-77-09.

WHISKER GROWTH IN TEST CELLS

Brian Foster

H.H. Wills Physics Laboratory

Royal Fort, Tyndall Avenue, Bristol BS8 1TL, United Kingdom

ABSTRACT

Polymerisation of drift chamber gases has been investigated using a high electric field in a test cell. Whisker growth on cathode wires is supported by mixtures containing hydrocarbons, whereas those containing carbon dioxide inhibit polymerisation and exhibit some therapeutic effects on chambers in which polymerisation has already begun.

There are many reasons for the failure in operation of drift chambers or similar detectors which amplify ionisation by an avalanche at the surface of a thin anode wire. One such cause is the spontaneous formation of a thin polymer cylinder or "whisker" which grows quickly and bridges the gap between the anode and cathode wires. We have experienced such problems during testing of the TASSO vertex detector¹ and initiated a program of studies using a simple test cell in order to find safe operating conditions for the detector. In the following I report the results of a series of tests carried out at Bristol and Imperial College, London.

The test cell is shown in figure 1. Gas mixed in a gas rig flows through cleaned copper tubing to a thick glass vessel of 5 cm internal diameter which contains a wire stretched between two insulating feedthrus. The distance of this wire from an earthed aluminium plate can be varied between 4 and 10 mm. High voltage (either positive or negative) can be applied to the wire with the option of including a high series resistance which acts as a crude current limiting device. The exhaust gas from the cell can be directed into a mass spectrometer of type Micromass 1/2 for analysis before it is vented.

In order to initiate the formation of whiskers, negative high voltage is applied to the wire and increased until current begins to be drawn. This usually takes place for a surface field on the cathode greater than about 100 kV/cm at which point glow discharge occurs at one point along the wire. Typically currents of about 10 μ A are drawn. If the voltage is then increased again, the glow discharge will recur but the position and threshold voltage are not in general reproducible. The behaviour as the current is allowed to continue or increase varies for different gases. In some, such as 50% Argon/50% Ethane, the current quickly grows and a black filament forms, almost invariably on the cathode, which grows across the gap to the anode plane. During growth the end of this whisker glows brightly as the glow discharge approaches the anode. Even if the high voltage is increased substantially so that many other centres of glow discharge form, after a few minutes one or at most two centres of discharge remain, from which whiskers propagate. Analysis of the exhaust gas during this process via the mass spectrometer indicates that Ethane is being used up, presumably forming $(CH_2)_n$ -type polymers in the whisker.²

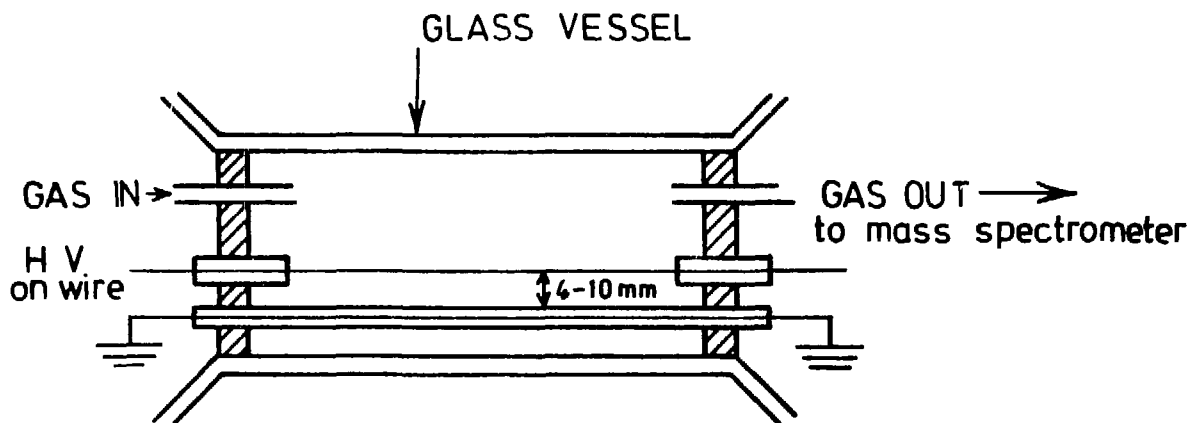


Figure 1. Section through the test cell used. The separation of the wire from the earthed aluminium plate can be varied between 4 and 10 mm.

In contrast, the behavior of gas mixtures containing only Argon and Carbon dioxide is very different. Whereas the surface field at which glow discharge begins is roughly comparable, no polymerisation leading to whisker growth has been observed. The current drawn remains constant at constant voltage, and the effect of increasing voltage is merely to allow more centres of glow discharge to form. At the highest attainable voltages, just before the onset of spontaneous sparking, the whole cathode is surrounded by a continuous glow discharge sheath. Areas of black, soot-like deposits are the only damage evident on the wire surface, which may be cleaned using a wire brush.

Argon-Carbon Dioxide mixtures can even be used to rehabilitate chambers damaged using Argon-Ethane which extended approximately half-way across the anode-cathode gap, at which point the voltage was removed and the Argon-Ethane was replaced by Argon-Carbon Dioxide. When the high voltage was reapplied the whisker was observed to glow red and slowly vanish, the end glowing and retreating back to the cathode surface. No further whisker was formed.

In addition to the gas mixtures mentioned above, we have tested the properties of several other mixtures and including, following a suggestion by Atac,³ Ethanol. The results of these tests are summarised in table 1. It seems that mixtures containing even as little as 5% Ethane or Methane can still grow whiskers; while Ethanol inhibits this process, it does not prevent it. In contrast, Argon-Carbon Dioxide mixtures seem not to support whisker growth.

Clearly, the process of glow discharge which is forced to occur in our test cell by increasing the high voltage well above normal operating conditions is atypical for a normal drift chamber in a particle physics experiment. However, our experiences with the TASSO vertex detector do indicate that, under sufficiently high cathode fields over many hundreds of wires the phenomenon of spontaneous whisker growth does occur, perhaps at an area of particularly poor surface quality. In addition, it is possible that the formation of deposits on cathode wires which is well documented in many experiments (see these proceedings) can sometimes lead to areas of local high field which initiate whisker growth of the type described here.

TABLE 1

Gas Mixture	Whisker growth allowed?	Comments
50:50 Argon-Ethane	yes	Whiskers grow down to concentrations of ethane of 5% or more
48:48:4 Argon-Ethane-Ethanol	yes	Whisker growth is suppressed by adding ethanol
40:40:20 Argon-Ethane	yes	
Argon-Carbon Dioxide	no	No mixtures of Argon-CO ₂ support whisker growth
70:25:5 Argon-Carbon Dioxide-Ethanol	no	
90:10 Argon-Methane	yes	
95:5 Argon-Methane	yes	
50:50 Argon Isobutane 60:60 Argon Isobutane 92:9 Argon Isobutane	yes	Threshold for whisker growth about 2 times higher than Argon-Ethane mixtures

In conclusion, we have tested various gas mixtures commonly used in drift chambers to see if they support whisker growth on cathode wires. Mixtures containing even quite small amounts of hydrocarbons, such as Ethane or Methane, allow whiskers to grow when a high surface field is applied to the cathode. In contrast, mixtures containing only an inert gas plus Carbon Dioxide fail to support whisker growth and, moreover, seem to be able to rehabilitate chambers in which whisker growth has begun.

ACKNOWLEDGEMENTS

This work has been carried out in collaboration with D.M. Binnie of Imperial College, London, E. Nordberg of Cornell University and N. Jennett and L. Taylor of Bristol University.

REFERENCES

- 1) D.M. Binnie, "Experience with the TASSO chambers", these proceedings.
- 2) D. Hess, these proceedings.
- 3) M. Atac, FERMILAB-FN-376, CDF Note 146, December 1982.

AGING EFFECTS IN A LARGE DRIFT CHAMBER IN THE FERMILAB TAGGED PHOTON SPECTROMETER

Penny Estabrooks
IPP/Ottawa-Carleton Institute for Physics

Fermilab Experiments E516 and E691

ABSTRACT

Aging effects have been observed in a large drift chamber in the Tagged Photon Spectrometer at Fermilab with a total collected charge of about 0.2 Coulomb/cm per central wire. The first problem, excessive current draw, was cured by bubbling the argon-ethane gas mixture through ethanol. A large inefficiency was observed in the central (high rate) area of the chamber, a region in which a thick layer of (mainly silicon) deposits was observed on the anode wires. The efficiency in this region slowly decreased as a function of time. Cleaning the wire planes resulted in a major restoration of efficiency.

Aging effects have been observed in a drift chamber (D2) during Fermilab experiments E516 and E691 which used the Tagged Photon Spectrometer. The experiments used a photon beam and this chamber was located downstream of the first analysing magnet (vertical field), so the flux, due primarily to pair production, was highest in a horizontal strip across the centre of the chamber. The chamber consisted of three assemblies, D2-1, D2-2 and D2-3, each with three sense planes: one with vertical wires, one with wires at an angle of 20.5 degrees from the vertical, and a third with wires at an angle of -20.5 degrees. The plane configuration was cathode plane, U sense plane (-20.5 degrees), cathode plane, X sense plane (vertical wires), cathode plane, V sense plane (+20.5 degrees), cathode plane. All cathode planes had vertical wires. The sense wires were .001" diameter gold plated tungsten while the field and cathode wires were .003" Cu-Be. The sense wire spacing was .375", and there was a field wire between each pair of sense wires. The spacing between sense planes was .625", as was the spacing between cathode planes. The wires were attached to G10 printed circuit boards supported by aluminum frames. All three assemblies were housed in the same aluminum gas box with Mylar windows. The gas mixture used was a 50/50 mixture of argon and ethane with, eventually, the addition of about 1.5% ethanol. Gas pressure in the chamber was just over atmospheric. Gas flow was such that there was a volume change about once a day. The sense wires were held at ground, field wires at about -2.1 kilovolts, and cathode wires at -2.4 kilovolts, resulting in a gas gain of about $2E+05$.

The chamber was used in the engineering and data-taking runs for E516 from 1979 to 1981. Early in the data-taking run, large current draws and high voltage breakdowns were observed. The current would increase steadily until it caused a high voltage trip, even with the high voltage ramped down to 80% of its full value between beam spills. Attempts to localize the problem were unsuccessful. After the chamber high voltage was turned off for an hour or so, it was possible to slowly increase the voltage to reasonable

operating conditions and the chamber would function properly for a few hours before the current draw began to grow again. We estimate that the total collected charge in the centre of the chamber was about .05 Coulomb/cm of wire at this time. Bubbling the gas through ethanol at zero degrees Celsius (yielding an alcohol concentration of 1.5%) was found to completely eliminate the excessive current draw. We estimate a total collected charge of 0.12 Coulomb/cm per central wire for the E516 run with ethanol in the gas mixture.

Before the re-commissioning of the chamber for E691, the most upstream D2 assembly (D2-1) was removed from the gas box and cleaned. Visual inspection revealed white crystal-like deposits, occasionally with associated whisker formation, more or less randomly distributed over the field and cathode wires. These deposits were not easily dissolved and were removed by rubbing the wires with an abrasive pad (3M product Scotch-Brite) and then cleaning the wires with trichloroethane. There were also black discoloured areas at the ends of many of these wires. These were very difficult to remove and required vigorous abrasive cleaning. The sense wires seemed reasonably clean. The only sign of a beam-related problem was a subtle difference in the reflectivity of the wires in the high flux region.

At this time also, D2-4, a new assembly of U,X,V planes, was constructed. This assembly differed from the others in that it had larger diameter (.005") field and cathode wires and had the outer cathode planes parallel to the sense planes, i.e., at ± 20.5 degrees from the vertical. This assembly sat in a separate aluminum gas box with aluminized mylar windows.

During the E691 run in 1985, the gas used was again a 50/50 mixture of argon and ethane bubbled through alcohol at zero degrees C. We estimate the charge accumulated per cm of wire in the chamber centre to be about 0.09 Coulomb for this experiment (see Table 1).

The first indication of chamber aging after the addition of alcohol to the gas mixture is illustrated in Fig. 1 which shows the y (vertical) distribution of found tracks from E516. Instead of peaking in the centre ($y=0$) as expected, this distribution actually has a dip at $y=0$. This dip was due to an inefficiency in the high flux central region of the chamber. There was no evidence that this effect was rate related . . . it was apparent even in extremely low intensity background muon runs. This inefficiency was also present in E691. The central region efficiency was high at the beginning of each twenty second beam spill, then decreased fairly rapidly as the spill progressed, as illustrated by Fig. 2 which shows the y distribution at various times within the spill. The inefficiency seems to grow during the first four seconds and then remain roughly constant for the duration of the spill. We attribute this effect to a space charge buildup.

There was also a much longer time dependence of this effect. Histograms of the y distribution of hits in D2-2, for example, show no evidence for a dip at the beginning of the E691 run in April. The same distribution for data taken later in the run shows a clear dip at $y=0$. These results are quantified in Fig. 3 which shows the ratio of efficiency in the hole region to that outside it for the four D2 assemblies as a function of the total accumulated charge in the centre of the chamber. A slow decrease of efficiency is apparent in all four assemblies. However, it is also clear that the efficiency is much higher in the new assembly, D2-4, than in the old assemblies which had already

TABLE 1

Summary of total charge accumulated per cm of wire		
Experiment	Gas mixture	Charge (Coulomb/cm)
E516	argon-ethane	.05
E516	argon-ethane + ethanol	.12
E691	argon-ethane + ethanol	.09

E516 Y DISTRIBUTION

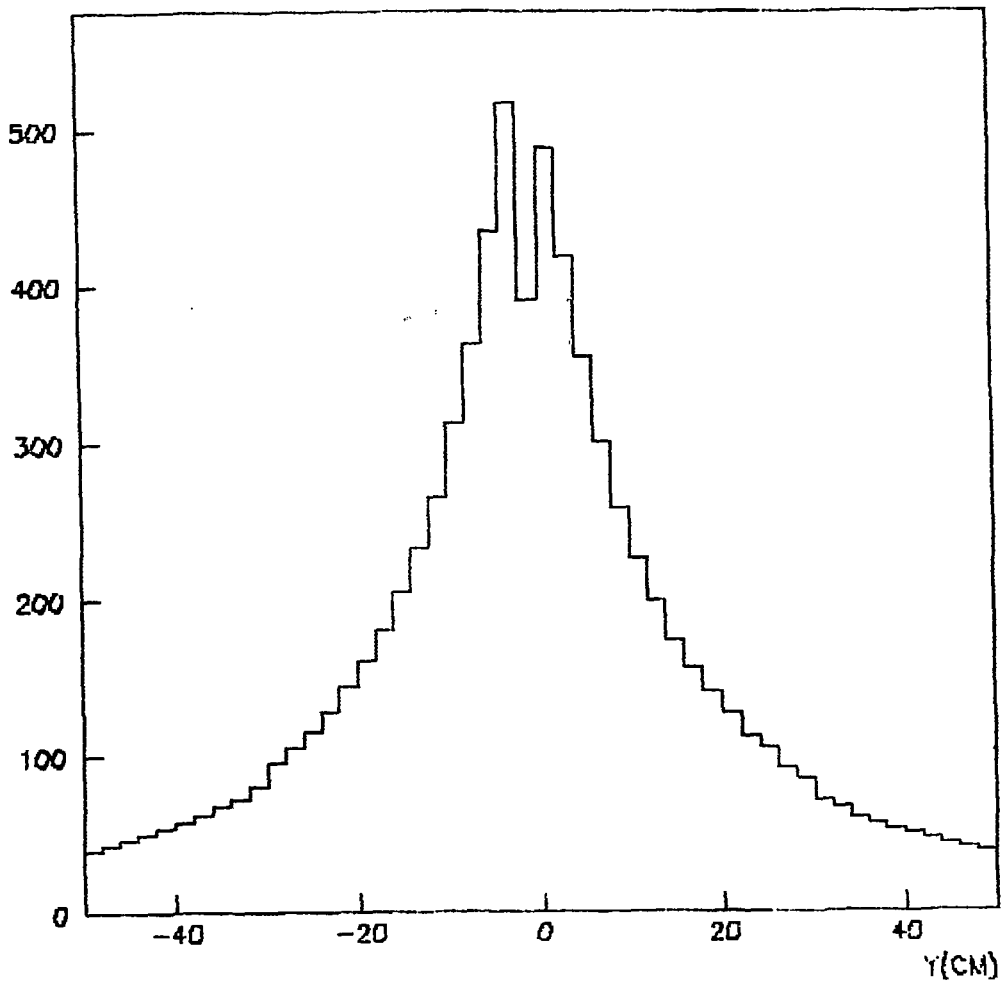


Fig. 1: y distribution of found tracks in E516.

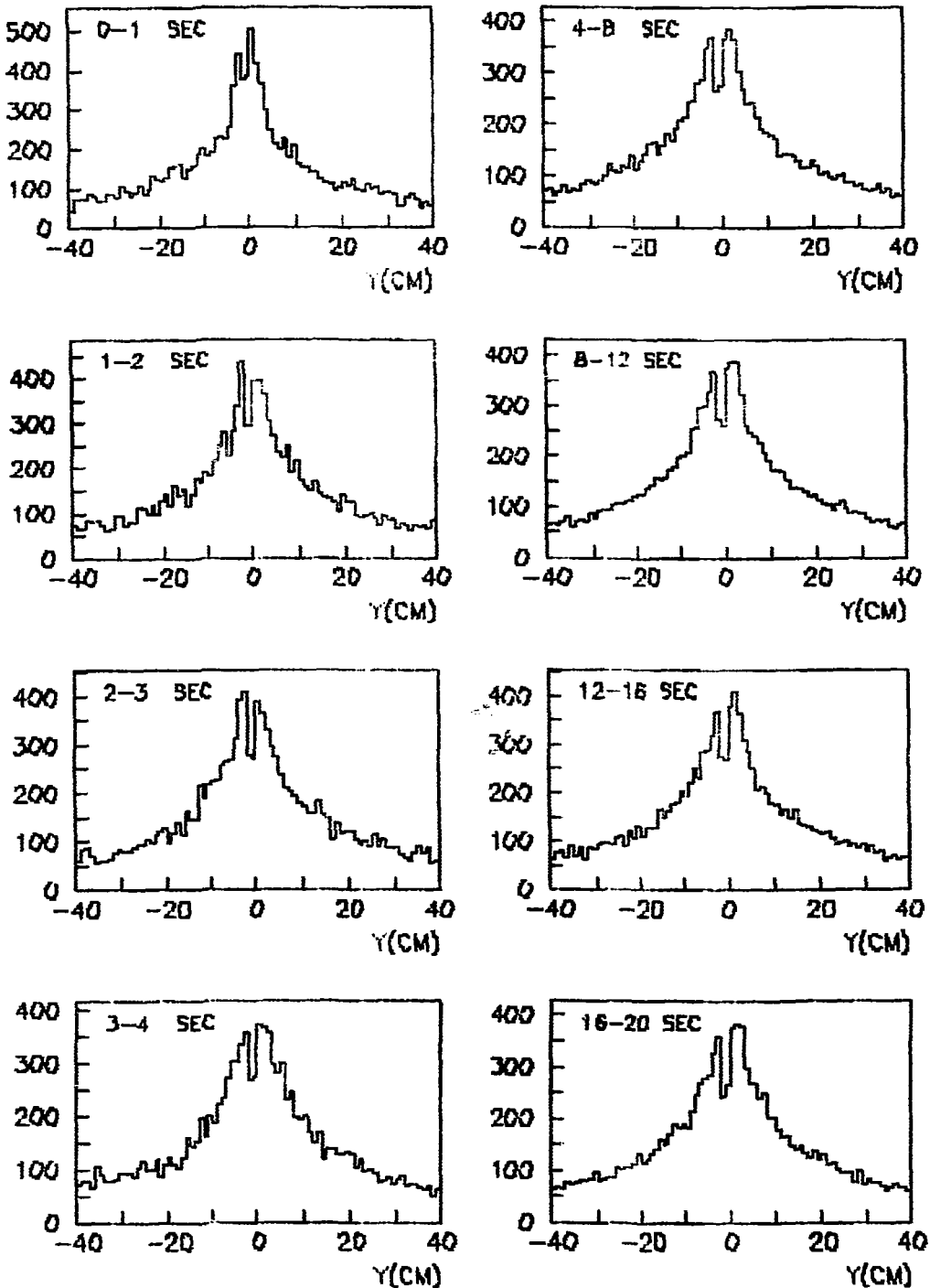
E691 γ (D2-2)

Fig. 2: y distribution of hits in D2-2 as a function of time in the spill in E691.

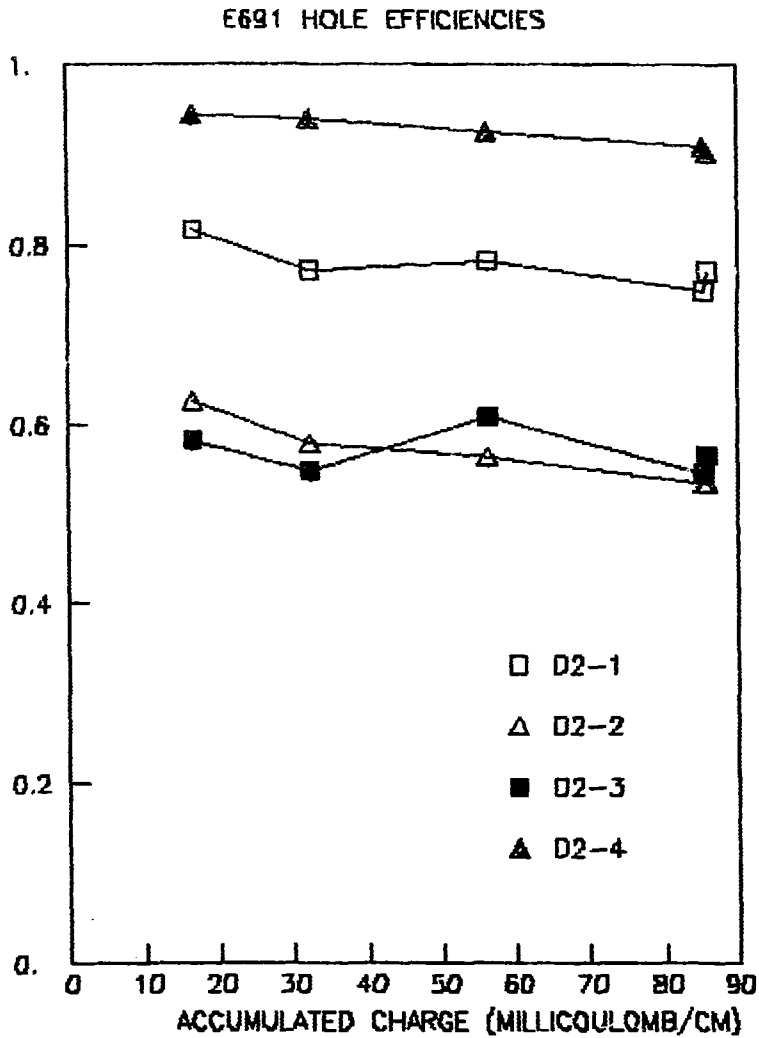


Fig. 3: Ratio of efficiency in the hole region to that outside for the four D2 assemblies as a function of the accumulated charge/cm of wire in the centre of the chamber.

accumulated about 0.17 Coulomb/cm by the beginning of E691. Moreover, the efficiency in D2-1, the assembly which was cleaned before the E691 run, is dramatically higher than in the two uncleaned assemblies, D2-2 and D2-3. The fact that both D2-1 and D2-4 efficiencies at the end of the run are much higher than D2-2 and D2-3 efficiencies at the beginning indicates that the addition of alcohol to the gas significantly retarded the aging process.

At the end of E691, D2-2 was removed from the gas box and its wires examined. Once again, white crystal-like deposits were found on cathode and field wires (see microphotographs of Fig. 4b and c) and, to a lesser extent, on the sense wires. The chemical composition of these deposits could not be determined using Auger Electron Spectroscopy due to charging problems. The black marks at the ends of the field and cathode wires were found to be cracks in an almost transparent hard film covering the wire (see Fig. 4a). AES indicated that this was a several micron thick layer containing mostly carbon with small amounts of nitrogen, chlorine and sulphur. There was no discernible difference between segments of wire in the hole region and segments outside the hole. On the other hand, the anode wires in the hole region were covered by a fairly thick layer of deposits, as shown in the microphotographs of Fig. 5. AES analysis was difficult due to charging problems, but indicated that the deposits were primarily silicon with substantial amounts of carbon and oxygen. These deposits were presumably the major cause of the inefficiency in the hole region. Outside this central region, the sense wires were fairly clean except for the scattered white deposits.

In summary, we have observed a steady decrease in efficiency in the highest rate region of our chambers as the total accumulated charge increased. This inefficiency appears to be well correlated with the existence of deposits on the sense wires, and is exacerbated by space charge effects. The addition of 1.5% ethanol to the argon-ethane gas mixture clearly retarded the aging effects. Cleaning the wire planes resulted in a major improvement in efficiency.

ACKNOWLEDGMENTS

The help of the entire Tagged Photon Collaboration, the Fermilab Physics Department and Facility Support Department is gratefully acknowledged. In particular, this work would not have been possible without the collaboration of Jeff Spalding and Jim Welch. We thank the Analytical Chemistry Division of the National Research Council of Canada, in particular, Irwin Sproule, for performing the chemical analyses. This work was partially supported by the U.S. Department of Energy, the National Science Foundation, the Natural Science and Engineering Research Council of Canada and the National Research Council of Canada.

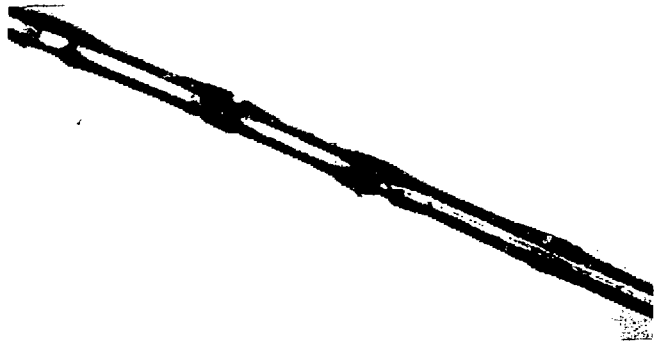


Fig. 4a: Bottom end of field wire (x30)

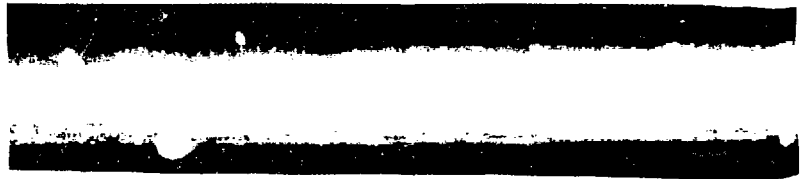


Fig. 4b: Cathode wire (x200)



Fig. 4c: Cathode wire

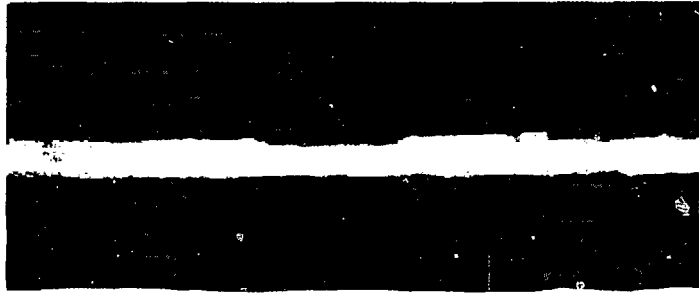


Fig. 5a: Central portion of sense wire (x100)

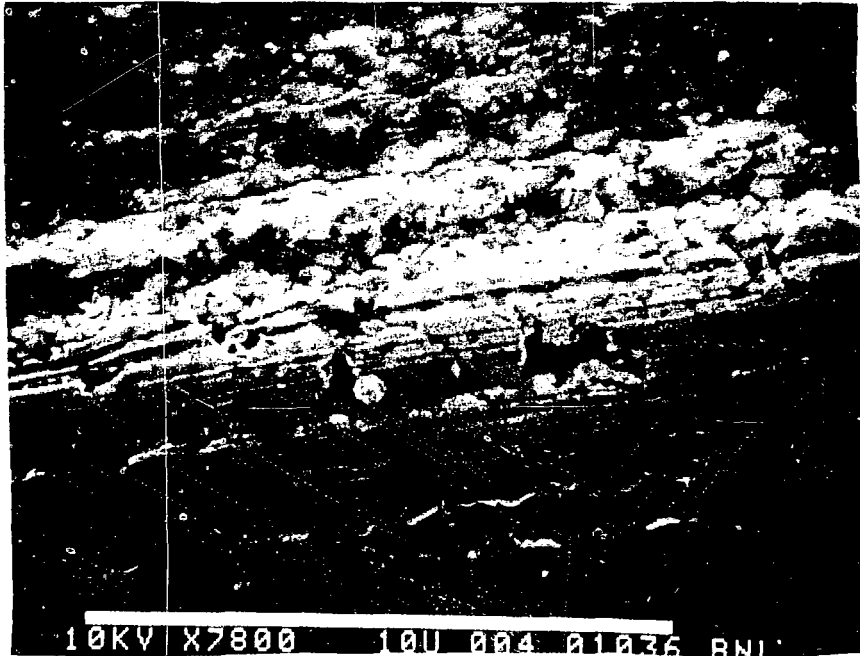


Fig. 5b: Central portion of sense wire

RESULTS ON AGEING AND STABILITY WITH PURE DME AND ISOBUTANE/
METHYLAL MIXTURE IN THIN HIGH-RATE MULTIWIRE CHAMBERS

STAN MAJEWSKI , UNIVERSITY OF FLORIDA

Abstract.

Thin chamber structures with 1 mm wire spacing were tested with isobutane/methylal mixture and pure dimethylether (DME). Results do not show serious ageing effects up to integrated charges of about 1 Coulomb per 1 cm length of wire. The actual limit is expected to be much higher. Additionally, the chambers with 50 micrometers wires are extremely mechanically durable, can accept heavy, short charge overloads without discharging and are fast, even with a "slow" gas - DME.

1. Introduction.

The results presented here were obtained during a wider study¹ of high-rate radiation-hard multiwire proportional chambers. This presentation will be limited to ageing tests and other subjects related to the problem of stability of operation of these detectors. Originally intended to focus exclusively on a new type of a detector with thick wires, the study expanded also to the improvement of the standard Fermilab beam chambers.

A very brief history of the search for a high intensity radiation-hard wire chamber will be presented to demonstrate the motivation for this work. In a very nice demonstration Walenta² has shown that the decrease in size of the elementary wire chamber cell (wire spacing * anode-to-cathode gap) can lead to a drastic improvement in the count rate capability before the space charge effect takes over. This gain is due to reduction in the charge accumulated in the column of slowly drifting positive ions. At the same time collection times of electrons are also shorter and a detector becomes faster. In the second very nice study which I want to mention, it was demonstrated³ that time resolutions of below 5 ns FWHM with an effective pulse duration (after shaping) of 8 ns are possible with very thin chambers of 0.635 mm gap thickness and fast gas mixture based on CF₄. Finally this author a few years ago worked on a thin chamber with thick wires and with highly quenching gases^{4,5}. The idea was to obtain high current saturated mode of operation in a thin active sampling chambers in a hadron calorimeter⁶. To some extent the present study is a continuation of this first one. It seemed obvious that a chamber with a very high gas multiplication factor for moderate rates should be a good candidate for very high rates but at lower multiplication factor, providing it is also fast. At the same time as the notion of radiation hardness became more important it was decided to try non-ageing gases.

2. Detectors.

Ageing tests were performed in three different multiwire detectors.

A. Standard Fermilab beam chamber, with 3.2 mm anode to cathode gap and 10 micrometers diameter gold-plated sense wires with 1 mm pitch⁷. Cathode material: aluminum foil,

B. Modified standard Fermilab beam chamber with anode to cathode gap decreased to 1.6 mm by simple mechanical modification. Cathode foils made out of aluminum and copper were used,

C. multiwire chamber with 1 mm spacing between 50 micrometers diameter gold-plated tungsten sense wires and 1.4 mm gap thickness. Cathode materials: aluminum and copper.

3. Gases.

In ageing tests we used 3 types of gases:

- pure isobutane from Matheson, of instrument purity (min 99.5%),
- isobutane with saturated vapor of methylal at 0°C. The methylal was of reagent certified purity from Fisher,
- pure dimethylether, DME, also from Matheson of 99.87% minimum purity.

4. Radiation sources.

Two beta-radioactive sources were used. Activity of the Ru^{106} source was between 1 and 2 mCi. The second source of $\text{Sr}^{90} + \text{Y}^{90}$ had a nominal activity of 10 mCi. Both sources were mounted in the brass beta guns, behind about 1 inch long and 1/4 inch diameter hole colimators. The actual size of irradiated spot was of about 8-10 mm FWHM diameter at the sense wire plane, depending on the source to chamber distance.

5. Test procedure and setup .

Because of shortage of time it was decided to perform highly time-compressed ageing tests. After establishing the high voltage working point, the current drawn from the high-voltage power supply, as the result of exposure to radiation from the sources, was monitored for periods from a few hours to a few days. The total charge deposited locally in the irradiated spot was in the range from 0.1 to 10 Coulombs. This charge and the current flowing in the chamber were the only two parameters defining the test conditions. We will soon start a new and much more detailed study, with dose-rate and amplification factor as independently variable parameters, in order to get better image of ageing process. No special gas filters were used, unless specified, but the precaution was taken not to poison the gas line between gas cylinders and the chamber and beyond (outlet line). A few meters long tube of Rilsan Nylon 11 was applied, because of worries that copper tubing could be contaminated with oils apparently used in the drawing process. Arbitrarily we have decided not to use stainless steel tubing. (In fact for short-type connections a nickel tubing seems to be a better,

cleaner choice). Rilsan tubing is made out of low-outgassing and highly chemically resistant Nylon 11 with low moisture absorption characteristics and was proven not to contaminate chamber gas, as was reported during this Workshop⁸. Nylon tubing was connected to the glass methylal container/bubbler via teflon joints. To avoid poisoning the gas flow was adjusted at the level of about 50 cc/min, though the inner active chamber volume (between cathode planes) was only between 45 to 150 cc, depending on structure. It also helps eventually to remove gas decomposition products from the active chamber volume and, therefore prolongs lifetime of a chamber.

6. Measurements.

Pure isobutane.

In a reference measurement, pure isobutane was used in the structure B (modified Fermilab beam chamber) with thin aluminum cathode foils. This chamber can operate quite well with "traditional" mixtures like Argon-Ethane-Ethyl Alcohol or Argon-Isobutane-Methylal, but our goal was to define limits of operation of such a detector under extreme conditions of heavy loads. Argon should certainly be avoided in the mixture because it is a source of ultraviolet photons. Also ethane, even without argon admixture, is not sufficiently self-quenching gas in such a compact thin-gap structure^{4,5}. In fact with Argon-46% Ethane-4% Methylal and Argon-30% Isobutane-4% Methylal mixtures in the chamber structure B, sparking was observed with the Ru¹⁰⁶ "2 mCi" source before reaching currents of 1 mA, while with pure isobutane no discharging was observed even at the working voltage of 3450 Volts and with the current reaching about 4 mA with the same source. In a short, about one minute long, test with 10 mCi Sr⁹⁰+Y⁹⁰ source at 3450 Volts the current increased to 150 microamperes and the chamber finally became unstable (because of growing parasitic current) but no sparking was produced. This clearly demonstrates the expected, improved quenching properties of pure isobutane. The additional advantage of avoiding argon is realized in much lower sensitivity of detectors to X-ray and gamma radiations (brehmstrahlung, etc). With 10 mCi source and at a working voltage of 2550 Volts in the structure B, the current drawn from the high voltage power supply was about 14 microamperes at the start and after 11 hours dropped only by 1 microampere, but became highly unstable. When high voltage was turned down just for a moment and then turned on again the actual drop in current (and gas multiplication factor) was measured to be 40%. The total charge deposited in a 1 cm diameter circular spot was 0.55 Coulombs. The chamber was opened for visual inspection and, as expected in the case of pure isobutane, some discoloration was found on sense wires in the irradiated region. The yellowish discoloration of the central - main part could not be removed by cleaning with solvents like acetone, methylal or isopropyl alcohol. The central spot was accompanied by a 3 to 4 mm wide ring of blueish deposit which was easily cleaned with

brush and solvents. Beyond this an even narrower ring followed with the same yellowish appearance and chemical resistance as the central spot. The yellow discoloration observed in the focus of an intense light beam could have been in fact due to a locally modified reflection properties of a gold surface. After carefully washing the sense wire plane with solvents, we mounted the chamber again and gas multiplication factors in the irradiated spot and in the outside regions were compared. This time no difference was found. No effort to analyse or understand the origin of these deposits was made. In a short repeat of this ageing measurement, the multiplication factor drop of 4% was measured for about 0.1 Coulombs of total deposited charge and this time current started to increase uncontrollably, probably proving that some permanent damage was done to the chamber in the first irradiation. Also this time the entire central region of the new spot had a blueish discoloration like the one of the ring in the first test, as described above, and also disappeared when cleaned using a brush and isopropyl alcohol.

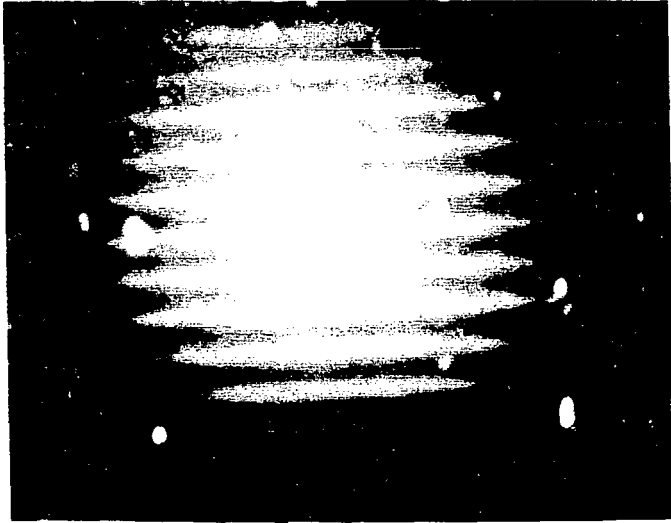
Isobutane and methylal mixture.

An obvious second try was to add methylal to isobutane in the same chamber (structure B). We quickly found that isobutane dissolves in the methylal bubbler kept at 0°C, and actually some time after connecting the gas system and opening valves (after all the air had already been flushed away from the gas system upstream from the bubbler), the gas flow at the output from the chamber was seen to halt (as observed in a second small silicone oil bubbler far away downstream from the chamber). The gas flow resumed after some time, depending on the flush rate, (usually high flow rate was used to accelerate this process) accompanied by the visible increase in the liquid level in the bubbler. After a total charge of 0.45 Coulombs, deposited at a rate of 16.9 microamperes, there was no change in current and no discoloration on the sense wires' plane, but a deposit-like whitish structure was revealed on the aluminum cathodes (Fig 1). It could not be removed by simple washing with solvents and a brush. One of the possible explanations is that it is an effect of aluminum oxidation⁹. Because we suspected that oxygen came from leaks or as a contamination in a gas, the measurement was repeated at higher flow rate after rechecking all gas connections and with Oxisorb filter installed at the outlet of the gas cylinder. This time after 0.3 Coulombs of charge the same, though less visible, "deposit" was found. And it was again astonishing to see the exact imprint of sense wires' structure on the foils, though the strength of the electric field close to cathodes should not depend much on the position relative to the wires and arriving positive ions are expected to be distributed more or less homogeneously over the cathode surface¹⁰. The deposit-like effects on aluminum were also obtained in other studies in chambers with much wider gaps^{11,12,8} and no explanation was given.

A



B



C



Figure 1. Discolorations of white color on the aluminum cathode plane after deposition of 0.45 Coulombs of charge in about 1 cm diameter spot in thin MWPC with 1 mm spacing of 10 micrometers sense wires, and filled with isobutane/methylal mixture. A/ natural size, B/under magnification of 5.5, C/ magnified 32 times.

We have heard at this workshop about the actual removal of aluminum in a case of aluminum deposited on a mylar foil ¹³. This makes us cautious about claiming that the whitish discolorations are of deposit nature. In fact observed optical effect could be due to differences in reflection (increased scattering of light) in this region of foils. We will soon analyze our old and new samples with surface analysis techniques, like proton induced X-ray emission (PIXE) and Auger-electrons technique. At present we want to state that etching (as discussed during the beautiful talk by J.Va'Vra ⁸) of the aluminum surface seems to be a viable hypothesis. After this measurement it was decided to try other cathode materials like copper foil and in the next measurement one of the aluminum cathode foils was replaced by copper. The same chamber as before was flushed with isobutane bubbling through a 0°C methylal bath. Again the 10 mCi $\text{Sr}^{90} + \text{Y}^{90}$ beta source was used to irradiate the chamber kept at 2600 Volts. Surprisingly, quite soon the current flowing in the chamber started to decrease and in 12 hours dropped from the original value of 18.8 to 11 microamperes, after only 0.6 Coulombs of deposited charge. Also a strange asymmetry in chamber response appeared when scanned with the beta beam, with spots of low multiplication close to the edges of frames, pointing definitely to some damage in the chamber. A very interesting almost irregular structure of white "deposits" was found on the aluminum cathode (Fig 2) with greasy spots in the place of irradiation and close to edges of the frames. Apparently during the time when the setup was left unattended (measurement was performed at night), the level of methylal plus dissolved isobutane in the bubbler reached the outlet connected to the tubing and some of the liquid has flown through the nylon tubing to the chamber inlet. In this chamber, as in all standard Fermilab beam-line chambers, gas sealing between frames is achieved with a little Apiezon grease squeezed between the frames. Some of the grease was dissolved and entered the active volume of the chamber in a gas phase, and was later deposited in the irradiated spot. Just after opening the chamber we saw that grease between frames was smelling strongly with methylal which confirms our hypothesis. Also the grease used to seal the connection between the nylon tubing and the bubbler was gone and the connector was found leaking. Greasy spots were very easy to remove with methylal and isopropyl alcohol. Nevertheless, a very important result of this unfortunate test was in finding that the copper foil did not show any traces of deposits, etching, etc except the greasy spots. Also it looks safer to use O-ring seals or other chemically inert ways to seal detectors to avoid additional potential sources of contamination in a gas (independently of this "accident" it is suspected that methylal even in the gaseous form can have a slow dissolving action on greases). The natural next step was to replace the second aluminum cathode with a copper foil and protect the chamber against

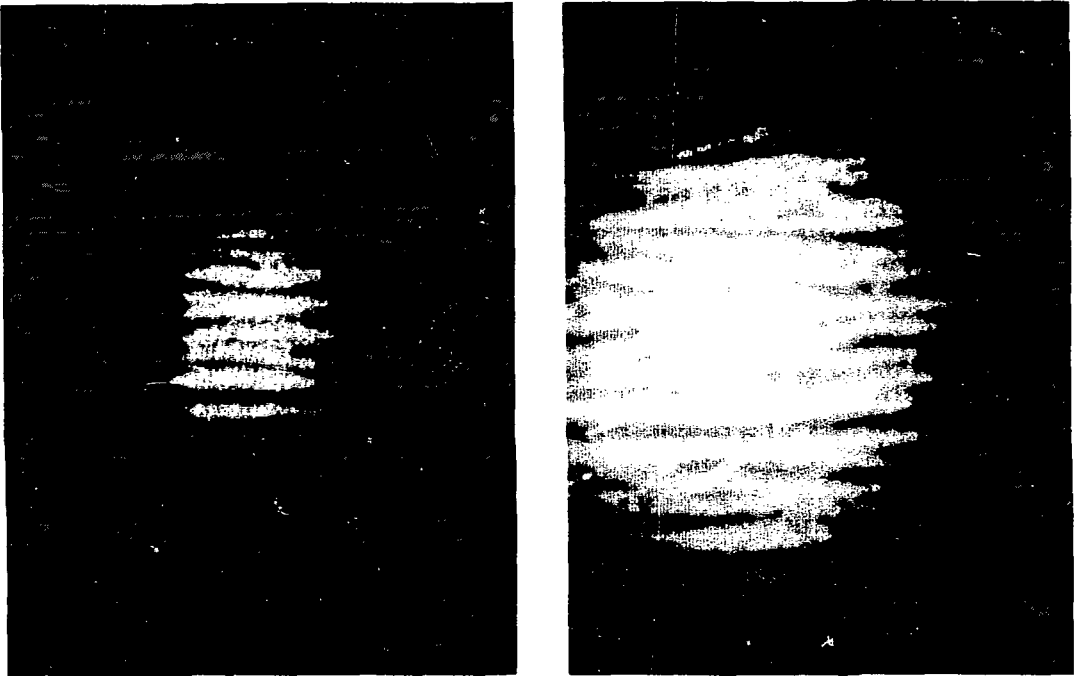


Figure 2. Irregular white discolorations on aluminum foil after an "accident" with methylal. Grease was removed before taking this picture. Chamber structure B, gas: isobutane/methylal. Total deposited charge: 0.6 Coulombs.

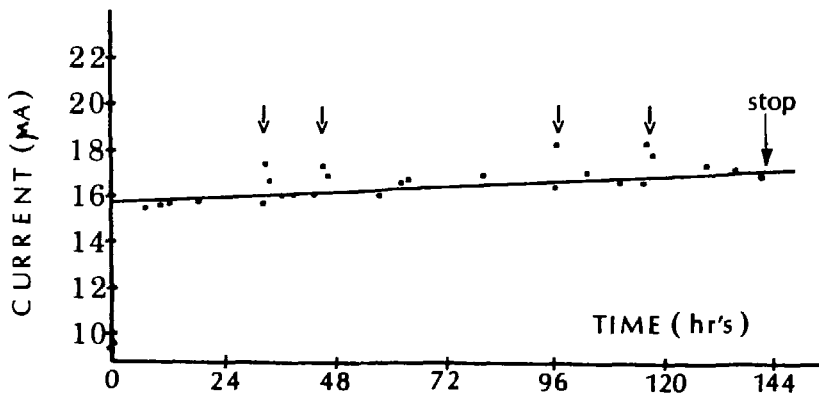


Figure 3. DC current measurement in the chamber structure B (1 mm step of 10 micrometers wires, 1.6 mm gap) filled with isobutane/ ^{90}Sr ^{90}Y ^{90}Zr methylal mixture and irradiated with 10 mCi ^{90}Sr ^{90}Y ^{90}Zr beta source. Total deposited charge in the 1 cm spot: 6.5 Coulombs. Arrows mark when refills of methylal container were done.

accidents like the one described. After these modifications were done, an almost completely successful ageing test was performed lasting about 145 hours (Fig 3). The working voltage was adjusted to 2550 Volts. During this time, frequent refills of the methylal container were necessary, and unfortunately each time the gas system had to be opened for a while leading to some small contamination with air. However, each time before resuming the test again, the chamber was flushed for periods of 5 - 15 minutes with a high flow of gas. Also, at the end of this measurement the chamber was found to be leaking. Nevertheless, even in these not completely clean conditions there was no external evidence of any deterioration after the total deposited charge of 6.5 Coulombs in the 8mm diameter FWHM spot. To our surprise we found again the same greasy spots on both cathodes, though this time they were only slightly visible and only in the irradiated region. This reinforces our statement of the necessity to avoid greases, though one cannot completely rule out contamination from the gases (isobutane and/or methylal). A slight 7% increase in current over the total test period was probably the result of other factors, like change in gas composition (contamination, slow outgassing, etc) or in temperature and/or pressure. No attempt to control all these parameters was made. The above supposition was confirmed by the direct comparison of the multiplication factors in the central spot and in the region around it, performed at the end of the test. No difference was found. In the properly directed, intense and almost transversal light beam, the greasy spots could be photographed revealing the same, though smeared, discrete structure (Fig 4). After cleaning with solvents no traces were left. We made only one observation on the nature of these spots, namely that they had an aromatic smell.

Pure dimethylether (DME).

DME was chosen because it is simpler to use than isobutane/methylal mixture. It has a similar structure to methylal but with only one oxygen bond between two CH_3 methyl groups. Importantly, the efficiency plateau in the structure C with DME was about 500 Volts lower than in isobutane/methylal mixture in the same chamber. However, the choice of DME appears to be like a contradiction to the claim of searching for a fast high-rate detector, because it is a well known "cool" and slow gas^{14,15} and at usual drift fields of around 1 kV/cm the drift velocity of electrons is below 1 cm/microsecond (Fig 5). However, in our chamber with thin gap, thick wires and a gas even more quenching than isobutane (absorption edge in DME is placed at 192 nm¹ to be compared with 170 nm for isobutane) electric fields in the drift region reach high values. For example at the bias voltage of 3500 Volts the drift electric field is 17.5 kV/cm. Electrons drift fast and time resolution measured between this chamber and plastic scintillator with relativistic electrons from Ru^{106} source was only 5-6 ns FWHM. Also positive ions drift faster in higher electric fields

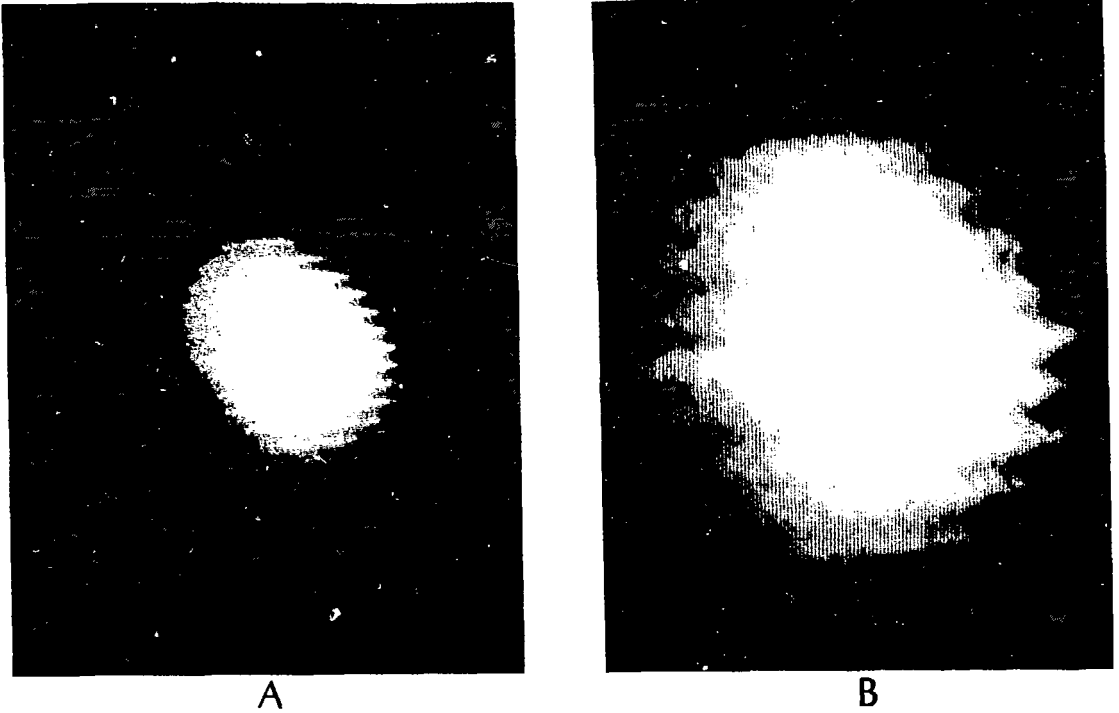


Figure 4. Greasy spots as seen on the cathode copper foil in the same measurement, as the one described in the caption to figure 3. A/ 2.5 times magnified, B/ 7 times magnified.

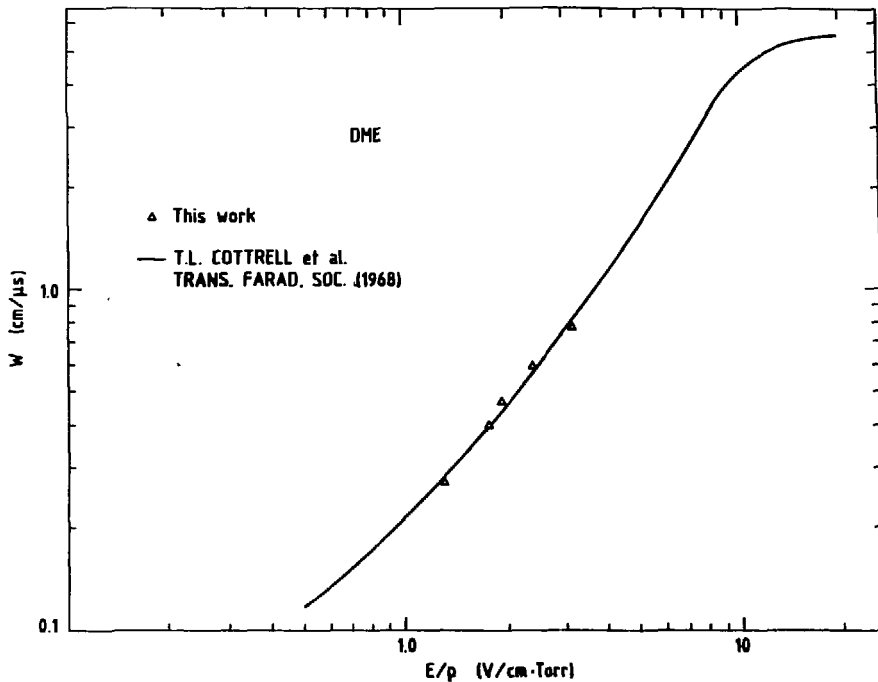


Figure 5. Drift velocity of electrons in DME versus strength of electric field at 1 atm pressure ¹⁵.

which, of course, helps prevent space charge effects. It took positive DME ions about 19 microseconds to drift 1.4 mm of distance to the cathode, at 3700 Volts of bias voltage (Fig 6) compared to about 32.5 microseconds in a modified Fermilab beam chamber (and expected twice this in a standard version) at 2300 Volts. DME was tested in the chamber structure C. The cathodes were made out of aluminum foil. The chamber was sealed with flat rubber O-rings without grease. With 10 mCi $\text{Sr}^{90} + \text{Y}^{90}$ source and at 3550 Volts working point placed well on the efficiency plateau, the constant current flowing in the chamber was about 9 microamperes. Because of lack of time (the chamber was being prepared for a beam test in the intense Fermilab beam) the test was interrupted after only about 40 hours, resulting in a total deposited charge of 1.2 Coulombs. No ageing effects were noticed but when the chamber was opened the same discoloration of white color of the cathodes was found as before for isobutane/methylal gas (Fig 7). As in all previous cases, centers of the white stripes were placed exactly opposite to the anode wires. No other deposits and no traces of oily substances were found. If the oxidation concept (contrary to etching) is true, one could try to explain it by noticing that DME (and methylal) is a source of oxygen-containing ions and probably no contamination by oxygen gas is necessary to account for the observed effect.

After this measurement, aluminum foils were replaced by copper, and the chamber was only briefly tested for ageing. No depositions were found and it was installed in the beam. The results of other studies will be published later ¹.

7. Electrostatic instability test with long wires.

One of the mechanical problems encountered when working with long wires is the necessity to estimate the maximum length of unsupported wires before an electrostatic instability will lead to discharges or other side effects, like changes in amplification factor etc. In fact in a typical multiwire chamber, where no precise position measurement of particle trajectories is performed, the only important criterion is that displacements of wires should not result in discharges, increased leakage current or other instability of operation, which will probably lead to a much faster ageing of a detector if not to an outright destruction by inducing discharges. Usually, to make a fast estimate of electrostatic operational limit for a planar multiwire chamber, say minimum mechanical critical tension T_C of wires for a given geometry of electrodes and fixed working voltage, the well-known formula is used ¹⁰:

$$(1) \quad T_C = \frac{(C \cdot V_0 \cdot l)^2}{4 \cdot \pi \cdot \epsilon_0 \cdot s^2} \quad \begin{array}{l} \text{(expressed in Newtons} \\ \text{in MKS units system)} \end{array}$$

where C stands for the wire capacity :

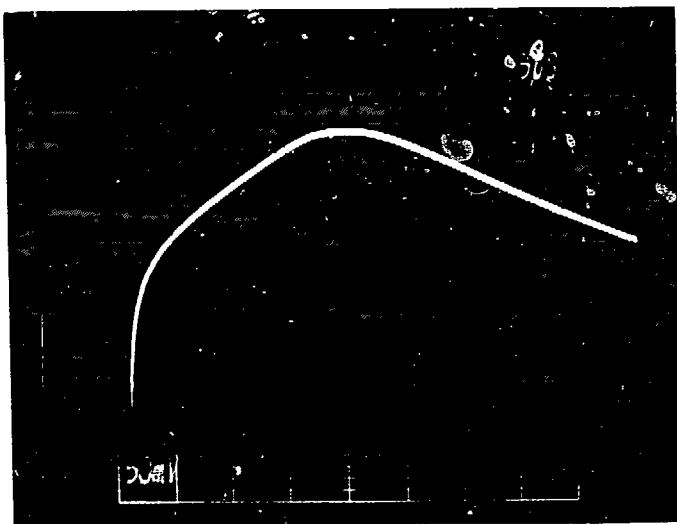


Figure 6. Single pulse from relativistic beta-electron as measured from the chamber C (1 mm wire spacing of 50 microm. diameter wires, 1.4 mm gap) at 3700 Volts in pure DME. Slow charge amplifier (ORTEC 109A) connected to the section of 8 sense wires. Electron and ion components are seen.

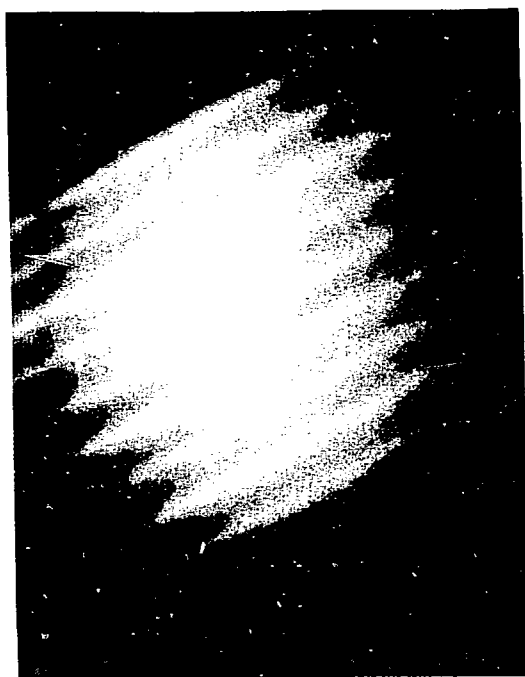


Figure 7. Skew pattern of discolorations of white color (due to inclined sense wires) on two aluminum foils from the chamber C after 1.2 Coulombs of charge was deposited locally. Gas: pure DME.

$$C = \frac{2\pi\epsilon_0}{\pi L/s - \ln(\pi d/s)}$$

V_0 is a working voltage, d is wire diameter, l , s and L are wire length, spacing and cathode to anode gap, respectively. ϵ_0 is the dielectric constant, for gases it is equal to about 8.85 pF/m. These formulae are obtained from a simple ideal model^{16,10} assuming that all the wires are at the beginning (at zero electric field) sitting perfectly placed in their theoretical equally spaced positions. On the other hand at a given mechanical tension T applied to the wires one may calculate in this model the maximum (critical) voltage U_0 still fulfilling the stability condition :

$$(2) \quad U_0 = \frac{(4\pi\epsilon_0 T_C)^{1/2} s}{C l}$$

But, as was pointed out by Alekseev et al¹⁷, in a much more realistic next approximation of the practical situation with one of the wires mounted with an original error dy out of the sense wire plane, the additional electrostatic deflection of this wire is non-zero even at low voltages. With the increasing bias voltage the wire increasingly bows out of the plane (Fig 8). To keep its maximum deflection in the middle below the maximum allowed value of y_{\max} , the mechanical tension of the wire must be higher than T_K , given by the formula:

$$(3) \quad T_K = \frac{T_C \pi^2}{4 \{\arccos(dy/y_{\max})\}^2} = k T_C$$

where y_{\max} is the maximum allowed deflection before problems listed above will occur, and T_C is expressed by the formula (1). For example if dy is equal to 50 micrometers and it is assumed that the maximum allowable additional electrostatic deflection is a further 50 micrometers, one finds k equal to $9/4 = 2.25$. This means that the actual mechanical tension on the wires should be more than twice the one obtained from the formula (1). However, even the improved formula cannot give an estimate when the troubles, like sparking, will start. That is why we decided to construct a test detector with 9 active 1 meter-long 50 micrometer wires spaced at 1.27 mm and placed between two flat aluminum bars at a distance of 1.6 mm from the sense wires' plane. No special care was taken to mount wires

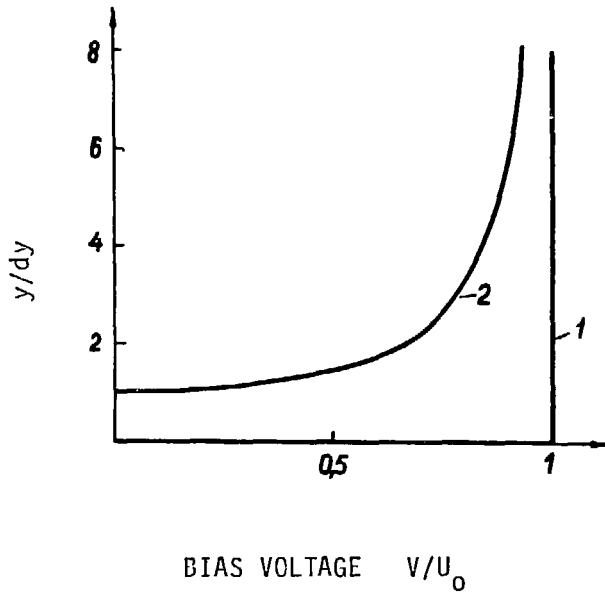


Figure 8. Dependence of the maximum deflection (in the middle of the wire) out of the sense wire plane on the bias voltage. Voltage is expressed in units of critical voltage U_0 . Deflection y is in dy units. Curve 1 is for the ideal case, as described in the text. Curve 2 is for the more realistic case of the wire mounted with an original error dy above the mean, geometrical sense wire plane.

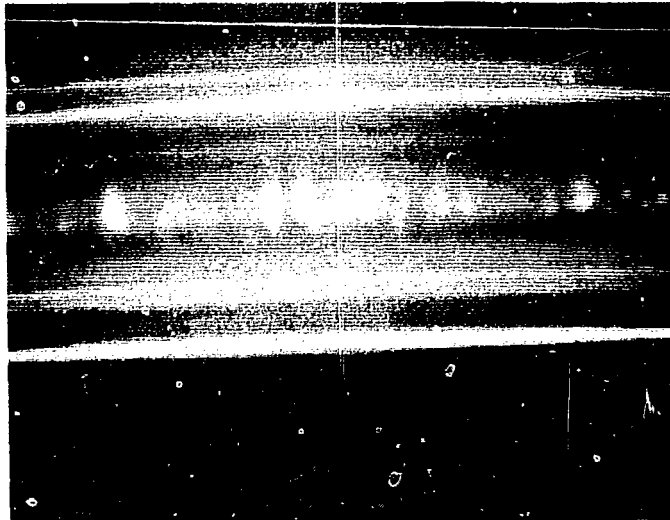


Figure 9. Picture of the pattern of displaced sense wires photographed in the middle of 70 cm-long 50 micrometers wires wired with 1.27 mm pitch, in the chamber with 1.6 mm gap. Gas: pure isobutane, bias voltage: 4000 Volts. Thick wire in the middle is the 250 micrometers diameter edge guard wire.

very precisely in order to simulate the realistic conditions of mass production. G-10 supports could be inserted to this chamber at any place along the wires and perpendicularly to them, to vary the active wire length from 1 m down. Through the mylar side window we could actually observe changes in transverse positions of the wires with a TV camera equipped with an amplifying zoom objective. The image was displayed on a TV screen and Polaroid pictures were taken.

As expected, it was quickly found that 1 meter long wires without a support will not be stable at working voltages required when filled with pure isobutane or DME even when mechanical stretching tension of 400 grams was applied to each wire. By cut-and-try we found that at 70 cm wire length the chamber was still quiet though the wires were substantially deflected. Effects observed when increasing slowly the bias voltage were in fact a combination of two different behaviours. In the first phase some of the wires were seen slightly out of geometry plane with the deflection increasing slowly with the bias voltage. Then at about 3725 Volts (with isobutane) a discontinuous transition was taking place with some more wires popping out and all of them rearranging their positions with apparently every second placed on the other side of the mean geometry plane, as predicted in the simple model^{16,10}. From this point there was a continuous and smooth increase in deflections of all the wires with increasing bias voltage. Finally at about 4100 Volts the sparking and vibrations initiated by sparking could be seen. The explanation of these vibrations is in the modification of the wire potential after each discharge and in the accompanying sudden change of electrostatic repulsions and attractions between different electrodes (wire to wire and wire to cathode). During these "sparking tests" none of the wires was broken and we confirmed the additional advantage of mechanical durability of thick wires. We checked that at the maximum stable working voltages of above 4000 Volts the multiplication factor in pure isobutane was higher than necessary to operate the chamber efficiently. In figure 9 the pattern of displaced wires is seen at the bias voltage of 4000 Volts. The thick wire in the middle with irregular surface structure is the last wire in the section of edge wires and is the closest to the TV camera. The camera was placed in the middle of the 70 cm-long wires where the displacement is maximal. The size of this 250 micrometers diameter wire defines the scale of the picture and we could estimate the displacement of some of the wires out of the middle plane to be as much as 0.4 mm. This amounts to 25% of 1.6 mm gap thickness, and nevertheless, the chamber was not discharging. This illustrates the point made earlier, that multiwire chambers can work acceptably even with wires substantially displaced by electrostatic forces. Of course in the real case we do not want to work with pure isobutane but the above conclusions on stability will still hold. From this short test one can draw a conclusion that thin gap

chambers with long 50 micrometers wires can be easily built provided support lines are used every, say, 50 cm (depending on the mechanical tension).

8. Summary and discussion.

Thin-gap chambers filled with isobutane/methylal or pure DME can operate safely at high rates, without intensity induced sparking and with relatively small ageing problems. With these strongly quenching gases, the electric field in a drift field region is stronger than when regular MWPC gas mixtures are used and positive ions reach cathodes in a shorter time, which leads to an improved high-rate operation. For a given gas the drift field is stronger in a chamber with thick wires. Full discussion of results and advantages of the new, thick-wire detector will be presented elsewhere¹. Here we will focus ourselves on the problems of radiation damage and stability of operation. The results of this brief pilot study do not permit one to draw a final conclusion where the realistic upper limit of the thin-gap detector operation lies and at which point damage will occur that would prevent proper functioning. With reasonable precautions a detector with clean seals and, for example, copper cathodes can operate with isobutane/methylal or DME up to charge deposits of at least 1 Coulomb per 1 cm of wire. We expect from these measurements that the actual limit is much higher but even this limit is good enough to consider application of this detector in a high intensity beam. For example, for a 2 x 1.4 mm thick MWPC working with a charge multiplication factor of 10^5 , each minimum ionizing particle will produce 1 pC of charge. This means that for each 10^{12} particles about 1 Coulomb of charge will be deposited in the chamber. This in turn can be translated to 10^5 beam spills of 10^7 particles/spill, which is close to 100 days of continuous 24 hours-a-day operation at Fermilab. In addition, we can conclude that the detector survives heavy current overloads without discharging and can be used in an environment with short-in-time heavy particle loads (spikes). Thin, large surface high-rate radiation-hard detectors are feasible because it is easy to support 50 micrometers wires with support lines, as is done on a large scale with the previous generation of this type of detector, used in the hadronic calorimeter in the flux return plug of OPAL⁶. Dimethylether seems to be the best choice for the working gas, though there were reports of contamination by Freon 11¹⁸, but it should be a solvable problem. However, it can turn out to be more practical, and less expensive to operate thin chambers with isobutane/methylal and also maybe with some third admixture like CO₂. Furthermore, some continuous cleaning of a gas takes place during bubbling through a cold methylal bath. Certainly more measurements of this promising detector are needed and we plan, among other things, to perform ageing tests with the same and new gases, this time with a full control of all parameters.

Acknowledgements.

I would like to thank all my colleagues and friends at Fermilab who helped me to arrange the ageing tests. My special thanks go to David Christian who provided the multiwire chamber, which was so masterly wired with thick wires and mounted by Frank Juravic. It is also David Christian who had an idea of modifying the standard Fermilab beam chamber. Also many thanks to Stephen Pordes and Vicky Frohne for providing me with few Fermilab beam chambers. Bill Cooper of E605 was extremely helpful in setting up the test stand.

Finally I would like to thank Jaroslav (Jerry) Va'Vra from SLAC for guiding my attention to DME gas as a best-guess non-ageing medium.

List of references.

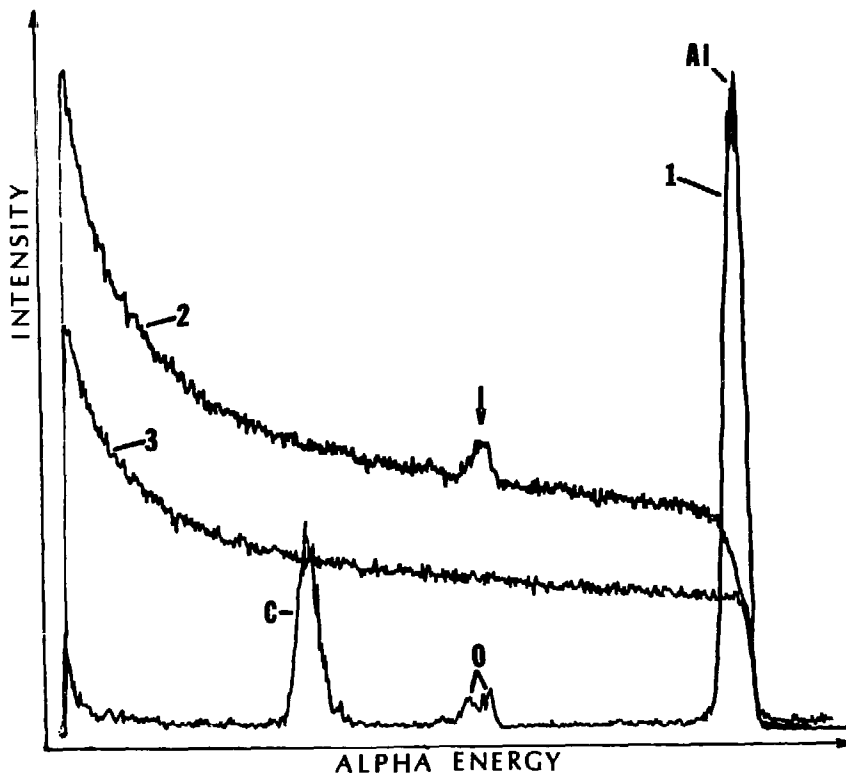
1. S.Majewski, Preliminary Results of the Study on the High-Rate Radiation-Hard Multiwire Chambers, in preparation.
2. A.H.Walenta, Nucl.Instrum.Meth.217(1983)65-76.
3. J.Fisher,A.Hrisoho,V.Radeka and P.Rehak, Nucl.Instrum.Meth. in Phys.Res.A238(1985)249-264.
4. S.Majewski and G.Charpak, A Thin Multiwire Chamber Operating in Saturated and Limited Streamer Modes - Preliminary Results, CERN EP Internal Report 82-02 (1982).
5. S.Majewski,G.Charpak,A.Breskin and G.Mikenberg,Nucl.Instrum.Meth.217(1983)265-271.
6. G.Mikenberg et al,Development of Calorimeters using Thin Chambers Operating in a High-Gain Mode, presented at the 1986 Wire Chamber Conference, Vienna, 25-28 February 1986.
7. H.Fenker, A Standard Beam PWC for Fermilab, Fermilab publication TM-1179, February 1983.
8. J.Va'Vra, Summary Talk, this Workshop.
9. M.Atac, Fermilab, private communication.
10. F.Sauli, Principles of Operation of Multiwire Proportional and Drift Chambers, CERN Report CERN 77-09, May 1977.
11. D.Friedrich and F.Sauli, Polymerization Properties of Ethane in Multiwire Proportional Chambers, CERN EP Internal Report 77-10, August 1977.
12. P.Le Du, P.Borgeaud,G.Burgun, R.Hammarstrom, R.Lorenzi and A.Michelini, Experimental Study of High Flux in Multiwire Proportional Chambers, CERN EP Internal Report 77-11, August 1977.
13. H.Nelson, Lifetime Tests on MAC Vertex Chamber, this Workshop.
14. F.Villa, Nucl.Instrum.Meth.217(1983)273.
15. M.Basile et al, Nucl.Instrum.Meth.in Phys.Res.A239(1985) 497-505.
16. T.Trippe, Minimum Tension Requirements for Charpak Chamber Wires, CERN NP Internal Report 69-18 ,June 1969.
17. G.D.Alekseev, N.A.Kalinina,W.W.Kruglov and D.M.Hazins, On the Accuracy of the Space Location and Tension of Wire Electrodes in Proportional Chambers,Probl.Techn.Exp.(Soviet) No.4(1978)47-50 (in Russian).
18. J.Kadyk, Some Results from Anode Wire Aging Tests, this Workshop.

Added in proof

The measurement with the backward scattering (170 deg) of the 2 MeV alpha particles from the aluminum foil with deposits of white color (obtained with DME gas, figure 7), has shown the presence of Oxygen in the surface layer (figure below). Three energy spectra of the scattered alphas measured with the silicon detector are:

- 1 - the calibration spectrum measured with the very thin carbon foil with vacuum deposited thin aluminum layer. Aluminum, Carbon and Oxygen peaks are seen. Oxygen peak is in fact a double peak from two oxide layers: on carbon and on aluminum ,
- 2 - the energy spectrum of backscattered alphas from the sample of the aluminum foil with the whitish deposits produced in the ageing test with pure DME. The Oxygen peak is observed on the background from Aluminum. The Aluminum spectrum has a continuous shape because of the energy loss of alpha particles in the foil ,
- 3 - the reference spectrum obtained with the clean sample from the same cathode foil.

The measurement was performed with the alpha particles beam from the Van de Graaff accelerator of the University of Florida, in the group led by Professor Henri Van Rinsvelt.



PROPORTIONAL TUBE LIFETIMES (MAGIC GAS, A-CO₂, DME)

Gary Godfrey - Stanford Linear Accelerator Center

Crystal Ball

ABSTRACT

Tube chamber lifetimes were measured (% gain change/ coul per cm) for Magic Gas (800), HRS Gas (<100), and DME (<5). Magic Gas failed due to an anode wire deposit. The DME test was ended due to sustained current from a cathode deposit.

The Crystal Ball tagging chambers (Figure 1) were installed in DORIS in September 1982. These chambers were built of thin walled (.002 inch thick) aluminum tubes and were designed to operate in the limited streamer mode (Magic Gas - gain 10^8) in order to have large pulse heights for good charge division. Table 1 lists some of the chambers' properties for the tubes nearest the beam pipe. The chambers degraded rapidly due to a build up of material on the anode wires. Figure 2 is an electron micrograph of a wire from the degraded chamber (.2 coul/cm of accumulated charge).

A small single tube test chamber was made (Figure 3). A lifetime test with a Sr⁹⁰ beta source using Magic Gas confirmed the short chamber lifetime (Table 2). HRS gas A(89%) - CO₂(10%) - CH₄(1%) was then tested (Table 2) and gave an acceptably long lifetime. By June 1984 all the Crystal Ball chambers had been rebuilt and are now using A(79%) - CO₂(20%) - CH₄(1%). This gas is being run at a substantially lower gain $\leq 10^6$. So far no effect on the chambers' operation has been seen for an accumulated charge of .05 coul/cm (Table 1).

Finally, dimethylether (DME) was tried in the same single tube test chamber. The gain curve (Figure 4) was measured for an Fe⁵⁵ source and for a single electron. The single electron curve was obtained by drilling a 1 mm diameter

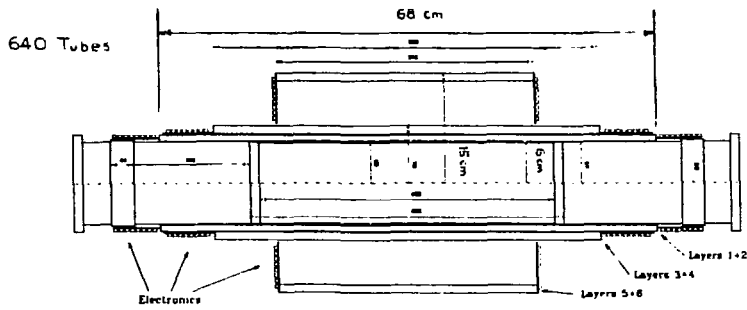


Figure 1: Crystal Ball chambers installed in DORIS 1982-83.

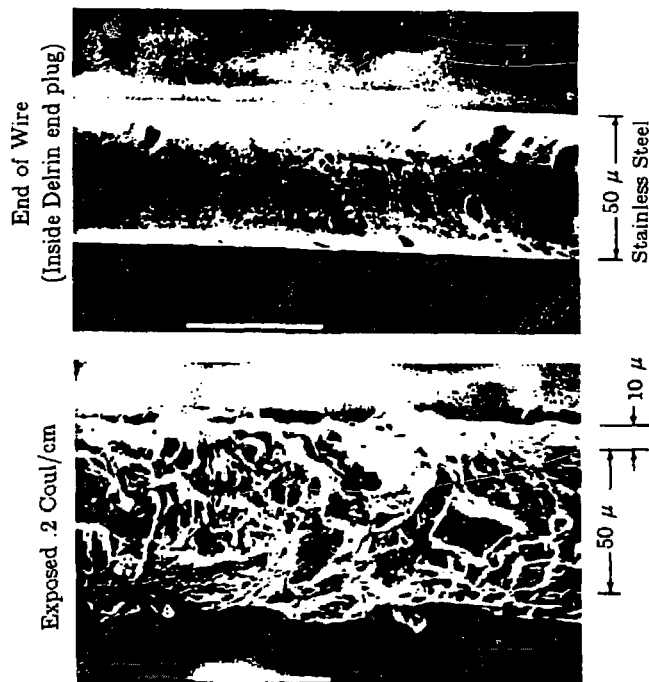


Figure 2: Electron micrograph of a wire from the Crystal Ball chambers (Magic Gas) after an accumulated exposure of .2 coul/cm.

Table 1. Lifetime results of Crystal Ball chambers at DORIS

Gas (1 atm absolute)	Magic: A(66%) <i>Isobutane</i> (30%) <i>Methylal</i> (4%) <i>Freon13B1</i> (.25%)	A(79%) <i>CO</i> ₂ (20%) <i>CH</i> ₄ (1%)
Anode wire diameter	50 μ	50 μ
(stainless steel)		
Cathode tube inner diameter	6 mm	6 mm
HV	2150 volts	1800 volts
Gain	10^8	$\leq 10^6$
Wire length irradiated	68 cm	62 cm
I_{wire}	1-2 μamp	.1 μamp
t_{run}	10^7 sec	3×10^7 sec
$Q_{accumulated}$.2 coul/cm	.05 coul/cm
Post mortem	Lost 150 v plateau 10 μ anode deposit	No changes seen

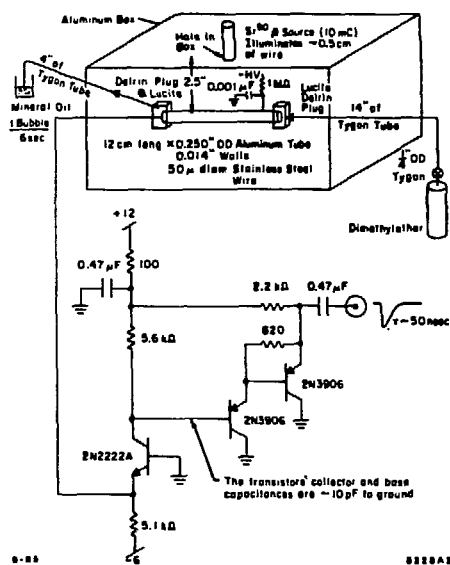


Figure 3: Single tube chamber used for lifetime tests.

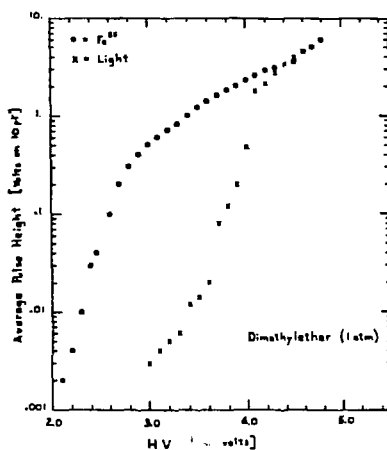


Figure 4: Gain curve for DME for both an Fe^{55} source and a single electron (generated by a flashlight).

Table 2. Lifetime results of test chamber

Gas (1 atm absolute)	Magic:A(66%) <i>Isobutane</i> (30%) <i>Methylal</i> (4%) <i>Freon13B1</i> (.25%)	HRS:A(89%) <i>CO</i> ₂ (10%) <i>CH</i> ₃ (1%)	DME
Anode diameter (stainless steel)	50 μ	50 μ	50 μ
Cathode inner diam	6 mm	6 mm	6 mm
HV	2250 volts	1700 volts	4300 volts
Gain	10^8	$\leq 10^6$	10^8
Irradiated length	1 cm	1 cm	1 cm
<i>I</i> _{wire}	.6 μ amp	.1 μ amp	2 μ amp
<i>t</i> _{run}	10^5 sec	10^6 sec	10^6 sec
<i>Q</i> _{accumulated}	.06 coul/cm	.1 coul/cm	2 coul/cm
% gain change/ coul per cm	800	<100	<5
Post mortem	Pulse height 1/2 in central 1cm of wire where irradiated.	No change.	Cathode deposit. Pulse height and current unchanged.

hole in the aluminum tube, covering it with scotch tape, and illuminating the hole with a flashlight. Presumably the single electrons came from the aluminum acting as a photocathode. It is interesting to note that the flashlight on the hole initially caused just a few electrons/sec. After a few minutes the aluminum became sensitized by several orders of magnitude, and the room lights had to be turned off to decrease the $1 \mu\text{amp}$ chamber current. This sensitization went away after about 10 minutes of darkness with no current being drawn. The properties of the DME lifetime test are listed in Table 2. After 2 coul/cm the chamber began to draw a sustained current with the source (and light) absent. This suggested the Malter effect due to an insulating deposit on the cathode wall of the tube. Replacing the anode wire with a new wire did not repair the chamber. A slightly darkened area could be seen on the inner wall of the tube where it was illuminated by the source. Washing out this deposit with ethanol succeeded in repairing the chamber.

In summary, the following lifetimes (% gain change/(coul/cm)) were measured: Magic Gas (800), HRS Gas (<100), DME (<5).

REVIEW OF WIRE CHAMBER AGING*

J. VA'VRA

*Stanford Linear Accelerator Center
Stanford University, Stanford, California 94305*

Abstract

This paper makes an overview of the wire chamber aging problems as a function of various chamber design parameters. It emphasizes the chemistry point of view and many examples are drawn from the plasma chemistry field as a guidance for a possible effort in the wire chamber field. The paper emphasizes the necessity of variable tuning, the importance of purity of the wire chamber environment, as well as it provides a practical list of presently known recommendations. In addition, several models of the wire chamber aging are qualitatively discussed. The paper is based on a summary talk given at the Wire Chamber Aging Workshop held at *LBL*, Berkeley on January 16-17, 1986. Presented also at Wire Chamber Conference, Vienna, February 25-28, 1986.

1. Introduction

The wire chamber aging problem is clearly very complex. A few years ago it seemed that it would never yield to rational analysis. The main difficulty was that each experiment or test had very specific conditions and it was very difficult to extrapolate given information to other circumstances. This is still basically true, but nevertheless, it appears that a pattern is emerging and one might even be able to draw some qualitative conclusions. However, a true quantitative understanding of the polymerization process and its control is a long way off. For that we would have to know:

- (a) All cross-sections for collisions of electrons and photons with all species involved, *i.e.* atoms, ions, molecules, radicals, ionized radicals, *etc.*
- (b) All cross-sections for atom-atom, atom-molecule, atom-radical, radical-radical interactions, *i.e.*, the probabilities for all chemical processes involved.
- (c) All this as a function of electron and photon energy, pressure, temperature, flow rate, chamber design, extremely high electric field ($\sim 200\text{--}300\text{ kV/cm.atm}$), *etc.*

Before we can start writing a complex Monte Carlo program simulating the avalanche and its polymerizing effects, we had better know all these parameters. Realizing these difficulties, it might be beneficial to learn as much as possible about the polymerization process from other branches of science. In fact, there does exist a branch of chemistry, called plasma chemistry, which deals empirically with the problem of plasma polymerization and polymer etching. Clearly, we should learn as much as possible about its methods and insights.

* Work supported by the Department of Energy, contract DE-AC03-76SF00515.

In the traditional polymerization process in chemistry, a necessary prerequisite to form polymers is to start with molecules containing double bonds between two carbon atoms. However, the polymerization in the plasma environment is much more complex.^[1,2] Although the process is complex, it is not hopelessly random or unstable, *i.e.*, one can tune the variables.

In this talk I will concentrate on the following subjects.

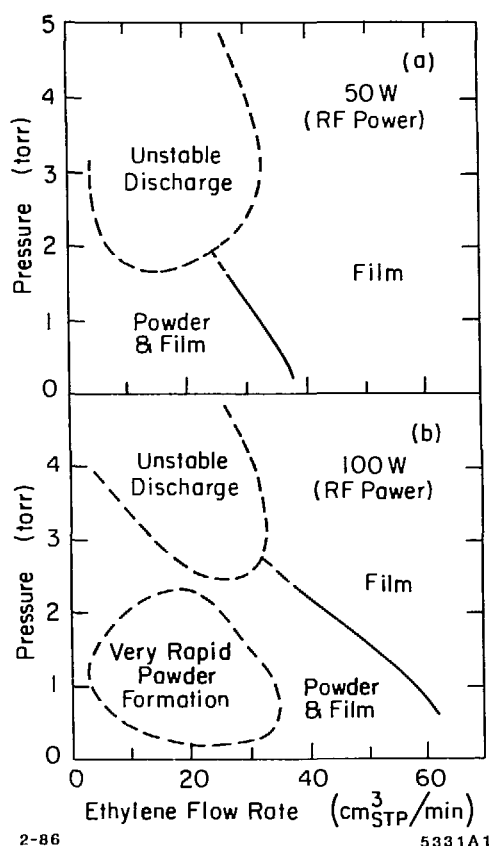
1. The importance of tuning variables.
2. A naive model of electrode coating.
3. Are present plasma chemistry studies in the same range of some basic parameters as we have in our avalanches?
4. Some of the design parameters for building chambers. Is anything known about their effect on aging?
5. Tests of aging in small accelerated tests.
6. A "cook book" of hints and suggestions.

2. Importance of Tuning of Variables

Plasma chemistry is a branch of science which deals with very complex reactions on a qualitative level of understanding and basically tunes a multi-variable process empirically. Typical variables are the choice of polymerizing gas, pressure, gas flow, *rf*-power density, impurity content, *etc.*, (*i.e.*, the variables which we typically also have to control). A typical example of such empirical tuning is shown in Fig. 1, the plasma polymerization of ethylene under various conditions. One can create film, powder or oil depending on operating conditions. Both the powder and the film are insoluble in common organic solvents, indicating a high degree of cross-linking of molecular chains. The oily products, on the other hand, are soluble in both acetone and xylene. (The possible structure of the molecular chains generated in a plasma condition can be seen on Fig. 2.)

These observations are not dissimilar to what many people have observed in our field, with one basic exception. In our field (wire chambers) we tend to choose the operating conditions rather arbitrarily from the aging point of view. In fact, one should always tune the additives level, the gas flow, the gain on the wires, tolerable level of impurities, *etc.* To illustrate this we cite as an example adding 1% of hydrogen to a gas mixture to improve aging. First of all, 1% is completely arbitrary. What we have to do is to tune the hydrogen content for the gas mixture, gain, gas flow, *etc.* If we change any of these variables we have to retune the hydrogen content. In comparison, the detailed understanding of the anatomy of the polymerized chains (Fig. 2) is perhaps not that important and should be left to specialists.

Fig. 1. Examples from plasma chemistry. Polymerization of ethylene and importance of tuning power, pressure and gas flow on a final appearance of polymerized species.^[51]



3. Naive Model of Electrode Coating

The avalanche can clearly produce a large variety of molecular species. However, as one can see in Table 1, to break a typical covalent molecular bond takes some 2–5 times less energy than to ionize the same molecule. When an electron or photon breaks a covalent bond, a radical molecule is formed. Such a molecule has no net electrical charge, but it typically has a large dipole moment, because it is frequently distorted. Because of a very high electric field near the anode, these radical molecules will be attracted towards the anode surface. They are chemically very active and will either recombine back to original molecules or form new molecular species.^[1,2] The concentration of these radicals in a typical avalanche is not known. To get a true distribution, the analysis of dissociated molecules would have to be done immediately during and inside the avalanche (of course, impossible). If we do it outside the chamber, many radicals are probably recombined by then. However, under plasma chemistry conditions, the typical concentrations of free radicals in the plasma is usually 5–6 orders of magnitude higher than that of ions.^[3]

We will make a simplifying working assumption, that the polymerization rate is proportional to the density of radical molecules. The density of radicals is in turn proportional to the density of electrons (and photons) in the avalanche and their energy distribution.

Unfortunately, we do not know how to calculate the density of electrons and their

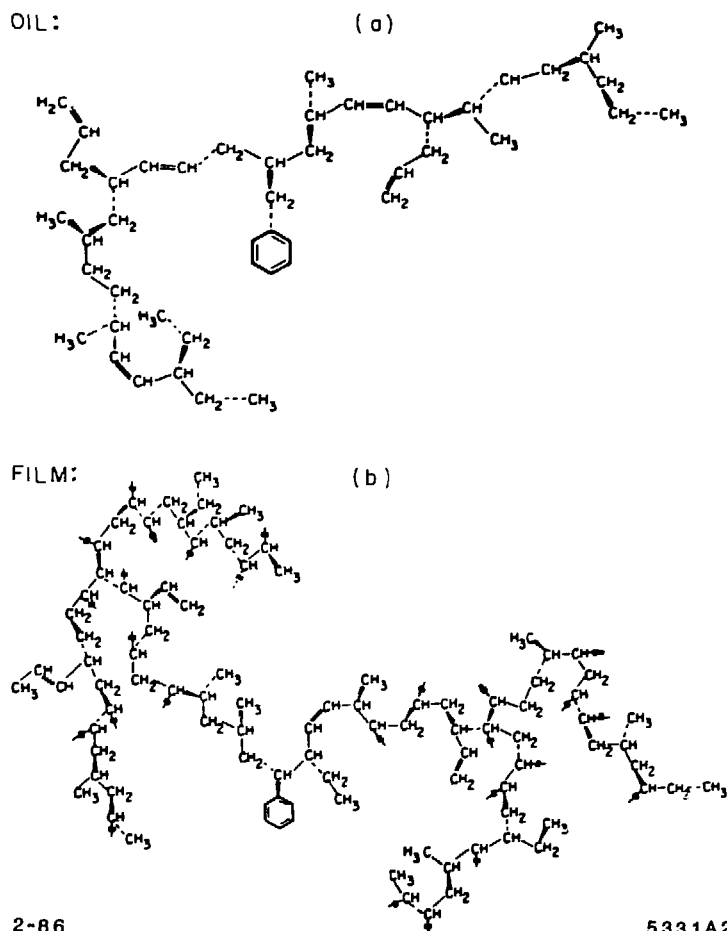


Fig. 2. A predicted structure of polyethylene produced in the plasma environment: a) oily product, b) film coating.^[52]

energy distribution. Recently, there has been an attempt to simulate an avalanche in Argon only^[4] The authors considered electron-Argon elastic, excitation and ionization cross-sections with a proper electron motion between the collisions and a proper treatment of energy balance and direction change after each collision. However, they neglected the photon emission, the photo-ionization processes and the effect of space charge within the avalanche. Nevertheless, as one can see in Fig. 3, they solved the problem in three dimensions and they predicted the electron density and energy distribution. We will use these predictions in the next section.

Figure 4 shows schematically a formation of polymers on the anode surface as caused by a large concentration of free radicals. Initially the polymer is held to the surface very weakly unless some additional chemical reaction takes place between the polymer atoms and atoms of the material of the wire, or unless the polymer completely surrounds the anode surface. That would mean that the polymers or free radicals can be blown away from the anode surface by a large gas flow. If a large polymerized macroscopic piece

TABLE 1 [74]

(1) Bond Energies of Typical Covalent Bonds:

$C - H$	4.3 eV	$C = C$	6.4 eV
$C - C$	3.6	$C = N$	9.3
$C - O$	3.7	$C = O$	7.8
$C - N$	3.2	$N \equiv N$	9.7
$N - H$	4.0	$C \equiv C$	8.6
$O - H$	4.8	$\left[CO_2 \rightleftharpoons O = C = O \right]$ is very stable	
$O - O$	1.5		
$F - H$	5.8		
$F - C$	5.4		
$C - Cl$	3.5		

(2) Dissociation Energy and Ionization Energy for Some Gases:

	<u>Dissociation Energy</u>	<u>Ionization Energy</u>
Ar	—	15.8 eV
Xe	—	12.1
H_2	4.5 eV	15.6
N_2	9.7	15.5
O_2	5.1	12.5
Ethanol	≥ 3.2	10.5
Iso-Propanol	≥ 3.2	10.2
DME	≥ 3.2	9.98
C_2H_6	≥ 3.6	11.5
H_2O Vapor	4.8	12.6
Methylal	≥ 3.2	10.0
CO_2	7.8	13.8
Iso-Buthane	≥ 3.2	10.6
CH_4	4.3	12.6

receives a positive charge in a subsequent avalanche, it will slowly drift toward the cathode (it is heavy). Again a large gas flow can successfully, according to this naive picture, prevent coating of the cathode. As F. Sauli^[5] pointed out, the deposit layer on the anode probably tends to carbonize under a heavy electron bombardment (he has always found only conductive black anode deposits).

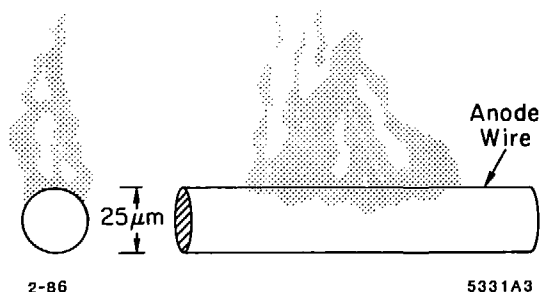


Fig. 3. Monte Carlo prediction of avalanche formation in pure argon.^[4]

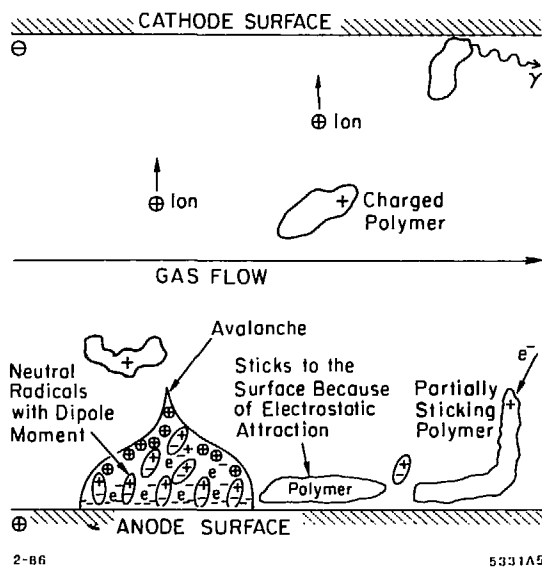


Fig. 4. A naive model of formation of polymers out of free radicals on the anode surface and an effect of gas flow on heavy positively charged species slowly drifting towards the cathode.

S. Majewski^[6] pointed out that a typical “wire pattern” image of deposits frequently found on the cathode foil^[5,6,40] is an important message any model should be able to explain. Because we argue that mainly very large molecules peel off and drift toward the cathode, we expect that the most likely flow direction will be perpendicular towards the cathode and therefore the cathode deposits will show the “wire pattern” structure.

There are, of course, a variety of other processes which could contribute to aging—see Table 2 for a summary. Notice, for instance, that above ~ 10 kV/cm one can multiply the number of electrons near the cathode surface (gain). CO_2 mixtures are known for carbon build-up, which occurs specifically at the cathode.^[33] We should mention the Malter effect^[31] which is an emission of electrons and occurs after the cathode has been coated by a thicker insulating film (oxides, polymer deposits, fingerprints^[5]). Finally, it appears that extremely thin cathode deposits or oxides can be very photosensitive,^[5,21,31,46,67] presumably due to lowering of electron work function, allowing even very low energetic photons to liberate electrons from the cathode. This may occur because the extremely thin layers of deposits or oxides may have electric dipole moment which helps to “pull” the electrons

from the metal.^[64] Clearly, if this happens, the chamber can deteriorate very quickly because of electron emission at the cathode and a subsequent positive feedback between this effect and the anode amplification. But we still believe that the primary process is polymer building at the anode according to the previously mentioned naive model.

We should also mention that the polymerization can be “primed” by a previous exposure of the wires to an atmosphere containing tiny droplets of oil and silicon dust. H. Hilke mentioned results of Christy^[65], who demonstrated that even 10^{-6} ppm (not a mistake) of silicon oil vapor can cause significant aging. These oil molecules get attached to the wires presumably due to their dipole moments. The details of manufacturing wires should also be closely examined,^[59] as well as gas processing procedures.

4. Is Plasma Chemistry in the Same Range as Some Basic Parameters We Have in Our Avalanches?

As we said there is considerable experience in plasma chemistry with the polymerization problem. The question is, are we operating in the same regime of variables? Table 3 shows this comparison, assuming anode diameters of $20 - 50 \mu\text{m}$, pressure of 1 atm, mean free path between the electron collisions, $\lambda \sim 1 \mu\text{m}$, mean free time between the collisions^[7] $\tau \sim 1$ psec, an average electron energy of about 5 eV and an effective volume according to naive pictures as shown in Fig. 5. We conclude that many parameters in the two fields are rather different. Nevertheless, in the absence of better information, we will continue to quote many examples from plasma chemistry and we will see that many are in agreement with what is observed in wire chambers.

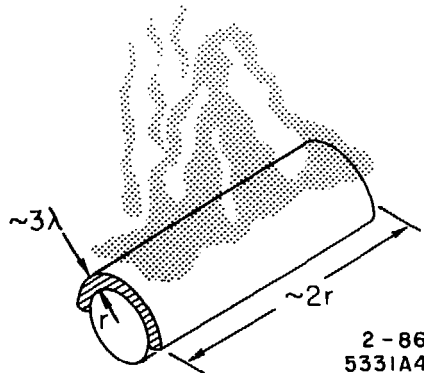


Fig. 5. A naive assumption about the avalanche effective volume needed to predict approximately effective volume of avalanche in Table 3.

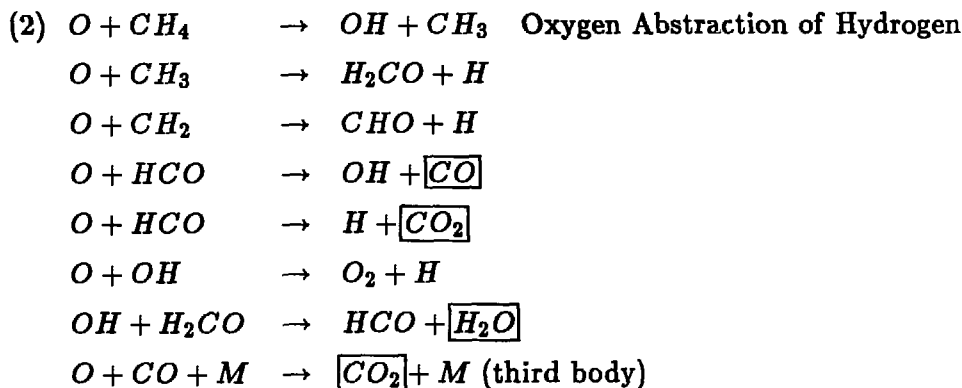
5. The Design Parameters for Building Chambers and Their Effect on Chamber Aging

In this section we will make a survey of what is known about the correlation between aging and chamber design parameters such as: gas [type (resistant or susceptible to

TABLE 3
Comparison of Basic Operating Conditions

Parameter	Plasma Chemistry [1]	Wire Chambers
Average Electron Energy	1 – 10 eV	5 – 10 eV (Ar)
Effective Volume	100 – 1000 cm ³	10 ⁻¹⁰ – 10 ⁻⁸ cm ³
Typical Electron Density	10 ⁹ – 10 ¹² e/cm ³	10 ¹⁴ – 10 ¹⁷ e/cm ³ /avalanche
Typical Power Density	0.01 – 10 watts/cm ³	10 ⁸ – 10 ¹² watts/cm ³ /avalanche
Gas Pressure	0.01 – 10 Torr	≥ 760 Torr
E/p	10 – 50 V/cm·Torr	100 – 400 V/cm·Torr (on the surface of the anode)
Type of Electric Field	RF	DC
Typical Gas Flow	~ 1 Gas Volume/1-10 minutes	~ 1 Gas Volume/1-8 hours

TABLE 4
 CH_4 Gas in Oxygen Plasma [70]



polymerization), impurities (undesirable), additives (desirable), flow rate, pressure, tubing material and temperature]; anode and cathode wire material; cathode type (wire versus continuous); electric field on anode and cathode surface; anode-cathode distance; chamber body material; glues and adhesives; and gain on the anode wires.

However, the most important variables probably are (apart from the gases):

- (a) effective volume of the avalanche (cm^3),
- (b) average electron and photon energy in the avalanche (eV), and
- (c) average electron and photon density ($\#/\text{cm}^3$).

All three variables then define the average power density (Watts/cm^3). These are the important variables because they control the density of the radicals, which according to our naive model, controls the rate of polymerization. Unfortunately, unlike in the plasma chemistry investigations, we really do not know how to calculate these basic variables and this probably contributes to our general confusion.

Before we start discussing good additives and bad impurities, we will review the electronegativity concept. In a bond between two atoms, the electron will be attracted more

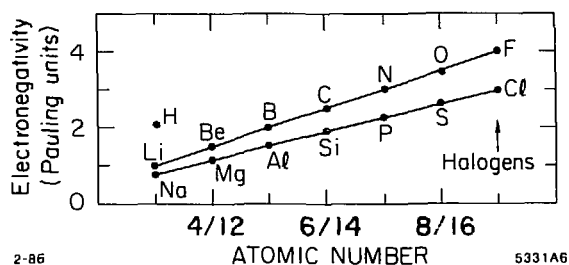


Fig. 6. Relative electronegativity of some of the more common elements.

strongly to the atom with larger electronegativity (or electron pulling power). As one can see in Fig. 6 the most electronegative atoms are halogens, however, oxygen is immediately behind fluorine in its reactivity. Notice also that carbon is similar in electronegativity to silicon. Figure 7 shows the fluorine atom has one missing electron in the valence shell and oxygen has two empty slots. As a result, the fluorine atom can make only a single bond, which as we can see in Table 1 is strong, but not as strong

as double bonds (two pairs of electrons in the covalent bond) which can be made, for instance, in oxygen reactions. This allows oxygen to make stronger species in the plasma reactions which will tend to terminate polymerization because the density of radicals is reduced. Silicon and carbon have similar valence shells (see Fig. 8) the only difference being that the silicon atom is heavier and its molecules are less volatile.

5.1 GOOD ADDITIVES

We will now discuss examples of additives which are believed to prolong chamber life.

5.1.1 Good additives – Oxygen

It is a well known fact in plasma chemistry that atomic oxygen O reacts with hydrocarbon radicals and it is generally found that the end products are CO, CO₂, H₂O and H₂. As we said earlier they are more stable molecules and they are volatile and can be blown away by a sufficient gas flow. In addition, the rate of removal of organic polymeric

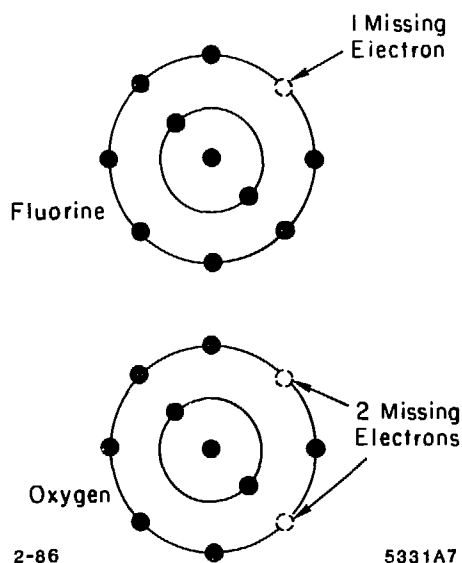


Fig. 7. A valence shell structure of fluorine and oxygen.

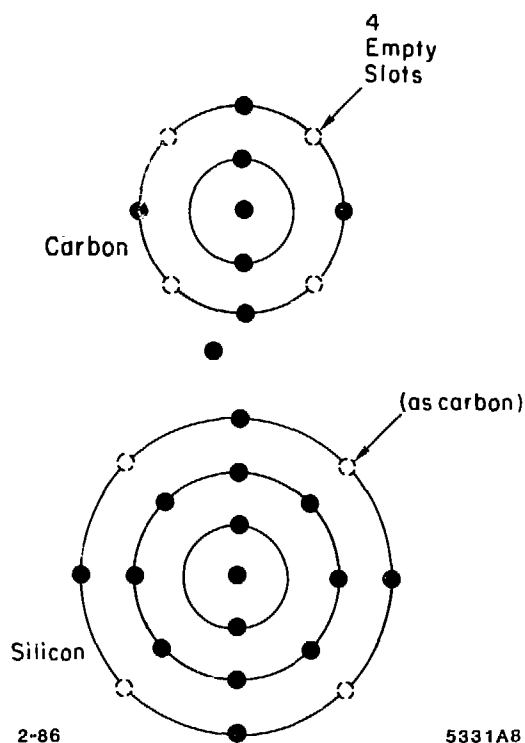


Fig. 8. A valence shell structure of carbon and silicon.

material can often be increased in an oxygen plasma by the addition^[9] of H_2O , H_2 , N_2 , NO , N_2O . These are empirical facts supported by qualitative models. Table 4 shows an example of such chain of reactions. The input is CH_4 gas and its radicals CH_3 , CH_2 , and the atomic oxygen produced in the plasma either from O_2 or from a molecule containing oxygen. Another example from plasma chemistry is the cleaning of contaminating films from mirrors in an oxygen plasma.^[8]

Yasuda^[13] in fact argues that in plasma chemistry most organic compounds with oxygen containing groups such as $-\text{COOH}$, $-\text{CO}-$, $-\text{OCO}-$, $-\text{OH}$, $-\text{O}-$, $-\text{C}=\text{O}$ are generally reluctant to form polymers in the plasma environment. This is not to say that it cannot happen. For instance $\text{CO} + \text{H}_2 + \text{N}_2$ in a discharge can form structures resembling proteins.^[14] Also, as we will see later, oxygen polymerizes with silicon to form various types of silicates (for instance a quartz).

In our field, I would like to mention two examples. The first one comes from the MARK II drift chamber,^[10] which ran for a year with 0.6% oxygen added to 50% Ar + 50% C_2H_6 gas. The oxygen is believed to stabilize the operation. The second example comes from Turala's talk,^[11] where he mentioned that excellent lifetimes were achieved with Ar + 8% N_2 mixture (~ 10 C/cm).

It is tempting to suggest that we can clean the wires if we simply run humid air in the chamber at large enough voltage so that there is a chance of producing atomic oxygen.

However, this may be practical only for chambers designed for high pressure operation, because typical feedthroughs would fail long before there was a gain on the wires. Another important point is that the gas flow has to be adequate, as one can see on Fig. 9, where nylon is removed in the oxygen plasma. Notice also that power is an important variable.

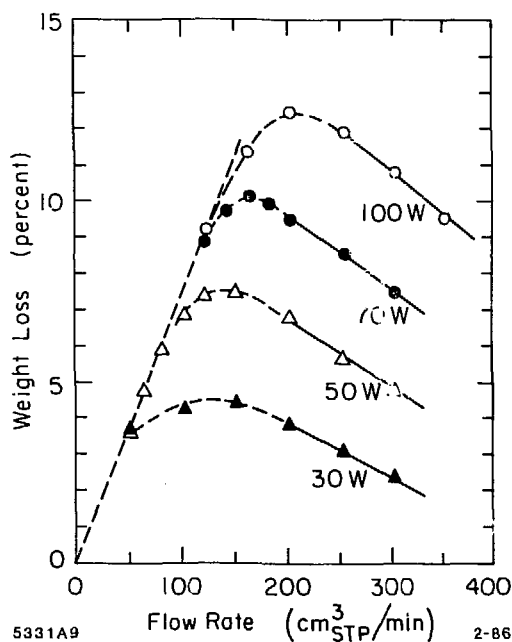
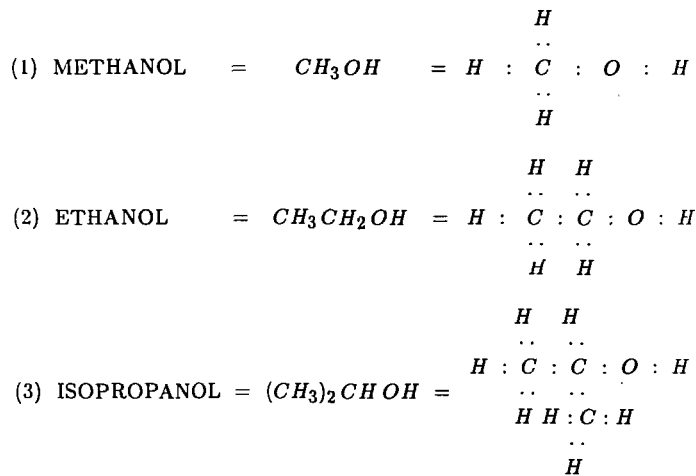
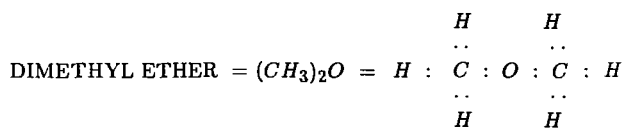


Fig. 9. Etching of nylon in an oxygen plasma under various conditions of flow rate and power in a plasma chemistry environment.^[71]

5.1.2 Good additives – H_2O , alcohols, ethers, methylal

There is more than one mechanism by which these additives help aging. Figure 10 and Table 5 show the molecular structure of these additives. As we can see they all have large dipole moment and as a result they tend to have large cross-sections for electron-molecule scattering, *i.e.*, the mean value of electron energy will get smaller in the avalanche, which is an important factor. As M. Atac pointed out a long time ago,^[12] they also have large cross-sections for absorption of *UV* photons. Because of the large dipole moment, these molecules will tend to concentrate near the anode and cathode surfaces. As we can see in Table 1, the ionization potential of these additives is lower than the ionization potential of typical hydrocarbon molecules (with the exception of water). Therefore, charge exchange is possible which will tend to protect the hydrocarbon molecule during its ionic neutralization at the cathode.^[5] Finally, if these molecules of the additives are broken, the electronegativity of oxygen will tend to repair them immediately, or, as we discussed in the previous section, the final oxygen products will tend to be volatile.

ALCOHOLS:**ETHERS:**

↑
DISSOCIATION ENERGY : 3.2 eV

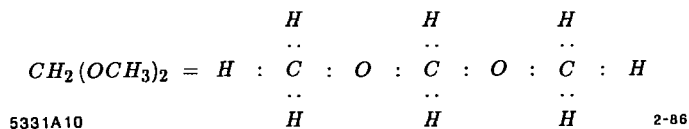
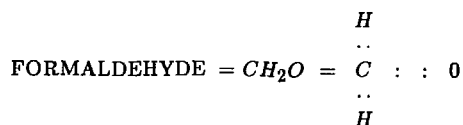
METHYLAL:

Fig. 10. A schematic molecular structure of some alcohols, dimethyl ether and methylal.



↑
DISSOCIATION ENERGY : 7.1 eV

(DIPOLE MOMENT : 2.8 D)

2-86
5331A11

Fig. 11. A schematic molecular structure of formaldehyde.

TABLE 5

Additive	Molecular Structure	Dipole Moment
Water	$H - O - H$	1.85 D *
Alcohols	$R - O - H$ ($R = CH_3, CH_3CH_2$, etc.)	1.66 – 1.7 D
Ethers	$R - O - R'$ (DME = $R = R' = CH_3$)	1.29 D
Methylal	$R - O - R' - O - R$ ($R = CH_3, R' = CH_2$)	

* D = Debye units

TABLE 6

Examples of Industrial Use of Halogens

Ethyl Chloride	CH_3CH_2Cl	Gasoline Production
Vinyl Chloride	$H_2C = CHCl$	Raincoat Production
Tetrachloroethylene	$Cl_2C = CCl_2$	Cleaning of Clothing
Tetrafluoroethylene	$F_2C = CF_2$	Teflon Production, Plasma Etching
Methylchloride	CH_3Cl	Paints and Varnish
Freon 11	$CFCl_3$	Refrigerant
Freon 12	CF_2Cl_2	Refrigerant
Freon 13-B1	CF_3Br	

Nevertheless, these molecules are fragile. For instance, the dimethyl ether molecule can be destroyed with only 3.2 eV! One can destroy these additive molecules successively to produce, for instance, formaldehyde (see Fig. 11) which can easily polymerize to produce paraformaldehyde $(\text{CH}_2\text{O})_n$. But still, the rate of this process tends to be lower than the polymerization rate of ordinary hydrocarbon molecules and therefore the addition of H_2O , alcohols, dimethylether, and methylal can be considered beneficial. As one can see in Table 10 (under "Conclusions") many of the experiments which reached at least 0.1 C/cm radiation dose, are using one or a combination of these additives. In addition, alcohols, DME, and methylal are used in many tests and experiments currently underway.^[27,48,54] (see also Table 11).

Water may have an additional value, *i.e.*, it tends to increase conductivity of deposits which are otherwise poorly conductive and as a result will prolong chamber lifetime.^[15,16,17,18,43,45,50,53]

5.1.3 Good additives – Hydrogen

It is believed that the addition of hydrogen would help to restore radicals to their original molecular form. For instance CH_2 radicals would get restored to CH_4 . The final outcome of this operation will depend on the competition of the polymerization rate of radicals with the rate of restoring them to the original molecular form by the hydrogen. As we said earlier, one should tune this balance. Because this is not generally done in our field, results of adding hydrogen are confusing. For instance, H. Sipilä and M. Järvinen^[19] have improved the life of a permanently sealed counter operating at very low gain (200) approximately twenty times by adding 0.1% H_2 to 90% Ar + 10% CH_4 . However, one should say that permanently sealed counters have very poor lifetimes nominally ($\sim 10^{-3}$ C/cm). Since 1983, H_2 has been used as an additive in commercial permanently sealed proportional counters to increase their lifetimes when hydrocarbons are used as a quenching gas.^[20] However, others tried hydrogen (usually 1%) and generally there was no observed improvement.^[18,21,22,23] Perhaps the problem is that tuning of hydrogen content was not attempted. The halogen impurities might also be a significant problem because they will react with the hydrogen in plasma and nullify its effect.

5.2 BAD IMPURITIES

In this section we will discuss several examples of undesirable impurities which generally accelerate chamber aging. An examination of analysis of deposits^[2,5,6,11,18,25,26,27,55,56] reveals that the *dominating* species usually found are carbon, carbon based polymers, silicon based species, halogen and sulphur elements,^[66] or their combination. It depends on a particular experimental setup whether a given element is found. For instance, F. Villa pointed out that most of the elements found on the wire could also be seen in the analysis of various materials used for building the chamber (delrin, O-rings, *etc.*).^[25]

5.2.1 Bad impurities – Halogens

Why should we worry about halogen contamination? Table 6 indicates that they are in widespread industrial use and therefore there is a good chance that our bottles have

been contaminated. This contamination level might be regionally dependent; in the San Francisco Bay Area it appears to be a problem.

As we discussed earlier the halogens are very reactive in the atomic form, because of their high electronegativity—see Fig. 6. In addition, they can form only single bonds (one electron pair), which are generally weaker than the double bonds. Finally, for instance C-Cl, and C-Br bonds are weaker than C-H bonds. Therefore, as we can see in Table 7 it takes more energy to dissociate, say CH_4 into free radicals than the halogenated hydrocarbons such as CF_2Cl_2 , CH_3Cl , $\text{C}_2\text{H}_3\text{Cl}$, $\text{C}_2\text{H}_3\text{F}$, *etc.* This would mean, according to our earlier naive model, some halogenated hydrocarbons create a higher density of free radicals in the plasma and will have a greater tendency to form polymers. This is in fact observed in plasma chemistry.^[24] Figure 12 shows that in the plasma chemistry environment a small addition of halogenated hydrocarbons can vastly increase the polymerization rate of CH_4 , C_2H_2 and C_2H_6 gases.

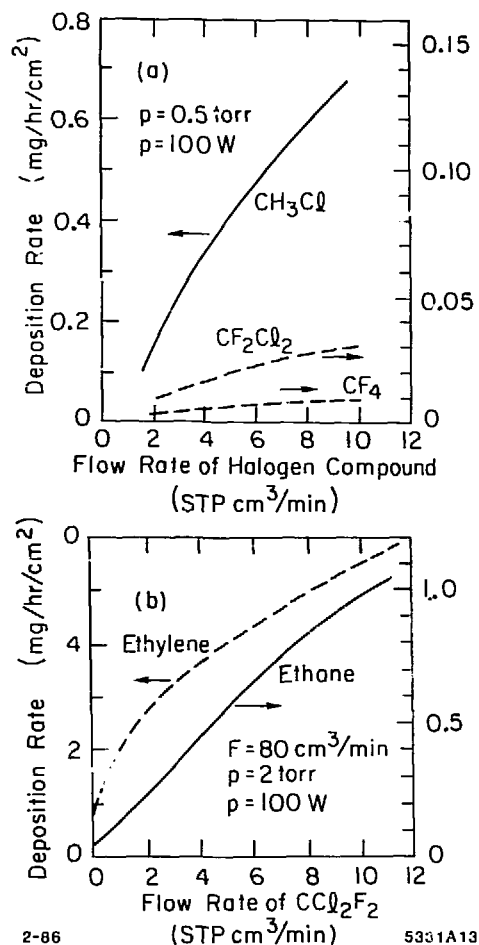


Fig. 12. An influence of halogens on the polymerization rate of methane, acetylene and ethane in a plasma chemistry environment.^[72]

TABLE 7

Energy Needed to Destroy Some Molecules [69]

(a)	$e^- + CH_4 \rightarrow CH_2 + H_2 + e^-$	4.6 eV
	$\rightarrow CH_3 + H + e^-$	4.5 eV
versus		
(b)	$e^- + CF_4 \rightarrow \boxed{CF_2} + F_2$	7.8 eV
	$e^- + CF_4 \rightarrow CF_3 + F$	5.2 eV
	$e^- + CF_2Cl_2 \rightarrow \boxed{CF_2} + Cl_2 + e^-$	3.2 eV
	$e^- + CH_3Cl \rightarrow \boxed{CH_2} + HCl + e^-$	3.9 eV
	$e^- + C_2H_3Cl \rightarrow \boxed{C_2H_2} + HCl + e^-$	1.1 eV
	$e^- + C_2H_3F \rightarrow \boxed{C_2H_2} + HF + e^-$	0.8 eV

TABLE 8

Wire Aging for Different Cathode Structures [32]

Type of Cathode	Lifetime Limit
(1) ϕ 100 μ m Cu-Be Wires	
(2) Stainless Steel Mesh	
(3) Continuous Sheet	
(4) As (3), But Add Methylal	
(5) As (1), But Add Isopropyl Alcohol (1%)	
(6) As (1), But Add 4% Methylal	

However, not all halogens are as fragile. For instance, CF_4 is more stable (bond strength is 5.2 eV — see Table 7) and as one can see in Fig. 12, it has a lower rate of polymerization. Apparently just a few eV in the bond strength makes a large difference in the polymerization rate. In fact, it has been used in wire chambers.^[60] It also has a wide industrial use etching metals in the plasma environment.

In our field I would like to quote J. Kadyk's measurement with *DME* gas.^[23] For no halogen contamination, he measured a gain drop of $\sim 10\%/ \text{C.cm}$. A gas bottle containing 10–20 ppm of Freon 11 gave a result more than fifty times worse. In addition, the preliminary results from a test with 2 and 4 ppm of Freon 11 contamination (specified by manufacturer) were 10–20 times worse compared to the reference ("pure") bottle. Does this means that we have to worry about 1 ppm contamination level? At that level we probably have many other types of halogens present! F. Villa^[25] and H. Spinka^[26] have also reported a good efficiency of transfer of halogen impurities on the chamber electrodes.

5.2.2 Bad impurities – Silicon

Silicon is the most abundant element on earth. It is present in gas bottles, in a form of a fine dust or gas impurities (silane SiH_4 , tetrafluorosilane SiF_4 , *etc.*). In addition, there are many products containing silicon (G-10, RTV, various oils, molecular sieves,^[57], *etc.*).

As we discussed earlier, Fig. 8 shows that the valence shell of silicon is the same as that of carbon. One therefore expects some similar features. Silicon can polymerize both

with hydrocarbons and oxygen to form a polysilicone $\left[\begin{array}{c} R \\ -\text{Si}-\text{O}- \\ R \end{array} \right]_n$, ($R = \text{CH}_3$) and a silicate $\left[\begin{array}{c} \text{O} \\ -\text{Si}-\text{O}- \\ \text{O} \end{array} \right]_n$. As discussed earlier, many products of oxygen and hydrocarbon

radicals are volatile and can be removed by a gas flow. This is not so much the case with the silicon species because they are heavier. In this sense, the silicon contamination is probably a more serious problem.

Many people reported problems with silicon based deposits—H. Hilke^[18], H. Spinka^[26], *etc.* As in case of the halogen contamination, the electrode coating by silicone products is very efficient. F. Villa suggested that this point could be utilized by removing them in a primary recirculation loop. D. Hess pointed out that the CF_4 gas could be used to remove silicon based products (to create, for instance, a volatile SiF_4) similar to the way oxygen might remove hydrocarbon based deposits. Certainly good filters should be used to prevent dust from getting into the active volumes of the chambers.^[28,58]

5.3 GAS TUBING

Figure 13 shows a polymer structure of several gas tubing materials. One can see that *PVC*, teflon and neoprene rubber contain halogen atoms in the molecular chains. It is conceivable that some parts of these chains will be broken off and they will contaminate the active volume of the wire chamber, *i.e.*, we will get halogen contamination. This may cause problems as discussed in Section 5.2.1. Kotthaus^[27] has measured the effect of *PVC*

tubing on the rate of polymerization. As one can see in Fig. 14, the introduction of *PVC* tubing initiated aging and this continued even after the tubing was replaced with the original stainless steel tubing. This indicates a potentially serious problem. Once aging is initiated, it will continue even if we introduce correct conditions to prevent aging. There has been good experience with *RILSAN* tubing which is a form of nylon.^[38] As we can see in Fig. 13, the molecular chain of this material doesn't contain halogens. Copper tubing can trap oxygen, react with some gas mixtures, and one should be aware that silicon oils^[6] are frequently used during a drawing process. Clearly, the safest way is to use stainless steel tubing.

GAS TUBING

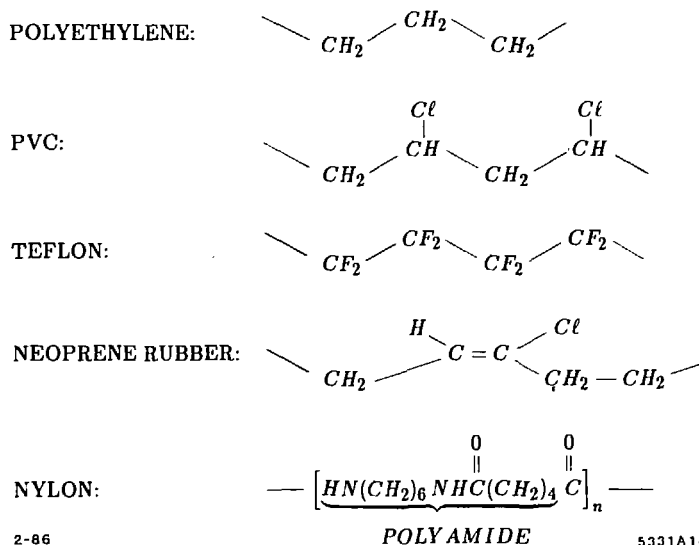


Fig. 13. Examples of chemical composition of some typical gas testing material (notice halogens).

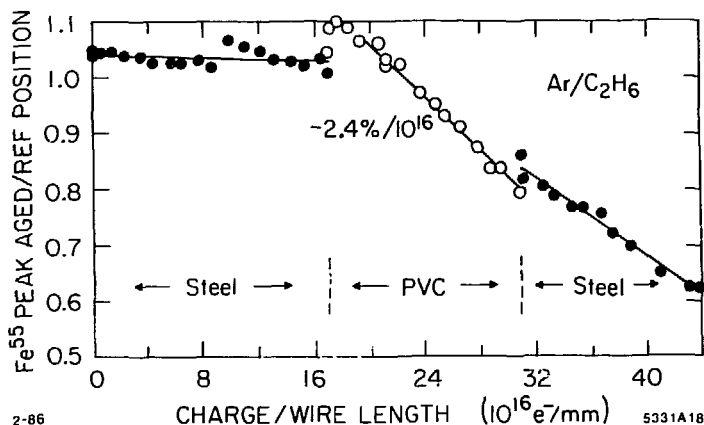


Fig. 14. The observed effect of the PVC tubing on the chamber aging (notice that aging continues even after switching to steel tubing).^[27]

5.4 GAS FLOW RATE

This is one of the most important variables to control in plasma chemistry whenever polymerization or etching is performed (Figs. 15 & 9 show typical examples of both types of behavior). The rate of polymerization (Fig. 15) is low for both a very high and very low flow rate. In plasma chemistry it is argued that at low flow rate there is not enough of the primary polymerization material (original hydrocarbon molecules), and at high flow rate one reduces the concentration of radicals by supplying more of the original hydrocarbon molecules and heavy positively charged polymers are swept away before they can reach the cathode.

How is it in our field? First of all, the gas pressure is typically ~ 1000 times higher and we usually find ourselves on a descending part of the Fig. 15 curve. In fact, the permanently sealed counters have some of the worst lifetimes measured. For instance, A. Smith and M. Turner have measured lifetimes of $\sim 2 \times 10^{-4}$ C/cm (90% Ar + 10% CH₄, 1.1 atm, 50 μ m anode diameter) and $\sim 5 \times 10^{-6}$ C/cm (90% Xe + 10% CH₄, 1.4 atm, 20 μ m anode diameter).^[29] J. Va'vra has measured a lifetime of about 4×10^{-4} C/cm in the micro-jet chamber (90% Ar + 10% C₄H₁₀, 6.1 atm, 7.8 μ m anode diameter).^[39] One criticism of such tests is, of course, possible confusion with an outgassing effect. It would be more direct to actually measure the lifetime as a function of flow. J. Kadyk^[23] has measured, for instance, a gain drop of $\sim 33\%/C.cm$ at a flow rate 105 cm³/min, and $\sim 69\%/C.cm$ at 50 cm³/min (50% Ar + 50% C₂H₆). He has reached similar conclusions in other gas flow tests.

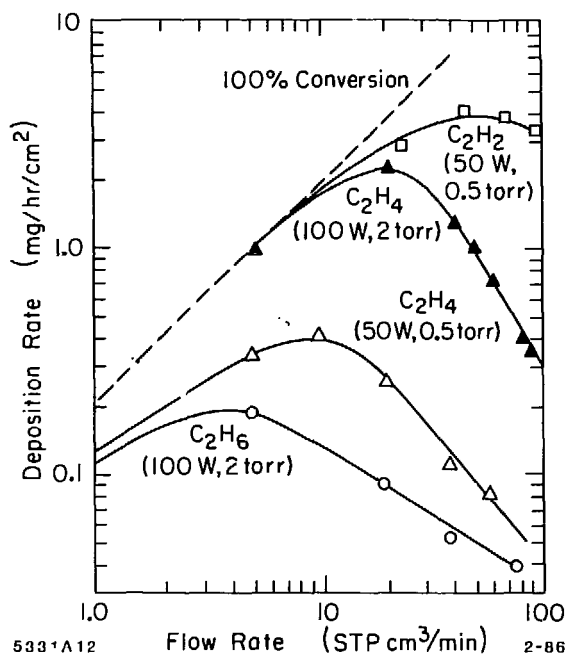


Fig. 15. An effect of a gas flow rate on the polymerization rate of acetylene, ethylene and ethane in a plasma chemistry environment.^[73]

5.5 ANODE-CATHODE DISTANCE

According to our naive model, if the cathode is very close to the anode and the gas flow is not sufficient, the large positively charged polymerized species will have a higher probability of reaching the cathode before the gas flow could remove them. In addition, the attenuation length ($1/e$) of photons which are capable of knocking out electrons from the cathode surface could be rather long. For instance, M. Atac^[12] has measured this length to be $\sim 480 \mu\text{m}$ in 50% Ar + 50% C_2H_6 and $\sim 160 \mu\text{m}$ when $\sim 1.5\%$ ethanol is added. This may be important for very closely spaced wires like pickup wires or grids.

An example of such a measurement is P. Drell's lifetime tests.^[30] With a grid structure 1.7 mm away from the anode plane the measured lifetime was $\sim 0.03\text{--}0.04 \text{ C/cm}$ with 92% $\text{CO}_2 + 8\% \text{C}_4\text{H}_{10}$. With a structure where the grid was 6 mm away the test obtained $\sim 0.15\text{--}0.4 \text{ C/cm}$. What is needed is to check if larger gas flow would improve the first measurement.

5.6 TYPE OF CATHODE (WIRE VERSUS CONTINUOUS)

The larger the cathode surface, the longer it takes to accumulate a certain thickness of insulating material. This material, as we said, is mostly produced at the anode and brought to the cathode by electrostatic forces (either positive charge or dipole moment). Once we accumulate a certain thickness of the insulating material, a continuous cathode will trigger the Malter effect^[31] later than the wire cathode, because it has a generally lower electric field at the surface—Table 8 shows experimental results supporting this mechanism (see Fig. 16). The measurements by G. Charpak et al^[32] were done with a magic gas mixture and a high gain. One can see that the continuous cathode is substantially better, from the aging point of view, than the wire cathode. However, this test also indicates that

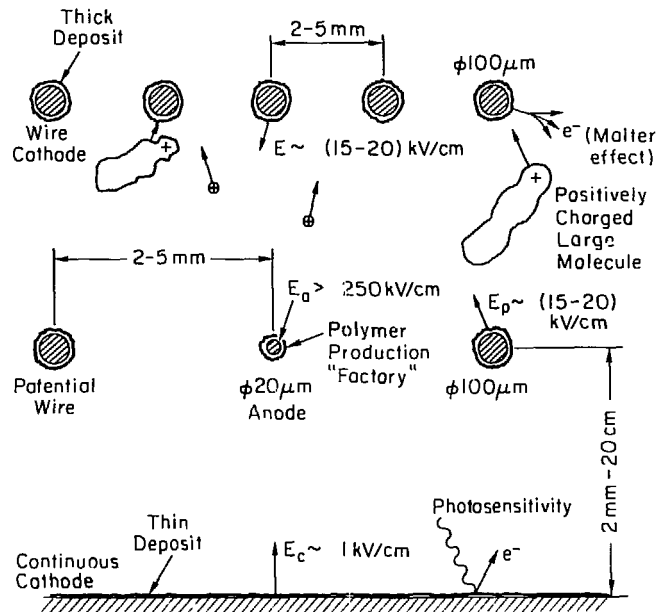


Fig. 16. Typical wire chamber structures, distances, electric fields on the surface and basic aging processes.

the continuous cathode + additive is equivalent, as far as aging, to the wire cathode + additive, where the additive is either methylal or isopropyl alcohol.

5.7 PRESSURE DEPENDENCE

This is certainly one of the least understood variables affecting aging. The aging is probably a delicate balance between two basic effects:

- (a) average electron energy $\sim E/P$, and
- (b) hydrocarbon molecule concentration $\sim P$.

For a fixed voltage, as one increases the pressure, the E/P value gets smaller, and the average electron energy is also reduced and therefore the production rate of free radicals is also reduced. This effect is offset by a higher concentration of hydrocarbon molecules (i.e., the primary building material). However, one should mention that the pressure increase will help to reduce the photon attenuation length and therefore reduce the photo effect processes at the cathode surfaces. H. Boenig^[35] predicts that in the plasma chemistry environment the final outcome will be a slow increase in the polymerization rate (for example ethylene polymerization).

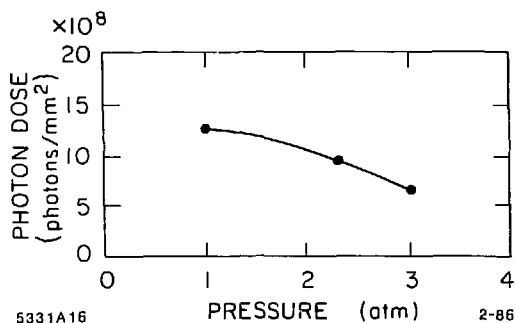


Fig. 17. The pressure dependence of aging (a photon dose required to reduce the plateau^[36] by 50%) in 70% Ar + 30% CO₂, voltage constant.

It is difficult to extrapolate this effect to our range of variables. Faruqi^[36] measured this dependence (see Fig. 17) and it appears to agree with H. Boenig's conclusion. A. Wagner^[43] reported on JADE experience. Innermost wires might have dropped the gain by about $\sim 11\%$ for a total charge dose of about 0.01 C/cm and in 88.8% Ar + 8.9% CH₄ + 2.6% C₄H₁₀ at 4 atm. However, since this experiment is a five year effort and many variables were changed, one cannot necessarily use it as an indication of the pressure effect.

5.8 TEMPERATURE

This is an even more confusing parameter. Nevertheless, one can find a number of examples in plasma chemistry where the polymerization rate decreases with increasing temperature. For instance, Fig. 18 shows this effect for a case of polymerization of C₂F₄.^[37]

In our field there is not much data, except H. Hilke^[18] reported preliminary data indicating agreement with an observation of the plasma chemistry people. If this correlation is proven true one might find a number of possible applications. For instance, aging in the CRID counters, which presently use TMAE and for which the remedies recommended in the previous sections might not apply (except a high gas flow rate). According to M. Atac, reporting on D. Anderson's preliminary measurements at 20 Torr of pressure, the gases containing TMAE have a rather poor lifetime ($\lesssim 0.1$ C/cm).

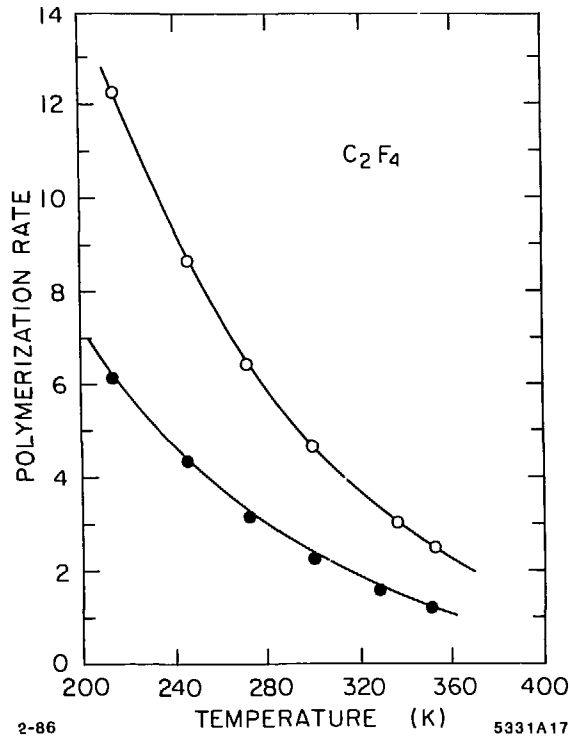


Fig. 18. Temperature dependence of the polymerization rate of C_2F_4 gas.^[37]

5.9 ANODE WIRE DIAMETER

For a general deposit on the anode, the gain behavior can be quite erratic. However, in many instances, the anode deposits can be quite uniform (oil or powder), and in that case the gain drop will be $G/G_0 \approx 1 - \alpha\epsilon/a$, where a is the anode radius, ϵ is the deposit thickness and α is a geometry and gas dependent constant (typically^[29] $\alpha \approx 5-10$). If we express the gain drop in terms of a volume per unit length of the deposited material (W), we get a formula $G/G_0 \approx 1 - \alpha W/2\pi a^2$, i.e., the smaller the anode wire diameter, the larger the gain drop, assuming a constant W .

5.10 ANODE AND CATHODE WIRE MATERIAL

There could be a complex chemical process going on either on the anode or cathode surface. For instance, if the anode wire is made of a complex alloy, which is not gold plated, some elements of the alloy might react with the gas or some of its additives (respectively, their radicals) and rapid aging may occur. As an example, J. Kadyk^[23] has compared the gain drop due to aging with two types of anode wires and 49.3% Ar + 49.3% C_2H_6 + 1.4% Ethanol. The Au/W wire gave a gain drop of $\sim 1.3\%/C.cm$ as compared to the Stabelohm wire (70% Ni, 25% Cr, 5% Al + Cu) giving $\sim 800\%/C.cm$. D. Hess suggested that Al and Cu might oxidize utilizing the oxygen from a destroyed ethanol molecule. In the second example, H. Nelson^[21] has reported a loss of thin Al coating in aluminized mylar straw tubes, when exposed to ~ 0.25 C/cm of ^{55}Fe source in the 50% Ar+50% CO_2 gas (Al was simply etched away). To indicate the complexity of the details of the aging, we

mention a test of P. Le Dû *et al.*,^[40] where they markedly improved the chamber lifetime by coating the mylar cathode with a graphite conducting paint (as compared to a bare Al surface). Clearly, the details of "sticking" (electrostatic attraction?) the polymers to the cathode surface are far from clear and will require more study.

6. How Should the Aging Test Be Done?

A basic message in this section is that it is far from easy to perform an accelerated aging test correctly. To name a few problems associated with such tests:

- (a) The most significant problem is that they typically do not test " $\sim 1\%$ tail effects" which are certainly very visible in a system with a large number of wires.
- (b) The gas flow, which is a very important parameter in plasma chemistry and probably also in our field, is usually much larger and more efficient in a small test compared to a typical large device.
- (c) The gas impurities are usually completely different in the small tests as compared to a real detector environment.
- (d) There is the usual question: "clean" versus "dirty (but realistic)" environment. If "clean," how clean? Is 10-20 ppm impurity level significant?

Our point is that if there is to be any chance of disentangling a many variable problem, we have to be able to separate the variables. It is better to introduce 10 ppm of O_2 , H_2O or freon into the system controllably, rather than have all of them at the same time. This has, however, one basic problem: how do we apply results of such "controlled" tests to a real environment where one has 15 variables at the same time? My answer would be that if we find exact conditions for extremely good lifetimes, we might try to reproduce them in the real detector.

In the next section we will discuss the question of ultra pure gases. It is obvious that it doesn't make sense to put the ultra pure gas into a dirty gas system. Therefore, these tests should also be made in an ultra-pure gas system, which allows recirculation with removal of oxygen, water, dust and other contaminants.

6.1 ULTRA PURE GASES?

There is clear evidence that one should buy the highest possible purity of gases. For instance, Hartman^[41] reports a stabilization of aging in the TASSO central detector after ethane (50% Ar + 50% C_2H_6) was cleaned from oil contaminants and gas filters were installed. Kotthaus^[27] reached 0.7% C/cm with 50% Ar + 50% C_2H_6 (no additives) in a very clean environment (MPI tests in Table 11). J. Kadyk^[23] has done several such comparisons, for instance the gain drop was 15 %/C.cm versus 147%/C.cm for "pure" and "regular" purity of 89% Ar + 10% CO_2 + 1% CH_4 gas, and -6%/C.cm versus 63%/C.cm in the case of 80% Ar + 20% CH_4 .

6.2 HIGH VERSUS LOW INTENSITY?

In a low source intensity test, each avalanche is realistic and such a test simulates an experiment correctly. However, in a high intensity test we start getting a modification of the avalanche strength due to several effects:

- (a) pile up of two ionization events on the same spot of wire,
- (b) saturation of ionization within the same event, and
- (c) modification of field due to a space charge.

These effects will generally tend to reduce the electron density (total charge is reduced) in each individual avalanche and to make up an overall integrated current, we have to either increase the intensity of the source or increase the voltage on the chamber (this causes the avalanche to spread, reducing the electron density). If we reduce the electron density in the avalanche, we expect, according to our wire model, to reduce the density of free radicals and therefore improve chamber life.

To calculate the gain drop due to the space charge, one either has to make a proper solution of Poisson equations in cylindrical coordinates, including the Z -coordinate dependence,^[43] or to get a feeling for the problem, one can neglect the Z -dependence and assume a Gauss law and a simple gain dependence $G \simeq \exp \{ \gamma (V - V_T) \}$. One obtains a formula for gain drop $G/G_0 \simeq \exp [-\gamma r_0^2 \ln(r_0/r_a) (\rho^+ / 2\epsilon_0)]$, where r_0 is the cathode radius, r_a is the anode radius and ρ^+ is the density of positive ions. For instance, for J. Kadyk's geometry^[23] one obtains the result that the anode current should be limited to ~ 50 nA/cm if one desires a gain drop in the center of the radiation flux to be less than 10%.^[44] J. Kadyk^[23] has done two types of tests addressing the intensity question:

1. Keeping the chamber voltage constant and varying the source strength (Al shims) and using the same bottle of high purity 50% Ar + 50% C₂H₆ he obtained a gain drop of $\sim 23\%$ /C.cm for the anode current 61 nA and $\sim 6\%$ /C.cm for the current ~ 392 nA.
2. Keeping the source strength constant and varying the chamber voltage, he obtained the following results: $\sim 99\%$ /C.cm for 95 nA, $\sim 66\%$ /C.cm for 372 nA and $\sim 34\%$ /C.cm for 1495 nA. In fact, all his ~ 1600 nA runs have rather good lifetimes.

Similar results have been reported by Kotthaus.^[27] Table 11 (under "Conclusions") shows results in typical tests where rather large radiation doses have been achieved. As one can see, many results were obtained at rather large current and therefore one needs to perform additional measurements at low source intensities before the test results can be extrapolated to large experiments. This emphasizes the point that aging tests are difficult to do. In order to see a dependence, we have to make an accelerated aging test. However, we need to normalize the final result with a low intensity test.

6.3 DELIBERATE SPARKING TESTS

One thing we cannot avoid is accidental sparking in the chamber due to beam losses. Each spark is a potential danger from the aging point of view because it can "prime" the

wire for subsequent deposit buildup. Therefore it makes sense to perform special tests under very high current conditions.^[12,34,45] One should point out that these are special tests where the plasma conditions are generally different compared to usual aging due to typical avalanche conditions. For instance, B. Foster concludes that gas mixtures containing even small quantities of hydrocarbon (ethane, for instance) are very prone to whiskers or deposits.^[34] Adding ethanol vapor inhibits but does not prevent this process. Ar/CO₂ mixtures generally do not grow whiskers and can rehabilitate chambers where whisker growth has started. H. Sadrozinski has performed similar tests with 89% Ar + 10% CO₂ + 1% CH₄ mixture and breakdown currents of $> 0.1 \mu\text{A}/\text{cm}$. If the content of CH₄ exceeded 5% in this mixture, the whiskers were grown on the cathode at a rate of $\sim 1\text{mm}/5\text{min}$.^[45]

7. A Cookbook of NO, NO ...

Table 9 shows a summary of various variables which may affect aging adversely. Clearly, the basic conclusion is that the chamber structure should be made of metals, ceramic and glass, perhaps with a possibility of baking (applicable to some designs).

8. Conclusions on Gases

- A. If we obtain regular purity gases, a basic conclusion of the workshop is that *Noble gas + hydrocarbon* mixture should not be trusted for more than^[11,18,21,46] 0.01–0.05 C/cm. The *Noble gas + CO₂* mixture appears to behave about ten times better.^[11,21,46]
- B. If we obtain the “highest possible” purity of a gas, there is a clear evidence that a considerable improvement can be gained. For instance, at least a factor of ten can be gained in the case of the *Noble gas + hydrocarbon* mixtures.^[23,27,41]
- C. There is a clear evidence that the oxygen containing additives (*H₂O, alcohols, etc.*,) can considerably improve the lifetime.^[12] — see also Tables 10 and 11.
- D. *DME* gas looks very attractive, but one should check for halogen impurities.^[23,25]

Conclusions

1. Chamber aging is clearly a very complex subject. If we are to make any significant headway in this field, we will have to consider it as a serious subject for scientific investigation and treat it correspondingly.
2. The gas impurities may be the most critical variable to control.
3. We should always tune the variables, such as gas flow, additive fraction, gas type, gain on the wire, impurities level, temperature, *etc.*
4. Perhaps one should look, as D. Nygren suggested, for a way to increase a conductivity of some of these insulating deposits.^[16]
5. One should limit the total radiation dose by limiting the gain on the wire (aging and cost of electronics are inversely proportional) and/or limit the primary amount of ionization through suitable geometry (small cells^[62] or restrictive curtains^[61]).

TABLE 9
List of NO, NO

- No halogens in the gas [23,25]
- No oil traces in the gas [23,41]
- No oil bubblers [27,38]
- No silicon rubber (RTV) to seal the chamber [23,47]
- No rubber O-rings [66, Fig. 14]
- No polyurethane adhesive [47]
- No PVC or teflon tubing [27]
- Avoid Cu-tubing [6]
- No soft epoxies or adhesives [47]
- No aggressive solder
- Avoid sparking with large capacitance in very early testing stages [12,34,45]
- Avoid unknown organic materials
- Avoid a large amount of G-10 (S_i) [18]
- During an entire operation of the chamber do not allow even a single case of bad gas! [63]
- Methanol and isopropanol attack dielectrics, methylal attacks mylar [12]
- No insulators on wires (lubricating oil, fingerprints, oxydized regions, etc.) [5]

TABLE 10

Experiments (Accept only those which accumulated more than 0.1 C/cm)

Gas	Charge Dose	Observed Change in Operation	Person and Detector
65% Ar + 35% C ₄ H ₁₀ + 1.5% Isopropanol	$\lesssim 0.1$ C/cm	Some (Traces of Deposits)	Beusch and Omega [38] CERN
50% Ar + 50% C ₂ H ₆ + Ethanol (2°C)	$\sim 0.2 - 0.4$ C/cm	Initially: Yes Now: No	Hartman and Tasso Central Detector [17]
Note: Initially observed aging. At that point add ethanol, and later filters in gas line, remove oil from ethane. No further deterioration seen and running well for two years. Alcohol added, not because shown necessary, but mainly in attempt to reduce anticipated high background currents.			
95% Ar + 5% CO ₂ + H ₂ O + Ethanol (4°C)	~ 0.25 C/cm	Yes	Binnie, Tasso Vertex Ch. [17]
Note: Onset of the Malter effect observed already at ~ 0.02 C/cm. Cured by adding H ₂ O and ethanol.			
53% Ar + 40% C ₄ H ₁₀ + 7% Methylal	~ 0.2 C/cm	Some ($\sim 1 \mu\text{m}$ Thick Deposits)	Ullaland SFM, CERN [38]
76% Ar + 20% C ₄ H ₁₀ + 4% Methylal	~ 0.2 C/cm	No	Pile, BNL Hypernuclear Spectrometer [47]
Note: However troubles seen in a chamber with a different construction			

TABLE 11

Tests (Accept only those which accumulated more than 0.1 C/cm)

NOTE: Many results done at large currents

⇒ Absolute Lifetime Suspect!!

Gas	Charge Dose C/cm	Observed Change in Operation	Anode Current (cm ⁻¹)	Person
50% Ar + 50% C ₂ H ₆ (with and without 0.7% H ₂ O)	~ 0.7	No	~ 1 μ A	Kotthaus [27] (MPI Test)
89% Ar + 10% CO ₂ + 1% CH ₄ (with and without 0.7% H ₂ O)	~ 0.7	Yes	~ 1 μ A	Kotthaus [27] (MPI Test)
50% Ar + 50% C ₂ H ₆	~ 0.15	10% Gain Drop	~ 1 μ A	Kotthaus [27] (KEK Test)
89% Ar + 10% CO ₂ + 1% CH ₄	~ 0.3	10% Gain Drop	~ 1 μ A	Kotthaus [27] (KEK Test)
50% Ar + 50% CO ₂ 50% Ar + 40% CO ₂ + 10% X _e 49% Ar + 50% CO ₂ + 1% CH ₄	~ 0.3 – 0.5	Yes	~ 1 μ A (20 kHz)	Nelson [21]
25% Ar + 50% CO ₂ + 25% n-Pentane	~ 1.0	Yes		Iaroci [49]
27% Ar + 73% C ₄ H ₁₀ + \geq 0.1% H ₂ O	~ 0.1	Yes		Seiden [50]
50% Ar + 50% C ₂ H ₆ + 1.4% Ethanol (Very Pure Gases)	~ 1.0	< 2% Gain Drop	~ 400 nA	J. Kadyk [23]
89% Ar + 10% CO ₂ + 1% CH ₄ (Very Pure Gases)	~ 1.0	9% Gain Drop	~ 400 nA	J. Kadyk [23]
DME (No Freon 11)	~ 1.0	< 10% Gain Drop	~ 400 nA	J. Kadyk [23]
DME	~ 4.0	Some	~ 5 μ A	F. Villa [25]
50% Ar + 50% C ₂ H ₆ + 0.5% Ethanol	~ 1.5	No	~ 440 nA	M. Atac [12]
DME	~ 1.0	Some	~ 3 μ A	Majewski [6]
DME	~ 2.0	Some	~ 2 μ A	Godfrey [46]
89% Ar + 10% CO ₂ + 1% CH ₄	~ 0.3	50% Gain Drop	~ 50 μ A/25 cm	Sadrozinski [45]
93% Ar + 3% CO ₂ + 4% CH ₄	~ 1.9	50% Gain Drop	~ 50 μ A/25 cm	Sadrozinski [45]
92% CO ₂ + 8% C ₄ H ₁₀	~ 0.15 – 0.4	Yes	~ 260 nA	Drell [30]

References

1. D. Hess, *Plasma Chemistry in Wire Coating*, LBL Workshop.
2. M. Williams, *Analysis of TPC Inner Drift Chamber Wire Coatings*, LBL Workshop.
3. Bell, *et al.*, *Macromol. Sci. Chem.* **A8**, 1354 (1974).
4. M. Matoba, *et al.*, *IEEE*, Vol. NS-32, 1985.
5. F. Sauli, *When Everything Was Clear*, LBL Workshop.
6. S. Majewski, *Results on Ageing and Stability with Pure DME and Isobutane/Methylal Mixture in Thin High-Rate Multi-Wire Chambers*, LBL Workshop.
7. G. Baranko, *et al.*, *Nucl. Instrum. Methods* **169**, 413 (1980).
8. R. Gillette, *et al.*, *Vac. Sci. Tech.* **7**, 534 (1970).
9. H. Boenig, *Plasma Science and Technology*, p. 281.
10. Old Mark II drift chamber, private communication with J. Kadyk.
11. M. Turala, *Ageing Effects in Gaseous Detectors and Search for Remedies*, LBL Workshop; and A. Dwurazny *et al.*, *Nucl. Instrum. Methods* **217**, 301 (1983).
12. M. Atac, *Wire Chamber Ageing*, LBL Workshop.
13. H. Yasuda, *Plasma Polymerization* (published by Academic Press, 1985), p. 113.
14. Hollahan, *et al.*, *Adv. Chem. Ser.* **80**, 272 (1969).
15. H. Kado, *Performance of the JADE Vertex Detector*, LBL Workshop.
16. H. Yasuda, *Plasma Polymerization*, p. 395.
17. D. M. Binnie, *Experience with the TASSC Chambers*, LBL Workshop.
18. H. Hilke, *Summary of Ageing Studies in Wire Chambers by AFS, DELPHI and EMC Groups*, LBL Workshop; and J. Adam *et al.*, *Nucl. Instrum. Methods* **217**, 291 (1983).
19. H. Sipilä, M. Järviäinen, *Nucl. Instrum. Methods* **217**, 298 (1983).
20. H. Sipilä, private communication.
21. H. Nelson, *Lifetime Tests for MAC Vertex Chamber*, LBL Workshop.
22. W. Mohr, a Summary Table contribution, LBL Workshop.
23. J. Kadyk, *Results from Some Anode Wire Aging Tests*, LBL Workshop.
24. H. Boeing, *Plasma Science and Technology*, p. 145.
25. F. Villa, *Aging Effects in DME*, LBL Workshop, oral contribution.
26. H. Spinka, *Wire Chamber Degradation at the Argonne ZGS*, LBL Workshop.
27. R. Kotthaus, *A Laboratory Study of Radiation Damage to Drift Chambers*, LBL Workshop.

28. Early experience of OPAL indicates this might be a very serious problem even with a stainless steel tubing. Filters had to be installed to prevent the dust getting into the chambers.
29. A. Smith and M. Turner, Nucl. Instrum. Methods **192**, 475 (1982).
30. P. Drell, a Summary Table contribution, LBL Workshop.
31. L. Malter, *Phys. Rev.*, Vol. 50 (1936); and Güntherschulze, *Zeits & Physik* **86**, 778 (1933).
32. G. Charpak, F. Sauli, *et al.*, Nucl. Instrum. Methods **99**, 279 (1972).
33. V. S. Bawdekar, IEEE, Vol. NS-22, 1975.
34. B. Foster, *Whisker Growth in Test Cells*, LBL Workshop.
35. H. Boenig, *Plasma Science and Technology* (published by Cornell University Press, Ithaca, NY, 1982), p. 127.
36. A. Faruqi, IEEE, Vol. NS-27, No. 1, 1980.
37. H. Yasuda, *Plasma Polymerization*, p. 198.
38. O. Ullaland, *The Omega and SFMD Experience in Intense Beams*, LBL Workshop.
39. J. Va'vra, a Summary Table contribution, LBL Workshop.
40. P. Le Dû *et al.*, CERN EP77-11 (1977).
41. H. Hartman, a Summary Table contribution, LBL Workshop.
42. H. Sipilä *et al.*, Nucl. Instrum. Methods **176**, 381 (1980).
43. A. Wagner, *Long Time Behavior of the Jet Chamber at JADE*, LBL Workshop.
44. J. Va'vra, *Field and Gain Modification During High Rate Lifetime Studies of Chambers*, SLAC EFD Memo, October 11, 1985, unpublished.
45. H. Sadrozinski, *Investigation of Breakdown Conditions of Drift Chambers*, LBL Workshop.
46. G. Godfrey, *Proportional Tube Lifetimes (Magic Gas, A-CO₂, DME)*, LBL Workshop.
47. P. Pile, *Radiation Damage Control in the BNL Hypernuclear Spectrometer Drift Chamber System*, LBL Workshop.
48. P. Estabrooks, *Ageing Effects in a Large Drift Chamber in the Fermilab Tagged Photon Spectrometer*, LBL Workshop.
49. E. Iaroci, a Summary Table contribution, LBL Workshop.
50. A. Seiden, a Summary Table Contribution, LBL Workshop.
51. H. Yasuda, *Plasma Polymerization*, p. 244.
52. H. Yasuda, *Plasma Polymerization*, p. 154.
53. W. Schmidt-Parzefall, a Summary Table contribution, Argus Central Detector, LBL Workshop.

54. T. Jensen, *One and One-Half Year's Experience with CLEO vertex detector*, LBL Workshop, oral contribution.
55. R. Heuer, *New Techniques to Analyze Wire Coatings*, LBL Workshop.
56. M. Yvert, *Our Ageing Experience with the UA1 Central Detector*, LBL Workshop.
57. Linde Molecular Sieve Type 3A has a chemical composition:
 $\text{K}_9\text{Na}_3[(\text{AlO}_2)_{12}(\text{SiO}_2)_{12}] \times \text{H}_2\text{O}$.
58. Mathison sells a mechanical filter absorbing $0.02\mu\text{m}$ size particles. But it has silicon O-ring and teflon parts(!)—private communication, L. Feely, Matheson Co., Newark, California.
59. A. Veltri, Little Falls Alloys, is using a lubricant, Lusol WD80, during the wire production (it doesn't contain silicon).
60. J. Fisher *et al.*, Nucl. Instrum. Methods **A238**, 249 (1985).
61. J. Va'vra, SLAC-PUB-3727, (1985).
62. R. Bouclier, G. Charpak, F. Sauli, CERN-EP-84-03 (1984).
63. P. Lennert, private communication.
64. Private discussion with R. Kirby, SLAC.
65. R. Christy, J. Appl. Phys. **31**, 1680 (1960).
66. M. Williams pointed out that sulphur is used to make a vulcanized rubber stronger (O-rings?).
67. H. Nelson pointed out that the photosensitivity of the cathode dramatically increased after a sparking, and then it slowly decreased (in minutes). In Ar-hydrocarbon mixtures the effect was very easy to create, in Ar-CO₂ mixtures it was much more difficult. This suggests that the hydrocarbon film is responsible for the effect.
68. B. Sadoulet, Physica Scripta, Vol. 23, 434 (1981).
69. H. V. Boenig, *Plasma Science and Technology*, pp. 115,116.
70. H. V. Boenig, *Plasma Science and Technology*, p. 280.
71. H. Yasuda, *Plasma Polymerization*, p. 186.
72. H. V. Boenig, *Plasma Science and Technology*, p. 147 and p. 116.
73. M. Shen, *Plasma Chemistry of Polymers* (published by Dekker, NY, 1976); M. Shen and A. Bell, *Plasma Polymerization* (published by American Chemistry Society, 1979).
74. G. B. Butler and K. D. Berlin, *Fundamentals of Organic Chemistry*; H. Yasuda, *Plasma Polymerization*, p. 74.

APPENDIX A

Discussion Sessions

FIRST DISCUSSION PERIOD, THURSDAY AM

(Speakers: Sauli to Atac)

Stevens (to M. Williams): Could the chlorine seen in analysis spectra be due to what was used to clean the chambers (chlorinated solvents)? What would the effect of this be on polymerization processes?

Layter: Ethyl alcohol is believed to have been used to clean the TPC Inner Drift Chamber [paper by M. Williams], and no chlorinated solvent.

Pile: What about polyvinyl chloride (PVC) tubing as a contaminating source?

Williams: PVC was in fact one of the possibilities that I mentioned; it is widely used in tubing and wire insulations. We looked at some wire insulation taken from the TPC chamber [IDC], using the MS, and this gave indications of various kinds of hydrocarbons that could come from the wire insulation: phthalate esters — plasticizers — the *same* ones seen in the wire deposits. If PVC was used as wire insulation, this would be a likely suspect as the source of chlorine.

Pile: Why wouldn't you suspect this to be the source of the aromatic hydrocarbons found on the sense wires?

Williams: Phthalates have an aromatic ring, but do not give the specific breakdown pattern observed. These could contribute, but do not seem to be the entire explanation, due to the strength and distribution of pattern.

Hilke: Could you comment on temperature dependence of polymerization?

Hess: Polymerization rate does go up with temperature, so will etching rate. The former leads to a solid product, the latter to a volatile product. The relative rates of these two processes determines which predominates. Evaporation of material off a surface (by laser) can be done using high temperatures. Generally, it is difficult to predict the temperature dependence when both polymerization and etching are competing unless the temperature dependence of each contributing reaction is known.

??: Could the chemists comment on the likely mechanisms by which the addition of ethanol or methylal increase chamber lifetimes so dramatically? The charge exchange mechanism in the case of methylal reduces the amount of ionized hydrocarbon species which can reach the cathode.

Hess: I already commented with respect to polymerization vs. etching. Have studies been done on concentration of ions that verify this charge exchange mechanism?

Sauli: From the timing curves, one can measure the drift velocity of ions. When one goes above 4-5% of methylal there is a transition from light hydrocarbon ions to a broad peak of correct timing for methylal. This does not prove there are not small amounts of other species present however. Also, it may be that methylal has such a high cross section for ionization in the avalanche itself that very little of the other hydrocarbon (methane) is ionized.

Hanson: I would like to have the speakers comment on whether the coating rate depends on whether or not the wire is gold plated, the surface characteristics of wire, and what

material the wire is made from.

Atac: John Kadyk will talk about Stablohm wire vs. gold plated wire; he does see a difference.

Pile: What kind of conditions are necessary to make a conductive coating on sense wires? Is it possible to have a conducting, carbon coating on sense wires and a polymer on the field wires? How does methylal prevent carbonaceous deposits on anode?

Hess: Indeed it is. If you have a coating that is primarily carbon, rather than normal polymers the conductivity will be much higher, so the energy of and amount of particle bombardment on the surface can very easily change the composition and therefore conductivity. Hydrogen can be easily removed by ion bombardment, so heavy bombardment leads to a more carbonaceous than polymer-like deposit. Conceivably methylal, which contains oxygen, can react with hydrocarbons which might otherwise cause deposits and oxidize them to volatile compounds.

Atac: If you use argon/ CO_2 and you use an aluminum cathode, then oxidation can occur giving aluminum oxide (sapphire), which is a very good insulator. I have seen such chalk-like substances on cathodes. Oxides of other metals (e.g. copper) are still conductive enough.

Nelson [to Hess]: You said there was no particular correlation between processes occurring on the cathode and on the anode?

Hess: I said there can be polymerization at both places. At the anode, the primary bombarding species are electrons, which are not efficient at sputtering. Negative ions can cause efficient sputtering at the anode, but if there are few of these, little sputtering at the anode is expected.

Nygren: I think the field at cathode is too low to allow sputtering — the ions are essentially of thermal energy. The heavier molecules, with lower ionization potentials, polymerize in the gas and have a good chance, through the charge-exchange processes, of getting to the cathode.

Odian: It appears as though oxygen, whether in alcohol or in water vapor, helps at the anode by making negative oxygen ions which are drawn into the anode, and sputtering off deposits or converting them to CO_2 .

Williams: I'd like to comment on the effects at the anode when oxygen-containing species are present. These are converted into free radicals, which are very inactive and stop the chain formation. They are free-radical scavengers, and can have the effect of quenching the chain formation which would result from polymerization of the hydrocarbon free radicals.

Kadyk: Can the *polar* nature of the oxygen-containing compounds ethanol, methylal, water result in concentrating them (as neutral species) near the wires by attraction in the inhomogeneous field? Then, due to the release of oxygen from the broken molecule, either etching or oxidation at the wire surface would be more efficient due to this oxygen concentration.

Atac: This may be the case. There is evidence dating from some time ago that after flowing gases, many layers of hydrocarbon molecules are attracted to the surface,

especially at the cathode.

Godfrey [to Hess]: Does CO_2 in a plasma polymerize?

Hess: No. You can reduce CO in a high energy discharge ending up with a porous carbon coating on the walls; I'm not aware that the same effect occurs with CO_2 , presumably a reflection of the C/O ratio.

Nelson: What was the gain and charge/cm of wire in the TPC inner drift chambers [see paper by M. Williams].

Layter: Initial gas gain was $2-3 \times 10^5$; the reduced gain on the replacement chamber was $5-6 \times 10^3$. The charge was something over 10^{17} e/cm.

Hilke: If both C and Si are competing for the polymerization process, do you know of parameters that can push the balance either way?

Williams: No. This is not a common situation; I don't think it has been studied.

Kozanecki: There is a "black magic" conditioning procedure that is sometimes used at beginning of chamber's life: force it to draw current, which then slowly dies away. Do any of the mechanisms that have been discussed explain this?

Atac: This could be from an increase in wire diameter due to deposits quickly formed at local "hot spots" and resulting gain drop here, or possibly due to hairs [dirt] being burned off.

Sauli: Ion bombardment can eliminate needles or points of dust, but the chamber life-time is much shorter, because with these discharges you produce polymers very quickly. If you are satisfied with low rate, that's fine, but at high rate, it is dead. This technique has been abandoned by most people.

Wagner [to Hess]: Can you comment on the relative polymerization rates of methane and isobutane?

Hess: No, not with any certainty. Probably isobutane [has a higher rate].

Williams: These are not common monomers commercially. I would agree with "isobutane," because its structure and bond strengths allow it to be broken up readily.

Lach: Does anybody have an explanation for where the silicon deposits come from?

Atac: Machined G10 looks fine to the eye, but it is full of dust and this can get onto the anode.

Williams: The silicon observed in the MS plot [of the TPC chamber] is what is associated with silicon polymer (polydimethylsiloxane). There may be other sources of silicon as well.

SECOND DISCUSSION PERIOD, THURSDAY PM

(Speakers: Yvert to Kadyk)

Questions to afternoon speakers:

Perez-Mendez: I would like to know what is the effect of self-quenched streamers on deterioration of chambers.

Atac: In self-quenched streamers we have an extreme condition. One has to be sure to use large enough diameter tubes. The CDF experience has been that when using aluminum tubes, regeneration was a problem. When we use stainless steel tubes, it was much better. This is possibly due to different work functions for the two metals.

Hilke: I think the effect you have seen has been seen quite often on aluminum chambers. It is well known that for proportional chambers, aluminum and magnesium are the two worst substances.

Kozanecki: You mentioned your work with argon-nitrogen gas in proportional tubes, and said it would not work in drift chambers. In what sense could you not operate?

Turala: We could not come to the gain to reach our electronic threshold. We saw some pulses, but came quickly to a sort of Geiger-Mueller condition; we estimated the gain to be about 2×10^3 , while in the proportional counters we could safely go above 10^4 . We think the gap was too small. We did some tests, but think they were not conclusive.

Parker: I should be surprised if a diatomic gas [as a quencher] would ever do much better than you have done. I have used pure argon and gotten [gains of about] a thousand; therefore, the diatomic gas [N_2] hasn't gotten much more.

Turala: Nitrogen has a quite high cross section for photons, but, of course, not as good as hydrocarbons, but better than hydrogen.

Videau: Aleph uses aluminum tubes with one side of graphite, and once this was filled [by mistake] with 50/50 argon/nitrogen. It gave an extremely narrow operating range.

Questions to morning speakers:

Parker [to M. Williams]: You showed a profile plot where layers were being sputtered off [argon etching] and there was an overlap region between gold and carbon. The question is: are the layers and sputtering uniform enough to be able to say that this overlap constituted a mixture or alloy of materials rather than a reflection of the non-uniformities?

Williams: I can't be absolutely sure of that; we would have to take a closer look. What I would like to do is to look on the wire with this method before installing it in the chamber to check surface features such as patchiness of coating, porosity, etc.

Perez-Mendez: I'm curious to know if anyone has done measurements using ammonia. Do you get deposits from ammonia?

Villa: Yes. You don't get any gain. You can get gains of 10^5 , but the gas can easily be poisoned by water vapor.

Hilke: Ammonia was used in proportional chambers which had quite long lifetimes.

Villa: The problem is that ammonia is very, very reactive, and will attack many substances. Plastics would be very vulnerable.

Binnie: Could I ask about flow rate? The tests just described [J. Kadyk] flowed the gas through quite quickly, ≈ 1 cm/sec, much faster than in a big chamber or sealed counter.

Kadyk: Sometimes when you increase the flow rate and expect the deposit rate to go down, it goes up instead. This is because there is some contaminant causing coating which gets used up as fast as it gets to the wire, and the faster you pump it, the higher the deposit rate.

Binnie: You had extremely high flow rates, essentially removing all the [avalanche] products. Nevertheless the flow rate made a factor of two or more difference in deposit rate.

Stevens: I don't remember if there was a comment from the chemistry side on those very uncertain but seemingly very high efficiencies for pulling substances like silicon out of the gas and depositing it on wires.

Williams: This morning I gave a talk showing very strong signals. There was data shown this afternoon indicating virtually 100% efficiency for silicon deposit. Why that should be so effective — far more so than, say, carbon contamination — I do not know.

Hilke: Mike, if you were to try to deposit silicon compounds, what kind of probability per electron would you expect for polymerizing, for electron energies around 20 eV?

Williams: You don't make silicone polymers by the same chemistry as for polyethylene, and I have a feeling that it is much harder to get chains to polymerize: it seems very unlikely that would be the structure. If you get a solid film, I should think this might be due to epitaxy, or making SiO_2 crystals. Has anybody looked for this?

Atac: I've seen silicon on the wires, very crystalline.

Hilke: There exists an old article in the literature where they tried to put down silicone layers on a metal surface by electron bombardment, starting with Dow-Corning 704 oil. The vapor pressure of this was only $\approx 2 \times 10^{-9}$ Torr, and yet it gave a high rate of deposition of layers.

Williams: It is conceivable that field ionization could go on right at the surface which could promote the surface chemistry.

Videau: I would like to see someone summarize, because I have the impression that in some cases silicone polymers are formed, sometimes SiO_2 , and sometimes even silicon crystals.

Hilke: We have no indication of whether or not these are silicon crystals, but have an indication of a composition of " SiO_2 ," which doesn't mean you have silicon dioxide, but just this elemental ratio, approximately. However, the layer was mechanically very strong, not easily removable by rubbing.

Godfrey: In the various pictures we've seen today, we've seen uniform deposits, a lot of

pictures with little stalks, and one spectacular picture with kind of spiked sabers. What characteristic of the radicals, or ions, or whatever is drifting in, tend to make these different structures?

Williams: We proposed an explanation, based upon pure conjecture, for "whiskers" in the paper that John Layter and I wrote. If there are "weak spots," or "cracks" in an otherwise insulating layer, the current flow will be primarily focused to these spots, causing epitaxial growth of some sort. It is conceivable that "whisker" growth occurs in these regions.

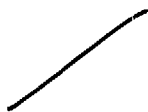
Godfrey: So the "stalks" are a second stage of growth?

Williams: Yes, in this picture, a smooth uniform growth could occur until the insulating layer is thick enough to make current flow difficult. Then the current will tend to flow to defects through the layer, thereby concentrating the growth at these points. The current densities there could be quite high, and temperatures could rise locally above the decomposition temperature of hydrocarbons, charring may occur there, and some kind of epitaxial structure may grow.

Pile [to Kadyk]: What is there about stablohm wire that seems to cause deposits to grow more rapidly than with gold plated tungsten?

Kadyk: I don't know whether it is a chemical reaction or surface catalytic action at the surface. Somehow it is important to have the ethanol vapor present for the reaction to occur. It does not appear to be due to initial surface defects: the stablohm wire is quite smooth. There could be other surface effects, however.

Williams: There could, for example, be local regions of higher surface energy.



THIRD DISCUSSION PERIOD, FRIDAY AM

(Speakers: Hilke to Villa)

Nelson [to Hess]: I and Gary Godfrey have noticed that the cathode of our tubular chambers can become very photosensitive after a discharge in argon/hydrocarbon gases. Does this have any significance in terms of chemistry at the cathode? It dies away after about a minute and does not occur in argon/CO₂.

Hess: I can only say that I'd expect that it is due to a coating on the surface and not the aluminum. Can you look at material while the surface is still photosensitive vs. after the effect has died off? It is probably not an oxide coating since CO₂ would give much more oxide.

Odian: We tried adding 1% DME to HRS gas, and the gain went up a factor of three.

Atac: Another issue than aging is the high voltage that is needed for DME, and the lack of saturation of that gas. It is okay at low rates but at high rates the field must be pushed very high.

Kadyk: Has DME been tried as an additive in the same way as ethanol, to suppress polymerization?

Perez-Mendez: Is a reasonable mixture of argon and DME, say 80% Ar/20% DME, a good quenching gas?

Villa: Yes, it works very well

Atac: One should do aging tests on this mixture.

Villa: A comment about high rates: We did a test with a chamber filled with DME in a beamspill of 10⁶ particles over ≈ 400 msec, which was sampled every 30 msec. We saw no difference in the results from beginning to end of spill.

??: Why does the gain go up when 1% DME is added to HRS gas?

Villa: Probably the 1st Townsend coefficient increases.

Sauli: Whenever triethylamine is added to a gas the working voltage changes by a factor of two — some kind of Penning effect.

??: Does DME tend to dissolve gasket material?

Villa: We have done some tests. We have a small vessel, putting in DME in liquid phase. G10 is mildly attacked after a few months; viton, teflon are not attacked; Al-loaded epoxy (from CERN) is not attacked.

Binnie: I'd like to ask about the neutral radicals. When you think of them forming polymers, does it have to be in the avalanche, or can they disperse through the gas and meet each other, slowly building up?

Hess: They'll diffuse around in the system, but I can't imagine them being adsorbed on something and then later being released, say after 5 minutes.

Va'vra: Radicals tend to have large dipole moments and will not diffuse far before being drawn to a surface [wire].

Kadyk: Can they diffuse as far as from the anode, where they may be created, to the cathode?

Va'vra: I think polymerization begins near the anode, then an entire ionized chain slowly drifts to the cathode.

Hess: If you have high enough mobility and you can remove them from the surface so that the vapor pressure is sufficient, yes. If you have an entire polymer film, then you have to break off fragments. For neutral species you may have a sizable dipole, but branch-type hydrocarbons may not have a significant dipole, compared to linear hydrocarbons. [To Williams] Is it possible that these would not be attracted to the wire as readily? Would that fit with your analysis of materials on anode vs. cathode?

Williams: There was evidence with the mass spectrometer of aromatics on the anode and not on the cathode, where more linear-type hydrocarbons were seen. I wanted to make a comment, in regard to the last talk [by Villa] on how to choose a gasket material for DME. You would be naturally drawn to halogenated, rubbery materials like viton and teflon because they would resist the swelling caused by solvents like DME. The chlorines and fluorines are likely to be stripped from the gasket, carrying with it silicon and sulphur [last talk] which may deposit. Solubility can be predicted with some confidence, but you can't always predict the transport of Si and S, in the presence of Cl and F.

Godfrey: The chambers have vastly more carbon in the gas than silicon. Since these elements have the same valence, what characteristic causes the silicon to make compounds so much more readily?

Williams: To give a counter example, even though Si and C are similar in their binding patterns, I think you'll agree that SiO_2 is very different from CO_2 .

Hess: Silicon compounds react very readily with oxygen. The kinematics of silicon reactions with oxygen are much more rapid than for carbon and oxygen. It is very difficult to make predictions; thermodynamics is of no help, since it applies only to equilibrium processes.

Williams: In regard to where the silicon comes from, we've heard about silicone rubbers, and about silica in silicate glass in G10, for example. Another possible source is sand; SiO_2 is used for strength as a reinforcing filler in synthetic and silicone rubbers; the latter is the weakest rubber and is strengthened by sand as a filler. Sulphur is used to cross-link polymeric rubbers (vulcanization), but is also used in some plastics. Speciality rubbers usually do not use sulphur vulcanization but depend on other processes.

Ritson: It is hard to see how silicon from sand [or G10 walls], having essentially zero vapor pressure, can get into the gas and migrate ≈ 10 cm to the wire.

Williams: How it would get out of the rubber isn't clear either. If it is stripped out with Cl or F, making volatile species, and then if oxygen were present in the system, the silicon could recombine with oxygen, making deposits. It would be interesting to take a real chamber and deposit some sand, and check for silicon on the wires while monitoring the gas outflow.

Majewski: One can easily fall into traps when not knowing where the contaminants come from. For example, silicone oil is commonly used in drawing copper tubing which may be used for plumbing wire chambers. Hard plastic, like nylon, may be much better. Checks should probably be made of every material [in the gas system] before building a full-sized detector.

Kadyk: Is it a possibility worth considering to "clean up" a damaged chamber by putting in pure fluorine and/or pure oxygen?

Hess: If the chamber is dead due to carbonaceous deposits, yes, that would be possible by generating oxygen atoms in a discharge. Simply flowing oxygen through will do nothing — oxygen atoms are necessary. But if there is silicon present, the oxygen will form a still more stable species. The fluorine can etch silicon compounds to remove it, but may remain behind on surfaces after the treatment process.

Nelson: I've been surprised by the results presented here that for a given no. of coulombs/cm, there is less aging at high gas gain. Is there an explanation?

Va'ura: There is probably a sensitivity to density of electrons [as seen in plasma chemistry literature], since this controls the free radical density. Increasing the gain can actually decrease the density because the avalanche spreads out.

Pile: The gain loss plotted vs. time instead of charge shows that higher gain actually accelerates the rate of aging of chambers.

Wagner [to Hess]: There is a group at Brookhaven that is using pure CF_4 . Would you like to comment on this gas relative to a hydrocarbon gas?

Hess: I think the advantage of having halogens present is that you can get both etching of carbonaceous residue as well as polymerization. With only hydrocarbons present, the hydrogen is not nearly as efficient in forming a volatile species, compared to a halogen. To etch thin films in microelectronic processes we will use compounds like CF_4 , dissociate them in a discharge and allow the F atoms to attack the film material. Secondly, the halogens have a high cross section for electron attachment and this will affect the properties of the chamber. Having the halogens present can definitely help in reducing the onset of polymerization.

FOURTH DISCUSSION PERIOD, FRIDAY PM

(After J. Va'vra's talk)

Sauli [to Va'vra]: Did I understand that the number of radicals produced in the avalanche is orders of magnitude larger than the number of ions? Possibly this is true in plasma chemistry studies, but there are two reasons to doubt that this is true for wire chambers. One is the measurement of methane disappearing from a sealed counter: the number of disappearing molecules is equal to the number of ions produced. The other reason has to do with the calculation of the avalanche itself. Models of the avalanche must take into account where the energy available to electrons is going, into different processes. The energy balance is rather good if half of the energy goes into elastic or inelastic *non-ionizing* processes, and the other half into ions. So I don't see where all the energy is coming from to make all these radicals.

Va'vra: The average electron energy in an avalanche may be around 10 eV, while it takes 3-4 eV to damage a molecule. In plasma chemistry studies the radicals are 4-5 orders of magnitude higher [than ions]. Finally, I do not believe in the validity of the modeling, since the cross sections are not known, and they are important. Nobody knows these numbers.

Sauli: It has been done [modeling] with rather good results in terms of energy resolution.

Williams: It is generally true that free radical lifetimes in a very dilute plasma will be long, and in a dense plasma will be short. This will tend to make the concentration of radicals smaller in the present case [wire chambers] than in the plasma chemistry case. I don't have a feeling for whether this could account for orders of magnitude difference. The radicals, which are neutral, will certainly not be swept out as readily as ions, but whether this accounts for orders of magnitude difference in density, I don't know.

Atac: One thing I would like to emphasize, the most important thing, is the need to stop glow discharge and breakdown in chambers, the fast aging mechanism that should be prevented. We have a result from the CELLO group that even with aged chambers they were able to stop breakdown using alcohol. If you start with alcohol, the aging can be very slow.

Hilke: It is my feeling that there may be more than one process involved in the various kinds of polymerization. In one example, there is the presence of oils, which I think is the case in a large number of big experiments, having oil bubblers, O-rings, or having copper tubes not well cleaned. In these cases you may not need radicals or ionization at all. Molecules can settle down on the wire before there is even an avalanche, due to attraction via their dipole moment in the very inhomogeneous electric field. Then the electrons, when they come, can very easily do the cross-linking. In the example I gave, 10^{-9} mm (or $\approx 10^{-6}$ ppm) of silicon oil vapor in the gas led to a very rapid growth of polymers on the anode.

Nelson [to Va'vra]: I did not understand how the density of electrons can be *lower* in an avalanche when operating at *higher* gas gain.

Va'vra: My naive understanding is that at higher gain the avalanche spreads so much that the electron density is actually lower, and therefore also the free radical density [which results in a lower per Coulomb aging rate].

Parker: In order to avoid oil bubblers, a long open exhaust tube is sufficient, with an "ebb/flow" region, to accommodate atmospheric pressure changes, calculated from the chamber volume and expected barometric changes to stay safely near the tube exit. Diffusion [of air] up the tube has a short attenuation length.

Pile: I have used oil bubbles over long periods and have never associated trouble with them. Is there really any evidence to suspect them?

Atac: I also have had no problems with silicon oil bubblers.

Odian: We have heard about two different kinds of diseases: those diseases associated with the anode wire where there was a loss of efficiency but the chamber did not draw current. Another disease is where the chamber suddenly begins drawing current. This may be not quite the Malter effect. The cathode wires are coated with a very thin film that makes them very photosensitive. The photons released at the anode can then easily release electrons from the cathode surface causing regeneration. Adding water or alcohol vapor, or possibly DME, absorbs these ultraviolet photons and helps break the "link."

Wagner: This mechanism should show the characteristic drift time for pulses resulting from electrons knocked out of the cathode. Is there any evidence for this?

Hilke: With plastic tubes run in the streamer mode, this effect could be very important. A higher ohmic resistivity usually means that some areas are conducting and others are at all not conducting, so there could be charging up of the insulating spots.

Binnie: Suppose I took a cathode wire 100 μm diameter and 20 kV/cm on the wire, and I released an electron from the wire, what would the amplification be? What would the chance be of a positive ion coming back?

Va'vra: At about 2.5 kV/cm you have elastic collisions, at about 10 kV/cm in argon you can create electrons and photons. The photon could eject an electron from the cathode surface.

Binnie: It would be interesting if there were a unit probability of making a second electron when you got to the "magic" 20 kV/cm.

Turala: Cerenkov ring imaging counters use photo-sensitive materials like TMAE in the gas. Does anybody know of the aging properties of this?

Atac: Dave Anderson at Fermilab is interested in TMAE, because he would like to collect photons from scintillating glass to do calorimetry. He did some tests. With 0.15C of charge he found the gain has dropped very substantially in TMAE plus isobutane. In TMAE plus ethanol, he again sees droplets on the anode wire, but it works better. With CO_2 aging is also visible. The lost gain could be partially restored by flowing alcohol vapors: 40-50% back up to 80-85%. Some deposits remained. These chambers run at about 20 Torr.

Hilke: I'm surprised that the question of water vapor did not come up again. Argus at DESY has had very big aging problems, with a mixture of propane, methylal and hydrogen, I think. They added about 0.6% water, and since then they have been operating without any problems whatsoever. The water does not *remove* the layer, since removing the water makes the old problem reappear immediately, and restoring the water makes it disappear again. I think water is a very nice additive; it doesn't help everywhere, but

is very often useful. Looking at their surfaces you see cracks in the layers, and my understanding is that water provides sufficient conductivity to remove the charge which would otherwise build up. They have been running with water vapor for about two years now with no further problems.

APPENDIX B

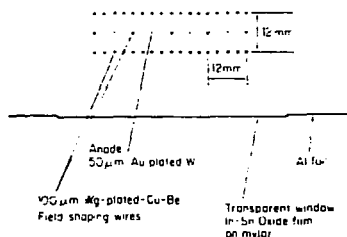
Result Summaries

SUMMARY OF RESULTS — WIRE AGING

Name and Institution: Muzaffer Atac / Fermilab
Telephone: (312) 840-3960
Laboratory test or result from experiment: Lab tests
Name of Detector (if from experiment): Drift Chamber

Significant degradation of performance: Did not occur
Describe the most significant change: Very little deterioration of pulse height spectrum with Fe^{56} source.

Make a small simple sketch of the cell:



Anode wire material and diameter: 50 μm , Au plated W
Cathode wire material and diameter (if applicable): 100 μm
Electric field on anode wire surface: 1.5×10^5 kV/cm
Electric field on cathode surface: 12-14 kV/cm
Electric field on potential wire surface (if applicable): 16 kV/cm

High/low intensity (particle rate in Hz/cm or anode current in nA/cm)?: 440 nA/cm
Approximate total integrated particle flux (No./cm²): 1.2×10^5
Approximate total gain (per primary electron): 5×10^4
Type of radiation (e.g. beam particles, Fe^{56} , Sr^{90} , etc.): $\text{Ru}^{106} \beta^-$
Number of primary electrons per ionization event: Varying
Approximate total charge dose (C/cm): 1.5

Type of gas (including "additives"): 50/50 $\text{Ar}/\text{C}_2\text{H}_6$ + 0.5% $\text{CH}_3\text{CH}_2\text{OH}$
Gas flow rate (gas volume/hour): 100 cc/min, 6 liters/hr
Gas flow condition: Vented
Gas impurities (water, oxygen, halogens, etc.): less than 10 ppm
Gas pressure (atm): atm
Can gas system be evacuated?: no
Length and material of gas tubing: 12 ft, Polyflow
List of other materials in the system: G10 and epoxy

Oils or greases in the system: no reason to have
Method of analysis of deposits: $\times 1000$ magnified microscopic picture
List the elements found in deposits:

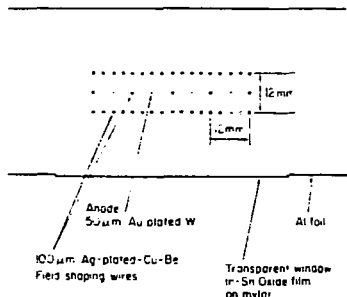
Major conclusion of the study (you can use the other side also): I do not think that there was any appreciable polymerization on the anode or cathode with this gas mixture after 1.5 C of charge per wire per cm. There may be very small amount of (possibly oxidation) impurity coating on the anode.

SUMMARY OF RESULTS — WIRE AGING

Name and Institution: Muzaffer Atac / Fermilab
Telephone: (312) 840-3960
Laboratory test or result from experiment: Lab tests
Name of Detector (if from experiment): Drift Chamber

Significant degradation of performance: Did not occur
 Describe the most significant change: Slight deterioration of pulse height distribution with Fe^{56} 5.9 KeV line width.

Make a small simple sketch of the cell:



Anode wire material and diameter: 50 μm , Au plated W
Cathode wire material and diameter (if applicable): 100 μm Au-plated Be-Cu
Electric field on anode wire surface: 1.6×10^5 kV/cm
Electric field on cathode surface: 12-14 kV/cm
Electric field on potential wire surface (if applicable): 16 kV/cm

High/low intensity (particle rate in Hz/cm or anode current in nA/cm)?: 500 nA/cm
Approximate total integrated particle flux (No./cm²): 1.2×10^5
Approximate total gain (per primary electron): 5×10^4
Type of radiation (e.g. beam particles, Fe^{56} , Sr^{90} , etc.): Ru^{106} β -source
Number of primary electrons per ionization event: Varies largely
Approximate total charge dose (C/cm): 2

Type of gas (including "additives"): 50/50 $\text{A}/\text{C}_2\text{H}_6$ + 0.7% $\text{CH}_3\text{CH}_2\text{OH}$
Gas flow rate (gas volume/hour): 100 cc/min, 6 liters/hr
Gas flow condition: Vented
Gas impurities (water, oxygen, halogens, etc.): less than 10 ppm
Gas pressure (atm): atm
Can gas system be evacuated?: no
Length and material of gas tubing: 12 ft, Polyflow
List of other materials in the system: G10 and epoxy

Oils or greases in the system: No
Method of analysis of deposits: $\times 1000$ magnified microscope
List the elements found in deposits:

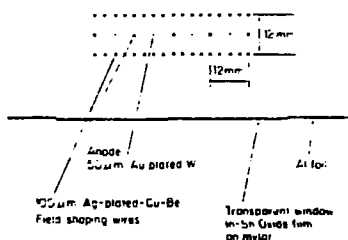
Major conclusion of the study (you can use the other side also): With clean system, clean gas and this gas mixture lifetime of wires can be long.

SUMMARY OF RESULTS — WIRE AGING

Name and Institution: Muzaffer Atac / Fermilab
Telephone: (312) 840-3960
Laboratory test or result from experiment: Lab tests
Name of Detector (if from experiment): Drift Chamber

Significant degradation of performance: Did not occur
Describe the most significant change: Very little deterioration of pulse height spectrum with Fe^{55} source.

Make a small simple sketch of the cell:



Anode wire material and diameter: 50 μm , Au plated W
Cathode wire material and diameter (if applicable): 100 μm
Electric field on anode wire surface: 1.65×10^5 kV/cm
Electric field on cathode surface: 12-14 kV/cm
Electric field on potential wire surface (if applicable): 16 kV/cm

High/low intensity (particle rate in Hz/cm or anode current in nA/cm)?: 600 nA/cm
Approximate total integrated particle flux (No./cm²): 1.2×10^6
Approximate total gain (per primary electron): 5×10^4
Type of radiation (e.g. beam particles, Fe^{55} , Sr^{90} , etc.): $\text{Ru}^{106} \beta^-$
Number of primary electrons per ionization event: Varying
Approximate total charge dose (C/cm): 1.0

Type of gas (including "additives"): 50/50 $\text{A}/\text{C}_2\text{H}_6 + 1.5\% \text{CH}_3\text{CH}_2\text{OH}$
Gas flow rate (gas volume/hour): 100 cc/min, 6 liters/hr
Gas flow condition: Vented
Gas impurities (water, oxygen, halogens, etc.): less than 10 ppm
Gas pressure (atm): atm
Can gas system be evacuated?: no
Length and material of gas tubing: 12 ft, Polyflow
List of other materials in the system: G10 and epoxy

Oils or greases in the system: no reason to have
Method of analysis of deposits: $\times 1000$ magnified microscopic picture
List the elements found in deposits:

Major conclusion of the study (you can use the other side also): I do not think that there was any appreciable polymerization on the anode or cathode with this gas mixture after 1.0 C of charge per wire per cm. There may be very small amount of (possibly oxidation) impurity coating on the anode.

SUMMARY OF RESULTS — WIRE AGING

Name and Institution: W. Beusch / CERN

Telephone: 3057

Laboratory test or result from experiment: Experiment

Name of Detector (if from experiment): OMEGA

Significant degradation of performance: Did not occur

Describe the most significant change:

Make a small simple sketch of the cell:



10 mm

Anode wire material and diameter: ϕ 20 μ m gold plated tungsten

Cathode wire material and diameter (if applicable): Flat

Electric field on anode wire surface: 293 kV/cm

Electric field on cathode surface: 4.6 kV/cm

Electric field on potential wire surface (if applicable):

High/low intensity (particle rate in Hz/cm or anode current in nA/cm)?:

$5 \cdot 10^7 / \text{cm}^2 / \text{sec}$

Approximate total integrated particle flux (No./cm²): $10^{13} / \text{cm}^2$

Approximate total gain (per primary electron): $6 \cdot 10^4$

Type of radiation (e.g. beam particles, Fe⁵⁶, Sr⁹⁰, etc.): Beam particles

Number of primary electrons per ionization event: 30

Approximate total charge dose (C/cm): 3 C/cm wire

Type of gas (including "additives"): 65% Ar, 35% isoButane, 1.5% Isopropanol

Gas flow rate (gas volume/hour): .025 detector volume/h

Gas flow condition: Vented

Gas impurities (water, oxygen, halogens, etc.):

Gas pressure (atm): 1 atm

Can gas system be evacuated?: No

Length and material of gas tubing: 50 m copper + 10 m Rilsan (polyamide 11)

List of other materials in the system: None

Oils or greases in the system: No

Method of analysis of deposits:

List the elements found in deposits:

Major conclusion of the study (you can use the other side also):

The chambers at OMEGA have been in the beam since 1979. Intensity used last 3 years: $(1-2) \cdot 10^7 / 2 \text{ sec}$. The beam region is not deadened but does not respond above about $10^5 / \text{cm}^2 / \text{sec}$ due to space charge.

SUMMARY OF RESULTS — WIRE AGING

Name and Institution: David M. Binnie / Imperial College

Telephone: 01-589-5111 (U.K.)

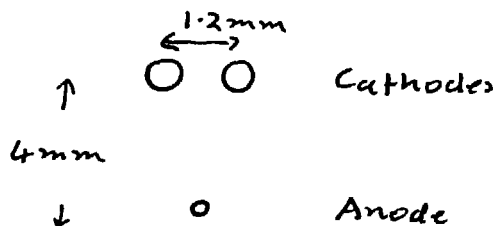
Laboratory test or result from experiment: Experiment

Name of Detector (if from experiment): TASSO VXD

Significant degradation of performance: Did not occur

Describe the most significant change: See qualification below

Make a small simple sketch of the cell:



Anode wire material and diameter: Tungsten-rhenium, gold plated, 20 μ

Cathode wire material and diameter (if applicable): Be-Cu, silver coated, 100 μ

Electric field on anode wire surface: 350 kV/cm

Electric field on cathode surface: 35 kV/cm

Electric field on potential wire surface (if applicable): —

High/low intensity (particle rate in Hz/cm or anode current in nA/cm)?: Up to ~ 10 nA/cm

Approximate total integrated particle flux (No./cm²):

Approximate total gain (per primary electron):

Type of radiation (e.g. beam particles, Fe⁵⁶, Sr⁹⁰, etc.): e^+e^- background

Number of primary electrons per ionization event:

Approximate total charge dose (C/cm): 0.22 C/cm

Type of gas (including "additives"): 95/5 Argon/CO₂. Argon through water, CO₂ through ethanol, both at 7.5 °C

Gas flow rate (gas volume/hour): 0.5 litres/hour at 3 atm

Gas flow condition: Vented

Gas impurities (water, oxygen, halogens, etc.):

Gas pressure (atm): 3 atm absolute

Can gas system be evacuated?: Probably, but don't

Length and material of gas tubing: 70 m copper

List of other materials in the system: short length of plastic tubing (not PVC)

Oils or greases in the system: Smear on 'O' rings. Non-silicon. Just downstream.

Method of analysis of deposits: — No analysis

List the elements found in deposits: —

Major conclusion of the study (you can use the other side also): Striking 'Matter-like' behaviour after approximately 0.02 C/cm. Eventually fixed as above. Clear evidence that water alone was insufficient. Present mixture gives very low ethanol content. Don't know if water is necessary or not.

Argon/CO₂ as above was reached by

- a) Need to avoid whiskers in Argon/ethane (evidence).
- b) Need to keep H.V. low.

SUMMARY OF RESULTS — WIRE AGING

Name and Institution: Penny Estabrooks / Carleton Univ.

Telephone: 613-564-7193

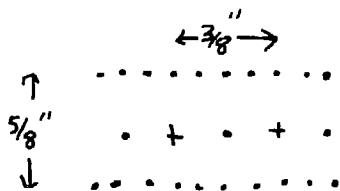
Laboratory test or result from experiment: Experiment

Name of Detector (if from experiment): Tagged Photon Spectrometer

Significant degradation of performance: Occurred

Describe the most significant change: Large inefficiency in high rate region of chamber

Make a small simple sketch of the cell:



Anode wire material and diameter: .001" Au plated tungsten

Cathode wire material and diameter (if applicable): Cu-Be, .003"

Electric field on anode wire surface:

Electric field on cathode surface:

Electric field on potential wire surface (if applicable):

High/low intensity (particle rate in Hz/cm or anode current in nA/cm)?: 30-50 kHz/cm

Approximate total integrated particle flux (No./cm²): 10¹¹

Approximate total gain (per primary electron): 2 × 10⁵

Type of radiation (e.g. beam particles, Fe⁵⁶, Sr⁹⁰, etc.): e⁺e⁻ pairs from γ beam

Number of primary electrons per ionization event: ~ 50

Approximate total charge dose (C/cm): ~ 0.3

Type of gas (including "additives"): 50-50 Ar-ethane (+1.5% ethanol)

Gas flow rate (gas volume/hour): 600 l/hour

Gas flow condition: Vented

Gas impurities (water, oxygen, halogens, etc.):

Gas pressure (atm): 1 + ε

Can gas system be evacuated?:

Length and material of gas tubing: ≥ 100 m Cu tubing

List of other materials in the system: Al, mylar, G10, RTV, epoxy ...

Oils or greases in the system:

Method of analysis of deposits: AES

List the elements found in deposits:

Major conclusion of the study (you can use the other side also):

- ethanol addition stopped excessive current draw to HV breakdown
- rate-related deposits observed on anodes, much less on cathodes

SUMMARY OF RESULTS — WIRE AGING

Name and Institution: Brian Foster / Bristol University, U.K.

Telephone: U.K. 0272 303030, ext. 3699

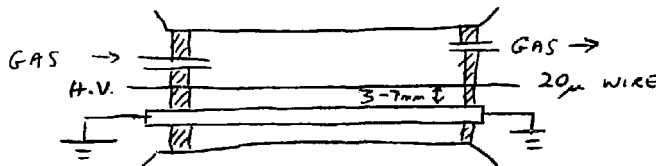
Laboratory test or result from experiment: Lab test

Name of Detector (if from experiment): —

Significant degradation of performance: Occurred

Describe the most significant change: Whisker growth and deposition on wire

Make a small simple sketch of the cell:



Anode wire material and diameter: Aluminium Bar

Cathode wire material and diameter (if applicable): 20 μ gold-plated Tungsten-Rhenium

Electric field on anode wire surface: —

Electric field on cathode surface: ~ 100 kV/cm

Electric field on potential wire surface (if applicable): —

High/low intensity (particle rate in Hz/cm or anode current in nA/cm)?: Forced discharge

Approximate total integrated particle flux (No./cm²): —

Approximate total gain (per primary electron): —

Type of radiation (e.g. beam particles, Fe⁵⁶, Sr⁹⁰, etc.): —

Number of primary electrons per ionization event: —

Approximate total charge dose (C/cm): —

Type of gas (including "additives"): Argon/Ethane 50/50; + Ethanol; CO₂; Ar/Methane; Ar/Isobutane

Gas flow rate (gas volume/hour): 12 l/hour

Gas flow condition: Vented

Gas impurities (water, oxygen, halogens, etc.): —

Gas pressure (atm): 1

Can gas system be evacuated?: No

Length and material of gas tubing: 5 m copper

List of other materials in the system: O-ring seal

Oils or greases in the system: None

Method of analysis of deposits: None

List the elements found in deposits: —

Major conclusion of the study (you can use the other side also):

Whisker growth investigated using forced discharge at sufficiently high fields, mixes containing Ethane with/without Ethanol would grow whiskers. Similar conclusions for Methane + Isobutane.

CO₂ mixtures would not support whisker growth, but do coat cathode with dark deposit.

CO₂ mixtures burn away grown whiskers formed in hydrocarbon gas mixtures.

SUMMARY OF RESULTS — WIRE AGING

Name and Institution: Persis Drell / LBL

Telephone: 486-7190

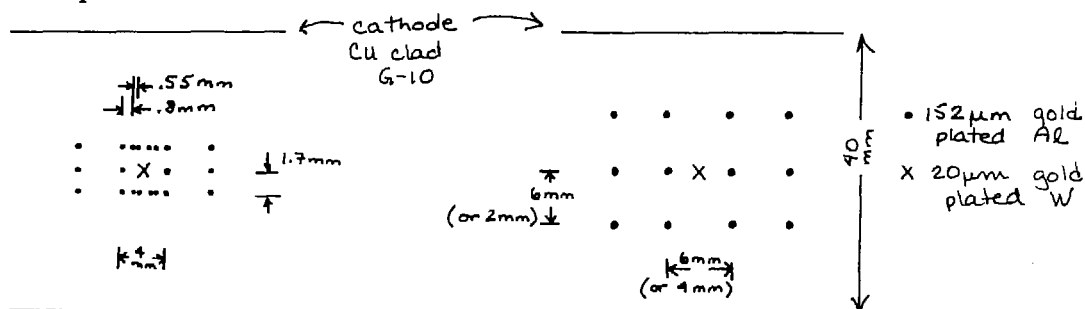
Laboratory test or result from experiment: Lab test

Name of Detector (if from experiment):

Significant degradation of performance: Occurred

Describe the most significant change: Sustained discharge in cell, Maltre effect

Make a small simple sketch of the cell:



Anode wire material and diameter: Gold plated tungsten, 20 μm diam.

Cathode wire material and diameter (if applicable): Gold plated Al, .006" D

Electric field on anode wire surface: 630 kV/cm

Electric field on cathode surface: < 1 kV/cm

Electric field on potential wire surface (if applicable): -10 kV/cm \rightarrow -16 kV/cm

High/low intensity (particle rate in Hz/cm or anode current in nA/cm)?: 24 kHz/cm,
150-400 nA in 1 cm of wire

Approximate total integrated particle flux (No./cm²):

Approximate total gain (per primary electron): 2×10^5

Type of radiation (e.g. beam particles, Fe⁵⁵, Sr⁹⁰, etc.): Fe⁵⁵

Number of primary electrons per ionization event: 200

Approximate total charge dose (C/cm): .03 C/cm \rightarrow .38 C/cm depending on test

Type of gas (including "additives"):

Gas flow rate (gas volume/hour): .07 scfh

Gas flow condition: Vented

Gas impurities (water, oxygen, halogens, etc.): H₂O, O₂ < 10 ppm

Gas pressure (atm): 3

Can gas system be evacuated?: yes

Length and material of gas tubing: Cu, 10 ft.

List of other materials in the system: Al, epoxy, G10, solder, Teflon cable, ceramic capacitors

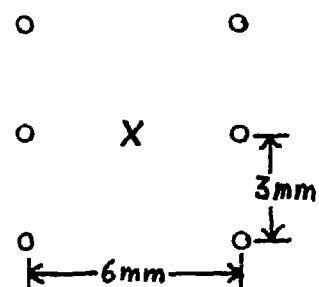
Oils or greases in the system: Mechanical pump oil — (10 ft away)

Method of analysis of deposits: Visual inspection only

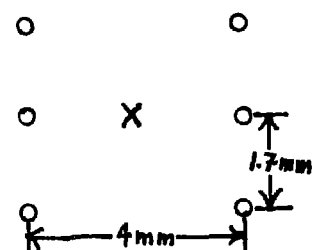
List the elements found in deposits:

Major conclusion of the study (you can use the other side also): Varying the spacing and number of potential wires about the sense wire had dramatic effects on wire lifetime. Listed below are the results for different wire configurations. (Cathode distance remained unchanged.)

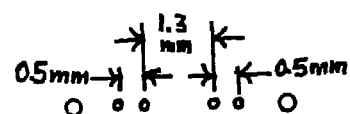
i (nA)	gain	max. surf. field (kV/cm)	Q_{tot} (C/m)
290	4×10^5	-16	.38



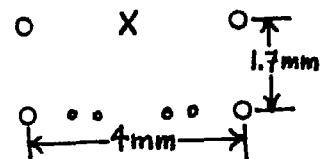
240	2×10^5	-14	.15
-----	-----------------	-----	-----



25*	2×10^5	-10	.031
-----	-----------------	-----	------



160	2.5×10^5	-10	.039
-----	-------------------	-----	------



250	4×10^5	-12	.03
-----	-----------------	-----	-----

*Middle gridwire had + charge.

SUMMARY OF RESULTS — WIRE AGING

Name and Institution: Dr. H. Hartmann / Bonn University (usually at DESY)

Telephone: DESY 49 40 89980

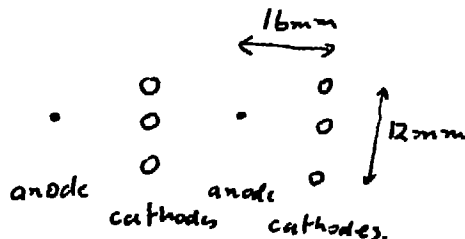
Laboratory test or result from experiment:

Name of Detector (if from experiment): TASSO Cylindrical Drift Chamber

Significant degradation of performance: Occurred

Describe the most significant change: Loss of gain after ~ 5 years. Now more stable.

Make a small simple sketch of the cell:



Anode wire material and diameter: Tungsten-rhenium, gold plated, $30\ \mu\text{m}$

Cathode wire material and diameter (if applicable): Molybdenum, gold plated, $120\ \mu\text{m}$

Electric field on anode wire surface: $230\ \text{kV/cm}$

Electric field on cathode surface: $18\text{--}20\ \text{kV/cm}$

Electric field on potential wire surface (if applicable): —

High/low intensity (particle rate in Hz/cm or anode current in nA/cm)?:

up to $\sim 5\ \text{nA/cm}$

Approximate total integrated particle flux (No./cm²):

Approximate total gain (per primary electron):

Type of radiation (e.g. beam particles, Fe⁵⁶, Sr⁹⁰, etc.): Background from e^+e^- machine

Number of primary electrons per ionization event:

Approximate total charge dose (C/cm): Inner wires, $0.2\text{--}0.4\ \text{C/cm}$. Outer, $\sim 0.07\ \text{C/cm}$.

Type of gas (including "additives"): Argon/Ethane through alcohol (ethyl) at 2°C

Gas flow rate (gas volume/hour): $600\ \text{l/hour}$

Gas flow condition: Vented

Gas impurities (water, oxygen, halogens, etc.): Argon very pure. Ethane, 99.5%. Gases filtered.

Gas pressure (atm): 1.0

Can gas system be evacuated?: No

Length and material of gas tubing: $70\ \text{m}$ copper + $\sim 10\ \text{m}$ 'good', not PVC, plastic tubing.

List of other materials in the system: Bubbler many metres downstream. Vac. oil. Al end plates.

Epoxy + glass fibre tube.

Oils or greases in the system:

Method of analysis of deposits: —

List the elements found in deposits: —

Major conclusion of the study (you can use the other side also):

After 1st year, changed from 90/10 Argon/methane to 50/50 Argon ethane. Alcohol (ethanol) was added in 1982. Some loss of gain noted at end of '83, on all wires; H.V. raised 100 V, oil removed from ethane and gas filtering improved. Since then, no clear evidence for further deterioration.

Apart from the 100 V increase in H.V. the chamber has continued to work for seven years.

SUMMARY OF RESULTS — WIRE AGING

Name and Institution: Hilke, H.J. / CERN

Telephone: 83 3789

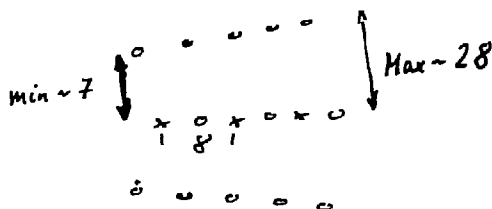
Laboratory test or result from experiment: Experiment R807

Name of Detector (if from experiment): Jet Chamber of AFS

Significant degradation of performance: Occurred

Describe the most significant change: Some $-\Delta PH \sim 20\%$

Make a small simple sketch of the cell:



Anode wire material and diameter: Stablohm (Ni, Cr; Al + Si + O/72.5, 22.5, 5%) $30 \mu m$

Cathode wire material and diameter (if applicable): Cu/Be $100 \mu m$

Electric field on anode wire surface: var. $\sim 230 \text{ KV/cm}$

Electric field on cathode surface: var. $\sim 10 \text{ KV/cm}$

Electric field on potential wire surface (if applicable): $< 10 \text{ KV/cm}$

High/low intensity (particle rate in Hz/cm or anode current in nA/cm)?: High

Approximate total integrated particle flux (No./cm²):

Approximate total gain (per primary electron): $(3-6) \times 10^4$

Type of radiation (e.g. beam particles, Fe⁵⁶, Sr⁹⁰, etc.): Beam particles

Number of primary electrons per ionization event: ~ 50

Approximate total charge dose (C/cm): 0.02

Type of gas (including "additives"): Ar/C₂H₆ (50/50)

Gas flow rate (gas volume/hour):

Gas flow condition: partly vented, partly recirculated (typ. 50%)

Gas impurities (water, oxygen, halogens, etc.): H₂O: $> 100 \text{ ppm}$

Gas pressure (atm): 1

Can gas system be evacuated?: No

Length and material of gas tubing: Metal, $> 50 \text{ m}$

List of other materials in the system: G10, Mylar/Aclar

Oils or greases in the system:

Method of analysis of deposits: Electron Microscope + Fluorescence; + Auger Au

List the elements found in deposits: b Si, O; $< 0.5\% \text{ C}$

Major conclusion of the study (you can use the other side also): From measurements with test chambers we know that after ~ 4 years of operation at the ISR the integrated charge was not far from values which likely would produce serious effects as discharges.

SUMMARY OF RESULTS — WIRE AGING

Name and Institution: Hilke, H.J. / CERN

Telephone: 83 3789

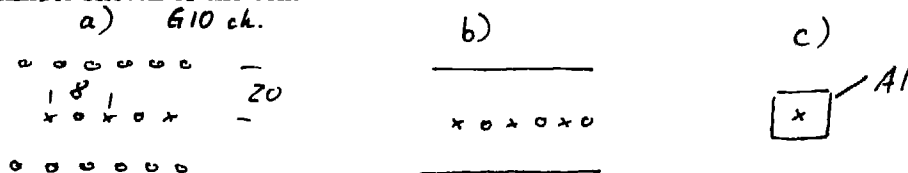
Laboratory test or result from experiment: Laboratory test

Name of Detector (if from experiment):

Significant degradation of performance: Occurred

Describe the most significant change: $-\Delta PH$ and finally often discharges

Make a small simple sketch of the cell:



a') Perspex Ch.

Anode wire material and diameter: Stablohm, 30 μm (Ni/Cr + Al, Si, ...)

Cathode wire material and diameter (if applicable): Cu/Be, 100 μm

Electric field on anode wire surface: ~ 200 kV/cm

Electric field on cathode surface: ≤ 10 kV/cm

Electric field on potential wire surface (if applicable): < 10 kV/cm

High/low intensity (particle rate in Hz/cm or anode current in nA/cm): High. ~ 100 nA/cm

Approximate total integrated particle flux (No./cm²):

Approximate total gain (per primary electron): 3×10^4

Type of radiation (e.g. beam particles, Fe⁵⁶, Sr⁹⁰, etc.): Fe⁵⁶

Number of primary electrons per ionization event: 220

Approximate total charge dose (C/cm): 0.02 - 0.3

Type of gas (including "additives"): α) C₂H₆, β) + Methylal, γ) + H₂, δ) + H₂O, ϵ) Ar/CO₂

Gas flow rate (gas volume/hour):

Gas flow condition: Vented

Gas impurities (water, oxygen, halogens, etc.): Small

Gas pressure (atm): 1

Can gas system be evacuated?: No

Length and material of gas tubing: > 2 m, Cu

List of other materials in the system: G10, oil bubbler

Oils or greases in the system: exc. for { c) and Perspex ch. a')

Method of analysis of deposits: Electron Microscope + Fluorescence Au.; sometimes Auger Au.

List the elements found in deposits: Mostly Si; O; sometimes S, Cl; little Si in [a), ϵ)]

Major conclusion of the study (you can use the other side also):

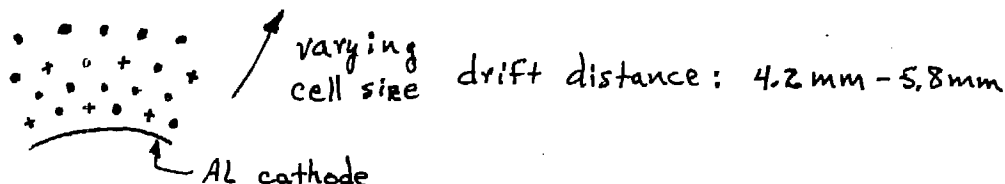
- Deposits only on anodes, insulating
- Mostly containing Si
- Appearance of layer can change easily: [a), α] shows strong, smooth layer; introduction of cold trap produces thin fibres
- Cathode important: ageing a) $>$ b) $>>$ c)!
- H₂O reduces ageing, H₂ not; (for our system) $\sim 10^3$ 200 $<< 150$ %/C/cm
- Suppression of G10 and oil bubbler suppressed Si, but chamber still aged, with deposits containing S, Cl, O.
- C detected in Auger analysis, but only on top 100 Å and same signal on unused wire
- Concerning Si-compound layers we assume: oil-like molecules (from bubbler, G10 surfaces, gas-impurities) adhere to the anode wire and are cross-linked under electron bombardment, to form solid deposits

SUMMARY OF RESULTS — WIRE AGING

Name and Institution:* T. Jensen / Ohio State University (Stationed at Cornell Univ.)
Telephone: 607-256-4882
Laboratory test or result from experiment: Experiment
Name of Detector (if from experiment): Cleo Vertex Detector

Significant degradation of performance: Did not occur
 Describe the most significant change: possible small change in pulse height

Make a small simple sketch of the cell:



Anode wire material and diameter: 0.8 mil Stableohm 800
Cathode wire material and diameter (if applicable): $\frac{6.4}{5.8}$ mil gold-plated Al (stress relieved 5056)
Electric field on anode wire surface: $\lesssim 300$ kV/cm
Electric field on cathode surface: 10-15 kV/cm
Electric field or potential wire surface (if applicable): N.A.

High/low intensity (particle rate in Hz/cm or anode current in nA/cm)?: .003 nA/cm averaged over entire wire

Approximate total integrated particle flux (No./cm²):

Approximate total gain (per primary electron): $\sim 4-8 \times 10^4$

Type of radiation (e.g. beam particles, Fe⁵⁵, Sr⁹⁰, etc.): particles + sync. rad. [e^+e^- machine ~ 10 GeV cm]

Number of primary electrons per ionization event:

Approximate total charge dose (C/cm): 0.035 - 0.04 C/cm (see conclusions)

Type of gas (including "additives"): Argon ($\approx 50\%$) + Ethane ($\approx 50\%$) + Ethanol ($\sim 0.3\%$)

Gas flow rate (gas volume/hour): 120 cc/min 0.16 volume/hr

Gas flow condition: Vented; constant pressure regulation

Gas impurities (water, oxygen, halogens, etc.): not tested

Gas pressure (atm): 1.0 atm. $\sim 60\%$ of data, $\sim 40\%$ of data @ 1.3 atm

Can gas system be evacuated?: no

Length and material of gas tubing: Copper $\left\{ \begin{array}{l} \sim 30 \text{ m inlet} \\ \sim 10 \text{ m outlet} \end{array} \right.$

List of other materials in the system: G10, delrin, epoxies, aluminized mylar, teflon, viton O-rings, flow meters

Oils or greases in the system: vacuum grease on O-rings

Method of analysis of deposits: not looked at

List the elements found in deposits:

Major conclusion of the study (you can use the other side also):

During 1-1/2 years of operation we have not observed any significant deterioration in chamber performance. Spatial resolution has remained in the range $\sigma \sim 80-100 \mu\text{m}$ for Bhabhas, and the efficiency for all layers has been $> 90\%$.

We estimate the **average** accumulated charge for the innermost cells to be 0.035-0.04 C/cm. We do not expect this charge to be distributed uniformly in ϕ or along the wire, but have no way of measuring this dependence.

We have observed a decrease in average pulse height for minimum-ionizing particles. However, this decrease seems to be limited to the synchrotron plane where background radiation is expected to be greater. We are presently studying this effect in more detail using Bhabha tracks.

*Collaborators in this project are: S. Behrends, T. Gentile, P. Haas, M. Hempstead, T. Jensen, H. Kagan, and R. Kass.

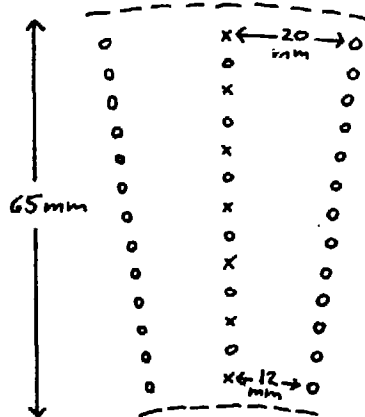
SUMMARY OF RESULTS — WIRE AGING

Name and Institution: Henning Kado / II. Inst. f. Exp. Physik
Telephone: 040/8998-2509 Universität Hamburg
Laboratory test or result from experiment: experiment
Name of Detector (if from experiment): JADE Vertex Detector

Significant degradation of performance: Did not occur
Describe the most significant change: increasing currents

Make a small simple sketch of the cell:

24 cells, 7 sense wires/cell
 wire spacing: 4.5 mm



Anode wire material and diameter: gold plated tungsten, 20 μm
Cathode wire material and diameter (if applicable): Cu Be, 700 μm
Electric field on anode wire surface: 240 kV/cm
Electric field on cathode surface: 20 ... 26 kV/cm
Electric field on potential wire surface (if applicable): 4 ... 5 kV/cm

High/low intensity (particle rate in Hz/cm or anode current in nA/cm)?: 6.3 nA/cm

Approximate total integrated particle flux (No./cm²):

Approximate total gain (per primary electron): $7 \cdot 10^4$

Type of radiation (e.g. beam particles, Fe⁵⁶, Sr⁹⁰, etc.): e^+e^- annihilation

Number of primary electrons per ionization event:

Approximate total charge dose (C/cm): 10^{-2} C/cm

Type of gas (including "additives"): Ar [89.1%] + CO₂ [9.9%] + CH₄ [1.0%]

Gas flow rate (gas volume/hour): 15 l/hr

Gas flow condition: Vented

Gas impurities (water, oxygen, halogens, etc.): ?

Gas pressure (atm): ~ 1.15 bar (constant density)

Can gas system be evacuated?: no

Length and material of gas tubing: ~ 90 m Cu pipe

List of other materials in the system: stainless steel, glass, brass, teflon, kapton

Oils or greases in the system: none

Method of analysis of deposits:

List the elements found in deposits:

Major conclusion of the study (you can use the other side also): The large standing currents observed in part of the JADE Vertex Chamber after six months' running, might be interpreted as a kind of "premature ageing" initiated by a mechanical imperfection in this area inside the chamber. The parasitic currents could be eliminated by adding a small amount of water to the chamber gas.

SUMMARY OF RESULTS — WIRE AGING

Name and Institution: Fabio Sauli / CERN

Telephone: (4122) 833670

Laboratory test or result from experiment: Laboratory test

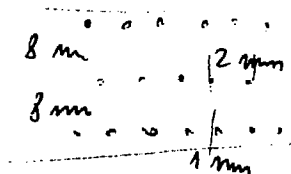
Name of Detector (if from experiment):

Significant degradation of performance: Occurred

Describe the most significant change: Lower gain — higher noise — DC current

Make a small simple sketch of the cell:

Standard MWPC with Wire Cathodes



Anode wire material and diameter: Tungsten, gold plated, \emptyset 20 μm

Cathode wire material and diameter (if applicable): Cu Be \emptyset 100 μm

Electric field on anode wire surface:

Electric field on cathode surface:

Electric field on potential wire surface (if applicable):

High/low intensity (particle rate in Hz/cm or anode current in nA/cm)?:

$\sim 10^4/\text{cm}^2 \cdot \text{sec}$

Approximate total integrated particle flux (No./cm²): 10^7 cm^2

Approximate total gain (per primary electron): 10^7

Type of radiation (e.g. beam particles, Fe⁵⁶, Sr⁹⁰, etc.): Sr⁹⁰

Number of primary electrons per ionization event: [Saturated gain: 1 electron sensitivity]

Approximate total charge dose (C/cm): 10^{-4} C/cm

Type of gas (including "additives"): "Magic" gas A 74.5, Iso C₄H₁₀ 25, CF₃Br 0.5

Gas flow rate (gas volume/hour): ~ 10 liters/hr

Gas flow condition:

Gas impurities (water, oxygen, halogens, etc.):

Gas pressure (atm): 1 Atm

Can gas system be evacuated?: No

Length and material of gas tubing: 5 m Teflon or Rilsen

List of other materials in the system: Mylar-Fiberglass-O-Rings

Oils or greases in the system: Oil bubbler

Method of analysis of deposits: Visual

List the elements found in deposits:

Major conclusion of the study (you can use the other side also):

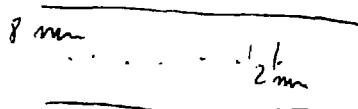
SUMMARY OF RESULTS — WIRE AGING

Name and Institution: Fabio Sauli / CERN
Telephone: (4122) 833670
Laboratory test or result from experiment: Laboratory test
Name of Detector (if from experiment):

Significant degradation of performance: Did not occur
 Describe the most significant change:

Make a small simple sketch of the cell:

Standard MWPC with Al Foil Cathodes



Anode wire material and diameter: Tungsten, gold-plated
Cathode wire material and diameter (if applicable):
Electric field on anode wire surface:
Electric field on cathode surface:
Electric field on potential wire surface (if applicable):

High/low intensity (particle rate in Hz/cm or anode current in nA/cm)?:

$\sim 10^5/\text{cm}^2 \cdot \text{sec}$

Approximate total integrated particle flux (No./cm²): $8 \cdot 10^{11}/\text{cm}^2$

Approximate total gain (per primary electron): 10^6

Type of radiation (e.g. beam particles, Fe⁵⁶, Sr⁹⁰, etc.): Fe⁵⁶

Number of primary electrons per ionization event: 200

Approximate total charge dose (C/cm): 0.1 C/cm

Type of gas (including "additives"): Argon-ethane 60-40

Gas flow rate (gas volume/hour): 10 liters/hr

Gas flow condition: Vented

Gas impurities (water, oxygen, halogens, etc.):

Gas pressure (atm): 1 Atm

Can gas system be evacuated?: No

Length and material of gas tubing: 5 m Rilson

List of other materials in the system: Fiberglass — O-Rings

Oils or greases in the system: Oil bubbler

Method of analysis of deposits:

List the elements found in deposits:

Major conclusion of the study (you can use the other side also): MWPC with foil electrodes and reasonably clean conditions live 0.1 C/cm or more in argon-ethane (without additives).

SUMMARY OF RESULTS — WIRE AGING

Name and Institution: Fabio Sauli / CERN

Telephone: (4122) 833670

Laboratory test or result from experiment: Laboratory test

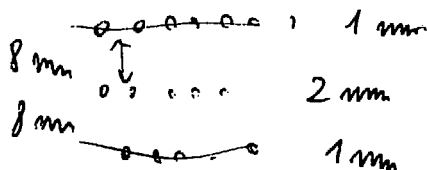
Name of Detector (if from experiment):

Significant degradation of performance: Did not occur

Describe the most significant change:

Make a small simple sketch of the cell:

Standard MWPC with Wire Cathodes



Anode wire material and diameter: Tungsten, Au plated, \emptyset 20 μm

Cathode wire material and diameter (if applicable): Cu Be \emptyset 100 μm

Electric field on anode wire surface:

Electric field on cathode surface:

Electric field on potential wire surface (if applicable):

High/low intensity (particle rate in Hz/cm or anode current in nA/cm)?:

$\sim 10^5 \text{ cm}^2/\text{sec}$

Approximate total integrated particle flux (No./cm²): $3 \cdot 10^{10}/\text{cm}^2$

Approximate total gain (per primary electron): 10^7

Type of radiation (e.g. beam particles, Fe⁵⁶, Sr⁹⁰, etc.): Sr⁹⁰

Number of primary electrons per ionization event: Single electron sensitivity (saturated gain)

Approximate total charge dose (C/cm): 0.3 C/cm

Type of gas (including "additives"): Magic + Methylal: A 74.5, i-C₄H₁₀ 25, CF₃Br 0.5, (O CH₃)₂CH₂ 4

Gas flow rate (gas volume/hour): ~ 10 liters/hr

Gas flow condition: Vented

Gas impurities (water, oxygen, halogens, etc.):

Gas pressure (atm): 1 Atm

Can gas system be evacuated?: No

Length and material of gas tubing: 5 m Rilson

List of other materials in the system: Mylar-Fiberglass-O-Rings

Oils or greases in the system: Oil bubbler

Method of analysis of deposits:

List the elements found in deposits:

Major conclusion of the study (you can use the other side also): Adding Methylal to magic gas improves lifetime by at least 3 orders of magnitude.

SUMMARY OF RESULTS — WIRE AGING

Name and Institution: D. Smith and D. Gee / UC Riverside

Telephone: (714) 787-5623

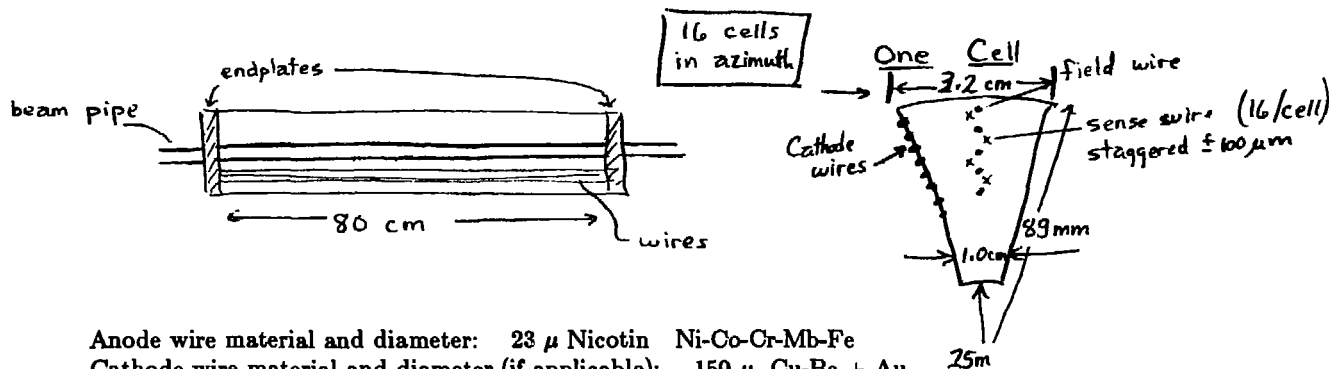
Laboratory test or result from experiment: UA1

Name of Detector (if from experiment): Microvertex Detector

Significant degradation of performance: Did not occur

Describe the most significant change:

Make a small simple sketch of the cell:



Anode wire material and diameter: $23\ \mu$ Nicotin Ni-Co-Cr-Mb-Fe

Cathode wire material and diameter (if applicable): $150\ \mu$ Cu-Be + Au

Electric field on anode wire surface: $442\ \text{kV/cm}$

Electric field on cathode surface: $34.8\ \text{kV/cm}$

Electric field on potential wire surface (if applicable): $6.0\ \text{kV/cm}$

High/low intensity (particle rate in Hz/cm or anode current in nA/cm)?:

Approximate total integrated particle flux (No./cm²): varies along the wire length in the SPS collider

Approximate total gain (per primary electron): $6 \pm 2 \times 10^4$ C

Type of radiation (e.g. beam particles, Fe⁵⁶, Sr⁹⁰, etc.): π, K, μ, e from $p\bar{p}$ collisions

Number of primary electrons per ionization event: ~ 30 primaries/cm \times 3 atmospheres

Approximate total charge dose (C/cm): 6×10^{-4}

Type of gas (including "additives"): Ar-C₂H₆ 53-47%

Gas flow rate (gas volume/hour): 15 liters/hour Chamber volume = 28 liters

Gas flow condition: Pre-mixed gas under pressure. Vented

Gas impurities (water, oxygen, halogens, etc.): No bubblers; all pre-mixed gas

Gas pressure (atm): 3

Can gas system be evacuated?: No

Length and material of gas tubing: ~ 20 meters teflon

List of other materials in the system:

Oils or greases in the system: Two gaskets to seal to the beam plate

Method of analysis of deposits: Electron microscope

List the elements found in deposits: Not enough deposits to warrant investigation at this time. However, we will go back and look.

Major conclusion of the study (you can use the other side also): We need to look at and investigate the chemical composition of the few residues we do have on our field wires. Sense wires appear clean under the microscope. Cathode wires appear clean under the electron microscope.

SUMMARY OF RESULTS — WIRE AGING

Name and Institution: Harold Spinka / Argonne National Lab

Telephone: (312) 972-6317

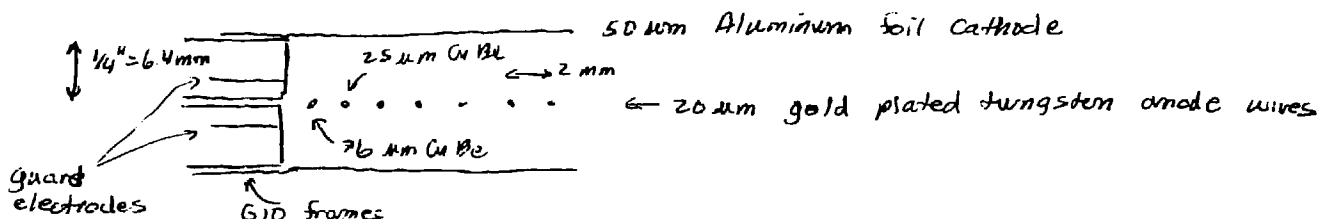
Laboratory test or result from experiment: experiments

Name of Detector (if from experiment):

Significant degradation of performance: Occurred

Describe the most significant change: silicon deposits on anode wire; fluorine deposits on cathode planes

Make a small simple sketch of the cell:



Anode wire material and diameter: 20 μm gold plated tungsten

Cathode wire material and diameter (if applicable): 50 μm aluminum foil

Electric field on anode wire surface:

Electric field on cathode surface:

Electric field on potential wire surface (if applicable):

High/low intensity (particle rate in Hz/cm or anode current in nA/cm):

Approximate total integrated particle flux (No./cm²): $10^{12}/\text{cm}^2/\text{experiment}$

Approximate total gain (per primary electron): 10^4

Type of radiation (e.g. beam particles, Fe⁵⁵, Sr⁹⁰, etc.): minimum ionizing beam protons

Number of primary electrons per ionization event: $\sim 100\text{-}150$

Approximate total charge dose (C/cm): 0.1-0.2 Coul/cm

Type of gas (including "additives"): 65% Ar, 35% CO₂, 0.5% freon 13B (CF₃ Br)

Gas flow rate (gas volume/hour): ~ 100 cc/hr

Gas flow condition: Vented

Gas impurities (water, oxygen, halogens, etc.): ≤ 100 ppm or perhaps ≤ 10 ppm of any impurity

Gas pressure (atm): atm

Can gas system be evacuated?: no

Length and material of gas tubing: $\sim 2 * (10 \text{ m polyflo} + 10 \text{ cm tygon})$

List of other materials in the system: mineral oil bubbler fluid, RTV gas seal

Oils or greases in the system: —

Method of analysis of deposits: ion microprobe mass analysis

List the elements found in deposits: Si, O mostly on anode wires, F mostly on aluminum foil planes, other elements seen (H, C, N, Na, K,...)

Major conclusion of the study (you can use the other side also):

- 1) $\geq 10,000$ angstroms Si, O layer on anode wires. The source of Si is not known.
- 2) $\sim 10^5$ Si deposited/incident beam particle.
- 3) Reasonably efficient mechanism to deposit silicon assuming it is present in the gas as an impurity.
- 4) No evidence for instabilities or breakdown.

SUMMARY OF RESULTS — WIRE AGING

Name and Institution: J. Va'vra / SLAC

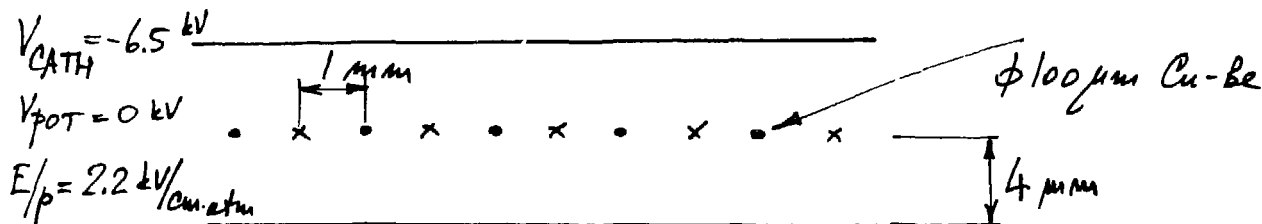
Telephone: (415) 854-3300 x 3299

Laboratory test or result from experiment: Test (Micro-Jet Chamber)

Name of Detector (if from experiment): —

Significant degradation of performance: Occurred

Describe the most significant change: HV instabilities, large currents



Anode wire material and diameter: $\phi 7.6 \mu\text{m}$, Ag (W)

Cathode wire material and diameter (if applicable): Continuous sheet, Cu

Electric field on anode wire surface: -760 kV/cm

Electric field on cathode surface: $+13.6 \text{ kV/cm}$

Electric field on potential wire surface (if applicable): -116 kV/cm

High/low intensity (particle rate in Hz/cm or anode current in nA/cm)?: Low, $\sim 100 \text{ Hz}$

Approximate total integrated particle flux (No./cm^2): $\sim 3 \times 10^8 / \text{cm}^2$

Approximate total gain (per primary electron): $\sim 10^5$

Type of radiation (e.g. beam particles, Fe^{55} , Sr^{90} , etc.): Fe^{55}

Number of primary electrons per ionization event: $\sim 220 \text{ e}^-$

Approximate total charge dose (C/cm): $\sim 4 \times 10^{-4} \text{ C/cm}$

Type of gas (including "additives"): 90% Ar + 10% C_4H_{10} ; "regular" purity

Gas flow rate (gas volume/hour): No flow

Gas flow condition: Sealed

Gas impurities (water, oxygen, halogens, etc.): Probably low, but not measured

Gas pressure (atm): 6.1 atm

Can gas system be evacuated?: Yes

Length and material of gas tubing: $\sim 10 \text{ m}$ Cu tubing

List of other materials in the system: Al pressure vessel, Cu, G-10, lemo cables, 5 min epoxy, teflon, lucite, rubber O-rings

Oils or greases in the system: Organic vacuum pump oil; Si based O-ring grease

Method of analysis of deposits: Visual and X-ray; deposits mostly on cathode (visual)

List the elements found in deposits: The method insensitive to organic compounds; other: Al, Au, Pd, Fe, Cr; no Si seen

Major conclusion of the study (you can use the other side also):

- Very poor lifetime measured, but consistent with similar results reported in literature about the permanently sealed counters
- The lifetime was also affected negatively by other variables:
 - a) Very thin anode wire
 - b) Use of a "regular purity" gas
 - c) High pressure operation (6.1 atm) — ?

SUMMARY OF RESULTS — WIRE AGING

Name and Institution: A. Wagner / Univ. Heidelberg

Telephone: (049-6221) 569220

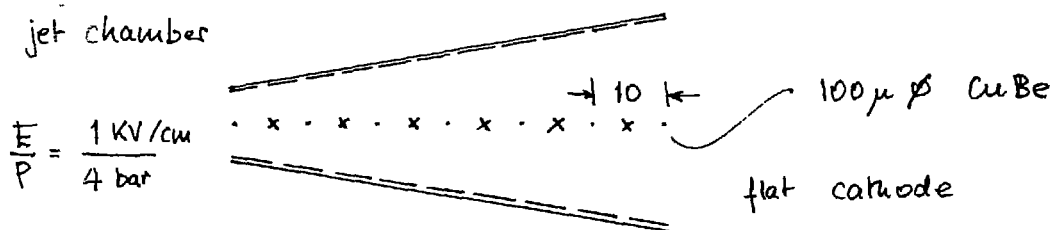
Laboratory test or result from experiment: experiment

Name of Detector (if from experiment): JADE

Significant degradation of performance: Occurred

Describe the most significant change: 20% drop in amplitude at wires closest to beam (over 6 years)

Make a small simple sketch of the cell:



Anode wire material and diameter: 20 μ W

Cathode wire material and diameter (if applicable): Cu on Kapton

Electric field on anode wire surface: 340 kV/cm

Electric field on cathode surface: 0.9

Electric field on potential wire surface (if applicable): 14.6 kV/cm

High/low intensity (particle rate in Hz/cm or anode current in nA/cm)?: ~ 0.5 μ A/cm

Approximate total integrated particle flux (No./cm²): 10^9 /cm²

Approximate total gain (per primary electron): $(3-4) \cdot 10^4$

Type of radiation (e.g. beam particles, Fe⁵⁶, Sr⁹⁰, etc.): (beam part) + synchrotron rad: $\langle E \rangle = 15$ KeV

Number of primary electrons per ionization event: 360/min ion part. cm

Approximate total charge dose (C/cm): 0.02 C/cm

Type of gas (including "additives"):

Gas flow rate (gas volume/hour): 10 l/s

Gas flow condition: sealed + circulated, no purific.

Gas impurities (water, oxygen, halogens, etc.): H₂O (0.05%); O₂ (.003%)

Gas pressure (atm): 4

Can gas system be evacuated?: yes

Length and material of gas tubing: ~ 50 m steel, copper

List of other materials in the system: G10, Rohacell, cables

Oils or greases in the system: ?

Method of analysis of deposits: —

List the elements found in deposits: —

Major conclusion of the study (you can use the other side also): In 3 ring jet chambers, the following amplification reduction was observed:

$$\begin{array}{cc} \text{ring 1} & \text{ring 2} \\ \frac{dA}{A} \cdot \frac{1}{Q} [\%/C/cm] & - (11 \pm 2) - (2 \pm 3) \end{array}$$

although the accumulated charge per wire in each ring is the same. Suspicion: radiation damage induced during filling of storage ring (in preamps, chamber material...)

SUMMARY OF RESULTS — WIRE AGING

Name and Institution: Michel Yvert / CERN/Annecy (LAPP)

Telephone: 83 4547 (CERN)

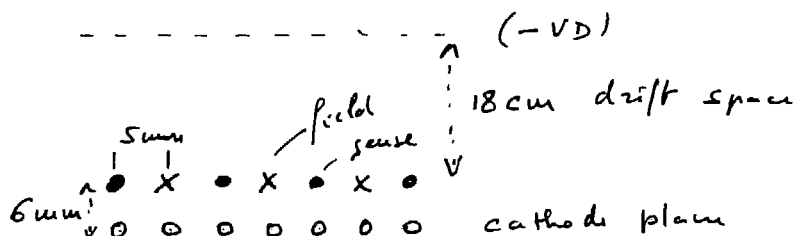
Laboratory test or result from experiment: Experiment

Name of Detector (if from experiment): UA1 Central Detector

Significant degradation of performance: Did not occur

Describe the most significant change:

Make a small simple sketch of the cell:



Anode wire material and diameter: $35\ \mu$ Ni-Cr

Cathode wire material and diameter (if applicable): Cu Be gold plated $100\ \mu$

Electric field on anode wire surface: $213\ \text{kV/cm}$

Electric field on cathode surface: $35\ \text{kV/cm}$

Electric field on potential wire surface (if applicable): Field wires $2.7\ \text{kV/cm}$

High/low intensity (particle rate in Hz/cm or anode current in nA/cm)?: Low: $3\ \text{nA/cm}$

Approximate total integrated particle flux (No./cm²):

Approximate total gain (per primary electron): $\simeq 10^5$

Type of radiation (e.g. beam particles, Fe⁵⁶, Sr⁹⁰, etc.): beam

Number of primary electrons per ionization event: $\simeq 100$

Approximate total charge dose (C/cm): $0.01\ \text{C/cm}$

Type of gas (including "additives"): Argon 40, Ethane 60

Gas flow rate (gas volume/hour):

Gas flow condition: $400\ \text{l/h}$ 10% Vented/90% recirculated

Gas impurities (water, oxygen, halogens, etc.): 20 ppm input H₂O, 30 ppm input O₂

Gas pressure (atm): 1

Can gas system be evacuated?: no

Length and material of gas tubing: inox (stainless steel) $\simeq 100\ \text{m}$ + nylon $10\ \text{m}$

List of other materials in the system:

Oils or greases in the system:

Method of analysis of deposits:

List the elements found in deposits:

Major conclusion of the study (you can use the other side also): Detector has not been opened yet — operates satisfactorily; no trace of ageing found (no drop in gain resolution).

SUMMARY OF RESULTS — WIRE AGING

Name and Institution: Michel Yvert / CERN/Annecy (LAPP)

Telephone: 83 4547 (CERN)

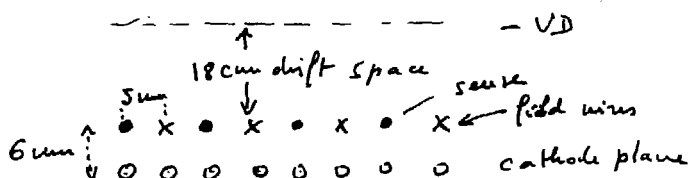
Laboratory test or result from experiment: Lab tests

Name of Detector (if from experiment):

Significant degradation of performance: Occurred

Describe the most significant change: One wire broke down (discharge). Wire removed, chamber still under irradiation.

Make a small simple sketch of the cell:



Anode wire material and diameter: 35 μm Ni-Cr

Cathode wire material and diameter (if applicable): Cu Be gold plated 100 μm \emptyset

Electric field on anode wire surface: 213 kV/cm

Electric field on cathode surface: 35 kV/cm

Electric field on potential wire surface (if applicable): Field wires 2.7 kV/cm

High/low intensity (particle rate in Hz/cm or anode current in nA/cm)?: High: 11.5 nA/cm

Approximate total integrated particle flux (No./cm²):

Approximate total gain (per primary electron): $\simeq 10^5$

Type of radiation (e.g. beam particles, Fe⁵⁶, Sr⁹⁰, etc.): Sr⁹⁰ source

Number of primary electrons per ionization event: Variable

Approximate total charge dose (C/cm): 0.038 C/cm

Type of gas (including "additives"): Argon Ethane 40-60%

Gas flow rate (gas volume/hour): 5 vol/hour

Gas flow condition: Vented

Gas impurities (water, oxygen, halogens, etc.): direct from bottle

Gas pressure (atm): 1

Can gas system be evacuated?: no

Length and material of gas tubing: Copper 5 m + 5 m rilson (nylon)

List of other materials in the system: glass + pressure regulator

Oils or greases in the system: no

Method of analysis of deposits: X-ray

List the elements found in deposits:

Major conclusion of the study (you can use the other side also):

- Measurement still in progress.
- Breakdown observed on a faulty wire. Analysis of faulty cell shows:
 - coating on cathode wire possibly polymerization
 - no deposit on field wire
 - sulfur on sense wire in the breakdown region
- On the wire still under irradiation, no change in resolution observed.

SUMMARY OF RESULTS — WIRE AGING

Name and Institution: M. Turala — UC Santa Cruz / INP Krakow

Telephone: SLAC: (415) 854-3300, x. 3305

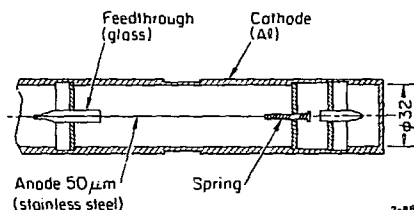
Laboratory test or result from experiment: lab test

Name of Detector (if from experiment): proportional chamber

Significant degradation of performance: Did not occur

Describe the most significant change: Small change in gas gain observed

Make a small simple sketch of the cell:



Anode wire material and diameter: SS, 50 μm

Cathode wire material and diameter (if applicable): Al

Electric field on anode wire surface:

Electric field on cathode surface:

Electric field on potential wire surface (if applicable):

High/low intensity (particle rate in Hz/cm or anode current in nA/cm)?: 200 nA (?)

Approximate total integrated particle flux (No./cm²):

Approximate total gain (per primary electron): $\sim 10^4$

Type of radiation (e.g. beam particles, Fe⁶⁶, Sr⁹⁰, etc.): ⁵⁶Fe

Number of primary electrons per ionization event: ~ 100

Approximate total charge dose (C/cm): ~ 2 C/cm

Type of gas (including "additives"): Ar + 8% N₂

Gas flow rate (gas volume/hour):

Gas flow condition: Sealed

Gas impurities (water, oxygen, halogens, etc.): below few ppm

Gas pressure (atm): 0.92 atm

Can gas system be evacuated?: yes

Length and material of gas tubing:

List of other materials in the system:

Oils or greases in the system: no

Method of analysis of deposits: Electron Scanning Microscope

List the elements found in deposits: no deposits

Major conclusion of the study (you can use the other side also):

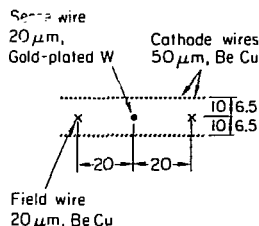
No deposits seen on the anode. Quenching properties of the mixture not very good. Slow reduction of gas amplification factor observed.

SUMMARY OF RESULTS — WIRE AGING

Name and Institution: M. Turala — UC Santa Cruz / INP Krakow
Telephone: SLAC: (415) 854-3300, x. 3305
Laboratory test or result from experiment: NA 32 at CERN
Name of Detector (if from experiment): drift chambers

Significant degradation of performance: Did not occur
 Describe the most significant change:

Make a small simple sketch of the cell:



Anode wire material and diameter: W + Au - 20 μm , SS - 25 μm
Cathode wire material and diameter (if applicable): Be-Cu - 50 μm
Electric field on anode wire surface: $\sim 10^5$ V/cm
Electric field on cathode surface:
Electric field on potential wire surface (if applicable):

High/low intensity (particle rate in Hz/cm or anode current in nA/cm)?: $10^6/\text{s}$
Approximate total integrated particle flux (No./cm²): $\sim 5 \cdot 10^{11}$
Approximate total gain (per primary electron): 10^4 – $2 \cdot 10^5$
Type of radiation (e.g. beam particles, Fe⁵⁶, Sr⁹⁰, etc.): beam
Number of primary electrons per ionization event: ~ 20
Approximate total charge dose (C/cm): 0.01 – 0.02 C/cm

Type of gas (including "additives"): 60:40 Ar + C₂H₆ + 0.1% iso-propyl alcohol
Gas flow rate (gas volume/hour): ~ 0.04
Gas flow condition: Vented
Gas impurities (water, oxygen, halogens, etc.): ?
Gas pressure (atm): 1 atm
Can gas system be evacuated?: no
Length and material of gas tubing: 50m, "tygon" + Cu
List of other materials in the system: stainless steel, ...

Oils or greases in the system: both (silicon)
Method of analysis of deposits:
List the elements found in deposits:

Major conclusion of the study (you can use the other side also):

We do not see (yet?) a degradation of drift chambers. In the past, for the similar gas mixture but without alcohol, we noticed a drop of efficiency at approximately the similar dose.

SUMMARY OF RESULTS — WIRE AGING

Name and Institution: M. Turala — UC Santa Cruz / INP Krakow

Telephone: SLAC: (415) 854-3300, x. 3305

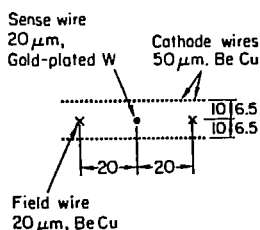
Laboratory test or result from experiment: lab test

Name of Detector (if from experiment):

Significant degradation of performance: Did not occur

Describe the most significant change:

Make a small simple sketch of the cell:



Anode wire material and diameter: W + Au, 20 μm

Cathode wire material and diameter (if applicable): Be-Cu, 50 μm

Electric field on anode wire surface: $\sim 10^5$

Electric field on cathode surface:

Electric field on potential wire surface (if applicable):

High/low intensity (particle rate in Hz/cm or anode current in nA/cm)?: ~ 100 nA/cm (?)

Approximate total integrated particle flux (No./cm²):

Approximate total gain (per primary electron): 10^4 – $3 \cdot 10^5$

Type of radiation (e.g. beam particles, Fe⁶⁵, Sr⁹⁰, etc.): ⁹⁰Sr

Number of primary electrons per ionization event: ~ 30

Approximate total charge dose (C/cm): 1 C/cm (?)

Type of gas (including "additives"): 50:50 Ar + C₂H₆ + 0.1% iso-propyl alcohol

Gas flow rate (gas volume/hour): ~ 5

Gas flow condition: Vented

Gas impurities (water, oxygen, halogens, etc.): ?

Gas pressure (atm): 1 atm

Can gas system be evacuated?: no

Length and material of gas tubing: 5m, "tygon"

List of other materials in the system: stainless steel, ...

Oils or greases in the system: yes (both)

Method of analysis of deposits: fluorescent analysis, ESM

List the elements found in deposits: Si, Au

Major conclusion of the study (you can use the other side also):

Even a small addition of iso-propyl alcohol significantly increased the lifetime of the test chamber (in comparison with its performance for gas mixture without alcohol).

SUMMARY OF RESULTS — WIRE AGING

Name and Institution: O. Ullaland / CERN

Telephone: 5915

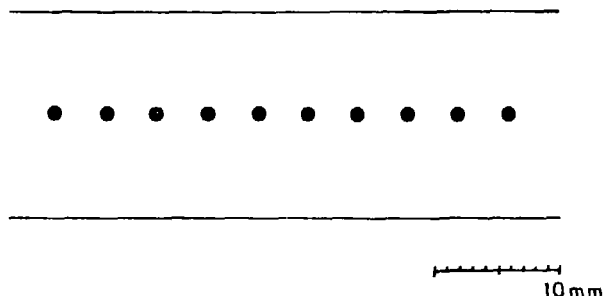
Laboratory test or result from experiment: Experiment

Name of Detector (if from experiment): SFMD

Significant degradation of performance: Occurred

Describe the most significant change: Change in HV plateau

Make a small simple sketch of the cell:



Anode wire material and diameter: ϕ 20 μ m gold plated tungsten

Cathode wire material and diameter (if applicable): Silver plated flat cathode

Electric field on anode wire surface: 335 kV/cm

Electric field on cathode surface:

Electric field on potential wire surface (if applicable):

High/low intensity (particle rate in Hz/cm or anode current in nA/cm)?:

$.75 \cdot 10^4 / \text{cm}^2 / \text{sec}$

Approximate total integrated particle flux (No./cm²): $2 \cdot 10^{11} / \text{cm}^2$

Approximate total gain (per primary electron): 10^5

Type of radiation (e.g. beam particles, Fe⁵⁶, Sr⁹⁰, etc.): Beam particles

Number of primary electrons per ionization event: 30

Approximate total charge dose (C/cm): .3 C/cm wire

Type of gas (including "additives"): 53% Ar, 40% isoButane, 7% Methylal

Gas flow rate (gas volume/hour): .1 detector volume/h

Gas flow condition: Vented

Gas impurities (water, oxygen, halogens, etc.):

Gas pressure (atm): 1 atm

Can gas system be evacuated?: No

Length and material of gas tubing: 60 m Stainless Steel + 25 m Rilsan (polyamide 11)

List of other materials in the system: None

Oils or greases in the system: Oil bubbler 25 m downstream

Method of analysis of deposits: Electron microscope

List the elements found in deposits:

Major conclusion of the study (you can use the other side also):

Maximum growth of the radius of the anode wire was about 1 μ m.

APPENDIX C

Bibliography

PARTIAL LIST OF REFERENCES ON POLYMERIZATION AND
WIRE CHAMBER DEGENERACY

- Friedland and Katzenstein, Rev. Sci. Instr. 24, 103 (1953).
- den Boggende et al., J. of Sci. Instr. (J. of Phys.)
2, 701 (1969).
- Charpak et al., NIM 99, 279 (1972).
- Spielberg et al., Rev. Sci. Instr. 46, 1086 (1975).
- Bawdekar, IEEE Trans. Nucl. Sci. NS-22, 282 (1975).
- Friedrich and Sauli, CERN EP 77-10 (1977).
- Le Du et al., CERN EP Internal Report 77-11 (1977).
- Faruqi, IEEE Trans. Nucl. Sci. NS-27, 644 (1980).
- Grady and Robertson, NIM 179, 317 (1981).
- Turala and Vermeulen, NIM 205, 141 (1983); CERN EP/82-79.
- Smith and Turner, NIM 192, 475 (1982).
- Sumner, IEEE Trans. Nucl. Sci. NS-29, 1410 (1982).
- Atac, Proceedings of Gas Calorimetry Workshop, 1982, pp. 303-340.
- Adam et al., NIM 217, 291 (1983).
- Sipila and Jarvinen, NIM 217, 298 (1983).
- Dwurazny et al., NIM 217, 301 (1983). Also NIM 228,
267 (1985).
- Binnie et al. (TASSO), Imperial College (London) Report HENP/84/2.
Also, NIM 28, 267 (1985).
- Artemiev et al., NIM 224, 408 (1984).
- Anderson et al., NIM 223, 29, 31 (1984).
- Fischer et al., NIM A238, 249 (1985).
- Kwong et al., NIM A238, 265 (1985).
- Lawrence Berkeley Laboratory, TPC Letter of Intent: Vertex
Chamber Proposal, TPC-LBL-85-20 (1985).

PARTIAL LIST OF BOOKS ON PLASMA POLYMERIZATION

1. M Shen, Plasma Chemistry of Polymers, published by Dekker, New York City, 1976.
2. M. Shen and A. Bell, Plasma Polymerization, published by American Chemical Society, 1979.
3. H. Boenig, Plasma Science and Technology, published by Cornell University Press, Ithaca, NY, 1982.
4. H. Yasuda, Plasma Polymerization, published by Academic Press, 1985.

APPENDIX D

List of Workshop Attendees

WORKSHOP ON RADIATION DAMAGE TO WIRE CHAMBERS

List of Participants

Hiroaki Aihara
50B-6208
Lawrence Berkeley Laboratory
1 Cyclotron Road
Berkeley, CA 94720
415/486-7355
FTS 451-7355

Muzaffer Atac
MS-223
Fermi National Accelerator Laboratory
P.O. Box 500
Batavia, IL 60510
312/840-3960
FTS 370-3960

David Binnie
Imperial College
Blackett Laboratory
Prince Consort Road
London SW7 2AZ
UNITED KINGDOM

James Bistirlich
50-205
Lawrence Berkeley Laboratory
1 Cyclotron Road
Berkeley, CA 94720
415/486-5021
FTS 451-5021

Kirk Bunnell
Bin 65
Stanford Linear Accelerator Center
P.O. Box 4349
Stanford, CA 94305
415/854-3300, x2543
FTS 461-9300, x2543

John Carr
High Energy Physics
University of Colorado
Campus Box 390
Boulder, CO 80309
303/492-1480

George Chadwick
Bin 95
Stanford Linear Accelerator Center
P.O. Box 4349
Stanford, CA 94305
415/854-3300, x2659
FTS 461-9300, x2659
GBC@SLACVM

David Christian
MS-122
Fermi National Accelerator Laboratory
P.O. Box 500
Batavia, IL 60510
312/840-4001
FTS 370-4001

Persis Drell
50A-2160
Lawrence Berkeley Laboratory
1 Cyclotron Road
Berkeley, CA 94720
415/486-7190
FTS 451-7190
PERSIS at SLACVM

Friedrich Dydak
CERN
CH-1211 Geneva 23
SWITZERLAND
(022) 834921

Al Erwin
High Energy Physics Department
University of Wisconsin
Madison, WI 53706

Penny Estabrooks
Department of Physics
Carleton University
Ottawa, Ontario K1S 5B6
CANADA
613/564-6630

Lyle Feely
Matheson
6775 Central Avenue
Newark, CA 94560

Norman Morgan
Physics Department
Purdue University
Lafayette, IN 47907
317/494-8748

Brian Foster
Physics Department
Bristol University
Royal Fort, Tyndall Avenue
Bristol BS8 1TL
UNITED KINGDOM
0272 303030, x3699
VAX PHYS::AIHP04

T. Freese
Stanford Linear Accelerator Center
P.O. Box 4349
Stanford, CA 94305
415/854-3300
FTS 461-9300

Yasuo Fukui
MS-223, CDF/RD
Fermi National Accelerator Laboratory
P.O. Box 500
Batavia, IL 60510
312/840-3231
FTS 370-3231

Raymond Fuzesy
80-101
Lawrence Berkeley Laboratory
1 Cyclotron Road
Berkeley, CA 94720
415/486-5464
FTS 451-5464

Dan Gee
Physics Department
University of California
Riverside, CA 92521
714/787-5330

Murdock G. D. Gilchriese
Laboratory for Nuclear Studies
Newman Laboratory
Cornell University
Ithaca, NY 14853
607/256-5197

Gary Godfrey
Bin 98
Stanford Linear Accelerator Center
P.O. Box 4349
Stanford, CA 94305
415/854-3300, x2919
FTS 461-9300, x2919

Christoph Grab
Bin 65
Stanford Linear Accelerator Center
P.O. Box 4349
Stanford, CA 94305
415/854-3300, x2636
FTS 461-9300, x2636

Gail Hanson
Bin 61
Stanford Linear Accelerator Center
P.O. Box 4349
Stanford, CA 94305
415/854-3300, x2510
FTS 461-9300, x2510

Dennis W. Hess
Chemical Engineering Department
University of California
Berkeley, CA 94720
415/642-4862

Rolf-Dieter Heuer
CERN
CH-1211 Geneva 23
SWITZERLAND
HEUER@CERNVM
(22) 834096

Hans Juergen Hilke
CERN
CH-1211 Geneva 23
SWITZERLAND

Christopher L. Hodges¹
San Francisco State University
1600 Holloway Avenue
San Francisco, CA 94132
415/469-2433

¹SLAC Address: Bin 96, 415/854-3300, x2696

George Igo
 Physics Department
 University of California
 405 Hilgard Avenue
 Los Angeles, CA 90024
 213/825-1308
 213/825-1376

Richard Jared
 29-100
 Lawrence Berkeley Laboratory
 1 Cyclotron Road
 Berkeley, CA 94720
 415/486-6616
 FTS 451-6616

John A. Jaros
 Bin 61
 Stanford Linear Accelerator Center
 P.O. Box 4349
 Stanford, CA 94305
 415/854-3300, x2852
 FTS 461-9300, x2852

Terrence Jensen²
 Wilson Laboratory
 Cornell University
 Ithaca, NY 14853
 607/256-4882

James Jones
 Idaho National Engineering Laboratory
 EG&G Idaho, Inc.
 P.O. Box 1625
 Idaho Falls, ID 83415
 (208) 526-1730
 FTS 583-1730

Henning Kado
 Inst. für Experimentalphysik der Univ. Hamburg
 Luruper Chaussee 149
 D-2000 Hamburg 50
 WEST GERMANY
 040 8998-2509

John Kadyk
 50A-2160
 Lawrence Berkeley Laboratory
 1 Cyclotron Road
 Berkeley, CA 94720
 415/486-7189
 FTS 451-7189

Harris Kagan
 High Energy Physics Group
 174 West 18th Avenue
 Ohio State University
 Columbus, OH 43210
 614/422-2745

Christopher B. Klopfenstein
 50-341
 Lawrence Berkeley Laboratory
 1 Cyclotron Road
 Berkeley, CA 94720
 415/486-7087
 FTS 451-7087

Rainer Kotthaus
 Max-Planck-Institut für Physik
 Fohringer Ring 6
 D-8000 München-40
 WEST GERMANY
 (089) 3189-3265

Witold Kozanecki
 Bin 95
 Stanford Linear Accelerator Center
 P.O. Box 4349
 Stanford, CA 94305
 415/854-3300, x2701
 FTS 461-9300, x2701

Joseph Lach
 MS-219
 Fermi National Accelerator Laboratory
 P.O. Box 500
 Batavia, IL 60510
 312/840-0107
 FTS 370-0107

²Home Institution: Ohio State University

John Layter³
 Bin 43
 Stanford Linear Accelerator Center
 P.O. Box 4349
 Stanford, CA 94305
 415/854-3300, x2361
 FTS 461-9300, x2361

David Lee
 MS H838, MP 13
 Los Alamos National Laboratory
 Los Alamos, NM 87545
 505/667-8888

Peter Lennert
 Physikal. Institut
 Philosophenweg 12
 D 6900 Heidelberg
 FED. REP. GERMANY
 49 6252 3312

Alain-Pierre Lilot
 Balteau S.A.
 Division Controle non Destructif
 Rue de Magnee, 54
 B-4610 Beyne-Heusay
 BELGIUM

Kaori Maeshima
 Physics Department
 University of California
 Davis, CA 95616
 (916) 752-6726

Stan Majewski⁴
 Physics Department
 University of Florida
 215 Williamson Hall
 Gainesville, FL 32611
 904/392-0521

Usha Mallik
 Bin 65
 Stanford Linear Accelerator Center
 P.O. Box 4349
 Stanford, CA 94305
 415/854-3300, x2635
 FTS 461-9300, x2635

Gholamali Mazaheri
 Bin 65
 Stanford Linear Accelerator Center
 P.O. Box 4349
 Stanford, CA 94305
 415/854-3300, x2716
 FTS 461-9300, x2716

Curtis Meyer
 50-205
 Lawrence Berkeley Laboratory
 1 Cyclotron Road
 Berkeley, CA 94720
 415/486-5021
 FTS 451-5021

W. Molzon
 University of Pennsylvania
 Philadelphia, PA 19104

Francis Muller
 CERN
 EP Division
 CH-1211 Geneva 23
 SWITZERLAND
 FGM\$XN at CERN

Uriel Nauenberg
 University of Colorado
 Department of Physics
 Campus Box 390
 Boulder, CO 80303
 (303) 492-7715

Francesco L. Navarria
 Physics Department
 University of Bologna
 Via Irnerio 46
 I-40126 Bologna
 ITALY
 003951 260991
 NVR\$VW at CERN

³Home Institution: University of California, Riverside

⁴FNAL Address: MS-222, Fermi National Accelerator Laboratory, P.O. Box 500, Batavia, IL 60510 (312/840-3471 FTS 370-3471)

Harry Nelson
Bin 94
Stanford Linear Accelerator Center
P.O. Box 4349
Stanford, CA 94305
415/854-3300, x3196
FTS 461-9300, x3196

David Nygren
50B-6208
Lawrence Berkeley Laboratory
1 Cyclotron Road
Berkeley, CA 94720
415/486-7162
FTS 451-7162

Allen Odian
Bin 65
Stanford Linear Accelerator Center
P.O. Box 4349
Stanford, CA 94305
415/854-3300, x3593
FTS 461-9300, x3593

Robert Openshaw
TRIUMF
4004 Westbrook Mall
Vancouver, B.C., Canada
(604) 228-4711

Andrea Palounek⁵
Bin 96
Stanford Linear Accelerator Center
P.O. Box 4349
Stanford, CA 94305
APTP@SLACVM

Sherwood Parker⁶
Department of Physics
University of Hawaii
Honolulu, HI 96822

Victor Perez-Mendez
50-348
Lawrence Berkeley Laboratory
1 Cyclotron Road,
Berkeley, CA 94720
415/486-6332
FTS 451-6332

Philip Pile
Bldg. 510 A
Brookhaven National Laboratory
Upton, NY 11973
516/282-3913

Dale Pitman
Bin 65
Stanford Linear Accelerator Center
P.O. Box 4349
Stanford, CA 94305
415/854-3300, x3594
FTS 461-9300, x3594
PITMAN at SLACVM

Richard Prepost⁷
Bin 94
Stanford Linear Accelerator Center
P.O. Box 4349
Stanford, CA 94305
415/854-3300, x2625
FTS 461-9300, x2625

Bill A. Rowe
Santa Cruz Institute for Particle Physics
University of California
1156 High Street
Santa Cruz, CA 95064
408/429-2694

Mario Ruscev
Giers Schlumberger
12 Place des Etats Unis
92120 Montrouge
FRANCE
(33) 1 47 46 65 36
Telex GIERS 206289F

⁵Home Institution: MIT

⁶LBL address: 50A-6141, Lawrence Berkeley Laboratory, 1 Cyclotron Road, Berkeley, CA 94720 (415/486-5859; FTS 451-5859)

⁷Home Institution: University of Wisconsin

Bernard Sadoulet
Physics Department
University of California
Berkeley, CA 94720
415/642-5719

Hartmut Sadrozinski
Santa Cruz Institute for Particle Physics
329 Nat. Sci. II
University of California
Santa Cruz, CA 95064
408/429-2923

Fabio Sauli
CERN
CH-1211 Geneva 23
SWITZERLAND
(4122) 833670

Rafe H. Schindler
Bin 65
Stanford Linear Accelerator Center
P.O. Box 4349
Stanford, CA 94305
415/854-3300, x3595
FTS 461-9300, x3595

Walter Selove
Physics Department
University of Pennsylvania
Philadelphia, PA 19104
215/898-8159

Ronald D. Settles
Max-Planck-Institut fur Physik
Fohringer Ring 6
D-8000 Munchen-40
WEST GERMANY
49/89-318931

Darrel Smith⁸
CERN
EP Division
CH-1211 Geneva 23
SWITZERLAND

Kevin Sparks
University of California
Davis, CA 95616
KBSUCD at SLACUCD

Harold M. Spinka
Bldg. 362
High Energy Physics Division
Argonne National Laboratory
9700 South Cass Avenue
Argonne, IL 60439
312/972-6317

George Stephans
Massachusetts Institute of Technology
70 Massachusetts Avenue
Cambridge, MA 02139
(617) 253-4237

Ian Stockdale
Bin 65
Stanford Linear Accelerator Center
P.O. Box 4349
Stanford, CA 94305
415/854-3300, x3579
FTS 461-9300, x3579

Wolfgang Stockhausen
Bin 65
Stanford Linear Accelerator Center
P.O. Box 4349
Stanford, CA 94305
415/854-3300, x3594
FTS 461-9300, x3594

Mark Strovink
50-341
Lawrence Berkeley Laboratory
1 Cyclotron Road
Berkeley, CA 94720
415/486-7087
FTS 451-7087

Mansour Taeed
Lawrence Berkeley Laboratory
1 Cyclotron Road
Berkeley, CA 94720

⁸Home Institution: University of California, Riverside

George E. Theodosiou⁹
 MS-221
 Fermi National Accelerator Laboratory
 P.O. Box 500
 Batavia, IL 60510
 312/840-4150
 FTS 370-4150

Walter Toki
 Bin 65
 Stanford Linear Accelerator Center
 P.O. Box 4349
 Stanford, CA 94305
 415/854-3300, x 2647 or 2646
 FTS 461-9300, x 2647 or 2646

Michal Turala¹⁰
 Bin 43
 Stanford Linear Accelerator Center
 P.O. Box 4349
 Stanford, CA 94305
 415/854-3300, x3305
 FTS 461-9300, x3305

O. Ullaland
 CERN
 CH-1211 Geneva 23
 SWITZERLAND
 (835709)

Jaroslav Va'vra
 Bin 20
 Stanford Linear Accelerator Center
 P.O. Box 4349
 Stanford, CA 94305
 415/854-3300, x3299
 FTS 461-9300, x3299

Henri Videau
 Lab. de Phys. Nucl. des Hautes Energies
 Ecole Polytechnique
 Route de Saclay
 F-91128 Palaiseau
 FRANCE

Francesco Villa
 Bin 65
 Stanford Linear Accelerator Center
 P.O. Box 4349
 Stanford, CA 94305
 415/854-3300, x3591
 FTS 461-9300, x3591

James Volk
 University of California
 Davis, CA 95616

Albrecht Wagner
 Physik. Institut
 D-6900 Heidelberg
 Philosophenweg 12
 WEST GERMANY
 WAGNER@DHDHEP1

Robert L. Wagner
 CDF MS-223
 Fermi National Accelerator Laboratory
 P.O. Box 500
 Batavia, IL 60510
 312/840-3112
 FTS 370-3112

Daria Walsh
 Santa Cruz Institute for Particle Physics
 University of California
 1156 High Street
 Santa Cruz, CA 95064
 408/429-2694

Crispin Williams
 Physics Department
 University of California
 Davis, CA 95616
 916/752-6726

Michael C. Williams
 Chemical Engineering Department
 University of California
 Berkeley, CA 94720
 415/642-4525

⁹Home Institution: University of Pennsylvania

¹⁰Visitor at the Department of Physics, University of California, Santa Cruz, CA 95064. Home Institution: Institute of Nuclear Physics, Krakow, Poland.

William Wisniewski
Bin 65
Stanford Linear Accelerator Center
P.O. Box 4349
Stanford, CA 94305
415/854-3300, x3596
FTS 461-9300, x3596

Stephen Wolbers
MS 122
Fermi National Accelerator Laboratory
P.O. Box 500
Batavia, IL 60510
312/840-4004, 840-3201
FTS 370-4004, 370-3201

Richard K. Yamamoto
Massachusetts Institute of Technology
Room 409, 575 Technology Square
Cambridge, MA 02139

Charles Young
Bin 96
Stanford Linear Accelerator Center
P.O. Box 4349
Stanford, CA 94305
415-854-3300, x2669
FTS 461-9300, x2669
YOUNG@SLACVM

Michel Yvert
CERN/LAPP Annecy
EP Division
CH-1211 Geneva 23
SWITZERLAND